



**The Synthesis, Structural  
Characterisation and Biological  
Evaluation of Potential  
Chemotherapeutic Agents**

**Brian W. Moran B.Sc. (Hons)**

**A thesis presented for the degree of Doctor of Philosophy**

**at**

*Dublin City University*



*Ollscoil Chathair Bhaile Átha Cliath  
School of Chemical Sciences  
National Institute for Cellular Biotechnology*

*September 2008*

*Dedicated to my little Princess*

## *Declaration*

I hereby certify that this material, which I now submit for assessment on the programme of study leading to the award of PhD is entirely my own work, that I have exercised reasonable care to ensure that the work is original, and does not to the best of my knowledge breach any law of copyright, and has not been taken from the work of others save and to the extent that such work has been cited and acknowledged within the text of my work.

Signed: \_\_\_\_\_  
Brian W. Moran

ID No.: 50097454

Date: \_\_\_\_\_

# *Acknowledgments*

I would like to thank my supervisor, Dr. Peter T. M. Kenny for giving me the opportunity to conduct research under his supervision, and for being so supportive and encouraging at both an academic level and a personal level.

I would also like to express my gratitude to:

The National Institute for Cellular Biotechnology and Dublin City University for funding my research to date;

Dr. Ciarán Ó Fagáin, Dr. Brendan O'Connor, Dr. Deborah M. Ruth and Dr. Pamela O'Brien in the School of Biotechnology for their invaluable assistance and use of equipment in my protease inhibition studies;

Dr. John P. Dalton in the Institute for the Biotechnology of Infectious Diseases, University of Technology, Sydney, PO Box 123, Broadway, NSW 2007, Australia for generously donating *Fasciola hepatica* cathepsin L protease;

Dr. Robert O'Connor and Aoife Devery in the National Institute for Cellular Biotechnology for carrying out cytotoxicity and synergistic studies;

Prof. Sylvia Draper in Trinity College Dublin for obtaining X-ray crystallographic data;

The entire technical staff of the School of Chemical Sciences and the National Institute for Cellular Biotechnology, especially, Damien, John, Mick, Ambrose, Veronica, Vinny, Mary, Mick and others;

The fourth year and exchange students that have worked with me over the past couple of years, including Yvonne Halpin, William Butler, Audrey Le Gall, Adeline Prêtre, Aymeric LePronier, Kahina Mammeri, Julian Dulcet.

A special thanks to my PKRG (Peter Kenny Research Group) colleagues, Frankie Anderson, Steven Alley, Paula Kelly, Alok Goel, Alan Corry, Áine Mooney, William Butler and Andy Harry.

Thanks to my fellow postgraduates and postdoctorals, including the occupants of X249 and GG23; especially Rob, Neil, Brian, Dan, Ewa, Haibo, Saibh, Bruce, Sarah, Fadi, Ger, Michael;

Very special thanks to my family, my parents John and Ann, sisters Maeve and Deirdre and brother Conor, for all their support and encouragement.

Finally, but certainly not least, a huge thank you to the two girls in my life, Aisling and my little princess Aoibheann. I could not wish for a better family to arrive home to each evening. Thank you from the bottom of my heart for putting up with me on this journey, through the many ups and downs and supporting me to the end.

## ***Abstract***

Cathepsin proteases have been identified in many parasitic organisms and are involved in roles as diverse as tissue and skin penetration, virulence and immune invasion. Involvement in these key functions renders them potential targets at which to direct novel chemotherapeutic agents. The inhibitor *N*-benzoyl-L-Leu-Gly nitrile prepared in this laboratory was shown to possess significantly greater inhibitory potency on the liver fluke *Fasciola hepatica* cysteine cathepsin L like endoproteases over the known commercial inhibitor *Z*-Phe-Ala-CHN<sub>2</sub> at varying concentrations.

The synthesis, structural characterisation and biological evaluation of a series of analogues of this active compound is now reported. Addition of fluorine atoms to the *N*-terminal benzoyl group and selective modification of the *N*-terminus is reported. These dipeptidyl derivatives were synthesized using the standard DCC/HOBt or EDC/HOBt protocols. These novel Cathepsin L inhibitors have been characterized by a wide range of spectroscopic techniques including <sup>1</sup>H, <sup>13</sup>C, <sup>19</sup>F NMR and ESIMS. The biological activity of these novel compounds was determined in a bioassay using *Z*-Phe-Arg-NHMec as a fluorogenic substrate.

Resveratrol is a naturally occurring phytoalexin found in several plants but mainly in the skins of grapes. It has been shown to be produced in response to bacterial and fungal infections. It has been shown to exhibit various biological activities including anticancer, antifungal, antiviral, neuroprotective, anti-aging, and anti-inflammatory effects. The synthesis of fluorinated stilbenes containing the 3,5,4'-substituted backbone was accomplished. The compounds were synthesised via the Wittig reaction and the decarbonylative Heck reaction. In conjunction with fluorine, nitrogen was also used as a replacement for the oxygen atoms of the resveratrol structure. Full structural characterisation of these compounds was carried out followed by preliminary biological screening.

## ***Table of contents:***

Title page	i
Dedication	ii
Declaration	iii
Acknowledgements	iv
Abstract	vi
Thesis Introduction	x

## **Section 1**

### **1.0 Proteases and their inhibition**

1.1	Introduction	2
1.2	Protease mechanism	4
1.3	Protease inhibitors	7
1.4	Inhibition kinetics	8
1.5	Types of Protease Inhibitors	10
	<i>1.5.1 Non specific inhibitors</i>	10
	<i>1.5.2 Class specific inhibitors</i>	13
	<i>1.5.2.1 Serine protease inhibitors</i>	14
	<i>1.5.2.2 Cysteine protease inhibitors</i>	25
	<i>1.5.2.3 Aspartic acid inhibitors</i>	33
	<i>1.5.2.4 Metalloprotease inhibitors</i>	47
1.6	Fluorine containing protease inhibitors	52
1.7	Conclusion & Aims	58
1.8	References	60

### **2.0 Synthesis & characterisation of novel dipeptide derivatives**

2.1	Introduction	70
2.2	Synthesis of dipeptidyl derivatives	71

2.2.1	<i>N</i> -fluorobenzoyl dipeptidyl nitriles	73
2.2.2	<i>N</i> -protected dipeptidyl nitriles	76
2.3	References	80
<b>3.0</b>	<b>Biological activity of novel dipeptide nitriles</b>	
3.1	Introduction	82
3.2	Fluorescent assay	83
3.3	Biological results	84
3.4	References	87
<b>4.0</b>	<b>Conclusion</b>	88
<b>5.0</b>	<b>Experimental</b>	89

## Section 2

<b>6.0</b>	<b>Resveratrol</b>	
6.1	Introduction	115
6.2	Biosynthetic pathway of resveratrol	118
6.3	Synthesis of resveratrol	120
6.4	Bioactivity of resveratrol	134
6.4.1	<i>Anticancer activity</i>	135
6.4.2	<i>Antioxidant activity</i>	142
6.5	Resveratrol derivatives	146
6.6	Conclusion & Aims	148
6.7	References	150
<b>7.0</b>	<b>Synthesis &amp; characterisation of novel fluoro-amino stilbenes</b>	
7.1	Introduction	155
7.2	Synthesis of 3,5-difluoro resveratrol analogues	156



7.2.1	<i>Synthesis of 3,5-difluoro-4'-nitro stilbene</i>	156
7.2.1.1	Determination of isomeric orientation	157
7.2.1.2	IR study of (E/Z)-3,5-difluoro-4'-nitrostilbene	163
7.2.1.3	NMR study of (E/Z)-3,5-difluoro-4'-nitrostilbene	165
7.2.2	<i>Synthesis of 4'-amino derivatives</i>	168
7.2.2.1	IR study of (E/Z)-3,5-difluoro-4'-aminostilbene	173
7.2.2.2	NMR study of (E/Z)-3,5-difluoro-4'-aminostilbene	174
7.2.3	<i>Basic resveratrol structure investigation</i>	182
7.2.4	<i>Synthesis of 4-aminobutan-1-ol derivative</i>	184
7.3	Synthesis of 4'-fluoro resveratrol analogues	189
7.3.1	<i>Synthesis of 3,5-dinitro-4'-fluoro stilbene</i>	189
7.3.1.1	IR study of (E/Z)-3,5-dinitro-4'-fluorostilbene	190
7.3.1.2	<sup>1</sup> H NMR study of (E/Z)-3,5-dinitro-4'-fluorostilbene	191
7.3.2	<i>Synthesis of 3,5-diamino derivatives</i>	196
7.3.2.1	IR NMR study of (E)-3,5-diamino derivatives	199
7.3.2.2	<sup>1</sup> H NMR study of (E)-3,5-diamino derivatives	201
7.4	References	210
<b>8.0</b>	<b>Biological activity of novel resveratrol analogues</b>	
8.1	Introduction	211
8.2	Lung cell carcinoma assays	214
8.3	Biological results	215
8.4	References	225
<b>9.0</b>	<b>Conclusion</b>	226
<b>10.0</b>	<b>Experimental</b>	228
	<b>Appendix I - List of abbreviations</b>	254

## Thesis Introduction

This thesis reports the synthesis, structural characterisation and biological activity of potential chemotherapeutic agents. Chemotherapy can be described as the treatment of disease using chemical agents or drugs that are selectively toxic to the causative agent of the disease, such as a virus, bacterium, or other microorganism. Chemotherapeutic agent is a generic term or description for any potential drug that displays biological activity against one or more bioorganisms. This thesis is divided into two separate sections, based on the disease targeted for inhibition and prevention. A common trait in this thesis is the inclusion of the fluorine atom in compounds synthesised. Fluorine has been shown to have many beneficial effects in medicinal chemistry and in today's world is an important factor in the preparation of many biologically potent compounds.

The initial section of this thesis concentrates on the preparation of potential inhibitors of an essential enzyme of the liver fluke parasite. By inhibiting this cysteine protease, cathepsin L, it is hoped to procure an increase in potency compared to what is currently available in the market place today. In recent years in Dublin City University, biologists have isolated the cathepsin L protease from this parasite and as a result studies have targeted this as a potential method of inhibiting this disease. From literature and past research experience in DCU, continued improvement of candidates for inhibition has led to the optimisation of a dipeptide structure. Modification of compounds has shown that the leucine glycine nitrile dipeptidyl scaffold as the most efficient for inhibition. As a result, a series of compounds with fluorobenzoyl *N*-terminal derivatives and a variety of substituted *N*-terminus dipeptides were prepared and evaluated for inhibitory potential.

The second section of this thesis involves the preparation of novel compounds with anti-cancer activity. Fluorinated derivatives of the stilbene resveratrol were synthesised. The triphenolic stilbene, resveratrol is a phytoalexin, *i.e.* produced in plant species in response to stress. Resveratrol has been shown to have a vast array of biological properties, ranging from anti-cancer activity to oestrogenic activity to inhibition of platelet aggregation. By maintaining the basic substitution pattern, fluorinated analogues were prepared containing hydroxyl bioisosteres, amines. Further to this, derivatives were synthesised containing substituted amines and also potential prodrugs amino acid substituted stilbenes were prepared.

# **Section 1**

## ***Protease Inhibitors***

# 1.0 Proteases and their inhibition

## 1.1 Introduction

Amino acids are essential basic building blocks of proteins. They are naturally occurring organic acids with an amine at one terminus and a carboxylic acid group at the other. These combine to form peptides which furthermore combine to form much larger macromolecules known as proteins.

A proteinase or protease is a catalyst for peptide bond cleavage. Proteolytic cleavage of peptide bonds is one of the most frequent and therefore one of the most important processes of enzymatic modification of proteins. Proteases can only catalyse the hydrolysis of a peptide bond. Despite this, their diversity of function has made them one of the most interesting and widely studied groups of enzymes. Regulation of physiological processes including differentiation, fertilization and growth is as a result of their control over protein synthesis. Various treatments of serious medical conditions such as cancer and HIV have resulted from the inhibition of such proteases<sup>1,2</sup>.

Investigations into inhibition, specificity, determination of amino acid sequence, kinetics and physical properties have led to the identification of their active sites. As a result of this determination of the mechanisms of action is also possible. Proteases can be classed into certain families or groups, dependent on similarity of structure and comparable mechanisms of action and active sites. They are split into four mechanistic classes, and within these classes, six families of proteases are present. Peptidases are members of the peptidase family. Proteolytic enzymes can be split into two categories; enzymes that require the presence of an unsubstituted *N*- or *C*-terminus in the substrate, these are known as exopeptidases whilst enzymes that do not have such a requirement are called endopeptidases. Exopeptidases can be further divided as follows:

- Aminopeptidases
- Dipeptidases

- Peptidyl-peptidases
- Dipeptidyl-peptidases
- Tripeptidyl-peptidases
- Carboxypeptidases
- Omega peptidases

Exopeptidases remove a single amino acid, dipeptide or tripeptide from one terminus, actions which are the basis for their definition. However, the secondary and tertiary structure formations of protein substrates usually foil attack by exopeptidases.

On the other hand, endopeptidases are categorised on their active sites and not on their mode of action. The action of the endopeptidase is generally not favoured by the presence of a free *N*- or *C*-terminus close to the scissile bond. The scissile bond is the bond to be cleaved. This category is subdivided into four main groups, as recognised by the International Union of Biochemistry, as follows<sup>3</sup>:

- Serine Proteases
- Cysteine Proteases
- Aspartic Proteases
- Metalloproteases

Serine peptidases react with organophosphate compounds in such a way that by acylating a single serine residue, they catalyse their own death at the active site, essentially an irreversible step. Essential to the catalytic mechanism of the cysteine peptidase is the thiol group of the individual cysteine moiety. This group is subject to oxidation and can react with a variety of reagents such as heavy metals, *e.g.* mercury (Hg). The aspartic peptidases are recognised by their highly acidic pH optima. The metallopeptidases are identified by their susceptibility to inhibition by chelating agents such as ethylenediamine tetraacetic acid (EDTA) **4**.

In terms of endopeptidases, it was clear from kinetic studies that the binding of substrates (and inhibitors) involved interaction at a number of active sites<sup>4</sup>. The nomenclature to describe this interaction is shown in **Figure 1.1**.

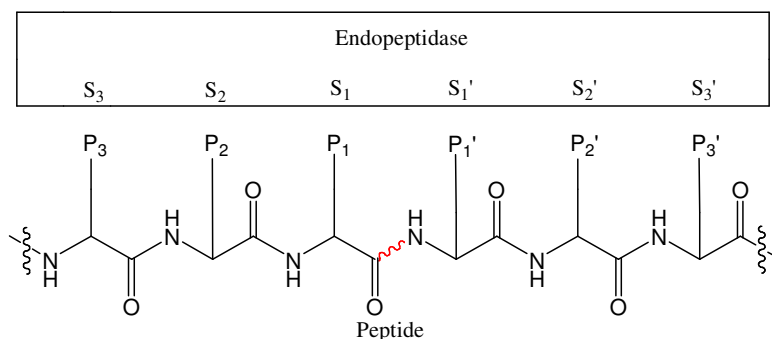


**Figure 1.1:** Subsite interactions between peptide substrate and endopeptidase active site

The amino acids of the polypeptide chain bind with the subsites in the endopeptidase active site. The subsite of the enzyme in the diagram is referred to as 'S' and the substrate amino acids 'P'. The amino acid adjacent to the scissile site (~~~~) on the *N*-terminus are labelled P<sub>1</sub>, P<sub>2</sub>, P<sub>3</sub> etc and on the *C*-terminus P<sub>1</sub>', P<sub>2</sub>', P<sub>3</sub>' etc, with the P<sub>1</sub>/P<sub>1</sub>' being closest to the cleavage site. The complementary sites on the endopeptidase are labelled S<sub>1</sub>, S<sub>1</sub>', S<sub>2</sub> etc. The specificity of different proteases is due to differing amino acid residue substitution in the primary substrate binding site P<sub>1</sub>/P<sub>1</sub>' and minor difference in the secondary binding sites (P<sub>2</sub>-P<sub>8</sub>/P<sub>2</sub>'-P<sub>8</sub>'). An example is the serine protease  $\alpha$ -chymotrypsin which prefers an aromatic side chain on the substrate at P<sub>1</sub>'. The reason for this preference is because the bulky aromatic side chain can fit tightly into a slit-like hydrophobic pocket near the active site<sup>5</sup>.

## 1.2 Protease Mechanism

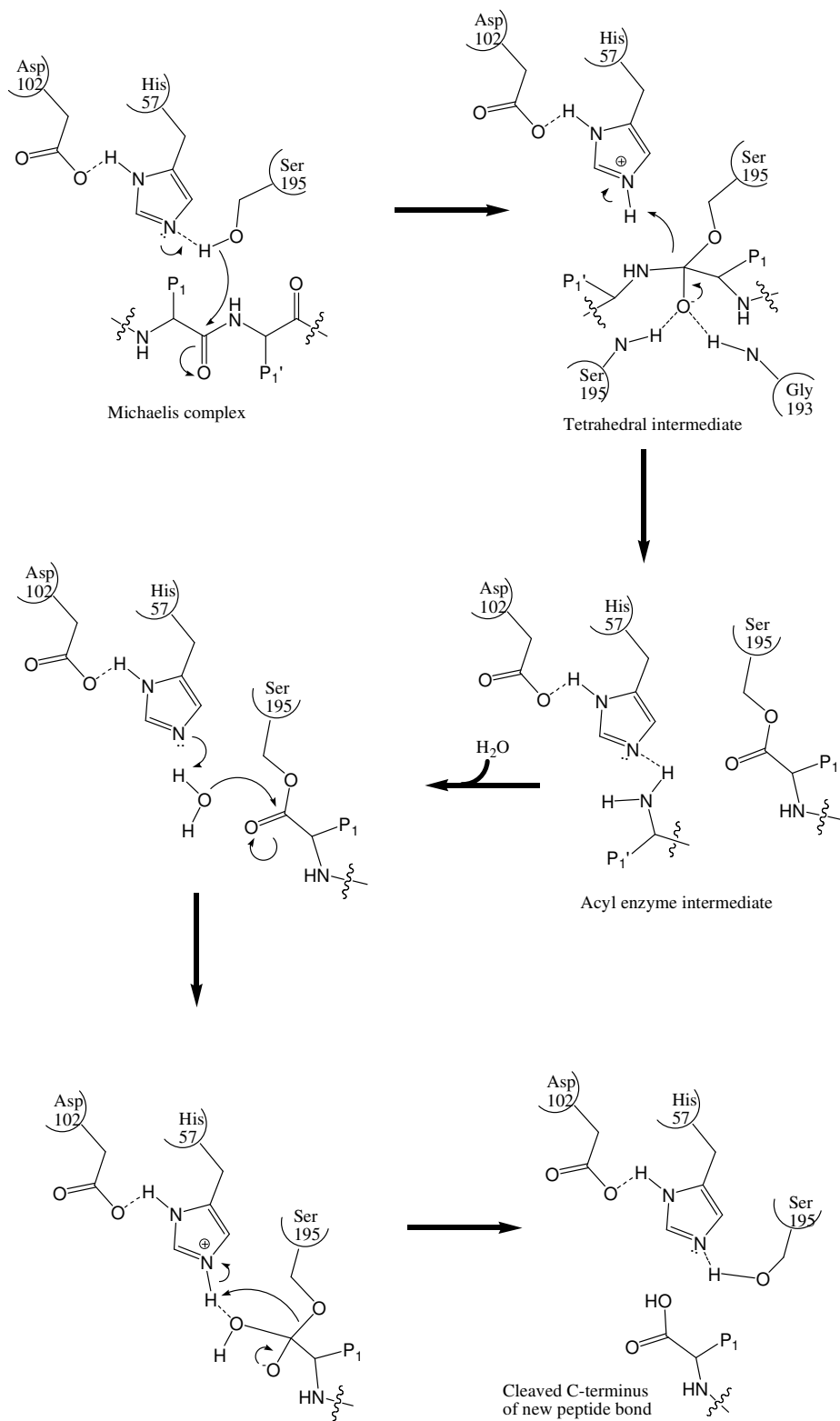
As previously mentioned, there are four classes of proteolytic enzyme each with independent mechanisms. These four classes can be subdivided further into two major mechanistic groups, which is of profound consequence since the strategy for inhibition is totally different for these two classes.

The two enzymes of the first mechanistic class, namely serine and cysteine proteases, form covalent enzyme complexes, and at the catalytic site have strongly nucleophilic amino acids. The second mechanistic group consists of aspartic and metalloproteases and do not form covalent enzyme complexes. These proteases catalyse the hydrolysis

of peptide bonds without nucleophilic attack by a functional group of the enzyme. They rely more on the acid/base catalysis of the attack of a water molecule and as a result the residues are lacking the aggressive nucleophilicity of the serine and cysteine peptidases.

The serine peptidases are the most extensively studied of all classes of proteases, possibly the most studied in all of enzymology. The important components of the mechanism of the serine peptidase enzymatic family are shown in *Scheme 1.1*. The key feature of this formation is the esterification reaction between the oxygen of serine 195 (chymotrypsin numbering system) and the acyl portion of the substrate, with the loss of the amino portion as the initial product, or P<sub>1</sub>. The ester formed will be the same for a series of substrates, which differ in their leaving groups. The other factor of importance in the serine protease mechanism is the presence of two backbone -NH- groups that are available for hydrogen bonding with the oxygen anion of the peptide substrate involved<sup>6</sup>. The mode of action of the serine proteases involves the binding of the substrate in the active site to form a Michaelis complex. This is shown in *Scheme 1.1*.

The active site serine hydroxyl, activated by the imidazole side chain of His<sup>57</sup>, nucleophilically attacks the carbonyl group of the scissile amide bond. The resulting tetrahedral intermediate then forms the oxyanion hole, stabilized by hydrogen bonding to the N-H backbone of Ser<sup>195</sup> and Gly<sup>193</sup>. Proton transfer from the His<sup>57</sup> residue to the amine of the tetrahedral intermediate eliminates the C-terminal fragment as a leaving group. The covalent acyl-enzyme complex is attacked by a water molecule activated by the imidazole side chain of His<sup>57</sup>, with formation of a new tetrahedral intermediate. This intermediate subsequently breaks down via acid catalysis to form the carboxy fragment of the cleaved substrate and regeneration of the Ser<sup>195</sup> residue of the active site.



**Scheme 1.1:** The mechanism of the serine peptidase enzymatic family.



Cysteine peptidases have a mode of action comparable to that of the serine peptidases, in that a covalent intermediate is formed<sup>7-9</sup>. In this mechanism, the nucleophile responsible for the attack is thought to be the sulphur atom of the cysteine residue. As in the serine protease mechanism, a histidine side chain is believed to be involved in the hydrogen binding to the oxygen anion formed from the attack of the sulphur based nucleophile. Full catalytic activity is still up for debate, regarding the involvement of the catalytic pair of Cys<sup>25</sup> and His<sup>159</sup> as being sufficient<sup>10</sup>.

The aspartic protease class of enzymes are believed to catalyse the cleavage of peptide bonds without the use of nucleophilic attack by a functional group of the enzyme<sup>11</sup>. Hence, there is no covalent or tetrahedral intermediate formed in the mechanism, between the enzyme and the substrate. The catalysis involves two aspartic acid side chains. Nucleophilic attack does not take place, as a carboxyl group is not known as an efficient nucleophile. However, the belief is that the carboxyl groups are involved in the catalysis, due to the low pH optimum of this group of enzymes.

Like aspartic peptidases, metalloproteases do not form covalent intermediates. The metalloproteases utilize coordination to a metal ion to exert the catalytic effect on the carbonyl group of the bond undergoing cleavage, rather than relying on the hydrogen bonding via an 'oxyanion hole'<sup>12</sup>. Zinc is the most common metal, but other transition metals can substitute. To assist in attack by a water molecule, the metal ion exerts a strong electrophilic 'pull'.

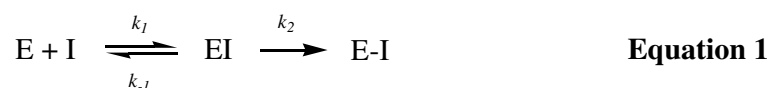
### 1.3 Protease Inhibitors

Protease inhibitors are compounds that have an adverse effect on the measured rate of hydrolysis of a given substrate. Whether discovering or characterizing protease inhibitors for therapeutic purposes or as functional tools, the kinetics of the reaction are important to the degree of inhibition achieved. The kinetics determine how effective the reaction in question will be. If suppression of the activity of a specific proteinase is required, knowledge of the kinetics allows for further information such

as amounts required and time needed for complete suppression. Most protease inhibitors can be defined as ‘active-site-directed’, *i.e.* formation of a tight and stable complex via combination with catalytic and substrate-binding sites of the protease<sup>13</sup>. Whether it is a natural or a synthetic inhibitor, they all mimic substrates. Protease inhibitors compete with substrates and many are extremely tight-binding. In fact, many proteinase inhibitors form irreversible complexes with proteinases. Irreversible or tight-binding inhibitors decrease the number of active sites available for the substrate<sup>3</sup>.

## 1.4 Inhibition kinetics

Describing the bimolecular reaction between protease (E) and inhibitor (I) which results in a stable complex (E-I) formation via an intermediate comparable to substrate binding (EI), the key equation for protease inhibition is:



The rates of the reactions are described by the rate constants,  $k_1$ ,  $k_{-1}$  and  $k_2$ . **Equation 1** describes an irreversible reaction. Irreversible inhibitors form covalent bonds with the enzyme, and often, on denaturation of the enzyme these bonds remain. The three rate constants mentioned for **equation 1**, are the parameters that govern the general reaction between a protease and an irreversible inhibitor. The apparent rate of inhibition (or association) known as  $k_{ass}$  is the most important quantity in this type of inhibition. For inhibitors following this mechanism,  $k_{ass}$  is defined as follows:

$$k_{ass} = k_1 \cdot k_2 / k_{-1} \quad \text{Equation 2}$$

For practical purposes  $k_{ass}$  is a sufficient value to describe the rate of reaction of irreversible inhibitors.

When an inhibitor binds to an enzyme by means of van der Waals, electrostatic, hydrogen bonding and hydrophobic forces, it is known as reversible inhibition.

Reversible inhibition can be divided into competitive and non-competitive inhibition. A reversible competitive inhibitor typically has close structural similarities to the normal substrate for the enzyme, thus it competes with the substrate to bind to the active site. The competitive inhibitor binds reversibly to the active site. A non-competitive inhibitor binds reversibly at a site other than the active site and causes a change in the overall three-dimensional shape of the enzyme that leads to a decrease in catalytic activity.



Characterising reversible inhibition, equilibrium is formed between the complexed form and free enzyme. The equilibrium constant for the reaction  $K_i$ , is given by:

$$K_i = \frac{[E][I]}{[EI]} = k_{-1}/k_1 \quad \text{Equation 4}$$

The estimation of the efficiency of an inhibitor is the practical side of the usage of kinetic constants. For a particular enzyme/inhibitor reaction,  $K_i$  and  $k_{ass}$  remain constant. Calculation of the  $IC_{50}$  or  $t_{1/2}$  can be made using these constants. The  $IC_{50}$  is the concentration of inhibitor required for a 50% reduction in enzyme activity. This value is dependent on substrate concentration and the Michaelis-Menten constant ( $k_m$ ) and is given by **Equation 5**. The  $IC_{50}$  value is one of the most common methods of comparing protease inhibitors.

$$IC_{50} = K_i(1+[S]/k_m) \quad \text{Equation 5}$$

Throughout this thesis, compounds will be shown and discussed in the context of their biological effects. However, depending on a number of factors, these results may be represented by either their  $IC_{50}$  or  $K_i$  value. The  $IC_{50}$  value represents the concentration of a drug that is required for 50% growth inhibition *in vitro*, while as mentioned above, the  $K_i$  value gives the equilibrium dissociation constant between enzyme and inhibitor, giving an idea of the efficiency of the inhibitor. In the case of compounds with potential for clinical use,  $IC_{50}$  values have been obtained and are stated. Where literature shows no data about the effects on cell growth of these compounds, only  $K_i$  values are stated.

## 1.5 Types of Protease Inhibitors

The history of protease inhibitors is intimately interwoven with that of the proteases. Protease inhibitors are as diversified as proteases themselves. Protease inhibitors can be divided into two distinct groups, naturally occurring protein protease inhibitors and active site-specific, low molecular weight synthetic inhibitors.

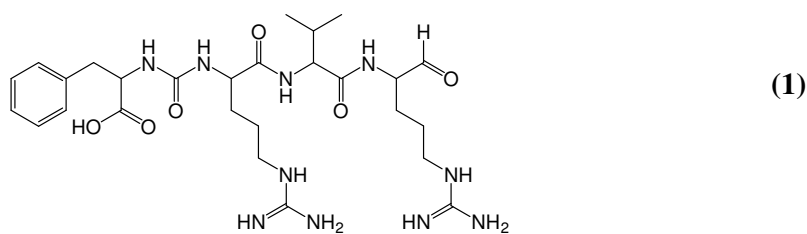
Hundreds of natural protein protease inhibitors have been isolated from plant, animal and bacterial organisms. Several natural crystalline inhibitors have been used as models to help explain the mechanism of protease inhibition. They combine irreversibly with the active site and are converted into a modified form in which a peptide bond, corresponding to the primary substrate specificity of the protease, is split. These inhibitors are usually large in nature but can vary in size from fifty residues (Bovine Pancreatic Trypsin Inhibitor) to over four hundred residues ( $\alpha$ -1-proteinase inhibitor)<sup>3</sup>.

Low molecular weight inhibitors can be either synthetic or of bacterial and fungal origin. They irreversibly modify an amino acid residue of the protease active site. The most efficient way of separating the different classes of these inhibitors is by their specificity, however, they are sometimes classified according to reaction mechanisms, origin or structural similarity. Generally low molecular weight inhibitors are classed according to the family of protease that they inhibit, although some are capable of inhibiting several enzyme classes.

### *1.5.1 Non-specific protease inhibitors*

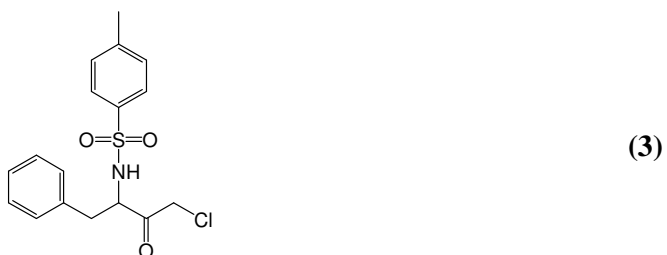
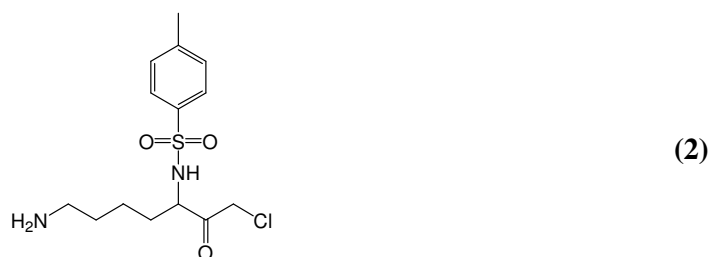
$\alpha$ -Macroglobulins are high molecular weight proteins that bind and inhibit most proteinases. These proteins are the only natural inhibitors that fail to discriminate among proteinase classes. Macroglobulins appear to physically entrap the reacting protease molecules, as a result of conformational changes following protease reaction<sup>14</sup>. For this reason they are mechanistically different from the active site directed protein inhibitors of proteases.

Peptide aldehydes (e.g. leupeptin, antipain **1**) are di-, tri- or tetrapeptides containing an aldehyde moiety in place of the usual carboxylate. Reversible inhibitors, they often are referred to as ‘transition-state analogues’ because they act by mimicking the tetrahedral intermediate formed during a peptide bond hydrolytic reaction. Antipain **1** is an example of a peptide aldehyde<sup>15</sup>, it has inhibitory capability against serine proteases (trypsin)<sup>3</sup> and cysteine proteases (calpain I)<sup>16</sup>. In an attempt to improve specificity, many peptide aldehyde derivatives have been synthesised<sup>17</sup>. In terms of being specific or selective inhibitors, there are two major failings of peptide aldehydes.



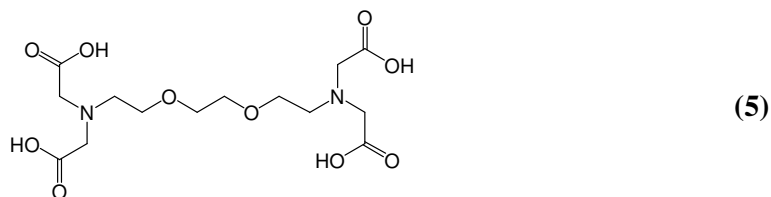
The first problem is that the lack of selectivity allows for inhibition of other proteases other than what is intended and the second drawback is the fact that in aqueous solution, most aldehydes exist mainly in the form of hydrates. Accordingly, the rate-limiting step for inhibition can be the formation of the aldehyde rather than the encounter with a suitable target enzyme<sup>18</sup>.

One of the first systematic approaches to the study of active site-directed proteinase-modifying reagents was with the irreversible inhibitors, peptide chloromethyl ketones<sup>19</sup>. Tosyl-lysine chloromethyl ketone **2** (TLCK) and tosylamido-2-phenylethylchloromethyl ketone **3** (TPCK) are the two most common members of this group of inhibitors.



From the mechanism of inactivation of serine proteases it is clear that inhibition results from the protease binding the inhibitor in a substrate-like manner, preceded by alkylation of the active site histidine by the chloromethyl moiety<sup>20</sup>. Although unproven, it is thought that chloromethyl ketones also inactivate cysteine proteinases in a similar mechanistic way.

The basis for the classification of the metalloproteinases is the presence of a metal ion (usually zinc), which participates in catalysis. This differentiates them from other proteases like calpains and some trypsin-like serine proteases, whose activities are stabilised by, but not necessarily dependent on, the presence of calcium. Chelating agents such as EDTA **4** and EGTA **5** can inactivate both the zinc-dependent metalloproteinase and some calcium-stabilised proteinases from other classes.



Inhibition by  $Zn^{2+}$  is due to the formation of zinc monohydroxide that bridges the catalytic zinc ion to a side chain in the active site of the enzyme<sup>21</sup>. This inhibition is therefore, competitive with the substrate. The non-competitive inhibition by the other heavy metal ions is attributed to binding of the ion to a site distinct from the active site<sup>22</sup>.

### 1.5.2 Class-Specific Inhibitors

Substrate specificity with particular emphasis placed on the nature of the residue present at  $P_1$ , is used to classify serine protease inhibitors. The most common types of inhibitors are trypsin-like, elastase-like, and chymotrypsin-like. The trypsin-like inhibitors prefer positively charged residues such as lysine and arginine at  $P_1$ , the elastase-like favour small hydrophobic residues like alanine and valine, while the chymotrypsin-like inhibitors prefer hydrophobic residues such as phenylalanine and leucine at  $P_1$ . The interactions with inhibitors, of various serine proteases such as trypsin,  $\alpha$ -chymotrypsin, thrombin etc., are available online and are demonstrated by X-ray crystal structural data (Protein Data Bank: <http://www.rcsb.org/pdb>). In order for an inhibitor to have the capability to inhibit only one protease in a mixture, maximum selectivity is the main target in inhibitor design and synthesis. Such inhibitors should have an inhibition rate constant ( $k_{ass}$ ) for that particular protease of one thousand fold less than for any other protease in the mixture.

### 1.5.2.1 Serine protease inhibitors

#### *Thrombin protease inhibition*

Thrombin is a trypsin-like serine protease, which plays a key role in blood coagulation and hemostasis<sup>23</sup>. In recent years this enzyme has become a highly investigated drug design target with potential use as antithrombotic drugs<sup>24,25</sup>.

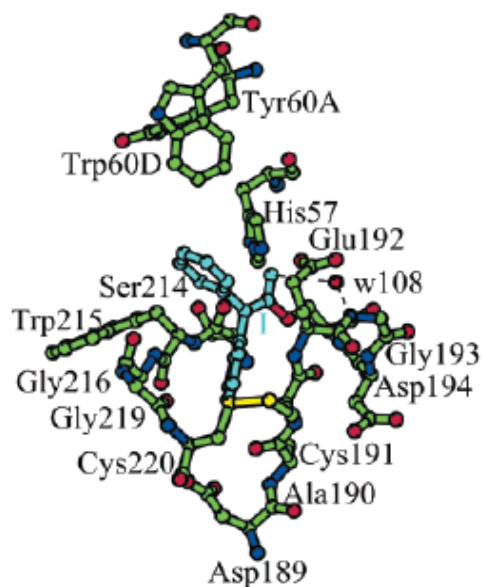
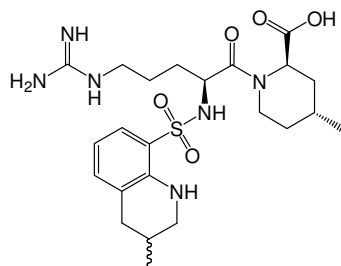


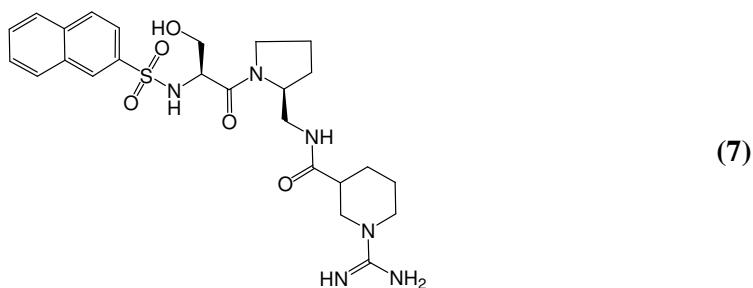
**Figure 1.2:** Stereoview of the active site region in the thrombin-*N,N*-diphenylcarbamoyl complex, showing the residues participating in recognition of the acylating *N,N*-diphenylcarbamoyl molecule (labelled I)<sup>23</sup>.

Thrombin is formed through the cleavage of prothrombin by the serine protease factor Xa (Fxa). It is responsible for many aspects in the blood coagulation cascade and cleaves numerous substrates such as blood factors V, VIII, XIII and fibrinogen, and is also responsible for activating the platelet thrombin receptor<sup>26</sup>. Thrombin converts fibrinogen to an active form that assembles into fibrin, which when polymerised



(6)





makes up the core of a blood clot. Thrombin therefore results in blood clotting, which in turn, prevents us from bleeding to death; but an excess of this protease can lead to internal clotting resulting in undesired thrombosis, often leading to death by stroke. The substrate pocket  $S_1$  of the thrombin protease is optimised for arginine side chain recognition. Argatroban **6** is a small synthetic molecule containing the arginine moiety<sup>27</sup> and inhibits platelet aggregation by clot-associated thrombin<sup>28</sup>. It is a mixture of 21-(*R*) and 21-(*S*) diastereomers with the latter being twice as potent in an *in vitro* assay but also less soluble in aqueous buffer<sup>29</sup>. In the mid 1990's, Bristol-Myers Squibb developed a potent thrombin inhibitor known as BMS-189090 **7**<sup>30</sup>. The ability of this compound to inhibit the thrombin hydrolysis of the chromogenic substrate S-2238 was tested and an  $IC_{50}$  value of 18  $\mu$ M reported. Because of its potency and selectivity, BMS-189090 was subjected to further evaluations *in vitro* and *in vivo*. The *in vivo* potency of BMS-189090 ( $ID_{50}$  = 0.11 mpk, iv; 29 mpk po) was significantly superior to that of Argatroban ( $ID_{50}$  = 1.6 mpk, iv; >100 mpk, po). BMS-189090 competitively and reversibly inhibited thrombin *in vitro* ( $K_i$  =  $3.44 \pm 0.05$  nM) without showing time dependent kinetics<sup>31</sup>. The binding of the thrombin protease with inhibitor **7** can be seen in the crystal structure shown in **Figure 1.3**. The three dimensional structure shows the bound conformation of the inhibitor, the active site residues and solvent molecules in the active site. From this crystal structure it can be seen that the binding of BMS-189090 and thrombin is in an antiparallel sequence. In the BMS-189090 complex, a water molecule fills the space left in the specificity pocket by the shortening of the arginine inhibitor side chain.

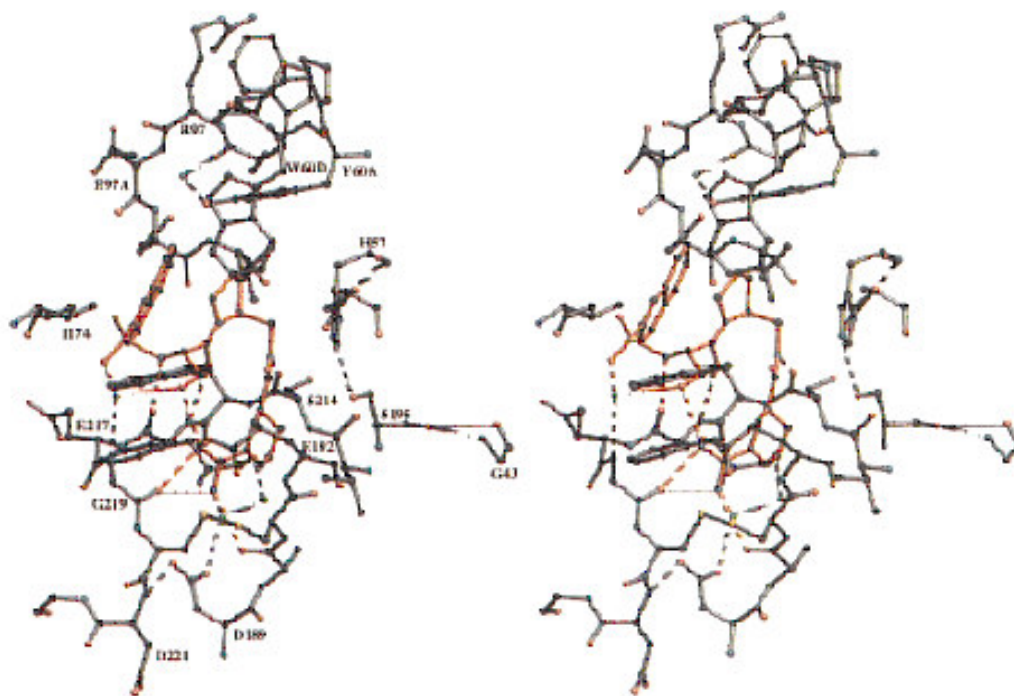
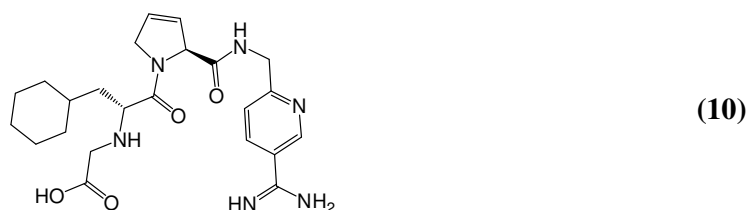
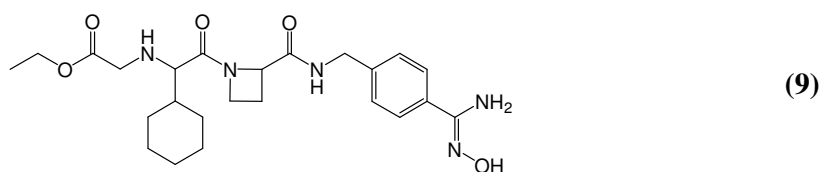
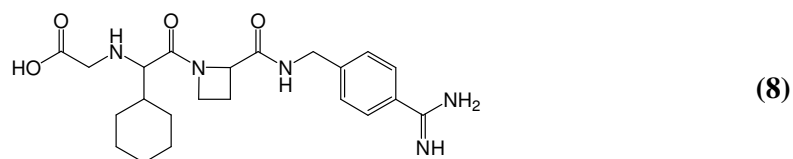


**Figure 1.3:** Three dimensional structure of  $\alpha$ -thrombin complexed with BMS-189090<sup>30</sup>.

From the crystal structure of the complex formed between compound **7** and human  $\alpha$ -thrombin, we can see that effective inhibitors form numerous close contacts (both hydrogen bonded and hydrophobic) with the protein.

Over the last few decades, antithrombotic activity via oral administration was the ultimate goal in developing potent inhibitors. This property was concentrated on in conjunction with selectivity over other serine proteases, appropriate half-life, and an improved side effect profile relative to warfarin. Melagatran **8** and its prodrug Ximelagatran **9** are the most advanced thrombin inhibitors and have recently been launched in a number of European countries for the prevention of venous thromboembolic events in elective hip or knee replacement surgery<sup>32,33</sup>.



Recent research into potent orally active thrombin inhibitors is concentrated on derivatives based on the D-Phe-Pro-Arg lead structure. One of the most active of these derivatives published to date is compound **10**<sup>34</sup>. The schematic representation and X-ray structure of inhibitor **10** shows binding to the active site of thrombin and can be seen in **Figure 1.4**. The cyclohexyl ring of the inhibitor is engaged in hydrophobic interactions in the lipophilic D pocket. The side chains of Ile<sup>174</sup>, Leu<sup>99</sup> and Trp<sup>215</sup> come in close contact with the cyclohexyl moiety of D-cyclohexylalanine. The pyrrolidine ring occupies the P pocket with contacts to Tyr<sup>60A</sup>, His<sup>57</sup> and Trp<sup>60D</sup>. The amidine group at the pyridyl ring of the inhibitor forms strong hydrogen bonds with the carboxylic group of Asp<sup>189</sup> at the bottom of the S pocket in thrombin.

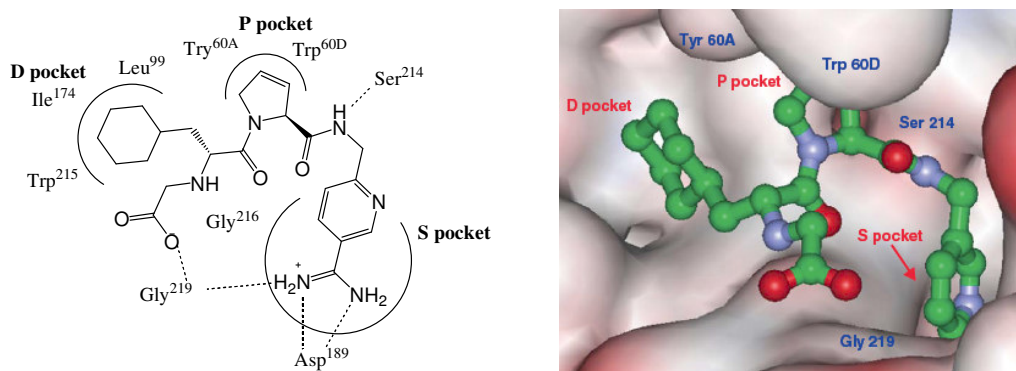
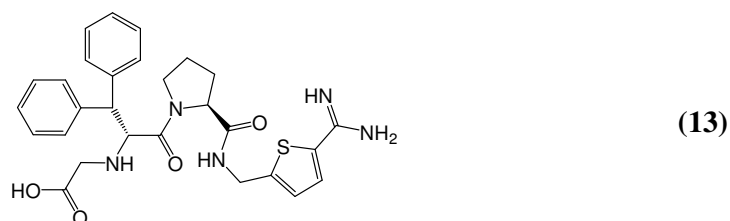
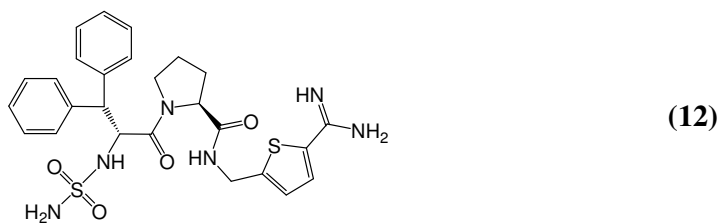
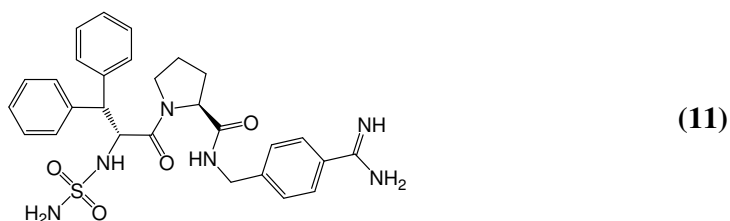


**Figure 1.4:** Schematic representation and X-ray structure of compound **10** bound to the active site of thrombin<sup>34</sup>.

The *in vitro* IC<sub>50</sub> value of inhibitor **10** was determined in a chromogenic substrate assay with S-2238 as substrate, against thrombin. The authors responsible for this research, in consecutive publications, have reported two differing IC<sub>50</sub> values, 1.00 nM and 1.80 nM, for the hydrochloride salt and for the corresponding acetate respectively<sup>34, 35</sup>.

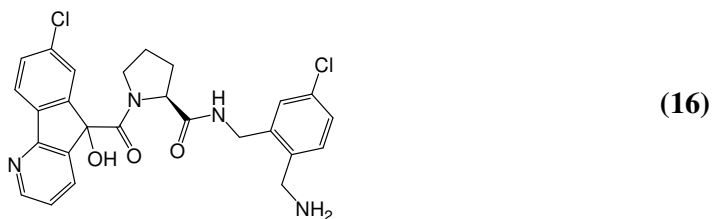
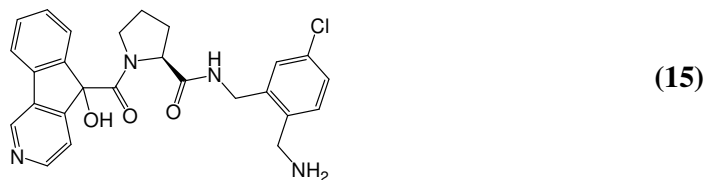
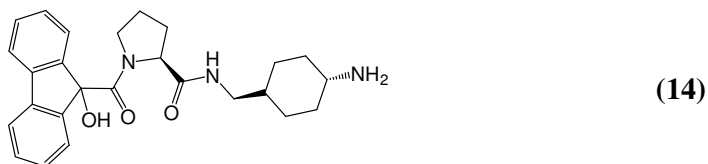
Lee *et al* have developed a highly potent orally active diphenylalanine derivative **12** ( $K_i = 0.004$  nM)<sup>36</sup>. This compound was synthesised based on the optimisation of known thrombin inhibitor **11**<sup>37</sup>. Although the initial inhibitor **11** showed a better  $K_i$  value of 0.003 nM *in vitro*, clinical trials revealed a short duration of action and bioavailability. The optimised inhibitor **12**, when tested showed slightly less potent inhibition than its predecessor, however the bioavailability was superior. Lee *et al* also synthesized inhibitor **13**, and this *N*-carboxymethyl derivative has a  $K_i$  value of 0.015 nM. Despite the five-fold higher  $K_i$  potency, the anticoagulant efficacy of **13** compares favourably to that of inhibitor **11**.



The *N*-carboxymethyl derivative **13**, demonstrated the best overall profile, which is potent, selective, metabolically stable and orally bioavailable. This inhibitor also displayed excellent anticoagulant and antithrombotic activity in venous thrombosis

models of rat and rabbit. In the last couple of years inhibitor **13** has undergone further preclinical and clinical development<sup>36</sup>.

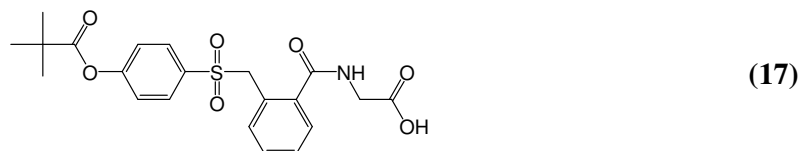
Based on a previously reported thrombin inhibitor **14**<sup>38</sup> ( $K_i = 1.5\text{nM}$ ), Stauffer *et al* optimised a series of potent thrombin inhibitors. Inhibitor **15**, with a  $K_i$  value of 0.4 nM showed a good improvement in potency. It also displayed good stability in human liver microsomal preparations, a long half-life, excellent pharmacokinetic properties in dogs and rhesus monkeys and a significant free fraction in human plasma protein binding experiments. Addition of a chlorine atom at the 7-position of the 4-azafluorenyl ring proved to produce an even more potent inhibitor **16**. It displayed the greatest absolute potency for trypsin in the series, with a  $K_i$  value of 0.042 nM. This is 38-fold more potent than the lead structure **14**. Despite this high potency, compound **16** did not maintain this improvement over **15** in the stability assays mentioned above<sup>39</sup>.



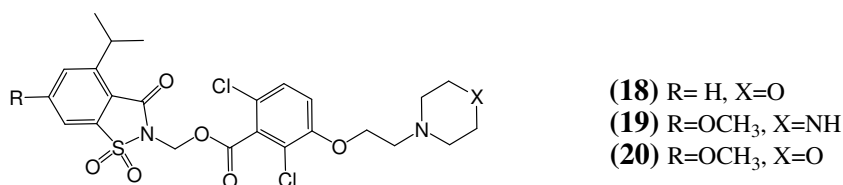
Taking into consideration all of the key preclinical properties of inhibitor **15**, it represents an inhibitor with considerable potential for development as an oral antithrombotic agent. These examples are useful to demonstrate that although an inhibitor can have a very high potency, it may not be the most suitable as chemotherapeutic agent.

### Elastase protease inhibition

Elastase is a serine protease that has been implicated as a primary mediator of various diseases such as adult respiratory distress syndrome (ARDS), cystic fibrosis, pulmonary emphysema, smoking related chronic bronchitis, rheumatoid arthritis and other inflammatory airway diseases<sup>40,41</sup>. Neutrophil elastase has plays a major role in the pathogenesis of acute lung injury<sup>42,43</sup>. Elastase released from activated neutrophils damages lung tissues, and causes epithelial injury<sup>44</sup>, vascular hyperpermeability<sup>45</sup> and airway hyperresponsiveness<sup>46</sup>. The inhibition of elastase has led to the development of numerous therapeutic agents. Ono Pharmaceuticals Co. Ltd. developed sivelestat **17**, a potent neutrophil elastase inhibitor. This compound has been shown to inhibit the early and late asthmatic responses in allergic sheep<sup>47</sup>. Sivelestat also improved the airway hyperresponsiveness caused by ozone exposure in guinea pigs<sup>48</sup>. Further studies have shown that with sivelestat treatment, airway hyperresponsiveness induced by epithelial injury or lipopolysaccharide (LPS), may be prevented by stopping elastase release<sup>49</sup>.



Emphysema is a condition resulting from destruction of the alveoli resulting from an imbalance in the lung between human leukocyte elastase (HLE) and endogenous inhibitor (elevated elastase or insufficient inhibitor). Hlasta *et al* have identified WIN 63294 **18** as a potent ( $K_i = 0.008$  nM) HLE inhibitor, however the bioavailability was poor compared to inhibitors **19** and **20**. These compounds are not as potent as **18** ( $K_i = 0.014$  &  $0.013$  nM respectively). WIN 64733 **19** and WIN 63759 **20** are selective, mechanism-based inhibitors of HLE which are also bioavailable<sup>40</sup>.

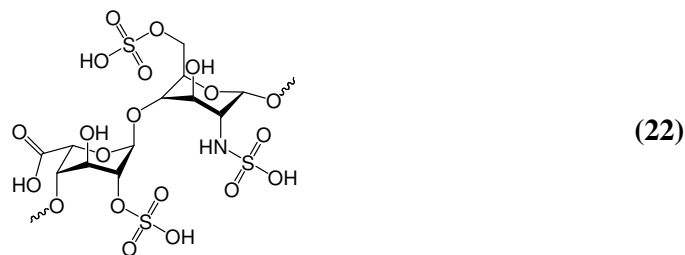


Chronic obstructive pulmonary disease (COPD) is a term referring to two lung diseases, chronic bronchitis and emphysema. A potent inhibitor used in the treatment

of COPD is the cyclic thiol inhibitor MR 889 **21**<sup>50</sup>. It is a slow binding, reversible inhibitor with specific activity towards neutrophil elastase ( $K_i = 1.38 \mu\text{M}$ ).

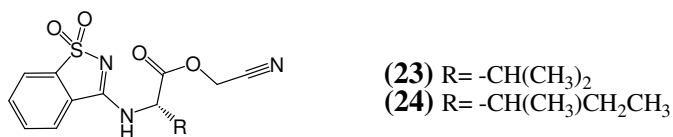


In the normal feedback mechanism of injury and repair in the lung, fragmented heparan sulphate proteoglycans (HSPGs) from damaged extracellular matrix and cells, are believed to interact with elastases to limit their activity. An imbalance in the HSPG-elastase response is thought to play a role in situations of uncontrolled lung injury, leading to diseases such as emphysema. The main option used for treating this imbalance is by supplementing the system with artificial elastase inhibitors. One inhibitor that circumvents some of these problems is heparin **22**, an anticoagulant drug that has been used for many years<sup>51</sup>. Native heparin is a polymer with a molecular weight ranging from 6 kDa to 40 kDa, although the average molecular weight of most commercial heparin preparations is in the range of 12 kDa to 15 kDa. As an inhibitor, heparin is extremely potent against human neutrophil elastases (HNEs), with studies confirming the activity of **22** and its derivatives, both *in vitro* and *in vivo*<sup>52</sup>. Activity is highly sensitive to specific properties of the heparin structure, including molecular mass, chain length, degree of sulphation charge density, specific rotation and iduronic acid content. Research has also shown that structural modification of heparin can remove the anticoagulant action, while retaining the inhibitory activity of **22**, which is a major advantage in clinical use<sup>53</sup>.



The ability of heparin and HSPGs to modulate proteolytic activity indicates that this ubiquitous class of complex polysaccharides plays a central role in regulating tissue injury. Current studies are investigating the full role of endogenous HSPGs in regulating elastase-mediated tissue injury<sup>51</sup>.

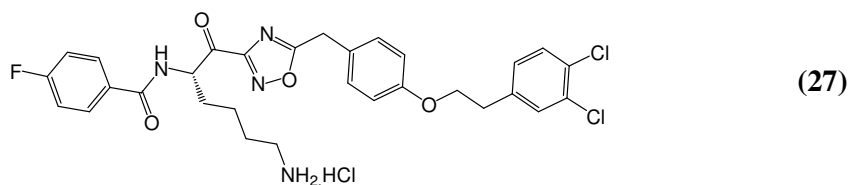
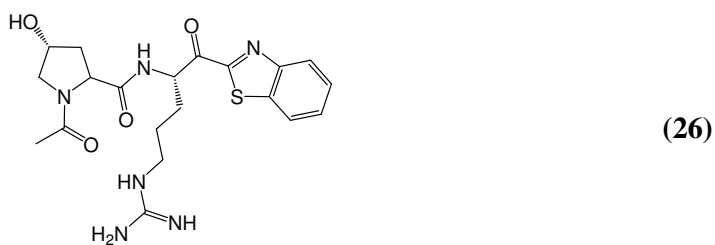
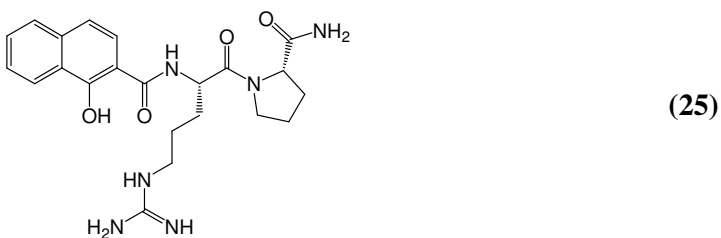
Otto *et al* synthesised potent pseudosaccharinamine derivatives that have shown good activity against human leukocyte elastase (HLE) and porcine pancreatic elastase (PPE)<sup>54</sup>. Compounds **23** and **24** showed the best activity, with  $K_i$  values for HLE of 1.3  $\mu$ M and 0.8  $\mu$ M, respectively. Inhibitor **23** showed 50% inhibition at 5  $\mu$ M concentration against HLE and 47% inhibition of PPE at 0.5 mM concentration. Inhibitor **24** showed 69% inhibition of HLE at 5  $\mu$ M concentration while a very weak inhibition of PPE (7% at 0.5 mM concentration) was observed. It is well reported that valine or alanine moieties (valine present in **23**) fit in the  $S_1$  pocket of HLE<sup>55</sup>. The presence of isoleucine at the  $P_1$  position of the inhibitor is also reported<sup>56</sup>.



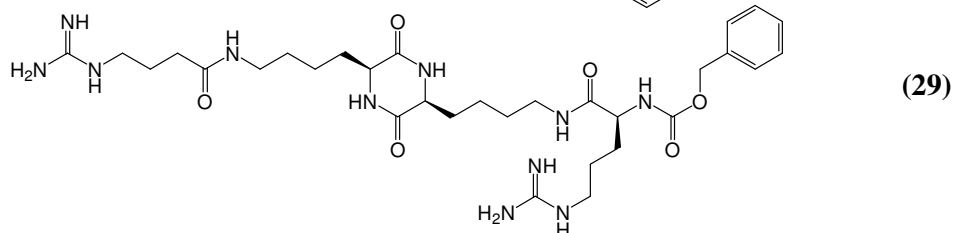
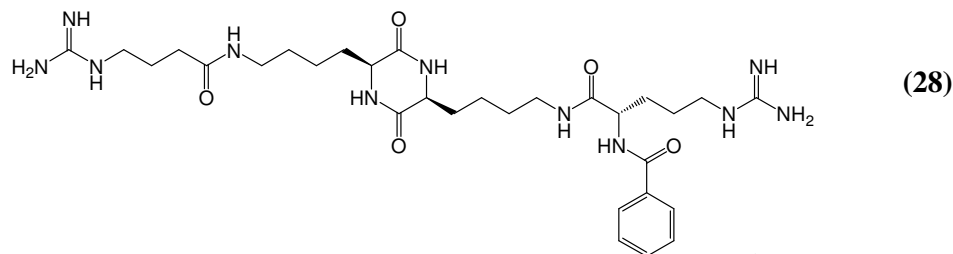
#### *Tryptase protease inhibitors*

Tryptase is a homotetrameric, trypsin-like serine protease that constitutes 20-25% of the total protein mast cells. Since it is stored in a catalytically active form within the secretory granules and released on stimulation, this enzyme is highly relevant to mast cell dependent inflammatory conditions. Indeed, tryptase has been directly implicated in the pathology of asthma<sup>57</sup>. Inhibitors of human mast cell tryptase have therapeutic potential for treating allergic or inflammatory disorders such as asthma, vascular injury (e.g. restenosis and atherosclerosis), inflammatory bowel disease and psoriasis<sup>58,59,60</sup>. Tryptase inhibitors are divided into four selective classes, of which three are synthetic and the fourth one is of natural origin<sup>59</sup>. The first class are called peptidic inhibitors and includes the Johnson & Johnson developed inhibitors APC-366 **25**, subsequently RWJ-56423 **26**<sup>57</sup>. Compound **25** has a  $K_i$  value of 330 nM and progressed to phase 2 clinical trials before being discontinued<sup>58,59</sup>. Resulting from this active inhibitor, Johnson & Johnson developed **26**, a potent, reversible inhibitor with a  $K_i$  value of 10 nM and it is currently undergoing clinical trials. Palmer *et al* synthesised another potent peptidic inhibitor **27**<sup>61</sup>. With a  $K_i$  value of 2.5 nM, this compound **27** is also undergoing preclinical trials at present.

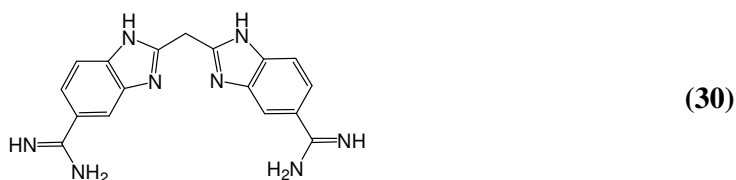




The second class of selective trypsin inhibitors is the dibasic inhibitors. This is the most studied group of trypsin inhibitors. Publication of a resolved crystal structure has revealed that the active enzyme consists of four identical subunits assembled with the four active sites pointing towards an oval central pore<sup>62</sup>. This array of the four negatively charged S<sub>1</sub> binding pockets represents an ideal basis for the rational design of divalent/dibasic inhibitors. Albericio *et al*<sup>63</sup> have developed two of these inhibitors, **28** and **29**, based on a 2,5-diketopiperazine scaffold. With  $K_i$  values of 2.4 and 2.2  $\mu\text{M}$  respectively, these two compounds represent highly potent dibasic trypsin inhibitors.



The third and last synthetic class of trypsin inhibitors are zinc-mediated inhibitors. The best known inhibitor of this type is bis(5-amidino-2-benzimidazolyl)methane (BABIM) **30**<sup>64</sup>. It has an inhibitor range of 10-25  $\mu\text{M}$ , and displays a high-affinity binding mode in which a  $\text{Zn}^{2+}$  ion is tetrahedrally coordinated between two chelating nitrogens of BABIM and two active site residues, His<sup>57</sup> and Ser<sup>195</sup>. The distinct  $\text{Zn}^{2+}$  coordination geometry implies a strong dependence of affinity on substituents<sup>65</sup>. This unique structural paradigm has enabled development of potent, highly selective,  $\text{Zn}^{2+}$  dependent inhibitors of several therapeutically important serine proteases, using a physiologically ubiquitous metal ion.



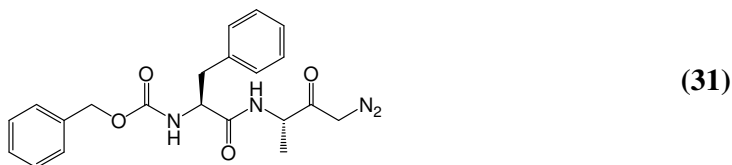
The final class of trypsin inhibitors are the compounds with natural origin and are known as heparin antagonists. An example of this type of inhibitor is lactoferrin<sup>63</sup>. This inhibitor is an iron transporting glycoprotein. It was originally isolated from bovine milk, where it is found as a minor protein component of whey proteins. Lactoferrin contains 703 amino acids and has a molecular weight of 80 kilodaltons. In addition to its presence in milk, it is also found in exocrine secretions of mammals and is released from neutrophil granules during inflammation.

### 1.5.2.2 Cysteine protease inhibitors

Cysteine proteases are generally classed into three structurally distinct groups, papain-like (e.g. cathepsins), ICE-like (interlukin-1 converting enzyme) or picorna-viral proteases. Cathepsins are the most common and therefore the most studied of the cysteine proteinases. At present, eleven human papain-like cysteine proteases have been described: the cathepsins A, B, C, F, K, L, O, S, V, W and X<sup>66</sup>. Cysteine proteases contain a thiol moiety that is involved in catalysis, much the same way as the hydroxy group of the serine protease is involved and this is the only real difference in the mechanism of amide hydrolysis of cysteine over serine proteinases. The biggest hurdle involved in the development of new cysteine proteases is the similarity in their substrate affinities and proteolytic mechanisms with serine proteases.

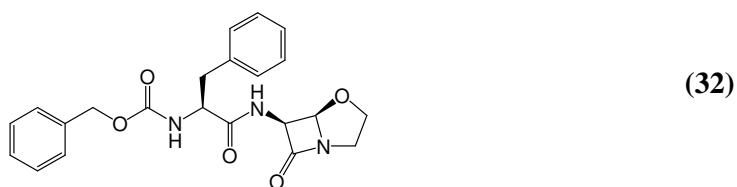
#### *Cathepsin protease inhibition*

In 1929, Willstätter and Bamann introduced the term cathepsins to describe a protease that is active at acidic pH but can be differentiated from pepsin<sup>10</sup>. Cathepsins A, B and C have been suggested as the intercellular counterparts of pepsin, trypsin and  $\alpha$ -chymotrypsin<sup>67</sup>. Cathepsins inhibitors are promising therapeutics for the treatment of diseases characterised by excessive bone loss such as osteoporosis and inflammatory and traumatic processes such as rheumatoid arthritis and cancer metastasis<sup>68</sup>.

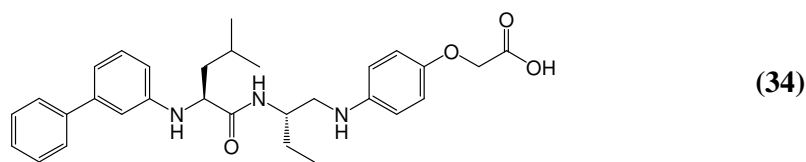
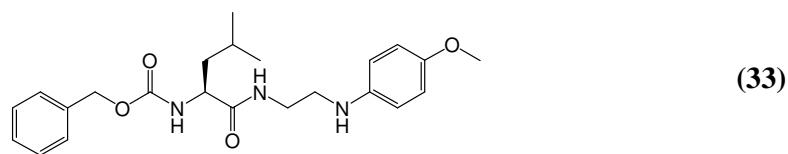


Among the earliest reported inhibitors were the peptidyl diazomethyl ketones and aldehydes. These are a group of peptidyl derivatives in which the hydroxyl of the terminal carboxylate is replaced with a diazomethyl moiety. Inhibition is irreversible and is thought to proceed, via a thiohemiketal intermediate, to the formation of an alkylated active-site cysteine existing as a thio-ether to the methyl group of the inhibitor. Diazomethyl ketones inactivate cathepsin B by alkylation of the active site cysteine residue. One of the most active inhibitors of this type is compound **31**. Reports have shown this inhibitor to be potent against cathepsin B and C<sup>69</sup>. This inhibitor is also the commercially available inhibitor of cathepsin L.

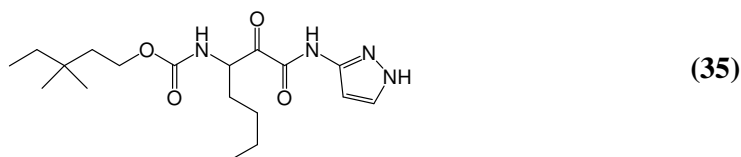
Singh *et al* have synthesised a series of potent cathepsin B protease inhibitors<sup>70</sup>. These 6-substituted amino-4-oxa-1-azabicyclo[3,2,0]heptan-7-one derivatives were synthesized on the basis of molecular modeling, with has suggested that the 1-N atom of the bicyclic side chain can be involved in hydrogen bonding to the protonated histidine in the active site of cysteine proteases, therefore acting as an effective inhibitor. Of the compounds reported by Singh *et al*, inhibitor **32** was the most potent against cathepsin B, with an  $IC_{50}$  value of 1.76  $\mu$ M. Unfortunately **32** was found to be potent against other cathepsins such as L, K and S, with nanomolar inhibition often occurring.



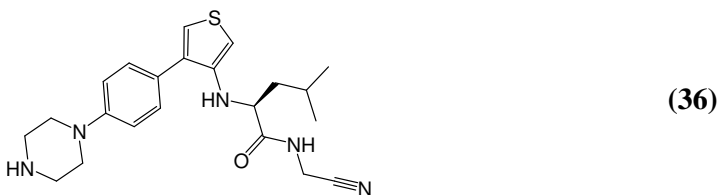
Cathepsin K is a cysteine protease that is highly expressed in osteoclasts, which are cells that break down bone and is responsible for bone resorption. The primary role of cathepsin K is the degradation of type I collagen, one of the main components of bone matrix. Bone mass is regulated by the continuous equilibrium between the bone resorbing and the bone forming processes. Thus, selective inhibition of cathepsin K provides efficient therapeutic treatment for bone diseases such as osteoporosis. The inhibitor **33** ( $IC_{50}$  = 6.4 nM) was developed by Novartis and has been shown to be a non-covalent binder and reversible<sup>71</sup>. This lead compound **33** has led to the synthesis of many new potent cathepsin inhibitors such as **34** ( $IC_{50}$  = 4.5 nM)<sup>72</sup>, which are undergoing preclinical and clinical studies.



GlaxoSmithKline have developed a series of potent ketoamide based inhibitors of cathepsin K<sup>73</sup>. Compound **35** is the most potent of this series with an IC<sub>50</sub> value of 1.6 nM, although it also is potent against cathepsin S (IC<sub>50</sub> = 2.56 nM). This lack of selectivity is a major disadvantage.

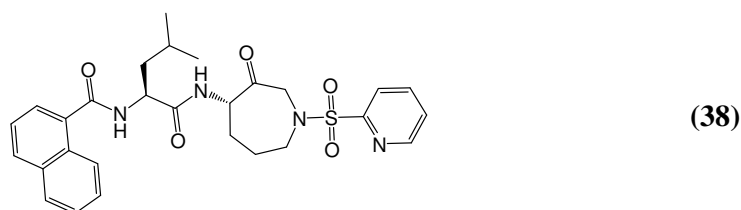
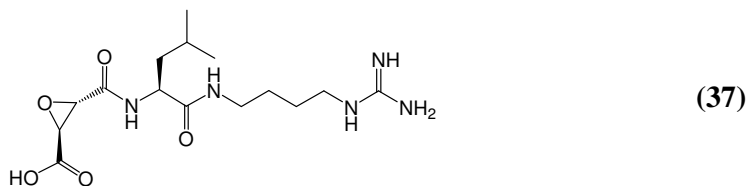


The peptidyl nitrile based compound **36** is another potent inhibitor and has been shown to reduce bone loss. The leucine glycine nitrile scaffold of the inhibitor has been a successful design feature of potent cysteine protease inhibitors. Inhibitor **36** has a reported IC<sub>50</sub> of 0.2 nM and at a concentration of 10 nM, has been shown to substantially reduce bone resorption.

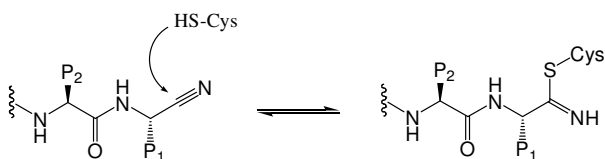


Human cathepsin L shows the highest proteolytic activity of all lysosomal proteases and is an ubiquitously expressed lysosomal cysteine endopeptidase. Cathepsin L has been implicated in a wide range of intra- and extracellular pathological and physiological processes including antigen presentation, ovulation, tumour metastasis<sup>74</sup>, progression, osteo and rheumatoid arthritis, as well as bone resorption<sup>75</sup>. *L-trans*-epoxysuccinyl-leucylamide-(4-guanido)-butane (E-64) **37** is a naturally occurring cysteine protease inhibitor with high potency against cathepsin B, F, K and L proteases<sup>76</sup>. E-64 offers a potential treatment for metastasis as the epoxide inhibitor **37** inhibits cathepsin L on a nanomolar scale (IC<sub>50</sub> = 0.9 nM). This was one of the early lead compounds for cathepsin L inhibition and remains to this day an important standard. Orally bioavailable azepanone-based inhibitors, which were initially designed to target cathepsin K<sup>77</sup>, but now provide a general template for the inhibition of cathepsin L. This is due to the similarities in the homologies of cathepsins K and L as well as reports that have suggested that cathepsin L may play a role in the

resorption phase of bone remodelling<sup>73</sup>. The azepanone **38** as reported by Marquis *et al*, has a  $K_i$  value of 0.43 nM and shows excellent selectivity towards cathepsin L over cathepsins K, S and B. Inhibitor **38** has a greater than 20,000-fold selectivity for cathepsin L over K ( $K_i = >10,000$  nM), a 36-fold selectivity over cathepsin S ( $K_i = 15.6$  nM) and a 340-fold selectivity over B ( $K_i = 150$  nM).



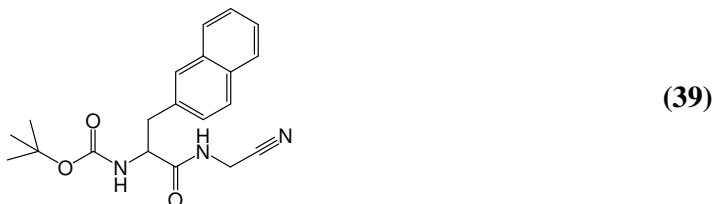
In recent years much emphasis has been directed at the synthesis of inhibitors with electrophilic sites able to interact with the active thiol, which has led to the investigation of peptidyl nitriles<sup>66</sup>. Peptide nitriles bind to the active site thiol via a reversible formation of a covalent thioimidate linkage as demonstrated in *Scheme 1.2*.



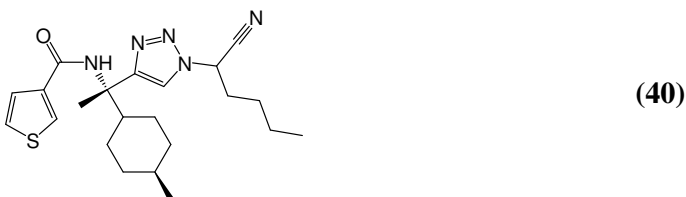
**Scheme 1.2:** Reversible formation of thioimidates from peptide nitriles and cysteine proteases.

Nitriles are class selective protease inhibitors, which strongly inhibit cysteine proteases while serine proteases are not or weakly affected. Gütschow *et al* have reported a structure-activity relationship study of dipeptide derived nitriles as inhibitors of cysteine proteases, namely cathepsins L, S and K<sup>66</sup>. Inhibitor **39** containing a bicyclic aromatic side chain was one of the most active compounds synthesised in this SAR study, showing good potency and selectivity against the three

cathepsins tested.  $K_i$  values of 0.12, 0.083 and 83  $\mu\text{M}$  were calculated for cathepsins L, S, and K, respectively.

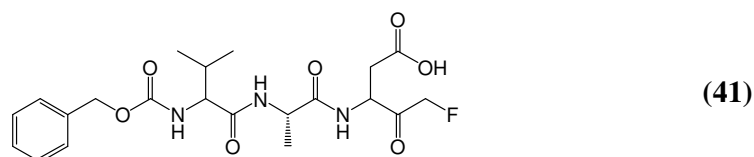


Using a substrate screening method, Ellman *et al* have synthesised a highly selective, nonpeptidic nitrile inhibitor of cathepsin S<sup>78</sup>. This 1,2,3-triazole inhibitor **40** is a potent ( $K_i = 15$  nM) and low molecular weight (413 Da) inhibitor of cathepsin S. This compound has shown to have greater than 1000-fold selectivity over all closely related human cathepsins, such as cathepsin B, K and L.



#### *Caspase protease inhibition*

Caspases are proteases that fit into the interleukin-1 converting enzyme-like group of cysteine proteases. Interleukin-1 converting enzyme is more commonly known as caspase-1, hence the group name ICE-like. Caspases are known to play major roles in the initiation and propagation of apoptotic signals<sup>79</sup> and neurodegenerative diseases such as Alzheimer's, Parkinson's and Huntington's disease<sup>80</sup>. Caspases cleave proteins after aspartic acid residues, hence their name being derived from cysteine-aspartate-specific proteases. To date, eleven caspases have been identified in humans, known as caspase-1, caspase-2 etc. The majority of early discovery programs targeting caspases centred on the development of reversible inhibitors of caspases-1<sup>81</sup>. One of the most commonly known and used inhibitors of ICE-like proteases was developed by Merck and is known as Z-VAD.FMK **41**<sup>82</sup>.



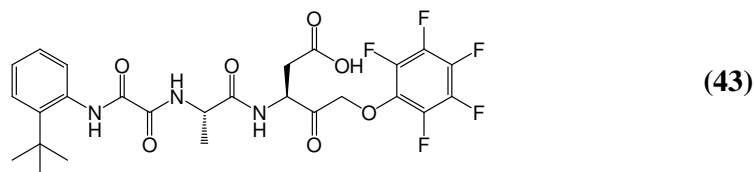
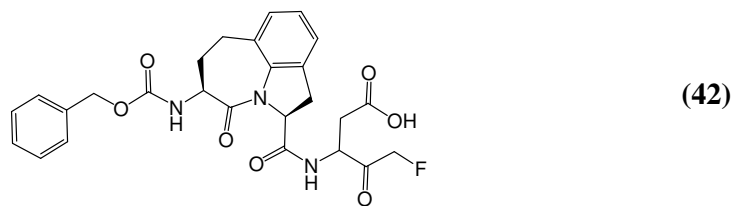
Carbobenzyloxy-valyl-alanyl-aspartyl-[o-methyl]-fluoromethyl ketone **41** is a broad-spectrum irreversible tripeptide inhibitor of caspases and is widely used for its apoptosis inhibition. **41** is also used for peripheral administration to treat cerebral ischemia in humans which is a condition that restricts the blood flow to the brain. Dissociation constants ( $K_i$ ) and first-order rate constants of irreversible caspase inactivation ( $k_3$ ) for inhibitors **41** and **42**, against mouse caspase 1 and human recombinant caspases 2, 3, 6, 8 and 9 are shown in *Table 1.1*.

	mCasp1	Casp2	Casp3	Casp6	Casp8	Casp9
<b>Z-VAD.FMK</b>						
$K_i$ (nM)	1.0	50	10	30	20	10
$k_3$ (1/min)	0.72	0.021	0.58	0.046	0.12	0.025
<b>IDN-5370</b>						
$K_i$ (nM)	10	180	820	590	10	2.1
$k_3$ (1/min)	0.13	0.028	0.54	0.1	0.05	0.032

**Table 1.1:** Profiles of caspases inhibition by the broad-spectrum irreversible caspases inhibitors **41** and **42**<sup>84</sup>.

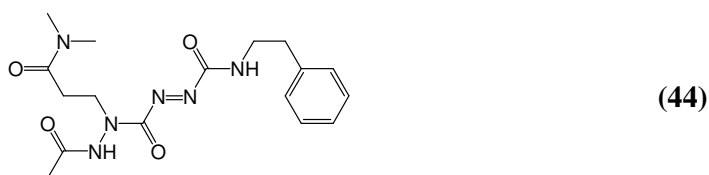
In the late 1990's Idun Pharmaceuticals reported highly potent irreversible caspase-3 inhibitors<sup>83</sup>. The oxoazepinoindoline IDN-5370 **42** was one of their earlier potent compounds, and showed a broad-spectrum activity of low nanomolar range against caspases 1, 2, 3, 6, 8 and 9. Compared to the commonly used broad-spectrum inhibitor Z-VAD.FMK **41**, the non-covalent binding of **42** to caspases 1 and 3 as measured by its  $K_i$  is about 10 and 100 times tighter, respectively, with comparable or better first order rate constants of irreversible inactivation<sup>84</sup>. Recently Idun Pharmaceuticals have developed IDN-6556 **43**, the first irreversible caspase-3 selective inhibitor to enter clinical development<sup>85</sup>. This compound is currently in Phase II clinical trials for the treatment of liver disease.



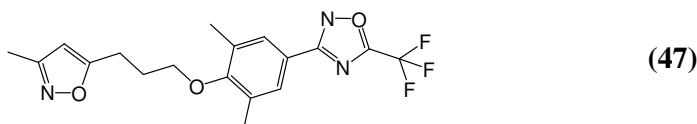
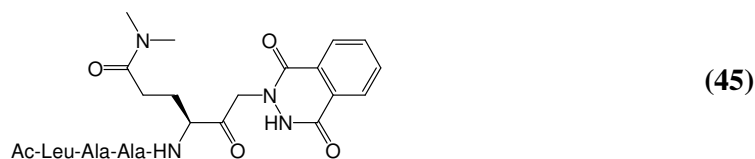


### *Picornaviral protease inhibition*

Picornaviral proteases are present in picornaviruses. Pathogens that belong to the picornavirus family include hepatitis A virus (HAV) and human rhinovirus (HRV). These viruses have a single-stranded, positive-sense RNA genome, which is translated into a polyprotein precursor. 3C and 2A picornaviral proteases process these precursors in order to generate mature viral proteins and functional enzymes and therefore ensure viral replication. These proteases are cysteine proteases, however these enzymes have a topology similar to those of the chymotrypsin-like serine proteinases. Vederas *et al*, based at the University of Alberta, have carried out an extensive study on new types of warheads (thiol reactive groups) as highly selective inhibitors of HAV and HRV 3C proteinases<sup>86</sup>. The azodicaboxamide inhibitor **44** has been shown to have potency against both HAV and HRV 3C proteases, with IC<sub>50</sub> values of 10 and 12 μM, respectively. These inhibitors were designed based on substrate specificity for HAV 3C, and contain the mimicked p1 (Gln) and P2' (Phe) residues important for enzyme recognition. It is believed that the active site cysteine thiolate adds to the azo nitrogen in a Michael type fashion, thereby forming a covalent adduct and irreversibly inactivating the enzyme.



A competitive series of phthalhydrazido analogues were also synthesised and tested for inhibition, with the most active inhibitor **45** having a  $K_i$  of 9  $\mu\text{M}$  against hepatitis A virus 3C protease, which is a 7-fold increase in activity compared to its precursor, which was lacking the tripeptide side chain required for enzymatic recognition. Vederas *et al* have also generated a series of pseudoxazolones, which they have shown to be good time-dependent inhibitors of HAV and HRV 3C proteases. Testing of the HAV proteases with the *trans* and *cis* isomer of **46** resulted in  $\text{IC}_{50}$ 's of 4 and 6  $\mu\text{M}$ , respectively, and when tested against the HRV 3C protease, the *trans* and *cis* isomers of **46** gave  $\text{IC}_{50}$ 's of 17 and 16  $\mu\text{M}$ , respectively. The time-dependent inhibition displayed by the pseudoxazolones is presumably the result of irreversible modification of the enzyme, likely from the addition of the enzyme's cysteine thiolate to the imine-carbon.



The human rhinovirus is the major cause of the common cold. At this moment, only symptomatic treatment is available to medicate rhinovirus infections. However, ViroPharma have developed a novel, orally bioavailable drug **47** that is in the late-stages of clinical trials<sup>87</sup>. Pleconaril<sup>88</sup> **47** is also able to cross the blood-brain barrier and target the viruses responsible for causing meningitis and is in clinical trials relating to this viral infection<sup>89</sup>.

To date there are very few electrophilic isosteres appropriate for developing selective, reversible inhibitors of cysteine proteases. This may be the reason for the lack of cysteine protease inhibitors that have progressed to clinical trials. C-terminal aldehydes and ketones, which react with the cysteine active site to form reversible

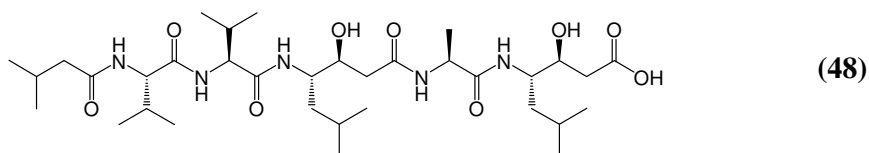
thioacetal transition state analogues, are the most common moieties for developing reversible cysteine protease inhibitors. The main problem with the aldehyde moiety is the lack of selectivity shown to proteases. In contrast to this, there have been many functional groups incorporated into peptides capable of irreversibly alkylating the active site cysteine, including epoxide, nitriles and diazomethyl ketones. These functional groups are activated electrophiles that are generally cysteine selective over the serine proteases. Even still, the vast majority of these compounds are too reactive towards various nucleophiles in the body. These concerns have severely limited the development of such irreversible inhibitors as therapeutic agents.

#### **1.5.2.3 Aspartic Acid protease inhibitors**

Aspartic acid proteases constitute a therapeutically relevant class of enzymes that play an important role in the regulation of various physiological processes, such as the control of blood pressure (renin)<sup>90</sup>, digestion (pepsin)<sup>91</sup>, or degradation of endocytosed proteins (cathepsin D)<sup>92</sup>. Further, they actively propagate the progression of severe diseases caused either by parasites, such as malaria (plasmepsin)<sup>93</sup>, or viruses, such as human immunodeficiency virus (HIV protease)<sup>94</sup>, or neurodegenerative disorders including Alzheimers disease ( $\beta$ -secretase)<sup>95</sup>. On the basis of the mechanism of peptide bond hydrolysis employed by aspartate proteases, several structurally diverse transition state analogues have been designed by replacing the dipeptide-encoded scissile bond within the specific substrates. A key structural element in most transition state isosteres is a hydroxy moiety that interacts with the catalytic site aspartic acid side chains via hydrogen bonds. This secondary hydroxy group further replaces the catalytic water molecule normally bound between both aspartates and simultaneously mimics the tetrahedral geometry that is intermediately formed in the initial steps of the amide bond hydrolysis of a peptide substrate.

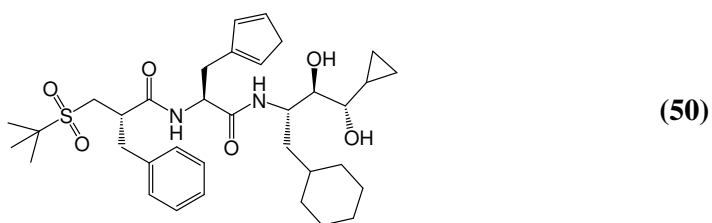
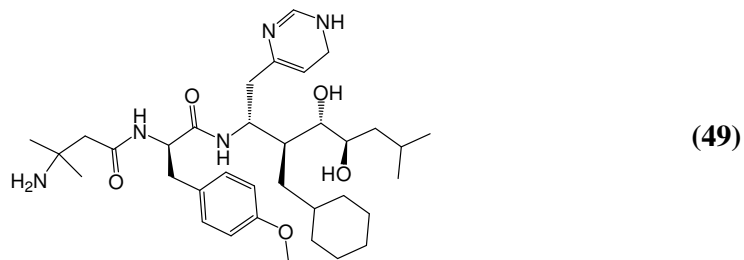
Raised blood pressure is associated with significant cardiovascular morbidity and mortality, and the incidence of cardiovascular complications (predominantly stroke and coronary heart disease) rises exponentially with increasing blood pressure. As the most common cause of strokes, reversible cause of heart failure and a preventable cause of ischaemic heart disease (IHD) in diabetics, hypertension is estimated to

affect approximately 1 billion people worldwide<sup>96</sup>. Renin represents a key player in the renin-angiotensin system (RAS) for controlling blood volume, arterial pressure and cardiac and vascular function, its manipulation also provides a means for the therapeutic treatment of hypertension and heart failure. In the renin-angiotensin system, angiotensin II is produced via a two-step process in which angiotensinogen, synthesised primarily in the liver, is cleaved by the aspartic peptidase, renin, produced in the kidney, to give rise to angiotensin I. This biologically inactive decapeptide is then converted to the active octapeptide angiotensin II by angiotensin converting enzyme (ACE). Angiotensin II acts to increase arterial tone, adrenal aldosterone secretion, renal sodium reabsorption, sympathetic neurotransmission, and cellular growth. Although the idea of renin or ACE inhibition as a method of blocking this system is well known, potent drugs identified have been abandoned as antihypertensive agents due to inadequate oral bioavailability properties (e.g. low stability, poor solubility). Furthermore, compared to the ACE targeting drugs, renin inhibitors require interaction with additional subsites for tight binding resulting in the requirement of higher molecular weight compounds and hence non-cost-effective syntheses. Nevertheless, in contrast to renin, ACE is implicated in alternative pathways and its inhibition therefore results in side effects (cough, angioneurotic edema).



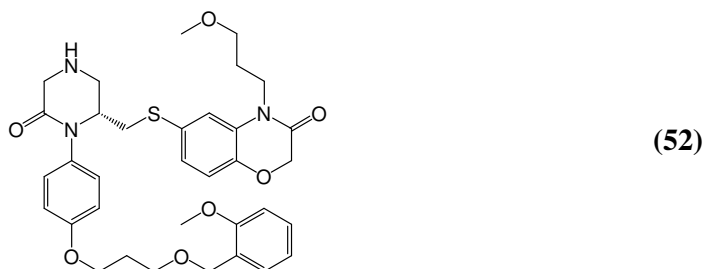
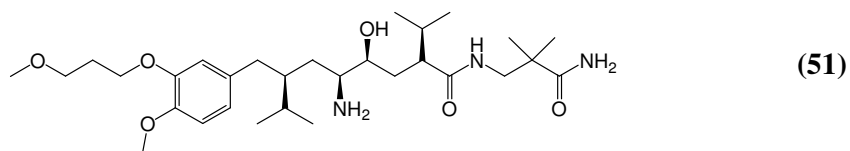
Pepstatin **48**, which is a naturally occurring compound, was the first known inhibitor<sup>97</sup>. Pepstatin (Iva-Val-Val-Sta-Ala-Sta) contains the novel amino acid statine [(3S,4S)-4-amino-3-hydroxy-6-methyl heptanoic acid], and inhibits most aspartic inhibitors. This inhibitor lacked the selectivity and bioavailability to be a success, but its isolation led to development of better compounds, such as the Abbott designed inhibitor, enalkiren **49** and remikiren **50** produced by Hoffman-La Roche. The reported IC<sub>50</sub>'s of **49** and **50** are 14 and 0.8 nmol/L with plasma half lives of 1.6±0.4 and 9.4±4.1 hours, respectively<sup>97</sup>. Enalkiren and remikien, as well as all of the first generation renin inhibitors failed to complete clinical testing. These inhibitors were

dropped due to low bioavailability attributable to poor gastrointestinal absorption with large variability between individuals and substantial first-pass metabolism, short duration of action and weak blood-pressure-lowering activity<sup>97,98</sup>.

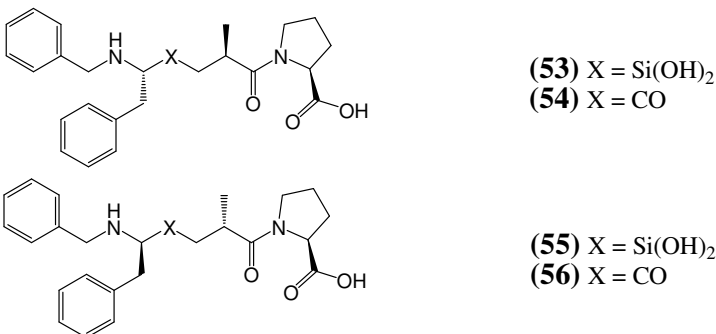


At this point in time, the first non-peptide orally active renin inhibitor, aliskiren **51**, developed by Novartis, is nearing the end of phase-III clinical trials<sup>99,100</sup>. Compound **51** has percentage oral bioavailability of 2.7%, IC<sub>50</sub> of 0.6 nmol/L and a plasma half life of 23.7±7.6 hours. With a half life at almost 24 hours, the compound is suitable for once-daily administration. Compared to other orally active renin inhibitors, such as enalkiren **49** and remikiren **50**, aliskiren **51** is the most of the most potent renin inhibitor identified, with high specificity for primate renin<sup>100</sup>. Aliskiren **51** is currently undergoing three phase-III trials at Novartis. The first trial is testing the effects of aliskiren **51** on intermediate markers of target-organ damage (ALLAY, reg. no. [<http://clinicaltrials.gov>] NCT00219141). The second trial that Novartis are undertaking (ALOFT, NCT00219011) is the comparison with a placebo given in addition to optimum standard treatment, with the primary endpoint is the fall of plasma concentration of brain natriuretic peptide. Finally, in the third trial (AVOID, NCT00219206), aliskiren and a placebo will be added to treatment with losartan to study the reduction in the urinary albumin-to-creatinine ratio. Each of these trials will be performed on 300-500 patients<sup>97</sup>.

Pfizer have published many compounds in a structure-activity relationship of novel substituted amino-aryl-piperidine-based renin inhibitors. Of the published results, the ketopiperazine-based inhibitor **52** is most active<sup>101</sup>. Compound **52** has shown a strong



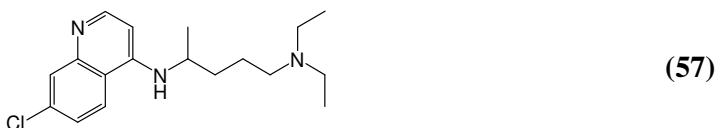
potency against renin as anticipated with an  $IC_{50}$  value of 0.18 nM. This inhibitor **52** was also evaluated for its propensity to inhibit the cytochrome P450 3Aa isozyme (CYP3A4)<sup>102</sup>, showed a potency with  $IC_{50}$  (BFC) value of 14 nM. In a review by Scott Sieburth, the potency of silanediol inhibitors and their corresponding ketone derivatives against angiotensin-converting enzyme (ACE) is reported<sup>103</sup>. Inclusion of the silanediol moiety is not a widely used group but this report has shown that various compounds have differing potencies to their corresponding ketone derivative, depending largely on the stereochemistry. Compounds **53** and **54**, and alternatively **55** and **56**, indicate that the orientation of the other substituents in vicinity of the relevant moiety largely affects the inhibitory potency of these compounds.



Inhibitors **53** and **54**, displaying the methyl group in *cis*-orientation and the benzyl group *trans*-, with respect to the carboxylic acid functionality, showed IC<sub>50</sub> values of 3.8 and 1.0 nM, respectfully. The inhibitors synthesized with the methyl *trans*- and the benzyl group *cis*- showed far less potency, with reported IC<sub>50</sub>'s of 72 and 3200 nM, respectfully.

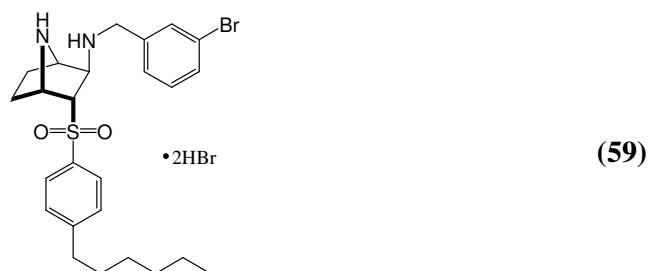
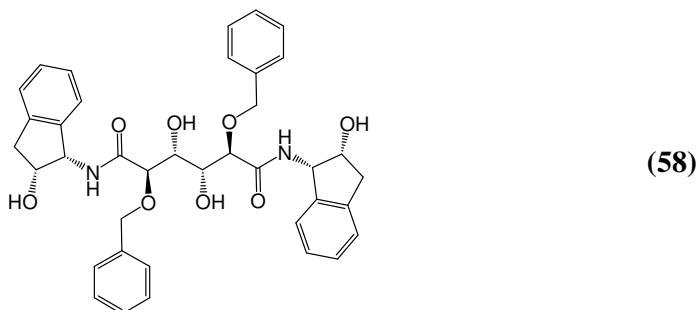
#### *Malaria protease inhibition*

Malaria has in recent years re-emerged as one of the most serious infectious diseases in the world. The most dangerous of the malaria-causing parasites, *Plasmodium falciparum*, infects 300-660 million people each year. The plasmepsins (PMs) are a family of *Plasmodium* aspartic proteases that digest human hemoglobin and deliver amino acids that are required for growth. In search for targets for new antimalarial therapies, the mutually redundant proteolytic activity of plasmepsins for hemoglobin requires inhibitors that are broadly active against all hemoglobin-degrading plasmepsins (PM I, PM II, PM IV and HAP, a histo-aspartic proteinase) while remaining inactive against the most closely related human aspartic proteases (cathepsins D and E; hCat D and E)<sup>104</sup>. Among the plasmepsins, only the structure of PM II has been extensively studied and characterized.

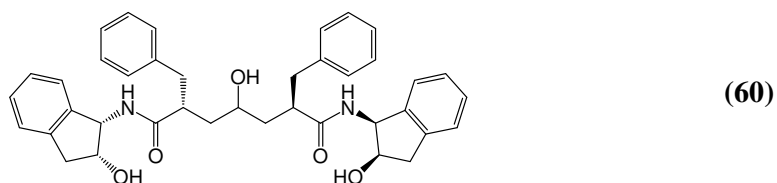


Unfortunately, no vaccine is currently available to stop the infection of malaria. Instead preventative drugs are taken continuously to reduce the risk of malaria. Such prophylactic drug treatments are simply too expensive for most individuals living in endemic areas. Malaria infections are treated through the use of antimalarial drugs such as chloroquine **57**, although drug resistance is increasingly common. Chloroquine is a 4-aminoquinoline drug long used in the treatment or prevention of malaria. As it also mildly suppresses the immune system, it is used in some autoimmune disorders, such as rheumatoid arthritis and lupus erythematosus. After the malaria parasite *Plasmodium falciparum* started to develop widespread resistance against chloroquine, new potential utilisations (e.g. HIV and cancer inhibition) of this

cheap and widely available drug have been investigated<sup>105</sup>. Combining chloroquine with other antimalarial inhibitors such as proguanil, may be more effective against chloroquine-resistant *Plasmodium falciparum* than treatment with chloroquine alone, but is no longer recommended by the Centres for Disease Control and Prevention in the United States, due to the availability of more effective combinations.



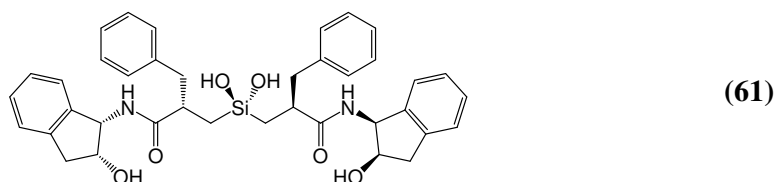
Due to the every increasing resistance to antimalarial treatments like chloroquine, research into developing efficient antiparasitic agents should target not only one but several of the plasmepsins. Hallberg *et al* have developed a series of nanomolar active PM I and II inhibitors with considerable discrimination versus the most homologous human aspartic protease cathepsin D. Inhibitor **58** has shown inhibitory activity against PM I and PM II with  $K_i$  values of 25 and 85 nM, respectively. This compares favourably to the  $K_i$  recorded against Cat D of >2000 nM<sup>106</sup>. Diederich *et al* have recently reported compound **59** which is active against PM I, II, IV and Cat D. However, it is only PM II and IV that are in the low nanomolar range ( $IC_{50}$  = 45 & 10, respectively) while the other two aspartic proteases are 100-fold higher<sup>104</sup>.





### *HIV protease inhibition*

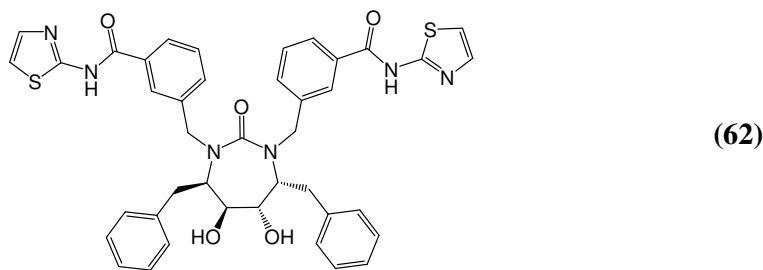
The human immunodeficiency virus type 1 (HIV-1) pandemic has emerged in many regions of the developing world already suffering from the burden of malaria<sup>107</sup>. In developed countries, HIV-1 protease inhibitors have dramatically reduced the effects of HIV disease. The target of these inhibitors is the HIV-1 protease, a member of the aspartic protease family. Inhibition of aspartic proteases as a way of hindering the human immunodeficiency virus is only a recent phenomenon. At the end of the 20th century, identification of the  $C_2$ -symmetric HIV protease enzyme was complete<sup>108,109</sup>. Development of  $C_2$ -symmetric inhibitors of this enzyme such as **60** followed quickly and presented less complex compounds for exploration<sup>110</sup>.



In the previously mentioned review by Sieburth, they demonstrated their silanediol derivative **61** of inhibitor **60** as having good inhibitory potency against the HIV protease enzyme. Sieburth reported a  $K_i$  value for **61** of 2.7 nM. While this is not as potently active as inhibitor **60** ( $K_i = 0.37$  nM), it not only inhibits the HIV protease enzyme, but also protects whole cells against HIV infection, indicating that it can penetrate cell walls<sup>106</sup>.

Recently, cyclic urea structures have been reported to constitute an entirely new class of potent and prospective non-peptidic inhibitors of aspartic proteases. A fundamental feature of the cyclic urea inhibitors is the carbonyl oxygen that mimics the hydrogen-bonding features of the key structural water molecule present in the active site of the aspartic protease<sup>111</sup>. The presence of this structural water distinguishes the retroviral protease from human aspartic proteases pepsin and renin. The success of the design in both displacing and mimicking the structural water molecule that bridges the substrate to the flaps of the protein by hydrogen bonds was confirmed by X-ray crystallographic studies<sup>112</sup>. Cyclic ureas proved to be highly selective structures with decreased conformational flexibility, low molecular weight, improved water solubility and oral bioavailability. DuPont Merck has developed a

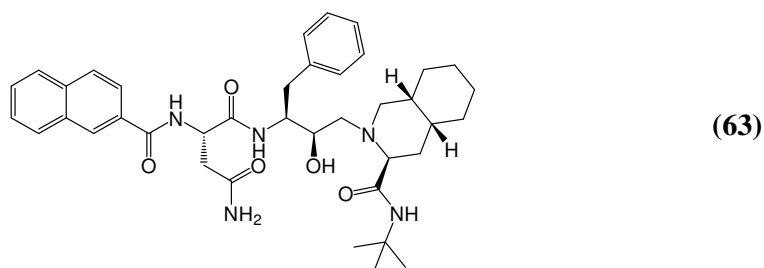
highly potent HIV inhibitor of wild-type HIV; XV638 **62** has a  $K_i$  value of 0.03 nM against reconstructed mutant viruses<sup>113</sup>



This inhibitor **62** was the most potent of a series of cyclic urea derivatives developed by DuPont Merck, and were optimised based on inhibitory potency of a set of viral strains selected for resistance to the four HIV aspartic protease inhibitors that were either approved for marketing (saquinavir **63**, zidovudine **64**, didanosine **65**, zalcitabine) or were in advanced clinical development (VX478) at the time. Developed by Vertex, amprenavir or VX478 was approved by the FDA in 1999 but production was discontinued by the manufacturer and licensee, GlaxoSmithKline, in 2004.

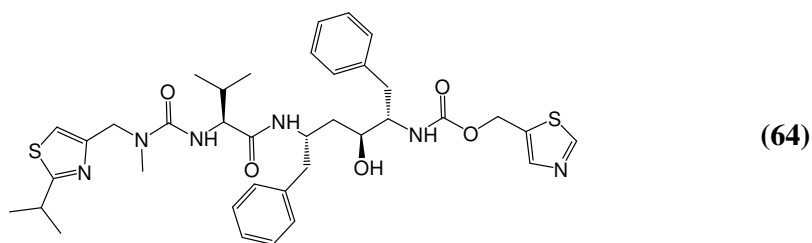
Inhibitor	Wild type ( $\mu\text{M}$ )	Knockout $\text{IC}_{50}$ (% of wild type $\text{IC}_{50}$ )
Saquinavir <b>63</b>	$5.7 \pm 0.8$	133
Ritonavir <b>64</b>	$7.9 \pm 1.1$	113
Atazanavir <b>65</b>	$35.0 \pm 0.4$	120

**Table 1.2:** Activity of HIV-1 protease inhibitors against *P. falciparum*-2 knockout parasites<sup>114</sup>.



Up to 2004, there were 19 compounds formally approved for the treatment of human immunodeficiency virus infections. They can be classified into 4 groups, (i) nucleoside reverse transcriptase inhibitors (NRTIs), (ii) nucleotide reverse

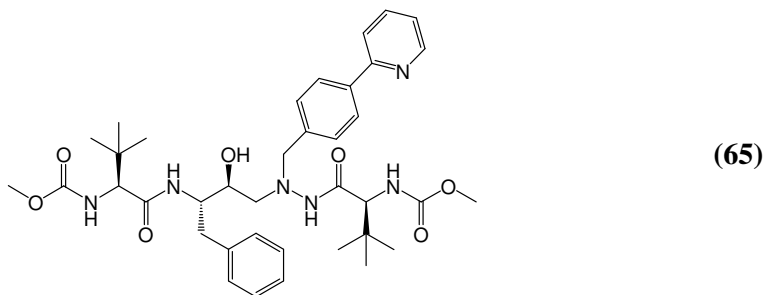
transcriptase inhibitor (NtRTI), (iii) non-nucleoside reverse transcriptase inhibitors (NNRTIs) and (iv) the protease inhibitors (PI). To achieve the highest possible benefit, these drugs have to be combined in multiple-drug regimens. Those that have generally been used consist of two NRTIs, or one NRTI and one NtRTI, to which is then often added one NNRTI or one PI<sup>115</sup>. Saquinavir **63** is manufactured and marketed by Roche Pharmaceuticals, and was the first HIV aspartic protease inhibitor to gain approval for use in the treatment of humans. Despite low bioavailability due to poor adsorption and extensive first pass degradation by cytochrome P450 3A4, it received FDA approval in 1995. Inhibitor **63** acts by restricting the enzyme, which cleaves viral protein molecules into smaller fragments, and this enzyme is vital for both the replication of the virus within the cell and also the release of mature viral particles from an infected cell. Saquinavir **63** was administered in combination with nucleoside analogues and is equally active in cell culture against both HIV-1 and HIV-2 viruses<sup>116</sup>. The most common side effects experienced from the use of inhibitor **63** are gastrointestinal including diarrhoea and nausea<sup>117</sup>. In the early part of 2006, Roche Pharmaceuticals issued a statement withdrawing the use of Saquinavir



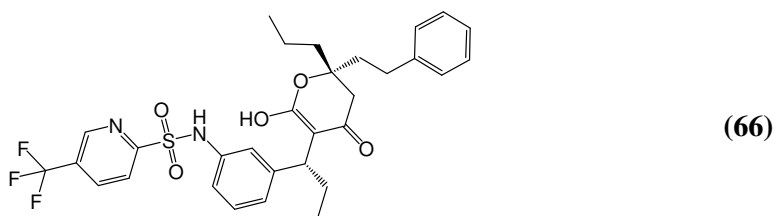
**63** in its initial form (Fortovase<sup>®</sup>) but remains in clinical use under the trade name Invirase<sup>®</sup>, which is combined with ritonavir **64**<sup>118</sup>.

Ritonavir **64** was another early protease inhibitor to receive approval in 1996. Developed by Abbott Laboratories, this inhibitor is used, as in **63**, in combination with nucleosides or as monotherapy for the treatment of HIV infection<sup>115</sup>. Considered both as a potent inhibitor and an inducer of the cytochrome P450 metabolic pathway, it is metabolised primarily through cytochrome P450 3A4<sup>117</sup>. As with inhibitor **63**, HIV-1 and -2 are equally susceptible to ritonavir inhibition. Nausea and vomiting are the two most common side effects that result from use of inhibitor **64**. The addition of ritonavir to a course of saquinavir therapy boosts inhibition levels 20-fold based on

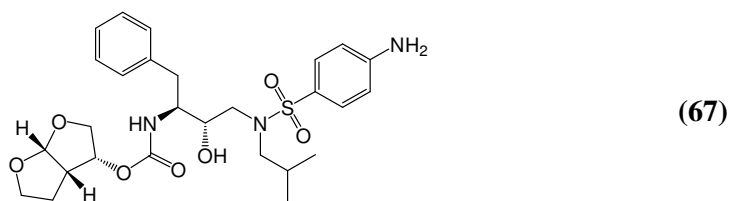
the ritonavir potent inhibition of the cytochrome P450 3A4. As a result, doses of both drugs can be reduced, thereby potentially limiting side effects.



One of the more widely used HIV protease inhibitors is known as atazanavir **65**, formerly known as BMS-232632, and now trading under the name Reyataz<sup>®</sup>. Atazanavir was approved for treatment in 2003 and is the first protease inhibitor approved for once-daily dosing<sup>115</sup>. The Bristol-Myers Squibb inhibitor **65** shows side effects common among HIV inhibitors, such as increased probability of kidney stones, metabolic abnormalities including cholesterol elevations and bizarre body shape alterations known as lipodystrophy, however in the case of atazanavir they are far less severe than its predecessors. In October 2006, the FDA approved a new formulation of atazanavir to be taken as part of combination drug therapy and should reduce the dosage amounts<sup>119</sup>. Atazanavir prevents the formation of mature virions by inhibiting the processing of viral gag and gag-pol polyproteins in HIV-infected cells. The unique, signature mutation for atazanavir resistance in isolates from antiretroviral therapy-naïve patients was an isoleucine to leucine substitution at amino acid residue 50 of the HIV-1 protease gene. This mutation was atazanavir **65** specific and conferred increased susceptibility to other protease inhibitors. However, in antiretroviral therapy-experienced patients who had never previously received atazanavir, susceptibility was reduced in the presence of multiple mutations associated with resistance to other protease inhibitors. There was a high cross-resistance to **65** in patients with prior exposure to at least three other PIs<sup>120</sup>.



Tipranavir **66**, is a nonpeptidic protease inhibitor (PI) with the trade name Aptivus<sup>®</sup> and developed by Boehringer Ingelheim Pharmaceuticals, Inc. Inhibitor **66** was approved by the FDA in 2005. It is used in combination therapy to treat HIV infection. Tipranavir has the ability to inhibit the replication of viruses that are resistant to other protease inhibitors. Resistance to tipranavir itself seems to require multiple mutations. Like most peptidomimetic protease inhibitors, tipranavir **66** is given in combination with low-dose ritonavir in order to boost its systemic availability. Like atazanavir **65**, it is very potent and is effective in salvage therapy for patients with some drug resistance. However, it tends to have more side effects<sup>121</sup>.

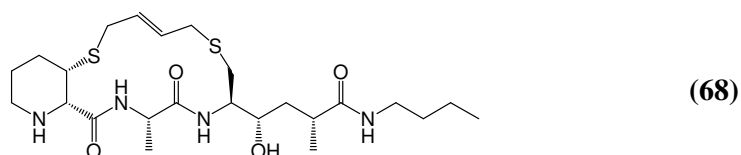


Inhibitor **67**, known as TMC-144 or darunavir, and prescribed under the name Prezista<sup>®</sup>, is the most recent HIV inhibitor to gain FDA approval. Receiving approval in June 2006, darunavir **67** is manufactured by Tibotec Therapeutics, a division of Ortho Biotech Products. Inhibitor **67** has exhibited a  $K_i$  value of 14 pM and antiviral  $IC_{50}$  of 3 nM<sup>122</sup>. Darunavir has been shown to have antiviral activity against the mutant and the wild type viruses<sup>123</sup>. Prezista is approved to be co-administered with a low-dose of ritonavir and other active anti-HIV agents. Ritonavir **64** slows the breakdown of Prezista in the body thereby increasing the concentration of **67** in the patient's system.

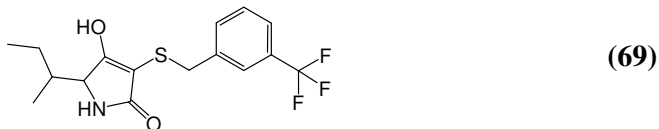
#### *Alzheimer's Disease protease inhibition*

Alzheimer's disease (AD) is the most common age-related neurodegenerative disorder and currently affects nearly 2% of the population in industrialized countries<sup>124</sup>. One in 10 individuals over 65, and nearly half of those over 85, are likely to be struck by the disease. The increase of the older population in the developed countries will turn AD into a dramatic issue for healthcare systems worldwide in the near future. Until now, there has been no cure for AD. Intensive investigation has provided insight into the biology of the disease and revealed several options for treatment. Brains of patients struck by AD are characterized by two

hallmark proteinaceous aggregates: amyloid plaques and neurofibrillary tangles<sup>125</sup>.  $\beta$ -Amyloid plaques are specific for AD<sup>126</sup>. The “amyloid hypothesis”, assigns the central role to the accumulation of  $\beta$ -amyloid peptide ( $A\beta$ ) in the brain.  $A\beta$  peptides derive from the abnormal cleavage of the  $\beta$ -amyloid precursor protein ( $\beta$ -APP), a protein found throughout the body whose normal function remains obscure.  $\beta$ -Secretase (BACE-1), a member of the pepsin family of aspartyl proteases, plays a critical role in this amyloid cascade. Recent reports have demonstrated a direct correlation between increased  $\beta$ -site amyloid precursor protein cleaving enzyme (BACE-1) activity and  $A\beta$  production in AD brain tissue<sup>127</sup>. Several aspartic proteases have been targeted successfully for drug development; therefore, BACE-1 inhibition has been recognized by several companies and academic groups as a suitable therapeutic approach to slow or halt the progression of AD<sup>128</sup>.

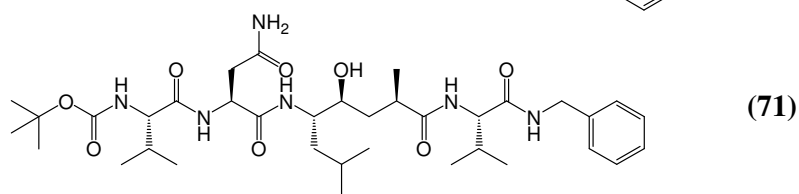
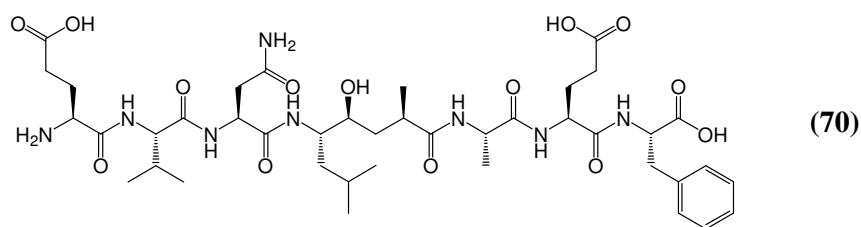


To date, numerous BACE-1 inhibitors have been published. Most of these inhibitors share a peptidic character and mimic the scissile amide bond of the natural substrate by a noncleavable transition state isostere. Up until recent years, most inhibitors were of this nature, peptidlike. Novartis have recently reported on the design and synthesis of 15- to 17-membered macroheterocyclic peptidomimetic inhibitors of  $\beta$ -secretase<sup>129</sup>. Inhibitor **68** was the most potent of these novel macrocyclic hydroxyethylene inhibitors and showed good activity against BACE-1 with an  $IC_{50}$  of 0.19  $\mu$ M. However, this inhibitor along with all in the series, when tested against two other aspartic protease enzymes (Cat D and pepsin), showed significantly better potency with  $IC_{50}$  values of 0.01 and <0.01  $\mu$ M, respectively.



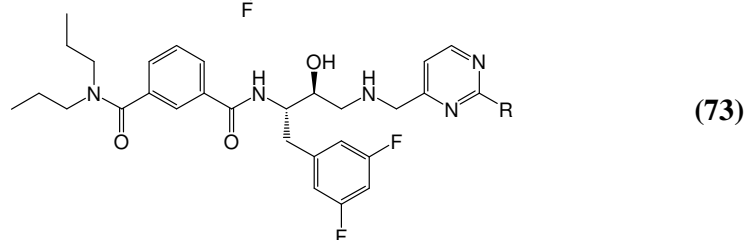
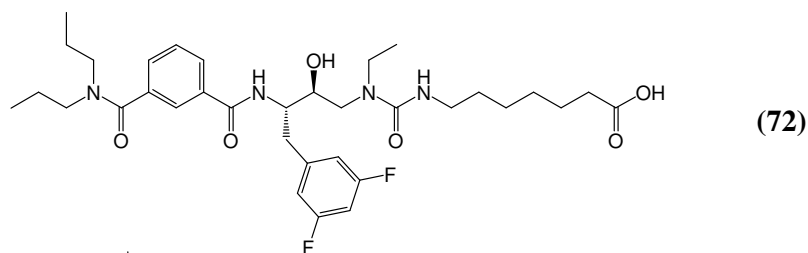
Despite all progress made in the design of peptidlike molecules, they have the same problems as all peptidic structures: low oral bioavailability and poor blood-brain

barrier permeation. Therefore, nonpeptidic compounds are now at the forefront in the hunt for a potent  $\beta$ -secretase inhibitor. The exploration of the potential of tetronates and tetramates as BACE-1 inhibitors is an exciting area that is showing promise, with Hoffman La Roche having recently applied for a patent in this area<sup>130</sup>. Schmidt *et al* have identified tetronic, tetramic, and N-substituted tetramic acids that inhibit BACE-1 in the micromolar range<sup>131</sup>. These scaffolds were chosen because they are related to the homologous 4-hydroxypyran-2-one class of HIV active site inhibitors, which includes tipranavir **66**. Of the vast library of compounds screened for  $\beta$ -secretase inhibition, only a select few showed potency in the micromolar range or better. The tetramic acid inhibitor **69** was the most active of all compounds assayed with a calculated IC<sub>50</sub> of 60  $\mu$ M. Further optimization is required and is in progress, based around modification of the enol functionality, as the results from the SAR indicate that the *m*-trifluoromethyl aryl group separated by a S-CH<sub>2</sub> moiety increases activity.

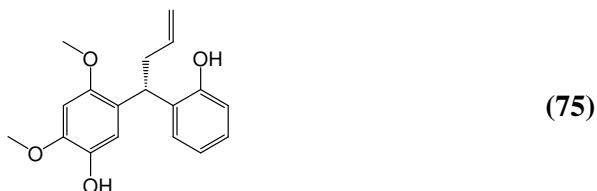
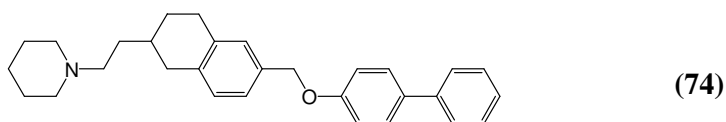


These recent publications show how difficult an enzyme  $\beta$ -secretase is to inhibit. Although active, the previously reported compounds are very weak in terms of potency. Several inhibitors of  $\beta$ -secretase have been identified in cellular assays but, more often than not, the true nature of the inhibition mechanism was not reported. Broad-spectrum protease inhibitors such as pepstatin **48**, known aspartic protease inhibitors from renin, and HIV protease programs, as well as cocktails thereof, have little inhibitory effect and gave misleading results. The consequent utilization of the Swedish mutation and the SAR of early compounds made by Bristol-Myers Squibb<sup>132</sup> resulted in the development of OM99-2 **70** and its successful cocrystallization with BACE. Activities have been reported for Leu-Ala hydroxyethylene isomers such as **71**, which provide insight into the binding mode. However, these compounds do not

really invite drug development because the obstacles for Alzheimer therapy are even higher in comparison to those for the inhibition of renin and HIV protease<sup>133,134</sup>.



Significant efforts were made to reduce the molecular weight and the flexibility of the lead structure. Inclusion of an alanine instead of a valine residue improved binding to the pocket S2'. This replacement and the omission of the small contributions from P4-Glu- and P4'-Phe-binding were first steps taken on a bumpy road towards optimization. The Elan compounds **72** and **73** have lost a good part of their peptidic heritage, which is mandatory to obtain sufficient oral absorption and blood-brain barrier penetration<sup>135,136,137</sup>.



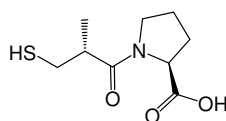
Despite all efforts made by pharmaceutical companies and academic groups, nonpeptidic lead structures for BACE inhibition are very scarce. Takeda reported the tetraline **74**, which is not an obvious scaffold for protease inhibition and is likely to originate from high-throughput screening efforts<sup>138</sup>. The activity is poor ( $IC_{50} = 100 \mu M$ ) and the mode of action is insecure. Latifolin **75**, isolated from the heartwood of *Dalbergia sissoo*, was found to inhibit  $A\beta$  synthesis with an  $IC_{50}$  value of  $180 \mu M$ ,



again a rather weak potency<sup>139</sup>. However, steady assay development will help provide further nonpeptidic leads. For example, protease-cleavable luciferases, which can be used in protease determination and screening for protease inhibitors, were suggested for use with the BACE sequence<sup>140</sup>, but the reported method needs improvement.

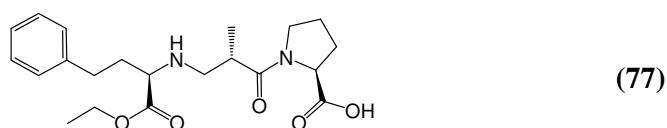
#### 1.5.2.4 Metalloprotease inhibitors

Metalloproteases, like aspartic proteases, do not form covalent intermediates, but have evolved with a more direct solution to the necessity for catalytic effect on the carbonyl group of the bond undergoing cleavage. Rather than rely on hydrogen bonding, the metalloproteases utilise coordination to a metal ion to exert this effect<sup>3</sup>. In the vast majority of cases this metal is zinc, although in some proteases other transition metals such as copper and nickel are present. The currently accepted mechanism of catalysis of the metalloproteases involves a  $Zn^{2+}$  ion tetrahedrally coordinated to three donor groups from the enzyme and a water molecule. By being hydrogen bonded to the carboxylic acid side chain of a glutamic acid residue, the water molecule is activated for nucleophilic attack. The coordination of the carbonyl moiety of the scissile amide bond to zinc is followed by nucleophilic attack by the water molecule with a proton transfer to the carboxylate giving a tetrahedral zinc intermediate. The transfer of a proton from the glutamic acid to the amide nitrogen is followed by collapse of the tetrahedral intermediate with the generation of a salt bridge between the glutamic acid and the free amine of the cleaved substrate. The design of inhibitors has focused on binding the catalytic zinc ion to hinder the mechanism. Synthetic inhibitors generally contain a moiety such as a thiol, carboxylic acid or hydroxamic acid moiety as the warhead, capable of coordinating to a zinc atom attached to a series of other groups that are designed to fit the specificity pockets of a particular protease<sup>141</sup>. With numerous selective and potent inhibitors of metalloproteases being approved for clinical administration, this hypothesis of inhibition has turned out to be very successful.

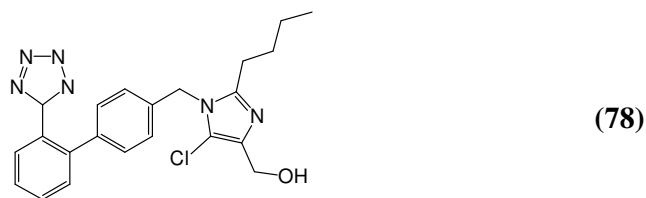


(76)

One of the most frequently expressed zinc metalloproteases, angiotensin converting enzyme (ACE) is found in tissues including the heart, the lungs and several regions of the brain. Due to its pivotal role in blood regulation, ACE has received huge amounts of attention. As mentioned earlier, ACE, as a catalyst is responsible for the conversion of angiotensin I to angiotensin II in the renin-angiotensin system<sup>97</sup>. The inhibition of this zinc metalloprotease decreases levels of angiotensin II in the body, ultimately leading to a reduction in blood pressure. ACE inhibition has been studied extensively for many years which has resulted in many potent inhibitors receiving approval for therapeutic use. The first ACE inhibitor to gain FDA approval was the Bristol-Myers Squibb inhibitor, captopril **76**, isolated from snake venom. Inhibitor **76** was patented in the late 1970's and received approval early in the 1980's for use in the treatment of hypertension and some types of congestive heart failure. The adverse effect and pharmacokinetic limitations of captopril stimulated the development of enalapril **77** by Merck & Co., and subsequent ACE inhibitors. These were specifically designed to lack the sulfhydryl moiety believed to be responsible for rash and taste disturbance<sup>142</sup>.



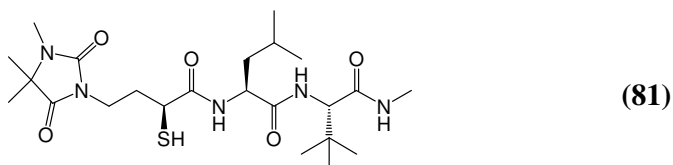
Enalapril **77** was the first member of the group of ACE inhibitors known as the dicarboxylate-containing ACE inhibitors. Both of these inhibitors employ a chelating group that binds to the active site zinc resulting in high inhibitory potency and selectivity. Most subsequent ACE inhibitors are given as prodrugs, to improve oral bioavailability.



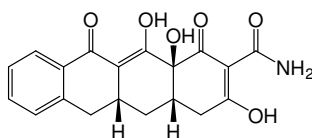
In recent times, low molecular weight, lipophilic inhibitors of ACE have been developed that are devoid of side effects. Losartan **78** is an angiotensin II receptor antagonist and was the first to be marketed. Developed by Merck & Co., losartan **78**



are still undergoing clinical trials. The first generation inhibitors were designed based on peptide substrates attached to a zinc-binding group (ZBG) such as a hydroxamate. These were mostly non-specific and broad based MMP inhibitors. More specific inhibitors have been designed using both peptidic and non-peptidic scaffolds, with the assistance of enzyme crystal structures. Also, several different types of ZBGs have been reported to work well with different scaffolds<sup>147</sup>. One of the most notable and well known of the first generation inhibitors was developed by British Biotech and is called marimastat **80**. This is a broad-based MMP inhibitor and is not specific against any one or group of MMP's. Marimastat **80** has undergone several Phase III clinical trials<sup>148</sup>. A trial for advanced pancreatic cancer failed to detect increased survival for the marimastat-treated groups. However, the highest dose of marimastat was not found to be more effective than the conventional therapy. The vast majority of the first generation matrix metalloprotease inhibitors have hydroxamic acid as the ZBG. So far progression of broad-spectrum matrix metalloprotease inhibitors (MMPIs) through these trials has been hampered due to a prevalent side effect known as musculoskeletal syndrome (MSS), which manifests itself as musculoskeletal pain and inflammation<sup>147</sup>.



The second generation of MMP inhibitors are nonpeptidic and are designed on the basis of the conformation of the MMP active site determined by NMR and X-ray crystallography. These inhibitors are more specific inhibitors. The first subgroup of these inhibitors also contain hydroxamic acids as ZBG, but the most potent has been with rebimastat (BMS 275191) **81**. This inhibitor is a thiol based instead of a hydroxamic acid based inhibitor and is undergoing cancer Phase II/III clinical trials. The second subgroup developed are tetracycline derivatives have been shown to inhibit both the activity and synthesis of MMPs. Tetracycline analogues with no antibiotic activity have been developed for the treatment of cancer. Metastat (CMT-2) **82** is one such analogue that is undergoing Phase II trials for Kaposi's sarcoma and advanced brain tumours<sup>146</sup>.

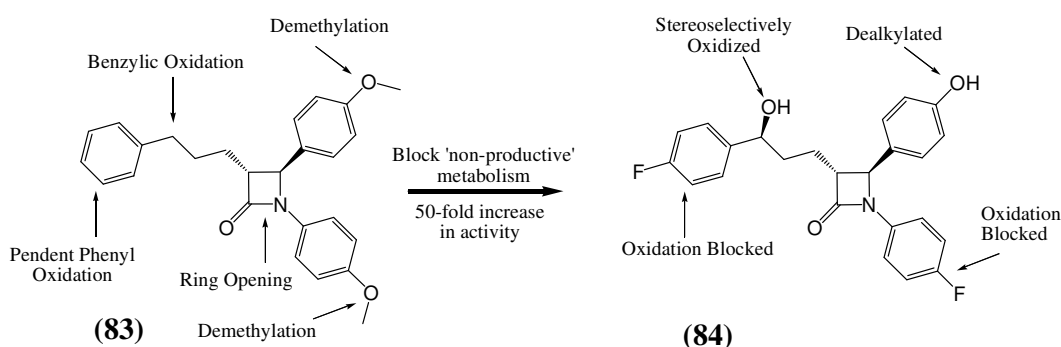


(82)

For numerous decades, matrix metalloproteinases have been heralded as promising targets for cancer therapy on the basis of their massive up-regulation in malignant tissues and their unique ability to degrade all components of the extracellular matrix. Matrisian *et al* has stated that a major reason for the failure of MMP inhibitors in the clinic appears to be faulty design of clinical trials<sup>149</sup>. Most preclinical studies have focused on the role of MMPs in the early stages (progression and metastases) of cancer, in which MMP inhibition seems to have its greatest effect. Unfortunately, clinical trials of MMP inhibitors were conducted almost uniformly in patients with advanced, metastatic disease, and all have failed to show any beneficial effect on patients. It is possible that these same trials could have had different outcomes if they were conducted in patients with earlier stages of disease. Secondly, lack of selectivity of the first generation inhibitors (marimastat **80**) may have contributed to this failure. The second generation inhibitors were designed to be selective for several specific MMPs. But the selectivity of the second generation may not be sufficient enough to cause significant inhibition of cancer growth. Further, most trials use the maximum tolerated dose of MMP inhibitors. At the highest tolerated doses, the inhibitors might lose selectivity for specific MMPs. In some trials, the dosage could have been too low to avoid the side effects (most commonly musculoskeletal pain) of MMP inhibitors. Some of these unfavorable side effects may have been caused by the hydroxamate group which is common to most of the clinical candidates<sup>150</sup>.

## 1.6 Fluorine containing protease inhibitors

The addition of fluorine atoms into a drug molecule has been around for many years as a fundamental element in the search for increased biological activity. The importance of fluorine substitution in pharmaceutical development is evident in the large number of fluorinated derivatives approved by the FDA for use as anticancer, antiviral, antidepressant and anesthetic agents. There are generally two consequences of introducing fluorine into a drug molecule<sup>151</sup>. Firstly there are the physicochemical properties. Fluorine has the ability to modulate electronic, lipophilic and steric parameters that can critically influence the pharmacological properties of a drug molecule. The introduction of a fluorine atom will generally increase lipophilicity, decrease basicity and alter the hydrogen bonding interactions of a molecule. Secondly, there is the influence of fluorine substitution on the biological stability of a drug molecule, *e.g.* through altering the metabolism of the drug<sup>152</sup>. A prime example of this is shown in **Scheme 1.3**, with the discovery of the cholesterol absorption inhibitor SCH 58235 **84**<sup>153</sup>. The expected modes of primary metabolism of **83** are dealkylation of the N1- and C4-methoxyphenyl groups, para hydroxylation of the pendent C3-side chain phenyl group, benzylic oxidation (hydroxylation potentially followed by ketone formation) and 2-azetidinone ring opening. Modification to form inhibitor **84** has shown a 50-fold increase in potency by blocking all but one of these modes of metabolism.



**Scheme 1.3:** Example of fluorine substitution on rational drug design.

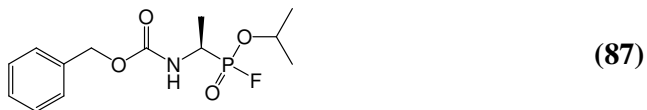
Compound **84** has been developed as a means of treating hyperlipidemia. Its half life of 22 hours is partly due to the presence of fluorine atoms blocking the unwanted metabolic processes mentioned previously. It has FDA approval for use in

combinatorial therapy with statin derivatives for the treatment of hypercholesterolemia. Fluorine has been used as a means to developing safer and more reactive pharmaceuticals due to the strength of the carbon-fluorine bond that is very difficult to metabolize, so harmful and unproductive side reactions are unlikely to occur.

The Van der Waals radius of the fluorine atom is 1.47 Å. This value is positioned between the values of hydrogen (1.20 Å) and oxygen (1.53 Å) allowing it to mimic a hydroxyl group and to participate in hydrogen bonding interactions. With an electronegativity value of 4.0, fluorine is the most electronegative element, much more than carbon (2.5) or hydrogen (2.1). As a result, the carbon-fluorine bond is one of the most stable chemical bonds, while hydrogen-fluorine bonds are the strongest of the secondary bonds. The concept of replacing the hydroxyl moiety of a bioactive molecule with a fluorine atom has been a prevalent method for the enhancement of biological activity. Medicinal chemists have recognized for some time that fluorine and hydroxyl groups are bioisosteres<sup>154</sup>. The introduction of a fluorine atom into a bioactive molecule also provides a marker for <sup>19</sup>F NMR studies where drug-protein interactions can be assessed *in vitro* and *in vivo* due to the absence of fluorine in living tissue<sup>155</sup>.

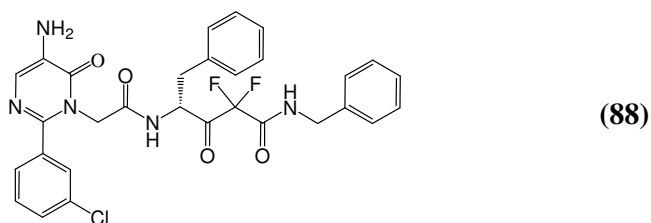


More than eighty years ago, the first fluorine containing protease inhibitors were developed and reported, these were phosphonyl and sulphonyl fluorides. The inhibitors diisopropylfluorophosphate (DFP) **85** and phenylmethylsulphonyl fluoride (PMSF) **86** are two of the most effective examples of protease inhibitors and are generally associated with serine inhibition<sup>156</sup>. These inhibitors phosphorylate or sulphonylate the active site serine hydroxy group due to the electrophilicity of the phosphorous or sulphur atom induced by the adjacent fluorine atom. These inhibitors show poor selectivity with regards to serine and cysteine proteases and are also extremely toxic. Lamden *et al* reported the synthesis of more selective phosphonyl



fluorides such as inhibitor **87**, which incorporates peptidyl character to improve potency<sup>157</sup>. Inhibitor **87** is a potent inhibitor of elastase with 6-fold selectivity over  $\alpha$ -chymotrypsin.

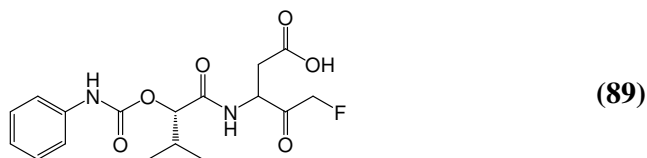
The incorporation of fluoromethyl ketone moieties into protease inhibitors has led to the development of potent transition state inhibitors for a variety of proteases including porcine pancreatic elastase and cathepsin B<sup>158</sup>. The introduction of a fluorine atom into a methyl ketone creates a highly reactive carbon centre that readily undergoes nucleophilic attack. Peptidyl derivatives containing fluoroketones have the ability to be potent inhibitors of proteases due to the vastly increased electrophilic nature of this carbon centre. Both di- and trifluoromethyl ketones exist almost entirely in the hydrated form in water and thus it seems likely that fluorinated ketones would form a hemiketal at the active site of a serine protease or in the case of the hydrate, bind tightly to both metallo or aspartyl proteases<sup>159</sup>. In contrast to chloromethyl ketones, the C-F bond in fluoromethyl ketones is much stronger than the C-Cl bond in the chloro analogues. This suggests that fluoromethyl ketones should be much poorer alkylating agents than chloromethyl ketones. This property should reduce the side effects associated with the use of chloromethyl ketones.



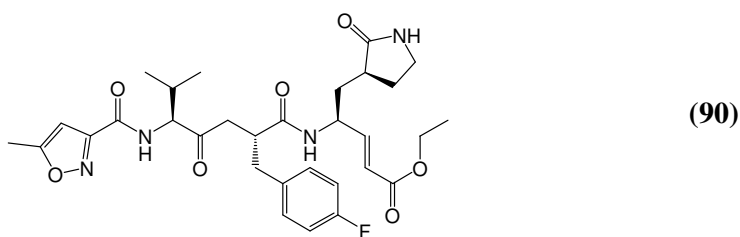
Akahoshi *et al* at the Welfide Corporation in Japan, developed a series of inhibitor analogues based on earlier work<sup>160</sup>. The synthesized compounds were developed as novel inhibitors of the chymotrypsin-like serine protease chymase. The most active inhibitor of the series is **88**, which was shown to have a  $K_i$  value of 2.62 nM towards human chymase, a  $K_i$  of 28.0 nM toward canine chymase, and high selectivity against chymase of other species and their representative human proteolytic enzymes. Along with the high potency towards chymase, the 3-chlorophenyl analogue **88** has a high



chymotrypsin/chymase selectivity ratio of 175. Pharmaceutical studies in rat and dog indicated that **88** was absorbed rapidly following oral administration and had satisfactory bioavailability (17% and 32%, respectively). Given its favorable biological profile, this inhibitor is undergoing further evaluation to determine its therapeutic potential against chymase-induced diseases such as asthma.

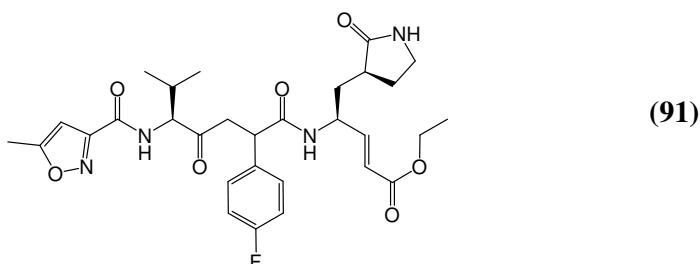


Recently, Cai *et al* (Maxim Pharmaceuticals) have been working on optimizing a series of dipeptidyl aspartyl fluoromethylketones as broad spectrum potent caspase inhibitors. MX1153 **89** was identified as having the best overall activity in the series, with  $IC_{50}$  values ranged between 11-50 nM against caspases-1, -3, -6, -7, -8 and -9. Compound **89** was found to be inactive against two cysteine proteases, calpain-1 and cathepsin B, as well as the serine protease, factor Xa. From the figures published, inhibitor **89** is >5000-fold selective for caspase-3 versus these three non-caspase proteases. This inhibitor was also shown to provide 50% cell protection against apoptosis induced by tumour necrosis factor- $\alpha$  (TNF- $\alpha$ ) at a concentration of 200 nM. It was found to be active in a mouse liver apoptosis model. Intravenous administration at a dosage of 10 mg/kg showed that there was 83% increase in the number of mice surviving after 3 days.



Perhaps the most successful example of a fluorinated protease inhibitor is the substrate derived tripeptidyl Michael acceptor-containing human rhinovirus (HRV) inhibitor Rupintrivir (AG7088) **90**. This inhibitor, developed by Agouron Pharmaceuticals Inc., has emerged as one of the lead candidates for this ailment and is presently undergoing phase III trials for intranasal delivery<sup>161</sup>. Rupintrivir is a potent irreversible inhibitor of HRV 3C protease with an  $EC_{50}$  value of 5 nM. It is a

selective inhibitor of HRV 3C protease with no inhibition of serine or cysteine (cathepsin) proteases occurring at a concentration of 10 nM and was shown to be stable in human plasma, dog plasma and  $\alpha$ -chymotrypsin with half lives of greater than 60 minutes. This drug was one of the first drugs utilized as a potential inhibitor of the SARS outbreak in 2003. Recently, investigative studies have shown that the *p*-fluorophenylalanine side chain is too long (or bulky) to fit into the relevant binding site of the SARS-coronavirus main proteinase (SARS-CoV M<sup>pro</sup>)<sup>162</sup>. Because of this, KZ7088 **91** has been developed with a modified side chain by removing the methylene (-CH<sub>2</sub>-), resulting in a more rigid, shorter side chain. It is hoped this inhibitor **91** will help lead to effective drug candidates for the treatment of SARS.



The incorporation of a fluorine atom has been shown to improve selectivity and bioactivity, and has led to development of some of the most successful pharmaceuticals on the market today. Despite this there are still very few examples of fluorinated protease inhibitors approved by the FDA for therapeutic use. The most potent series of derivatives have been based on a fluoromethyl ketone scaffold. Examples of such derivatives have shown high levels of activity towards both serine and cysteine proteases. They are considerable more stable than their chlorine analogues although their alkylating ability often induced toxic aide effects. The introduction of a trifluoromethyl moiety may be a more successful route for the inhibition of nucleophilic proteases given the steric size of the CF<sub>3</sub> moiety is similar to a chlorine atom and also it has the ability to induce an electrophilic centre. The development of potent selective inhibitors such as KZ7088 **91** furnishes optimism for the development of further fluorinated protease inhibitors.

Dipeptidyl derivatives have been shown to be effective inhibitors of the liver fluke *Fasciola hepatica* cysteine cathepsin L over the known commercial inhibitor Z-Phe-Ala-CHN<sub>2</sub> **31** at varying concentrations<sup>163,164</sup>. Over the past decade, research in our

group has looked at ways of producing potent dipeptidyl protease inhibitors. It is well documented that the inhibition of the protease is due to binding of the inhibitor via the *iso*-butyl side chain. This has been confirmed by our group by modifying the first amino acid in the dipeptide at the P1 position from glycine to phenylalanine. IC<sub>50</sub>'s

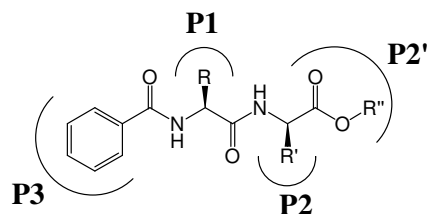


**Figure 1.5:** Points of modification of dipeptide protease inhibitors.

calculated from these derivatives range from 11 to >200  $\mu\text{M}$  for *N-trans*-cinnamoyl-L-Leu glycine nitrile and *N*-nicotinoyl-L-Leu-Ala-OMe, respectively<sup>163</sup>.

Modification at of the second amino acid, at the P2 position and also at the P2' C-terminus has also been done. As with the P1 site, the amino acid was altered to compare the effect of changing the R' group. Also, using unnatural amino acids such as  $\beta$ -alanine and  $\gamma$ -aminobutyric acid, the P2' position was lengthened. Alteration of the C-terminus of the dipeptide from the esters to nitriles to benzyl amides were synthesised. All the synthesised inhibitors were assayed against the cathepsin L endoprotease and the IC<sub>50</sub>'s compared. The resulting optimized dipeptide, containing, L-leucine at P1, glycine nitrile at the P2 and P2' positions and a *para*-substituted fluorine at the P3 position was found to have a 50% inhibitory concentration of 3  $\mu\text{M}$ <sup>164</sup>. This report outlines further investigation into optimizing a potent dipeptidyl inhibitor of the *Fasciola hepatica* cysteine cathepsin L endoprotease.

## 1.7 Conclusion and Aims

Historically, the design of protease inhibitors has incorporated highly reactive electrophilic warheads that alkylate, acylate, phosphorylate or sulphonate the active site residues of proteases. The initial generation of inhibitors, although very potent, showed severe side effects due to their high reactivity and poor selectivity, largely due to their lack of peptidyl character. The incorporation of peptides into potential inhibitors has greatly reduced complications associated with the first generation. The replacement of the peptide backbone with peptidomimetics has been very successful in further improving the bioavailability and stability of inhibitors in biological systems. Finally, the incorporation of moieties such as thiols and hydroxymates, capable of binding to the  $Zn^{2+}$  ion, has results in the most effective metalloproteases inhibitors. Although the degree of potency and selectivity of these metalloprotease inhibitors has been high, the majority have lacked good bioavailability. In recent years, the use of molecular modelling in tandem with crystal structures of the enzyme-inhibitor complexes has played a major role in drug development. These complexes offer important guidelines in the design of inhibitors by displaying a clear picture of the relationship between the conformation of the inhibitor and the active site of the enzyme. When used in combination with library screening, this mechanism of design has been particularly productive.

The inhibition of proteases offers great potential for the treatment of various diseases. Unfortunately there are very few inhibitors that are on the market today. Despite the impressive progress, there is much to learn about the cross talk between signal transduction pathways and protease activation cascades. Additionally, development of successful protease inhibitors for clinical use is reliant on maximising bioavailability, specificity and potency of inhibition of the target enzyme. Ideally, localising protease inhibitors to a single target area of the body may also help minimise the potential for complications and detrimental side effects.

The aim of this project was to develop an inhibitor of the cysteine protease, cathepsin L. This protease has been isolated from a parasite responsible for the disease liver fluke. Previous studies have shown that the L-leucine glycine nitrile scaffold has good potency against this protease. A series of novel dipeptidyl analogues were synthesised investigating fluorine substitution at the *N*-terminus substituent of this dipeptide. Further to this, dipeptides with a variety of *N*-terminal modifications were also prepared.

## 1.8 References

- 1 Jedinak, A., Maliar, T.; *Neoplasma* **2005**, *52*, 3
- 2 Johnson, L.L., Dyer, R., Hupe D.J.; *Curr. Opin. Chem. Biol.* **1998**, 466.
- 3 Baynon, R.J., Bond, J.; “*Proteolytic Enzymes, a practical approach*”, Oxford  
University Press, **1989**.
- 4 Schechter, I., Berger, A.; *Biochem. Biophys. Res. Comm.* **1927**, *27*, 157.
- 5 Harel, M., Su, C.T., Frolow, F., Silman, I., Sussman, J.L.; *Biochemistry* **1991**,  
*30*, 5217.
- 6 Fersht, A.R., Blow, D.M., Fastrez, J.; *Biochemistry* **1973**, *12*, 2035.
- 7 Smith, E.L.; *J. Biol. Chem.* **1958**, *233*, 1392.
- 8 Bender, M.L., Brubacher, L.J.; *J. Amer. Chem. Soc.* **1964**, *86*, 5333.
- 9 Lowe, G.; *Tetrahedron* **1976**, *32*, 291.
- 10 Otto, H.H., Schirmeister, T.; *Chem. Rev.* **1997**, *97*, 133.
- 11 Hofmann, T., Dunn, B.M., Fink, A.L.; *Biochemistry* **1984**, *23*, 5241.
- 12 Powers, J.C., Harper, J.W.; “*Proteinase Inhibitors*”, Elsevier, Amsterdam,  
**1986**.
- 3 Travis, J., Salvesen, G.S.; *Ann. Rev. Biochem.* **1983**, *52*, 655.
- 4 Barrett, A.J., Starkey, P.M.; *Biochem. J.* **1973**, *133*, 709.
- 5 Suda, H., Aoyagi, T., Hamada, M., Takeuchi, T., Umezawa, H.; *J. Antibiot.*  
**1972**, *25*, *4*, 263.
- 6 Sasaki, T., Kikuchi, T., Yumoto, N., Yoshimura, N., Murachi, T.; *J. Biol.*  
*Chem.* **1984**, *259*, 12489.
- 7 Fukiage, C., Azuma, M., Nakamura, Y., Tamada, Y., Nakamura, M., Shearer,  
T.; *Biochem. Biophys. Acta.* **1997**, *1361*, 304.
- 8 Schultz, R.M., Varma-Nelson, K.A., Kozlowski, A.T., Ortiz, R., Orawski, P.,  
Pagast, P., Frankfater, A.; *J. Biol. Chem.* **1988**, *264*, 1497.
- 9 Shaw, E., Mares-Guia, M., Cohen, W.; *Biochemistry* **1965**, *4*, 2219.
- 20 Rauber, P., Angliker, H., Walker, B., Shaw, E.; *Biochem. J.* **1986**, *239*, 633.
- 21 Larsen, K.S., Auld, D.S.; *FASEB J.* **1988**, *2*, 4754.
- 22 Mallya, S.K., Van Wart, H.E.; *J. Biol. Chem.* **1988**, *264*, 1594.
- 23 De Simone, G., Menchise, V., Omaggio, S., Pedone, C., Scozzafava, A.,  
Supuran, C.T.; *Biochemistry* **2003**, *42*, 9013.

- 24 Vacca, J.P.; *Curr. Opin. Chem. Biol.* **2000**, *4*, 394.
- 25 Leung, D., Abbenante, G., Fairlie, D.P.; *J. Med. Chem.* **2000**, *43*, 305.
- 26 Danilewicz, J.C., Abel, S.M., Brown, A.D., Fish, P.V., Hawkeswood, E.,  
Holland, S.J., James, K., McElroy, A.B., Overington, J., Powling, M.J., Rance,  
D.J.; *J. Med. Chem.* **2002**, *45*, 2432.
- 27 Hursting, M.J., Alford, K.L., Becker, J.C.; *Semin. Thromb. Hemost.* **1997**, *23*,  
503.
- 28 Rawson, T.E., Van Gorp, K.A., Yang, J., Kogan, T.P.; *J. Pharm. Sci.* **1993**,  
*82*, 672.
- 29 Yeh, R.W., Jang, I.K.; *American Heart Journal* **2006**, *151*, 6, 1131.
- 30 Malley, M.F., Taberero, L., Chang, C.J., Ohringer, S.I., Roberts, D.G.M.,  
Das, J., Sack, J.S.; *Protein Science* **1996**, *5*, 221.
- 31 Das, J., Kimball, D.S., Reid, J.A., Wang, T.C., Lau, W.F., Roberts, D.G.M.,  
Seiler, S.M., Schumacher, W.A., Ogletree, M.L.; *Bioorg. Med. Chem. Lett.*  
**2002**, *12*, 41.
- 32 Gustafsson, D., Bylund, R., Antonsson, T., Nilsson, I., Nyström, J.E.,  
Eriksson, U., Bredberg, U., Teger-Nilsson, A.; *Nat. Rev. Drug Disc.* **2004**, *3*,  
649.
- 33 Iddb3 database: Drug Report on Ximelagatran.
- 34 Mack, H., Baucke, D., Hornberger, W., Lange, U.E.W., Seitz, W., Höffken,  
H.W.; *Bioorg. Med. Chem. Lett.* **2006**, *16*, 2641.
- 35 Lange, U.E.W., Baucke, D., Hornberger, W., Mack, H., Seitz, W., Höffken,  
H.W.; *Bioorg. Med. Chem. Lett.* **2006**, *16*, 2648.
- 36 Lee, K., Park, C.W., Jung, W.H., Park, H.D., Lee, S.H., Chung, K.H., Park,  
S.K., Kwon, O.H., Kang, M., Park, D.H., Lee, S.K., Kim, E.E., Yoon, S.K.,  
Kim, A.; *J. Med. Chem.* **2003**, *46*, 3612.
- 37 Lee, K., Jung, W.H., Hwang, S.Y., Lee, S.H.; *Bioorg. Med. Chem. Lett.* **2002**,  
*12*, 1017.
- 38 Brady, S.F., Stauffer, K.J., Lumma, W.C., Smith, G.M., Ramjit, H.G., Lewis,  
S.D., Lucas, B.J., Gravel, S.J., Lyle, E.A., Appleby, S.D., Cook, J.J., Harahan,  
M.A., Strainer, M.T., Lynch, J.J., Lin, J.H., Chen, I.W., Vista, K., Naylor-  
Olsen, A.M., Vacca, J.P.; *J. Med. Chem.* **1998**, *41*, 401.
- 39 Stauffer, K.J., Williams, P.D., Slick, H.G., Nattered, P.G., Newton, C.L.,  
Hummock, C.F., Radar, M.M., Lewis, S.D., Lucas, B.J., Krueger, J.A., Pieta,

- B.L., Lyle, E.A., Singh, R., Miller-Stein, C., White, R.B., Wong, B., Wallace, A.A., Sitka, G.R., Cook, J.J., Harahan, M.A., Stranieri-Michener, M.T., Leonard, Y.M., Lynch, J.J., McMasters, D.R., Yan, Y.; *J. Med. Chem.* **2005**, *48*, 2282.
- 40 Hlasta, D.J., Subramanyam, C., Bell, M.R., Carabateas, P.M., Court, J.J., Desai, R.C., Drozd, M.L., Eickhoff, W.M., Ferguson, E.W., Gordon, R.J., Johnson, J.A., Kumar, V., Maycock, A.L., Mueller, K.R., Pagani, E.D., Robinson, D.T., Saindane, M.T., Silver, P.J., Subramanian, S.; *J. Med. Chem.* **1995**, *38*, 5, 739.
- 41 Ohbayashi, H.; *Expert Opin. Ther. Patents* **2002**, *12*, 1, 65.
- 42 Kawabata, K., Hagio, T., Matsuoka, S.; *Eur. J. Pharmacol.* **2002**, *451*, 1.
- 43 Kawabata, K., Hagio, T., Matsuoka, S.; *Folia Pharmacol. Jpn.* **2003**, *122*, 151.
- 44 Amitani, R., Wilson, R., Rutman, A., Read, R., Ward, C., Burnett, D., Stockley, R.A., Cole, P.J.; *Am. J. Respir. Cell Mol. Biol.* **1991**, *4*, 26.
- 45 Hagio, T., Nakao, S., Matsuoka, S., Matsumoto, S., Kawabata, K., Ohno, H.; *Eur. J. Pharmacol.* **2001**, *426*, 131.
- 46 Suzuki, T., Wang, W., Lin, J.T., Shirato, K., Mitsuhashi, H., Inoue, H.; *Am. J. Respir. Crit. Care Med.* **1996**, *153*, 1405.
- 47 Fujimoto, K., Kubo, K., Shinozaki, S., Okada, K., Matsuzawa, Y., Kobayashi, T., Sugane, K.; *Respir. Physiol.* **1995**, *100*, 91.
- 48 Matsumoto, K., Aizawa, H., Inoue, H., Koto, H., Nakano, H., Hara, N.; *Eur. Respir. J.* **1999**, *14*, 1088.
- 49 Takayama, N., Uchida, K.; *J. Smooth Muscle Res.* **2005**, *41*, 5, 257.
- 50 Luisetti, M., Sturani, C., Sella, D., Madonini, E., Galavotti, V., Bruno, G., Peona, V., Kucich, U., Dagnino, G., Rosenbloom, J., Starcher, B., Grassi, C.; *Eur Respir J.* **1996**, *9*, 1482.
- 51 Lever, R., Page, C.P.; *Nat. Rev. Drug Discovery* **2002**, 140.
- 52 Spencer, J.L., Stone, P.J., Nugent, M.A.; *Biochemistry* **2006**, *45*, 9104.
- 53 Fryer, A., Huang, Y.C., Rao, G., Jacoby, D., Mancilla, E., Whortan, R., Piantadosi, C.A., Kennedy, T., Hoidal, J.; *J. Pharmacol. Exp. Ther.* **1997**, *282*, 208.
- 54 Rode, H., Koerbe, S., Besch, A., Methling, K., Loose, J., Otto, H.H.; *Bioorg. Med. Chem.* **2006**, *14*, 2789.
- 55 Edwards, P.D., Bernstein, P.R.; *Med. Res. Rev.* **1994**, *14*, 2, 127.



- 56 Takahashi, L.H., Radhakrishnan, R., Rosenfield, R.E., Meyer, E.F.;  
*Biochemistry* **1989**, *28*, 7610.
- 57 Costanzo, M.J., Yabut, S.C., Almond, H.R., Andrade-Gordon, P., Corcoran,  
T.W., De Garavilla, L., Kauffman, J.A., Abraham, W.M., Recacha, R.,  
Chattopadhyay, D., Maryanoff, B.E.; *J. Med. Chem.* **2003**, *46*, 3865.
- 58 Clark, J.M., Moore, W.R., Tanaka, R.D.; *Drugs Future* **1996**, *21*, 811. (Update:  
Anon. APC-3 66. *Drugs Future* **1998**, *23*, 903.)
- 59 Rice, K.D., Tankaka, R.D., Katz, B.A., Numerof, R.P., Moore, W.A.; *Curr.*  
*Pharm. Design* **1998**, *4*, 381.
- 60 Burgess, L.E.; *Drug News Perspect.* **2000**, *13*, 147.
- 61 Palmer, J.T., Rydzewski, R.M., Mendonca, R.V., Sperandio, D., Spencer, J.R.,  
Hirschbein, B.L., Lohman, J., Beltma, J., Nguyen, M., Liu, L.; *Bioorg. Med.*  
*Chem. Lett.* **2006**, *16*, 3434.
- 62 Pereira, P.J.B., Bergner, A., Macedo-Ribeiro, S., Huber, R., Mastchiner, G.,  
Fritz, H., Sommerhoff, C.P., Bode, W.; *Nature* **1998**, *392*, 306.
- 63 Del Fresno, M., Fernandez-Forner, D., Miralpeix, M., Segarra, V., Ryder, H,  
Royo, M., Albericio, F.; *Bioorg. Med. Chem. Lett.* **2005**, *15*, 1659.
- 64 Caughey, G.H., Raymond, W.W., Bacci, E., Lombardy, R.J., Tidwell, R.R.; *J.*  
*Pharm. Exp. Ther.* **1993**, *264*, 676.
- 65 Katz, B.A., Clark, J.M., Finer-Moore, J.S., Jenkins, T.E., Johnson, C.R., Ross,  
M.J., Luong, C., Moore, W.R., Stroud, R.M.; *Nature* **1993**, *391*, 608.
- 66 Löser, R., Schilling, K., Dimmig, E., Gütschow, M.; *J. Med. Chem.* **2005**, *48*,  
7688.
- 67 Tallen, H., Jones, M., Fruton, J.; *J. Biol. Chem.* **1952**, *194*, 793.
- 68 Mendonca, R.V., Venkatraman, S., Palmer, J.T.; *Bioorg. Med. Chem. Lett.*  
**2002**, *12*, 2887.
- 69 Fried, B., Graczyk, T.K.; “*Advances in Trematode Biology*”, CRC Press, LLC,  
New York, **1997**.
- 70 Zhou, N.E., Guo, D., Kaleta, J., Purisima, E., Menard, R., Micetich, R.G.,  
Singh, R.; *Bioorg. Med. Chem. Lett.* **2002**, *12*, 3413.
- 71 Altmann, E., Renaud, J., Green, J., Farley, D., Cutting, B., Jahnke, W.; *J. Med.*  
*Chem.* **2002**, *45*, 2352.

- 72 Shinozuka, T., Shimada, K., Matsui, S., Yamane, T., Ama, M., Fukuda, T., Taki, M., Takeda, Y., Otsuka, E., Yamato, M., Mochizuki, S., Ohhata, K., Naito, S.; *Bioorg. Med. Chem.* **2006**, *14*, 20, 6789.
- 73 Tavares, F.X., Deaton, D.N., Miller, A.B., Miller, L.R., Wright, L.L., Zhou, H.Q.; *J. Med. Chem.* **2004**, *47*, 5049.
- 74 Rousselet, N., Mills, L., Jean, D., Tellez, C., Bar-Eli, M., Frade, R.; *Cancer Res.* **2004**, *64*, 146.
- 75 Marquis, R.W., James, I., Zeng, J., Trout, R.E.L., Thompson, S., Rahman, A., Yamashita, D.S., Xie, R., Ru, Y., Gress, C.J., Blake, S., Lark, M.A., Hwang, S.M., Tomaszek, T., Offen, P., Head, M.S., Cummings, M.D., Veber, D.F.; *J. Med. Chem.* **2005**, *48*, 6870.
- 76 Barret, A.J., Kembhavi, A.A., Brown, M.A., Kirschke, H., Knight, C.G., Tamai, M., Hanada, K.; *Biochem. J.* **1982**, *201*, 189.
- 77 Marquis, R. W., Ru, Y., LoCastro, S. M., Zeng, J., Yamashita, D. S., Oh, H.-J., Erhard, K. E., Davis, L. D., Tomaszek, T. A., Tew, D., Salyers, K., Proksch, J., Ward, K., Smith, B., Levy, M., Cummings, M. D., Haltiwanger, R. C., Trescher, G., Wang, B., Hemling, M. E., Quinn, C. J., Cheng, H.-Y., Lin, F., Smith, W. W., Janson, C. A., Zhao, B., McQueney, M. S., D'Alessio, K., Lee, C.-P., Marzulli, A., Dodds, R. A., Blake, S., Hwang, S.-M., James, I. E., Gress, C. J., Bradley, B. R., Lark, M. W., Gowen, M., Veber, D. F.; *J. Med. Chem.* **2001**, *44*, 1380.
- 78 Patterson, A.W., Wood, W.J.L., Hornsby, M., Lesley, S., Spraggon, G., Ellman, J.A.; *J. Med. Chem.* **2006**, *49*, 6298.
- 79 Budihardjo, I., Oliver, H., Lutter, M., Luo, X., Wang, X.; *Annu. Rev. Cell Dev. Biol.* **1999**, *15*, 269.
- 80 Cohen, G.M.; *Biochem. J.* **1997**, *326*, 1.
- 8 Ashwell, S.; *Exp. Opin. Ther. Pat.* **2001**, *11*, 1593.
- 82 Zhu, H., Fearnhead, H. O., Cohen, G.A.; *FEBS Lett.* **1995**, *374*, 303.
- 83 Karanewsky, D.S., Bai, X., Linton, S.D., Krebs, J.F., Wu, J., Pham, B., Tomaselli, K.J.; *Bioorg. Med. Chem. Lett.* **1998**, *8*, 2757.
- 84 Deckwerth, T.L., Adams, L.M., Weissner, C., Allegrini, P.R., Rudin, M., Sauter, A., Hengerer, B., Sayers, R.O., Rovelli, G., Aja, T., May, R., Nalley, K., Linton, S., Karanewsky, D.S., Wu, J.C., Roggo, S., Schmitz, A., Contreras, P.C., Tomaselli, K.J.; *Drug. Dev. Res.* **2001**, *52*, 579.

- 85 Linton, S.D., Aja, T., Armstrong, R.A., Bai, X., Chen, L.-S., Chen, L., Ching, B., Contreras, P., Diaz, J.L., Fisher, C.D., Fritz, L.C., Gladstone, P., Groessal, T., Gu, X., Herrmann, J., Hirakawa, B.P., Hoglen, N.C., Jahangiri, K.G., Kalish, V.J., Karanwsky, D.S., Kodandapani, L., Krebs, J., McQuiston, J., Meduna, S.P., Nalley, K., Robinson, E.D., Sayers, R.O., Sebring, K., Spada, A.P., Ternansky, R.J., Tomaselli, K.J., Ullman, B.R., Valentino, K.L., Weeks, S., Winn, D., Wu, J.C., Yeo, P., Zhang, C.; *J. Med. Chem.* **2005**, *48*, 6779.
- 86 Lall, M.S., Jain, R.P., Vederas, J.C.; *Curr. Top. Med. Chem.* **2004**, *4*, 1239.
- 87 Ma, J.D., Nafziger, A.,N., Rhodes G., Liu S., Gartung A.M., Bertino Jr, J.S.; *J. Clin. Pharmacol.* **2006**, *46*, 103.
- 88 Pevear, D.C., Tull, T.M., Seipel, M.E., Groarke, J.M.; *Antimicrob. Agents Ch.* **1999**, *43*, 9, 2109.
- 89 Desmond, R.A., Accortt, N.A., Talley, L., Villano, S.A., Soong, S.J., Whitley, R.J.; *Antimicrob. Agents Ch.* **2006**, *50*, 7, 2409.
- 90 Lien, E.J., Gao, H., Lien, L.L.; *Prog. Drug Res.* **1994**, *43*, 43.
- 9 Seijffers, M.J., Miller, L.L., Segal, H.L.; *Biochemistry* **1964**, *3*, 1203.
- 92 Gulnik, S., Baldwin, E.T., Tarasova, N., Erickson, J.; *J. Mol. Biol.* **1992**, *227*, 265.
- 93 Silva, A.M., Lee, A.Y., Gulnik, S.V., Maier, P., Collins, J., Bhat, T.N., Collins, P.J., Cachau, R.E., Luker, K.E., Gluzman, I.Y., Francis, S.E., Oksman, A., Goldberg, D.E., Erickson, J.W.; *Proc. Natl. Acad. Sci., U.S.A.* **1996**, *93*, 10034.
- 94 Drake, P.L., Huff, J.R.; *Adv. Pharmacol., (San Diego)* **1994**, *5*, 399.
- 95 Vassar, R., Bennet, B.D., Babu-Khan, S., Kahn, S., Mendiaz, E.A., Denis, P., Teplow, D.B., Ross, S., Amarante, P., Loeloff, R., Luo, Y., Fisher, S., Fuller, J., Edneson, S., Lile, J., Jarosinski, M.A., Biere, A.L., Curran, E., Burgess, T., Louis, J.-C., Collins, F., Treanor, J., Rogere, G., Citron, M.; *Science* **1999**, *286*, 735.
- 96 Ferro, A., Gilbert, R., Krum, H.; *Int. J. Clin. Pract.* **2006**, *60*, 5, 577.
- 97 Umezawa, H., Aoyagi, T., Morishima, H., Matsuzaki, M., Hamada, M., Takeuchi, T.; *J. Antibiot. (Japan)* **1970**, *23*, 259.
- 98 Glassman, H.N., Kleinert H.D., Boger R.S., Moyse D.M., Griffiths A.N., Luther R.R.; *J. Cardiovasc. Pharmacol.* **1990**, *16* Suppl 4 S76-81.
- 99 Staessen, J.S., Li, Y., Richart, T.; *Lancet* **2006**, *368*, 1449.

- 100 Wood, J.M., Maibaum, J., Rahuel, J.; *Biochem. Biophys. Res. Commun.* **2003**,  
308, 698.
- 101 Holsworth, D.D., Cai, C., Cheng, X.M., Cody, W.L., Downing, D.M., Erasga,  
N., Lee, C., Powell, N.A., Edmunds, J.J., Stier, M., Jalaie, M., Zhang, E.,  
McConnell, P., Ryan, M.J., Bryant, J., Li, T., Kasani, A., Hall, E., Subedi, R.,  
Rahim, M., Maiti, S.; *Bioorg. Med. Chem. Lett.* **2006**, 16, 2500.
- 102 Wrighton, S. A., Schuetz, E. G., Thummel, K. E., Shen, D. D., Korzekwa, K.  
R., Watkins, P. B.; *Drug Metab. Rev.* **2000**, 32, 339.
- 103 Sieburth, S., Chen, C.-A.; *Eur. J. Org. Chem.* **2006**, 311.
- 104 Hof, F., Schütz, A., Fäh, C., Meyer, S., Bur, D., Liu, J., Goldberg, D.E.,  
Diederich, F.; *Angew. Chem. Int. Ed.* **2006**, 45, 2138.
- 105 Joshi, A.A., Viswanathan, C.L.; *Anti-Infect. Agents Med. Chem.* **2006**, 5, 1,  
105.
- 106 Ersmark, K., Nervall, M., Gutierrez-de-Teran, H., Hamelink, E., Janka, L.K.,  
Clemente, J.C., Dunn, B.M., Gogoll, A., Samuelsson, B., Aqvist, J., Hallberg,  
A.; *Bioorg. Med. Chem.* **2006**, 14, 2197.
- 107 Corbett, E. L., Steketee, R. W., ter Kuile, F. O., Latif, A. S., Kamali, A.,  
Hayes, R. J.; *Lancet* **2002**, 359, 2177.
- 108 Wlodawer, A., Vondrasek, J.; *Annu. Rev. Biophys. Biomol. Struct.* **1998**, 27,  
249.
- 109 Erickson, J.W., Eissenstat, M.A.; "Proteases of Infectious Agents" (Ed.: B.M.  
Dunn), Academic, New York, **1999**
- 10 Kempf, D.J.; *Methods Enzymol.* **1994**, 241, 334.
- 111 De Lucca, G.V., Jadhav, P.K., Waltermire, R.E., Aungst, B.J., Erickson-  
Viitanen, S., Lam, P.Y.; *Pharm. Biotechnol.* **1998**, 11, 257.
- 112 Lam, P.Y., Ru, Y., Jadhav, P.K., Aldrich, P.E., DeLucca, G.V., Eyermann,  
C.J., Chang, C.H., Emmett, G., Holler, E.R., Daneker, W.F., Li, L., Confalone,  
P.N., McHugh, R.J., Han, Q., Li, R., Markwalder, J.A., Seitz, S.P., Sharpe,  
T.R., Bacheler, L.T., Rayner, M.M., Klabe, R.M., Shum, L., Winslow, D.L.,  
Kornhauser, D.M., Hodge, C.N.; *J. Med. Chem.* **1996**, 39, 3514.
- 113 Jadhav, P.K., Francis, P.A., Woerner, J., Chang, C.-H., Garber, S.S., Anton,  
E.D., Bacheler, L.T.; *J. Med. Chem.* **1997**, 40, 181.
- 114 Parikh, S., Liu, J., Sijwali, P., Gut, J., Goldberg, D.E., Rosenthal, P.J.;  
*Antimicrob. Agents Ch.* **2006**, 50, 6, 2207.

115 De Clercq, E.; *J. Clin. Virol.* **2004**, *30*, 115.

116 Witvrow, M., Pannecouque, C., Switzer, W.M., Folks, T.M., De Clercq, E.,  
Heneine, W.; *Antiviral Ther.* **2004**, *9*, 57.

117 Pakyz, A., Israel, D.; *J. Am. Pharm. Assoc.* **1997**, *5*, 543.

118 <http://www.rocheusa.com>

119 Reuters, October 20, **2006**.

120 Swainston Harrison, T., Scott, L.J.; *Drugs* **2005**, *65*, 16, 2309.

121 Croom, K.F., Keam, S.J.; *Drugs* **2005**, *65*, 12, 1669.

122 Ghosh, A.K., Sridhar, P.R., Leshchenko, S., Hussain, A.K., Li, J., Kovalevsky,  
A.Y., Walters, D.E., Wedekind, J.E., Grum-Tokars, V., Das, D., Koh, Y.,  
Maeda, K., Gatanaga, H., Weber, I.T., Mitsuya, H.; *J. Med. Chem.* **2006**, *49*,  
5252.

123 Surleraux, D.L.N.G., Tahri, A., Verschueren, W.G., Pille, G.M.E., de Kock,  
H.A., Jonckers, T.H.M., Peeters, A., De Meyer, S., Azijn, H., Pauwels, R., de  
Bethune, M.-P., King, N.M., Prabu- Jeyabalan, M., Schiffer, C. A., Wigerinck,  
P.B.T.P.; *J. Med. Chem.* **2005**, *48*, 1813.

124 Mattson, M.P.; *Nature* **2004**, *430*, 631.

125 LaFerla, F.M., Oddo, S.; *Trends Mol. Med.* **2005**, *11*, 170.

126 Joachim, C.L., Selkoe, D.J.; *Alzheimer Dis. Assoc. Disord.* **1992**, *6*, 7.

127 Li, R., Lindholm, K., Yang, L.-B., Yue, X., Citron, M., Yan, R., Beach, T.,  
Sue, L., Sabbagh, M., Cai, H., Wong, P., Price, D., Shen, Y.; *Proc. Natl. Acad.*  
*Sci., U.S.A.* **2004**, *101*, 3632.

128 Schmidt, B.; *ChemBioChem.* **2003**, *4*, 366.

129 Hanessian, S., Yang, G., Rondeau, J.-M., Neumann, U., Betschart, C.,  
Tintelnot-Blomley, M.; *J. Med. Chem.* **2006**, *49*, 4544.

130 Godel, T., Hilpert, H., Humm, R., Rogers-Evans, M., Rombach, D., Stahl, C.  
M., Weiss, P., Wostl, W., *U.S. Patent*, 2005119329, **2005**.

131 Larbig, G., Schmidt, B.; *J. Comb. Chem.* **2006**, *8*, 480.

132 Felsenstein, K., Smith, D.W., Poss, M.A., Chaturvedula, P., Sloan, C.P.;  
(Bristol-Myers Squibb Co., USA), EP 778266 **1997**.

133 Ghosh, A.K., Bilcer, G., Harwood, C., Kawahama, R., Shin, D., Hussain,  
K.A., Hong, L., Loy, J.A., Nguyen, C., Koelsch, G., Ermolieff, J., Tang, J.; *J.*  
*Med. Chem.* **2001**, *44*, 2865.

- 134 Ghosh, A.K., Shin, D., Downs, D., Koelsch, G., Lin, X., Ermolieff, J., Tang,  
J.; *J. Am. Chem. Soc.* **2000**, *122*, 3522.
- 135 Maillaird, M., Hom, C., Gailunas, A., Jagodzinska, B., Fang, L.Y., John, V.,  
Freskos, J.N., Pulley, S.R., Beck, J.P., Tenbrink, R.E.; (Elan Pharmaceuticals,  
Inc., USA; Pharmacia & Upjohn Company), WO 0202512, **2002**.
- 136 Beck, J.P., Gailunas, A., Hom, R., Jagodzinska, B., John, V., Maillaird, M.;  
(Elan Pharmaceuticals, Inc., USA; Pharmacia & Upjohn Company), *PCT Int.*  
*Appl.*, WO 0202520, **2002**.
- 137 Latimer, L.H., Stappenbeck, F., Jenkins, S., Nagarajan, L., Wu, J., Thorsett,  
E.D., Wogulis, M., Powell, K., Cunningham, D., Rydel, R.E., Seubert, P.;  
*Abstr. Pap.-Am. Chem. Soc.* **2001**, 221st.
- 138 Miyamoto, M., Matsui, J., Fukumoto, H., Tarui, N.; (Takeda Chemical  
Industries, Ltd., Japan), WO 0187293, **2001**.
- 139 Ramakrishna, N.V.S., Kumar, E.K.S.V., Kulkarni, A.S., Jain, A.K., Bhat,  
R.G., Parikh, S., Quadros, A., Deuskar, N., Kalakoti, B.S.; *Indian J. Chem.*  
*Sect B: Org. Chem. Incl. Med. Chem.* **2001**, *40*, 539.
- 140 Leng, J.; (Chemicon International, Inc., USA), WO 0206458, **2002**.
- 141 Hanessian, S., Moitessier, N., Gauchet, C., Viau, M.; *J. Med. Chem.* **2001**, *44*,  
3066.
- 142 Patchett, A.A., Harris, E., Tristram, E.Q.; *Nature* **1980**, *288*, 5788, 280.
- 143 <http://www.diovan.com>
- 144 Foda, H.D., Zucker, S.; *Drug Discovery Today* **2001**, *9*, 478.
- 145 Whittaker, M., Floyd, C.D., Brown, P., Gearing, A.J.H.; *Chem. Rev.* **1999**, *99*,  
2735.
- 146 Rao, B.G.; *Curr. Pharm. Design* **2005**, *11*, 295.
- 147 Kontogiorgis, C.A., Papaioannou, P., Hadjipavlou-Litina, D.J.; *Curr. Med.*  
*Chem.* **2005**, *12*, 339.
- 148 Coussens, L.M., Fingleton, B., Rothenberg, M.L., Matrisian, L.M.; *Science*  
**2002**, *295*, 2387.
- 149 Coussens, L.M., Fingleton, B., Matrisian, L.M.; *Science* **2002**, *295*, 2387.
- 150 Borkakoti, N.; *Biochem. Soc. T.* **2004**, *32*, 1, 17.
- 151 Emeléus, H.J.; “*The Chemistry of Fluorine and its Compounds*”, Academic  
Press, New York, London, **1969**.

- 152 Park, B.K., Kitteringham, N.R., O'Neill, P.M.; *Annu. Rev. Pharamcol. Toxicol.* **2001**, *41*, 443
- 153 Rosenblum, S.B., Huynh, T., Afonso, A., Davis, Jr., H.R., Yumibe, N., Clader, J.W., Burnett, D.A.; *J. Med. Chem.* **1998**, *41*, 973.
- 154 Welch, J.T., Eswarakrishnan, S.; “*Fluorine in Bioorganic Chemistry*”, Wiley and Sons, New York, **1991**.
- 155 Frutos, S., Tarrago, T., Giralt, E.; *Bioorg. Med. Chem. Lett.* **2006**, *16*, 2677.
- 156 Ni, L.M., Powers, J.C.; *Bioorg. Med. Chem.* **1998**, *6*, 1767.
- 157 Bartlett, P.A., Lamden, L.A.; *Bioorg. Chem.* **1986**, *14*, 356.
- 158 Imperiali, B., Abeles, R.H.; *Biochemistry* **1986**, *25*, 3760.
- 159 Gelb, M.H., Svaren, J.P., Abeles, R.H.; *Biochemistry* **1985**, *24*, 1813.
- 160 Akahoshi, F., Ashimori, A., Sakashita, H., Yoshimura, T., Eda, M., Imada, T., Nakajima, M., Mitsutomi, N., Kuwahara, S., Ohtsuka, T., Fukaya, C., Miyazaki, M., Nakamura, N.; *J. Med. Chem.* **2001**, *44*, 1297.
- 161 Binford, S.L., Maldonado, F., Brothers, M.A., Weady, P.T., Zalman, L.S., Meador III, J.W., Matthews, D.A., Patick, A.K.; *Antimicro. Agents Ch.* **2005**, *49*, 2, 619.
- 162 Chou, K.-C., Wei, D.-Q., Zhong, W.-Z.; *Biochem. Biophys. Res. Comm.* **2003**, *308*, 148.
- 163 Sheehy, M.J.; “*The design and synthesis of novel peptide derivatives as malarial protease inhibitors and electrochemical anion sensing receptors*”, Dublin City University, *PhD Thesis*, **1999**.
- 164 Anderson, F.P.; “*The synthesis, structural characterisation and biological evaluation of potential chemotherapeutic agents*”, Dublin City University, *PhD Thesis*, **2005**.

## 2.0 Synthesis and characterisation of novel dipeptide derivatives

### 2.1 Introduction

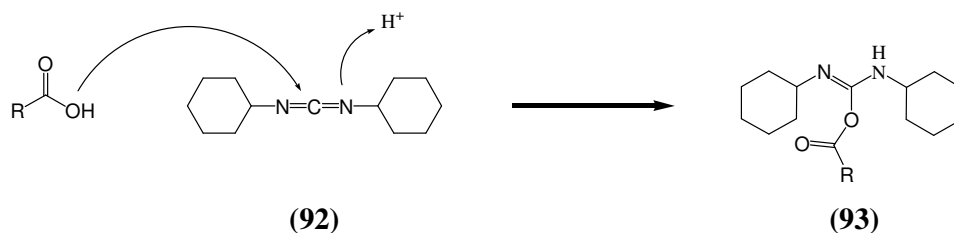
The group of cysteine proteases known as the cathepsins have been shown to play a crucial part in diseases such as osteoporosis, rheumatoid arthritis, cancer metastasis and infectious diseases<sup>1</sup>. Cathepsins are important targets for the development of inhibitors as therapeutic agents. Fasciolosis is caused by infection with *Fasciola hepatica* (temperate) and *Fasciola gigantica* (tropical) parasites. It is not only an important human disease but also affects cattle and sheep. In 1999 it was estimated that Fasciolosis was causing annual worldwide economic losses in the region of two billion dollars. It was also estimated at this time that 2.4 million people are infected with liver fluke worldwide<sup>2,3</sup>. Fasciolosis is acquired following the ingestion of vegetation or water contaminated with the encysted infectious liver fluke larvae, known as metacercariae<sup>4</sup>. It has long been known that the predominant protease activity in this parasite was associated with cells of the gut epithelium<sup>5</sup>. Like many other parasitic helminthes, *Fasciola hepatica* liver flukes release proteolytic enzymes that belong to the group of cysteine proteases. It has been suggested by Heffernan *et al*, that these proteases may be required for preventing attack by the host immune system, against the parasite<sup>6</sup>. The majority of the more recent methodology towards cathepsin inhibition utilises molecules of a peptidic nature. An electrophilic moiety is used to replace the hydrolysable amide bond and the catalytic thiol of the enzyme reacts with the inhibitor to form a covalent complex. Electrophilic groups such as an aldehyde, halomethyl ketone and epoxide have been shown to be potent cysteine protease inhibitors<sup>7,8</sup>. Peptidic molecules bearing the electrophilic nitrile moiety have been reported as having inhibitory activity towards cathepsins. One of the first such examples was the dipeptidyl derivative *N*-benzoyl-Leu-Gly-CN synthesised by Suzue *et al* in 1968<sup>9</sup>. Previous work in this laboratory has shown this to be a potent inhibitor of the *Fasciola hepatica* protease<sup>10,11</sup>. For this study all of the compounds are based on a dipeptidyl scaffold, with the initial study using a fluorobenzoyl dipeptide. The second protease inhibitor study will concentrate on modifying the *N*-terminal of the



dipeptide scaffold. The fluorobenzoyl moiety has been shown to be an effective *N*-terminal substitution in various potent inhibitors<sup>12</sup>. There are generally two consequences of introducing fluorine into a drug molecule, the physiochemical properties and the altering of susceptibility to metabolism of the drug molecule. The physiochemical properties that are affected by fluorine substitution are an increase in lipophilicity, increased acidity, decreased basicity and an alteration in the hydrogen bonding properties. The inductive electron withdrawing effect of fluorine is expected due to its electronegative nature, but electron donation by resonance effects attributed to the three lone pair electrons is a distinctive property of fluorine. The second consequence of fluorine introduction comes about as a result of the strength of the carbon-fluorine bond, which is very difficult to metabolise. Therefore, potentially harmful and unproductive side reactions due to the metabolism of the molecule are significantly reduced.

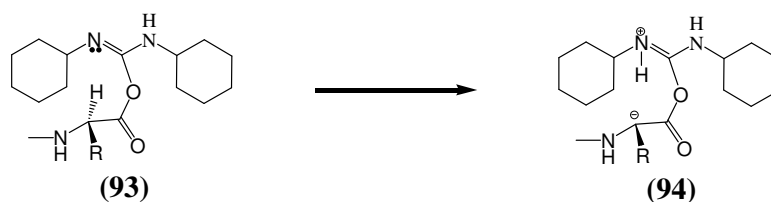
## 2.2 Synthesis of the dipeptidyl derivatives

The synthesis of dipeptides containing the amino acids L-leucine and glycine with *N*- and *C*-terminal modifications was carried out. The amino acids were coupled using an activation agent 1,3-dicyclohexylcarbodiimide (DCC) **92**. The mode of action of DCC involves the formation of an *O*-acylisourea intermediate **93** that is a potent acylating agent.



**Scheme 2.1:** Mode of action of peptide coupling with DCC

Unfortunately there are some disadvantages in using DCC as a coupling agent. Activation by **92** is shown to cause racemisation of the carboxy terminal residue. Reactive intermediates produced during coupling contain a basic centre, which causes an intramolecular proton abstraction from the chiral carbon atom.

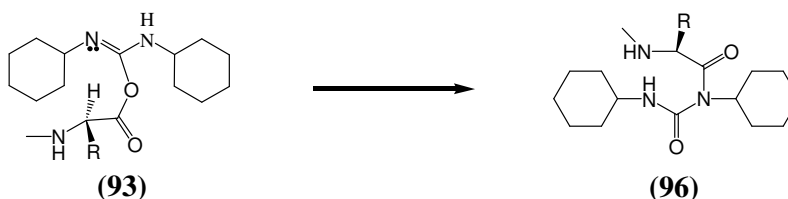


**Scheme 2.2:** Mode of racemisation of the carbonyl terminal residue upon activation with DCC

Chiral integrity can be preserved by the use of 1-hydroxybenzotriazole (HOBt) **95**. HOBt acts as an auxiliary nucleophile and reduces the lifetime of the *O*-acylisourea intermediate thus decreasing the occurrence of racemisation. An acylating agent of lower potency is formed which is still reactive to aminolysis, but is less susceptible to racemisation or other side reactions. 1-Hydroxybenzotriazole also offers an acidic hydrogen that can be more easily removed by bases than the proton at the chiral centre.



Low yields are often another feature of peptide coupling using DCC **92**. These low yields can be accounted for due to the formation of an *N*-acylurea derivative **96** via an intramolecular rearrangement of the *O*-acyl derivative **93** formed by activation with DCC **92**. The attack of the activated carbonyl group by the nearby nucleophilic  $\text{-NH-}$  results in an *O* to *N* shift yielding an *N*-acylurea side product **96**.



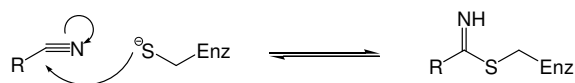
**Scheme 2.3:** Formation of an *N*-acyl derivative **96** via intramolecular rearrangement of the *O*-acylisourea derivative.

Another disadvantage of coupling peptides with 1,3-dicyclohexylcarbodiimide is poor reaction rates. The employment of HOBt and similar derivatives has greatly enhanced the ability of DCC to couple amino acids effectively. More recently, the design of peptide coupling reagents has concentrated in the ability of the reagent to

limit the onset of racemisation while at the same time offering a highly competent coupling agent whose side products can be easily removed. This method of design has resulted in coupling reagents incorporating the coupling ability of DCC and the racemisation suppression activity of HOBT being developed and utilised as effective combination type reagents<sup>13</sup>.

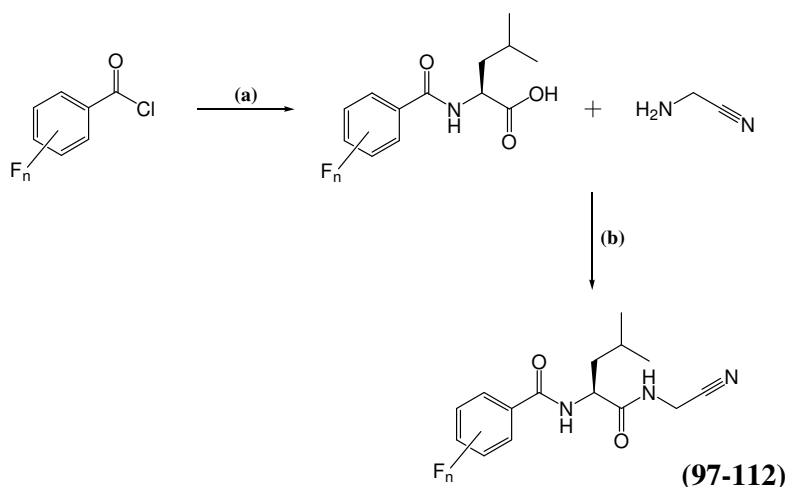
### 2.2.1 *N*-fluorobenzoyl dipeptidyl nitriles

The majority of recent research with nitrile derivatives has concentrated on developing the N-terminal substituent next to the P2 position with the fluorobenzyl moiety showing increased selectivity<sup>14</sup>. Dipeptidyl nitrile derivatives are believed to function as reversible inhibitors with the nitrile moiety undergoing attack by the activated thiol group of cysteine in the active site of the protease (**Scheme 2.4**). <sup>1</sup>H NMR studies have shown that inhibition occurs through the formation of a thioimide intermediate and this process is fully reversible<sup>15</sup>.



**Scheme 2.4:** Mechanism of nitrile inhibition of cysteine proteases

Dipeptidyl derivatives have been shown to be effective inhibitors of the liver fluke *Fasciola hepatica* cysteine cathepin L over the known commercial inhibitor Z-Phe-Ala-CHN<sub>2</sub> **31**<sup>10,11</sup>. The introduction of a fluorine atom into a system can drastically change the biological potency of a drug<sup>16</sup>. The synthesis of a series of benzoyl dipeptidyl nitriles incorporating fluorine atoms at various positions on the phenyl ring was undertaken to assess the effect of the fluorobenzoyl substituent. It has been shown that molecules containing the electrophilic nitrile warhead are potent inhibitors of cathepsin proteases<sup>17</sup>. A series of derivatives were synthesised as illustrated in **Scheme 2.5**.



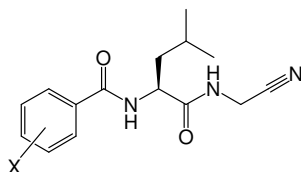
**Scheme 2.5:** Synthesis of N-fluorobenzoyl-L-leucine glycine nitrile derivatives

(a) L-Leu, H<sub>2</sub>O, NaOH, HCl (b) DCC, HOBT, TEA, DCM

The dipeptidyl nitrile derivatives gave yields varying from 20 to 66 % (**Table 2.1**). The highest yield recorded was for the 2,4-difluoro derivative, with a value of 66 %. The lowest yield was the 3,4-difluoro compound with an overall value of 20 %. These fluorobenzoyl dipeptidyl nitriles were found to be partially insoluble in organic solvents while they were completely insoluble in aqueous media. These solubility problems often hindered complete and successful isolation. A large amount of solvent was often required to dissolve the nitriles completely. The pentafluoro derivatives were found to be the least soluble in organic solvents such as dichloromethane, chloroform, ethyl acetate or methanol.

The <sup>1</sup>H NMR spectra of these compounds show distinctive amide proton splitting patterns. The amide proton from the L-leucine portion is split into a doublet by the α-hydrogen and appears in the range of δ 8.50 and 9.28. The second amide in the molecule, the glycine nitrile amide is split into a triplet by the adjacent methylene group and is seen between δ 8.75 and 9.01. The α-hydrogen of leucine appears as a multiplet (δ 4.4 - 4.8) coupling with the amide and protons of the isobutyl side chain. The <sup>13</sup>C NMR spectrum shows a distinctive peak for the nitrile moiety at approximately δ 118. The chemical shifts of the attached methylene units have been shifted upfield due to the effect of the nitrile group. The methylene carbon of the amino acid glycine, usually appears at about δ 40.5, but the methylene unit of the glycine nitrile was seen to appear at δ 27.5. The fluorobenzoyl moiety causes the carbon atoms of the phenyl ring to appear as doublets and triplets due to <sup>13</sup>C-<sup>19</sup>F

coupling. The  $^{19}\text{F}$  NMR spectra of these compounds shows the fluorine peaks appearing as multiplets due to  $^{19}\text{F}$ - $^1\text{H}$  coupling, with the exception of the trifluoromethyl derivatives (**110-112**).

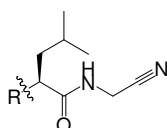


Compound	X	% Yield
<b>97</b>	3-F	25
<b>98</b>	2,3-F	48
<b>99</b>	2,4-F	66
<b>100</b>	2,5-F	60
<b>101</b>	2,6-F	38
<b>102</b>	3,4-F	20
<b>103</b>	3,5-F	28
<b>104</b>	2,3,6-F	24
<b>105</b>	2,3,4-F	44
<b>106</b>	2,4,5-F	55
<b>107</b>	3,4,5-F	45
<b>108</b>	2,3,4,5-F	42
<b>109</b>	<i>Penta</i> -F	40
<b>110</b>	<i>o</i> -CF <sub>3</sub>	43
<b>111</b>	<i>m</i> -CF <sub>3</sub>	37
<b>112</b>	<i>p</i> -CF <sub>3</sub>	33

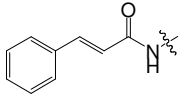
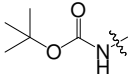
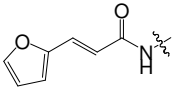
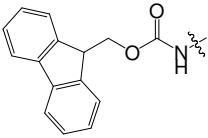
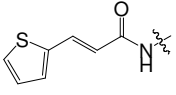
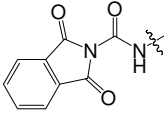
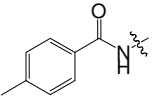
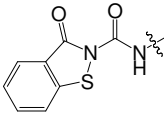
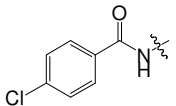
**Table 2.1:** N-fluorobenzoyl dipeptidyl nitrile derivatives



The *N*-modified derivatives gave a broad range of yields from 12 to 95% (**Table 2.2**). The highest yield of 95 % was found for the Fmoc protected dipeptide **131**, which was also the initial step in the synthetic scheme of these compounds. The lowest yield calculated was for 1,2-benzisothiazolin-3-one L-leucine glycine nitrile **133**, at 12 %, as isolation of this compound required several columns. This compound came about serendipitously. The anticipated compound would have had a free thiol group at the *ortho* position. On isolation, it was proposed that the thiol had cyclised with the leucine amide, which was confirmed by a combination of NMR and mass spectrometry. Insolubility problems of some of these products proved a hindrance for complete and successful isolation. Yields reported are for final step of reaction sequence, previous steps generally provided quantitative yields.



Compound	R	% Yield	Compound	R	% Yield
(115)		82	(125)		65
(116)		74	(126)		75
(117)		47	(127)		55
(118)		60	(128)		63
(119)		58	(129)		39

(120)		35	(130)		52
(121)		80	(131)		95
(122)		45	(132)		62
(123)		74	(133)		12
(124)		54			

**Table 2.2:** *N*-substituted dipeptidyl nitrile derivatives

The  $^1\text{H}$  NMR spectra of these compounds show distinctive amide proton splitting patterns, as seen in the previous series of fluorinated dipeptide inhibitors. The amide proton from the L-leucine amino acid is split into a doublet by the  $\alpha$ -hydrogen. The second amide in the molecule, the glycine nitrile amide, is split into a triplet by the adjacent methylene group. Both these amides have different chemical shifts depending on its environment in the molecule and these are outlined in **Table 2.3**. The  $\alpha$ -hydrogen of leucine appears as a multiplet ( $\delta$  4.0 - 4.8) due to coupling with the amide and protons of the isobutyl side chain. The exception to this is for compound **133**, where the  $\alpha$ -hydrogen appears further up field at  $\delta$  5.34 – 5.38. The  $^{13}\text{C}$  NMR spectrum shows a distinctive peak for the nitrile moiety at approximately  $\delta$  118. Due to the nitrile moiety, the doublet of the attached methylene units has shifted upfield. The methylene carbon of the amino acid glycine, usually appears at about  $\delta$  40.5, but the methylene unit of the glycine nitrile was seen to appear at  $\delta$  27.5.



<b>Compound</b>	<b>Leucine amide (<math>\delta</math>)</b>	<b>Glycine amide (<math>\delta</math>)</b>
<b>115</b>	8.59	8.73
<b>116*</b>	8.76 - 8.81	8.76 - 8.81
<b>117</b>	8.72	8.84
<b>118</b>	8.46	8.74
<b>119</b>	8.62	8.77
<b>120</b>	8.39	8.82
<b>121</b>	8.42	8.80
<b>122</b>	8.37	8.81
<b>123</b>	8.41	8.71
<b>124</b>	8.69	8.75
<b>125</b>	8.97	8.80
<b>126</b>	8.80	8.89
<b>127</b>	8.56	8.71
<b>128</b>	8.51	8.70
<b>129</b>	6.99	8.61
<b>130</b>	7.00	8.57
<b>131</b>	7.68	8.75
<b>132</b>	N/A	8.89
<b>133</b>	N/A	7.54

**Table 2.3:** Chemical shifts of amide protons in *N*-substituted dipeptidyl nitrile derivatives

\* both amides appear together as a multiplet

## 2.3 References

- 1 Otto, H.H., Schirmeister, T.; *Chem. Rev.* **1997**, *97*, 133.
- 2 Torgerson, P.R., Claxton, J.R.; **1999**. In: Dalton, J.P. (Ed.), *Fasciolosis*, CAB International, Oxford, p465.
- 3 Mas-Coma, S., Bargues, M.D., Esteban, J.G.; **1999**. In: Dalton, J.P. (Ed.), *Fasciolosis*, CAB International, Wallingford, UK, p411.
- 4 Dalton, J.P., O'Neill, S., Stack, C., Collins, P., Walshe, A., Sekiya, M., Doyle, S., Mulcahy, G., Hoyle, D., Khaznadji, E., Moire', N., Brennan, G., Mousley, A., Kreshchenko, N., Maule, A.G., Donnelly, S.M.; *Int. J. Parasitol.* **2003**, *33*, 1173.
- 5 Howell, R.M.; *Nature* **1966**, *209*, 713.
- 6 Dalton, J.P., Heffernan, M.; *Mol. Biochem. Parasitol.* **1989**, *35*, 161.
- 7 Leung, D., Abbenante, G., Farilie, D.P.; *J. Med. Chem.* **2000**, *43*, 3, 305.
- 8 Dubin, G.; *Cell. Mol. Life Sci.* **2005**, *62*, 653.
- 9 Suzue, S., Irikura, T.; *Chem. Pharm. Bull.* **1968**, *16*, 1417.
- 10 Sheehy, M.J.; "The design and synthesis of novel peptide derivatives as malarial protease inhibitors and electrochemical anion sensing receptors", Dublin City University, *PhD Thesis*, **1999**.
- 11 Anderson, F.P.; "The synthesis, structural characterisation and biological evaluation of potential chemotherapeutic agents", Dublin City University, *PhD Thesis*, **2005**.
- 12 Lim, I.T., Meroueh, S.O., Lee, M., Heeg, M.J., Mobashery, S.; *J. Am. Chem. Soc.* **2004**, *126*, 10271.
- 13 Han, S.Y., Kim, Y.A.; *Tetrahedron* **2004**, *60*, 11, 2447.
- 14 Greenspan, P.D., Clark, K.L., Cowen, S.D., McQuire, L.W., Tomassi, R.A., Farley, D.L., Quadros, E, Coppa, D.E., Du, Z., Fang, Z., Zhou, H., Doughty, J.R., Toscano, K.T., Wigg, A.M., Zhou, S.; *Bioorg. Med. Chem. Lett.* **2003**, *13*, 4121.
- 15 Greenspan, P.D., Clark, K.L., Tomassi, R.A., Cowen, S.D., McQuire, L.W., Farley, D.L., van Duzer, J.H., Goldberg, R.L., Zhou, H., Du, Z., Fitt, J.J., Coppa, D.E., Fang, Z., Macchia, W., Zhu, L., Capparelli, M.P., Goldstein, R.,

- Wigg, A.M., Doughty, J.R., Bohacek, R.S., Knap, A.K.; *J. Med. Chem.* **2001**, *44*, 4524.
- <sup>16</sup> O'Brien, S.E., Browne, H.L., Bradshaw, T.D., Westwell, A.D., Stevens, M.F.G., Laughton, C.A.; *Bioorg. Chem.* **1994**, *22*, 227.
- <sup>17</sup> Robichaud, J., Bayly, C., Oballa, R., Prasit, P., Mellon, C., Falgueyret, J.-P., Percival, M.D., Wesolowski, G., Rodan, S.B.; *Bioorg. Med. Chem. Lett.* **2004**, *14*, 4291.

## 3.0 Biological activity of novel dipeptide derivatives

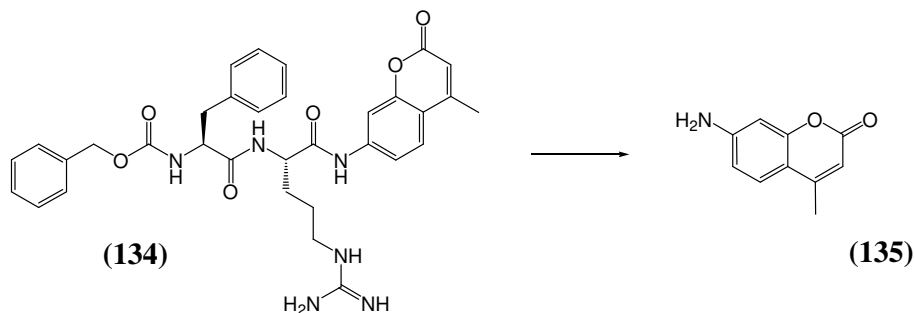
### 3.1 Introduction

Cathepsins are a complex group of cysteine proteases that cleave peptide bonds. They have been implicated as essential components of various diseases such as liver fluke, rheumatoid arthritis, cancer and malaria<sup>1</sup>. Their broad spectrum biological activity renders them as key therapeutic targets. Fasciolosis or liver fluke as it is commonly known, has been estimated to be present in up to 2 million humans worldwide and its economic losses on cattle and sheep livestock is estimated at \$2 billion annually<sup>2,3</sup>. Increasing resistance to the present chemotherapy against fasciolosis in animals asks for novel chemotherapeutic approaches. A series of potential cathepsin inhibitors have been developed and their bioactivity was assessed with the cathepsin protease *Fasciola hepatica* that has been implicated in the reproduction of the parasites<sup>4</sup>.

Commercially available peptide substrates with substituents added to either the *N*- or *C*-termini are most commonly used to assay, characterise and perform inhibition studies on proteases. The *C*-terminal substituents usually involve a chromophoric amine such as 4-naphthylamine (-NHNap) or a fluorogenic group such as 7-amino-4-methylcoumarin (-NHMec). These species are highly absorbant or fluorescent when cleaved from the substrate and can be detected spectrophotometrically or fluorometrically. The fluorogenic substrates are far more sensitive due to the ability of fluorescence to be detected against a low background in contrast to absorption spectrophotometry that requires measurement of transmitted light relative to high incident light levels at the same wavelength<sup>5</sup>. Although these substrates are useful in evaluating the inhibitory potency of potential therapeutic agents, *in vivo* testing has shown the physiochemical properties of the enzyme can vary against natural protein substrates.

## 3.2 Fluorescent assay

A standard fluorometric assay has been developed using a fluorogenic substrate to test the activity of dipeptidyl derivatives. In this assay, activity was determined by measuring the release of the fluorescent species 7-amino-4-methyl-coumarin (-NHMec) **135** from the substrate Z-Phe-Arg-NHMec **134**, upon enzymatic hydrolysis by a cathepsin L protease isolated from *Fasciola hepatica*.

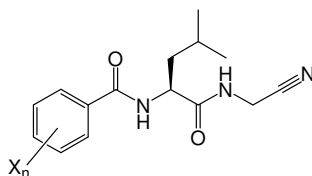


**Scheme 3.1:** Hydrolysis of Z-Phe-Arg-NHMec **134** by cathepsin L protease with liberation of the fluorescent 7-amino-4-methylcoumarin (-NHMec) **135**.

Assays were carried out using a final concentration of 10  $\mu\text{M}$  substrate in 0.1 M sodium acetate buffer pH 5, containing 100 mM dithiothreitol (DTT) and 500 mM ethylenediaminetetraacetic acid (EDTA), in a final volume of 1 ml. The mixture of enzyme and inhibitor were incubated together at 37°C for 15 mins. The substrate was then added and the mixture was further incubated for 30 mins. The reaction was stopped by the addition of 10% acetic acid solution. The amount of 7-amino-4-methyl-coumarin (-NHMec) **135** released was measured using a Perkin-Elmer fluorescence spectrophotometer with excitation at 370 nm and emission at 440 nm. The positive control contained only the enzyme extract and the substrate Z-Phe-Arg-NHMec **134**. There were two negative controls used. One contained the enzyme and inhibitor while the second contained just the inhibitor and the substrate. All assays were performed in triplicate with the mean result being taken.

### 3.3 Biological Results

The *N*-benzoyl-L-leucine-glycine nitrile scaffold has been shown to be an effective inhibitor of *Fasciola hepatica* cathepsin L endoproteases<sup>6,7</sup>. The electrophilic nature of the nitrile moiety is believed to be crucial for the effectiveness of this compound as a potent protease inhibitor. It is hoped that fluorination of the benzoyl *N*-terminus can increase the activity. The inhibition displayed by the entire series of fluorinated derivatives were all in the low micromolar range, with the exception of the *meta*-trifluoromethyl derivative. The IC<sub>50</sub> of this derivative was approximately 10-fold higher than the series average. The most active analogue was 3,5-difluorobenzoyl-L-leu-gly-CN **103** with an IC<sub>50</sub> of 3.0 μM. From the assays undertaken in this study it is clear that the addition of fluorine to the molecule has had a significant impact on the inhibition of cathepsin L. From the calculated inhibitory concentrations, it is clear that the position and number of fluorine atoms on the benzoyl group has little effect on the activity of the molecule. However, when compared to the non-fluorinated dipeptide, *N*-benzoyl-L-leucine-glycine (IC<sub>50</sub> = 11 μM)<sup>6</sup>, the combination of fluorine substitution and conversion of the *C*-terminus to a nitrile, reduced the IC<sub>50</sub> value.



Compound	X	IC <sub>50</sub> μM
<b>97</b>	3-F	3.1
<b>98</b>	2,3-F	3.4
<b>99</b>	2,4-F	5.5
<b>100</b>	2,5-F	3.1
<b>101</b>	2,6-F	3.7
<b>102</b>	3,4-F	3.1
<b>103</b>	3,5-F	3.0

<b>104</b>	2,3,6-F	6.0
<b>105</b>	2,3,4-F	4.1
<b>106</b>	2,4,5-F	4.5
<b>107</b>	3,4,5-F	3.4
<b>108</b>	2,3,4,5-F	3.4
<b>109</b>	<i>Penta</i> -F	4.4
<b>110</b>	<i>o</i> -CF <sub>3</sub>	4.1
<b>111</b>	<i>m</i> -CF <sub>3</sub>	29.1
<b>112</b>	<i>p</i> -CF <sub>3</sub>	3.2

**Table 3.1:** Inhibitory activity of *N*-fluorobenzoyl dipeptidyl nitrile derivatives

The activity of *Fasciola hepatica* cysteine cathepsin L endoprotease against the substrate *Z*-Phe-Arg-NHMec **134** can be blocked by micromolar concentrations of the commercially available diazomethane *Z*-Phe-Ala-CHN<sub>2</sub> **31**<sup>8</sup>. From the previous studies carried out in our laboratories, the IC<sub>50</sub> of inhibitor **31** was found to be 3.0 μM<sup>11</sup>, which is comparable to the inhibitory concentrations found for the majority of the *N*-fluorobenzoyl-L-leucine glycine nitrile derivatives, particularly compound **103**. From the variable concentration assays preformed, it can be seen that the commercially available inhibitor **31** is more potent at lower concentrations up to about 50% inhibition where inhibitors **97**, **103** and **112** showed comparable results. At higher concentrations, greater than 5 μM, the nitrile derivatives showed higher inhibition in contrast to the substrate *Z*-Phe-Arg-NHMec **134** towards *Fasciola hepatica* cysteine cathepsin L endoprotease. A representative bar chart showing these values is displayed in *Figure 3.1*

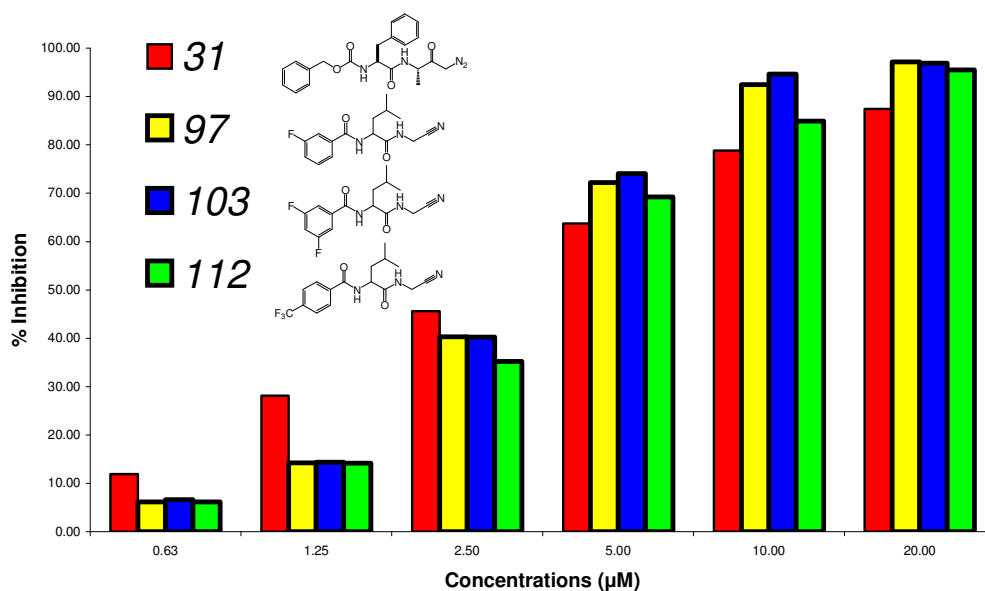


**Figure 3.1:** Bar chart illustration of the % inhibition of compounds **31**, **97**, **103** and **112** towards *Fasciola hepatica* cysteine cathepsin L endoprotease at varying concentration (μM)

To date, of the second series of modified *N*-terminal dipeptides, biological activity has been carried out on two of the compounds isolated. Compounds **129** and **133** were assayed again using the standard fluorometric assay mentioned previously using *Z*-Phe-Arg-NHMec **134** as substrate. Dipeptide **129**, cyclopentanoyl-L-leucine glycine nitrile showed comparable activity to that of the first series of fluorinated analogues and an  $IC_{50}$  value of 4.3 μM was calculated for the fluorescence readings. The second inhibitor assayed was the 1,2-benzisothiazolin-3-one dipeptide **133**. The  $IC_{50}$  of this analogue was calculated to be 1.4 μM, which makes it the most biologically active compound tested. Compounds **115-128** and **130-132** are set for assaying in the near future.



### 3.4 References

- <sup>1</sup> Otto, H.H., Schirmeister, T.; *Chem. Rev.* **1997**, *97*, 133.
- <sup>2</sup> Torgerson, P.R., Claxton, J.R.; **1999**. In: Dalton, J.P. (Ed.), *Fasciolosis*, CAB International, Oxford, p465.
- <sup>3</sup> Mas-Coma, S., Bargues, M.D., Esteban, J.G.; **1999**. In: Dalton, J.P. (Ed.), *Fasciolosis*, CAB International, Wallingford, UK, p411.
- <sup>4</sup> Zurita, M., Bieber, D., Mansour, T.E.; *Mol. Biochem. Parasitol.* **1989**, *37*, 11.
- <sup>5</sup> Valeur., B.; “*Molecular Fluorescence*” Wiley-VCH, **2002**.
- <sup>6</sup> Sheehy, M.J.; “*The design and synthesis of novel peptide derivatives as malarial protease inhibitors and electrochemical anion sensing receptors*”, Dublin City University, *PhD Thesis*, **1999**.
- <sup>7</sup> Anderson, F.P.; “*The synthesis, structural characterisation and biological evaluation of potential chemotherapeutic agents*”, Dublin City University, *PhD Thesis*, **2005**.
- <sup>8</sup> Fried, B., Graczyk, T.K.; “*Advances in Trematode Biology*”, CRC Press LLC, New York, **1997**.

## 4.0 Conclusion

In summary, we have identified potent inhibitors of the *Fasciola hepatica* liver fluke cathepsin L proteases with the two most successful derivatives being the nitrile compounds **103** and **133**. From the protease inhibition results it is very clear that the presence of an electrophilic isostere adjacent to the P1 position is essential for effective inhibition. However, it has been shown from the initial series of fluorinated analogues that the position of the isostere may not be of major importance to the activity of the inhibitor. Further to this, the number of fluorine substituents attached to the *N*-terminal benzoyl group has little if any improvement on the biological activity. Despite this, it is evident that almost all of the derivatives offer real inhibitory potency against *Fasciola hepatica* cysteine cathepsin L endoprotease. It is hoped that with continuing testing, further improvement in bioactivity can be made. The inhibitory potency of the nitrile compounds *N*-3,5-difluorobenzoyl-L-leucine-glycine nitrile **103** and 1,2-benzisothiazolin-3-one-L-leucine-glycine nitrile **133** relative to the commercial inhibitor Z-Phe-Ala-CHN<sub>2</sub> **31** shows that such benzoyl dipeptidyl derivatives may have a role to play as commercial inhibitors of *Fasciola hepatica* cathepsin L endoproteases.

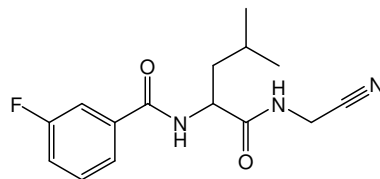
## 5.0 Experimental

All chemicals were purchased from Sigma-Aldrich, Lennox Chemicals or Fluorochem Limited; and used as received. Commercial grade reagents were used without further purification procedures. When necessary all solvents were purified and dried; and stored under argon. Tetrahydrofuran was distilled from Na/benzophenone and triethylamine distilled and stored over potassium hydroxide pellets. Riedel-Haën silica gel was used for thin layer and column chromatography. Melting point determinations were carried out using a Griffin melting point apparatus and are uncorrected. Elemental Analysis was carried out by the Microanalytical Laboratory at Univeristy College Dublin. Electrospray ionisation mass spectra were obtained on a Bruker Esquire 3000 series ion trap mass spectrometer. IR spectra were obtained on a Perkin-Elmer Spectrum GX FT-IR system. NMR spectra were obtained on a Bruker AC 400 NMR spectrometer operating at 400 MHz for  $^1\text{H}$  NMR 376 MHz for  $^{19}\text{F}$  NMR and 100 MHz for  $^{13}\text{C}$  NMR. The  $^1\text{H}$  and  $^{13}\text{C}$  NMR chemical shifts ( $\delta$ ) are relative to trimethylsilane and the  $^{19}\text{F}$  NMR chemical shifts ( $\delta$ ) are relative to trifluoroacetic acid. All coupling constants ( $J$ ) are in Hertz (Hz).

### ***General procedure for the synthesis of N-fluorobenzoyl dipeptides:***

#### ***N-3-fluorobenzoyl-L-leucine-glycine nitrile 97***

*N*-3-Fluorobenzoyl-L-leucine (2.59 g, 10.24mmol) was dissolved in dichloromethane (50ml) with glycine nitrile hydrochloride (0.95 g, 10.24 mmol), 1-hydroxybenzotriazole (1.38 g, 10.24 mmol) and triethylamine (1.42 ml, 10.24 mmol).



The mixture was cooled to 0 °C, and 1,3-dicyclohexylcarbodiimide (2.11 g, 10.24 mmol) was added. After 30 min. the solution was raised to room temperature and the reaction was allowed to proceed for 48 hrs. The precipitated *N,N*-dicyclohexylurea was removed by filtration and the filtrate was washed with brine, sat. potassium hydrogen carbonate, 10% citric acid and dried over sodium sulphate. The solvent was evaporated *in vacuo* and isolation by column chromatography and recrystallisation from ethyl acetate/hexane furnished **97** as a white powder (1.72 g, 57%).

m.p. 131-134 °C.

$[\alpha]_D^{25} = -10.0^\circ$  (c, 2.1, EtOH).

Anal. calcd. for  $C_{15}H_{18}N_3O_2F_1$ : C, 61.84; H, 6.23; N, 14.42.

Found C, 61.88; H, 6.16; N, 14.35.

IR (KBr):  $\nu$  3329, 2927, 2106, 1637, 1552, 1493, 1050, 842  $cm^{-1}$ .

Mass Spectrum:  $\{M+Na\}^+$  found 314.1.

$C_{15}H_{18}N_3O_2F_1Na_1$  requires 314.31.

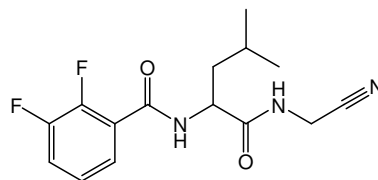
$^1H$  NMR (400 MHz, DMSO- $d_6$ ):  $\delta$  8.75 (1H, t,  $J = 5.6$  Hz, -NH-), 8.69-8.71 (1H, d,  $J = 8$  Hz, -NH-), 7.72-7.79 (2H, m, -ArH 2 & 6), 7.51-7.56 (1H, m, -ArH 5), 7.40-7.43 (1H, m, -ArH 4), 4.48-4.53 (1H, m,  $\alpha$ -H), 4.14 (2H, d,  $J = 5.6$  Hz, -CH<sub>2</sub>-), 1.48-1.75 (3H, m, -CH<sub>2</sub>- & -CH-), 0.91 (3H, d,  $J = 6.4$  Hz, -CH<sub>3</sub>), 0.87 (3H, d,  $J = 6.4$  Hz, -CH<sub>3</sub>).

$^{13}C$  NMR (100 MHz, DMSO- $d_6$ ):  $\delta$  173.2 (-CONH-), 165.5 (-ArCO-), 163.45 (d, -ArC 3), 136.5 (d, -ArC 1), 130.7 (d, -ArC 5), 124.2 (d, -ArC 6), 118.6 (d, -ArC 4), 118.0 (-CN), 114.8 (d, -ArC 2), 52.0 ( $\alpha$ -C), 40.3 (-CH<sub>2</sub>, -VE DEPT), 27.5 (-CH<sub>2</sub>, -VE DEPT), 24.8 (-CH), 23.4 (-CH<sub>3</sub>), 21.5 (-CH<sub>3</sub>).

$^{19}F$  NMR (376 MHz, DMSO- $d_6$ ):  $\delta$  -36.94 - -37.01 (m).

### ***N*-2,3-difluorobenzoyl-L-leucine-glycine nitrile **98****

*N*-2,3-difluorobenzoyl-L-leucine (1.33 g, 4.9 mmol) and glycine nitrile hydrochloride (0.45 g, 4.9 mmol) were used. Isolation by column chromatography and recrystallisation from ethyl acetate/hexane furnished **98** as a white powder (0.73 g, 48%).



m.p. 103-105 °C.

$[\alpha]_D^{25} = -13.0^\circ$  (c, 2.1, EtOH).

Anal. calcd. for  $C_{15}H_{17}N_3O_2F_2$ : C, 58.25; H, 5.54; N, 13.59.

Found C, 57.95; H, 5.52; N, 13.36.

IR (KBr):  $\nu$  3280, 2928, 2198, 1637, 1548, 1483, 1272, 1050, 803  $cm^{-1}$ .

Mass Spectrum:  $\{M+Na\}^+$  found 332.2.

$C_{15}H_{18}N_3O_2F_1Na_1$  requires 332.3.

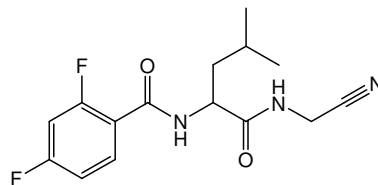
$^1H$  NMR (400 MHz, DMSO- $d_6$ ):  $\delta$  8.82-8.85 (1H, t,  $J = 5.4$  Hz, -NH-), 8.74-8.76 (1H, d,  $J = 8$  Hz, -NH-), 7.57-7.60 (1H, m, -ArH 6), 7.43-7.46 (1H, m, -ArH 5), 7.31-7.35 (1H, m, -ArH 4), 4.53-4.55 (1H, m,  $\alpha$ -H), 4.21 (2H, d,  $J = 4$  Hz, -CH<sub>2</sub>-), 1.49-1.82 (3H, m, -CH<sub>2</sub>- & -CH-), 0.95 (6H, t,  $J = 8.4$  Hz, -CH<sub>3</sub>).

$^{13}\text{C}$  NMR (100 MHz, DMSO- $d_6$ ):  $\delta$  172.8 (-CONH-), 163.2 (-ArCO-), 151.2 (dd, -ArC 3), 146.3 (dd, -ArC 2), 126.5 (d, -ArC 1), 125.5 (d, -ArC 4), 125.1 (d, -ArC 5), 119.6 (d, -ArC 6), 117.9 (-CN), 51.8 ( $\alpha$ -C), 40.5 (-CH<sub>2</sub>, -VE DEPT), 27.5 (-CH<sub>2</sub>, -VE DEPT), 24.6 (-CH-), 23.3 (-CH<sub>3</sub>), 21.6 (-CH<sub>3</sub>).

$^{19}\text{F}$  NMR (376 MHz, DMSO- $d_6$ ):  $\delta$  -62.40 - -62.51 (m), -64.0 - -64.10 (m).

#### ***N*-2,4-difluorobenzoyl-L-leucine-glycine nitrile **99****

*N*-2,4-difluorobenzoyl-L-leucine (1.47 g, 5.4 mmol) and glycine nitrile hydrochloride (0.5 g, 5.4 mmol) were used. Isolation by column chromatography and recrystallisation from ethyl acetate/hexane furnished **99** as a white powder (1.1 g, 66%).



m.p. 108-111 °C.

$[\alpha]_D^{25} = -10.9^\circ$  (c, 2.1, EtOH).

Anal. calcd. for C<sub>15</sub>H<sub>17</sub>N<sub>3</sub>O<sub>2</sub>F<sub>2</sub>: C, 58.25; H, 5.54; N, 13.59.

Found C, 57.96; H, 5.50; N, 13.37.

IR (KBr):  $\nu$  3201, 2987, 2110, 1640, 1507, 1301, 1089, 775 cm<sup>-1</sup>.

Mass Spectrum: {M+Na}<sup>+</sup> found 332.2.

C<sub>15</sub>H<sub>18</sub>N<sub>3</sub>O<sub>2</sub>F<sub>1</sub>Na<sub>1</sub> requires 332.3.

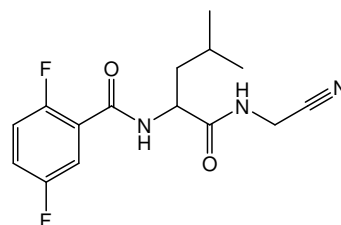
$^1\text{H}$  NMR (400 MHz, DMSO- $d_6$ ):  $\delta$  8.77-8.79 (1H, t,  $J = 4$  Hz, -NH-), 8.50-8.52 (1H, d,  $J = 9.2$  Hz, -NH-), 7.71-7.73 (1H, m, -ArH 6), 7.31-7.40 (1H, m, -ArH 5), 7.17-7.25 (1H, m, -ArH 3), 4.45-4.55 (1H, m,  $\alpha$ -H), 4.17 (2H, d,  $J = 5.2$  Hz, -CH<sub>2</sub>-), 1.46-1.78 (3H, m, -CH<sub>2</sub>- & -CH-), 0.91 (6H, t,  $J = 6.8$  Hz, -CH<sub>3</sub>).

$^{13}\text{C}$  NMR (100 MHz, DMSO- $d_6$ ):  $\delta$  172.9 (-CONH-), 163.4 (d, -ArC 4), 162.5 (-ArCO-), 158.9 (dd, -ArC 2), 132.4 (dd, -ArC 6), 120.8 (dd, -ArC 1), 117.9 (-CN), 111.8 (dd, -ArC 3), 104.7 (t, -ArC 5), 51.8 ( $\alpha$ -C), 40.6 (-CH<sub>2</sub>, -VE DEPT), 27.5 (-CH<sub>2</sub>, -VE DEPT), 24.6 (-CH-), 23.3 (-CH<sub>3</sub>), 21.6 (-CH<sub>3</sub>).

$^{19}\text{F}$  NMR (376 MHz, DMSO- $d_6$ ):  $\delta$  -30.29 - -30.38 (m), -32.90 - -32.98 (m).

#### ***N*-2,5-difluorobenzoyl-L-leucine-glycine nitrile **100****

*N*-2,5-difluorobenzoyl-L-leucine (2.1 g, 7.75 mmol) and glycine nitrile hydrochloride (0.72 g, 7.75 mmol) were used. Isolation by column chromatography and



recrystallisation from ethyl acetate/hexane furnished **100** as a white powder (1.43 g, 60%).

m.p. 101-104 °C.

$[\alpha]_D^{25} = -9.3^\circ$  (c, 2.1, EtOH).

Anal. calcd. for C<sub>15</sub>H<sub>17</sub>N<sub>3</sub>O<sub>2</sub>F<sub>2</sub>: C, 58.25; H, 5.54; N, 13.59.

Found C, 58.28; H, 5.56; N, 13.40.

IR (KBr):  $\nu$  3290, 2911, 2102, 1651, 1437, 1078, 985 cm<sup>-1</sup>.

<sup>1</sup>H NMR (400 MHz, DMSO-*d*<sub>6</sub>):  $\delta$  8.75-8.78 (1H, t, *J* = 5.6 Hz, -NH-), 8.62-8.64 (1H, d, *J* = 7.6 Hz, -NH-), 7.36-7.46 (3H, m, -ArH 3,4 & 6), 4.46-4.8 (1H, m,  $\alpha$ -H), 4.17 (2H, d, *J* = 5.6 Hz, -CH<sub>2</sub>-), 1.60-1.68 (3H, m, -CH<sub>2</sub>- & -CH-), 0.91 (6H, t, *J* = 6.4 Hz, -CH<sub>3</sub>).

<sup>13</sup>C NMR (100 MHz, DMSO-*d*<sub>6</sub>):  $\delta$  172.3 (-CONH-), 162.7 (-ArCO-), 157.5 (d, -ArC 2), 155.5 (d, -ArC 5), 125.1 (dd, -ArC 1), 118.9 (dd, -ArC 6), 117.9 (dd, -ArC 3), 117.5 (-CN), 116.3 (dd, -ArC 4), 51.5 ( $\alpha$ -C), 39.9 (-CH<sub>2</sub>, -VE DEPT), 27.1 (-CH<sub>2</sub>, -VE DEPT), 24.2 (-CH-), 22.9 (-CH<sub>3</sub>), 21.3 (-CH<sub>3</sub>).

<sup>19</sup>F NMR (376 MHz, DMSO-*d*<sub>6</sub>):  $\delta$  -42.38 - -42.48 (m), -43.38 - -43.45 (m).

### *N*-2,6-difluorobenzoyl-*L*-leucine-glycine nitrile **101**

*N*-2,6-difluorobenzoyl-*L*-leucine (2.23 g, 8.23 mmol)

and glycine nitrile hydrochloride (0.76 g, 8.23 mmol)

were used. Isolation by column chromatography and recrystallisation from ethyl acetate/hexane furnished

**101** as a white powder (0.98 g, 39%).

m.p. 159-163 °C.

$[\alpha]_D^{25} = -20.3^\circ$  (c, 2.1, EtOH).

Anal. calcd. for C<sub>15</sub>H<sub>17</sub>N<sub>3</sub>O<sub>2</sub>F<sub>2</sub>: C, 58.25; H, 5.54; N, 13.59.

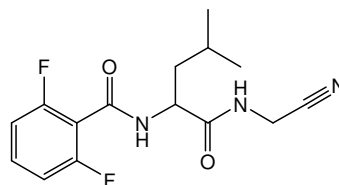
Found C, 58.18; H, 5.49; N, 13.51.

IR (KBr):  $\nu$  3190, 2875, 2055, 1675, 1688, 1402, 1075, 626 cm<sup>-1</sup>.

Mass Spectrum: {M+Na}<sup>+</sup> found 332.1

C<sub>15</sub>H<sub>18</sub>N<sub>3</sub>O<sub>2</sub>F<sub>1</sub>Na<sub>1</sub> requires 332.3.

<sup>1</sup>H NMR (400 MHz, DMSO-*d*<sub>6</sub>):  $\delta$  9.03-9.01 (1H, d, *J* = 8.4 Hz, -NH-), 8.85-8.88 (1H, t, *J* = 5.6 Hz, -NH-), 7.10-7.55 (1H, m, -ArH 4), 7.13-7.17 (2H, m, -ArH 3 & 5), 4.40-4.57 (1H, m,  $\alpha$ -H), 4.18 (2H, d, *J* = 2.4 Hz, -CH<sub>2</sub>-), 1.41-1.78 (3H, m, -CH<sub>2</sub>- & -CH-), 0.91 (3H, d, *J* = 4.4 Hz, -CH<sub>3</sub>), 0.89 (3H, d, *J* = 4.4 Hz, -CH<sub>3</sub>).

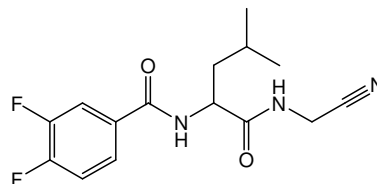


$^{13}\text{C}$  NMR (100 MHz, DMSO- $d_6$ ):  $\delta$  172.5 (-CONH-), 160.45 (d, -ArC 2), 159.96 (-ArCO-), 157.95 (d, -ArC 6), 131.91 (-ArC 4), 117.9 (-CN), 115.5 (t, -ArC 1), 112.1 (dd, -ArC 3 & 5), 51.5 ( $\alpha$ -C), 40.8 (-CH<sub>2</sub>, -VE DEPT), 27.4 (-CH<sub>2</sub>, -VE DEPT), 24.5 (-CH-), 23.3 (-CH<sub>3</sub>), 21.6 (-CH<sub>3</sub>).

$^{19}\text{F}$  NMR (376 MHz, DMSO- $d_6$ ):  $\delta$  -37.54 - -37.58 (m).

### *N*-3,4-difluorobenzoyl-L-leucine-glycine nitrile **102**

*N*-3,4-difluorobenzoyl-L-leucine (2.3 g, 8.5 mmol) and glycine nitrile hydrochloride (0.79 g, 8.5 mmol) were used. Isolation by column chromatography and recrystallisation from ethyl acetate/hexane furnished **102** as a white powder (0.52 g, 20%).



m.p. 139-142 °C.

$[\alpha]_D^{25} = -19.6^\circ$  (c, 2.1, EtOH).

Anal. calcd. for C<sub>15</sub>H<sub>17</sub>N<sub>3</sub>O<sub>2</sub>F<sub>2</sub>: C, 58.25; H, 5.54; N, 13.59.

Found C, 58.05; H, 5.51; N, 13.29.

IR (KBr):  $\nu$  3198, 2654, 2063, 1641, 1567, 1246, 1098, 803 cm<sup>-1</sup>.

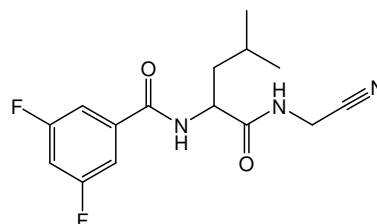
$^1\text{H}$  NMR (400 MHz, DMSO- $d_6$ ):  $\delta$  8.76-8.82 (1H, t,  $J = 11.4$  Hz, -NH-), 8.71-8.73 (1H, d,  $J = 7.7$  Hz, -NH-), 7.97-8.00 (1H, m, -ArH 6), 7.81-7.84 (1H, m, -ArH 2), 7.54-7.61 (1H, m, -ArH 5), 4.47-4.52 (1H, m,  $\alpha$ -H), 4.14 (2H, d,  $J = 5.6$  Hz, -CH<sub>2</sub>-), 1.59-1.75 (3H, m, -CH<sub>2</sub>- & -CH-), 0.91 (3H, d,  $J = 6.4$  Hz, -CH<sub>3</sub>), 0.86 (3H, d,  $J = 6.4$  Hz, -CH<sub>3</sub>).

$^{13}\text{C}$  NMR (100 MHz, DMSO- $d_6$ ):  $\delta$  173.1 (-CONH-), 164.64 (-ArCO-), 153.0 & 150.64 (dd, -ArC 4), 150.52 & 148.16 (dd, -ArC 3), 131.55 (t -ArC 1), 125.52 (dd, -ArC 2), 117.9 (-CN), 117.8 (d, -ArC 5), 117.3 (d, -ArC 6), 52.0 ( $\alpha$ -C), 40.3 (-CH<sub>2</sub>, -VE DEPT), 27.5 (-CH<sub>2</sub>, -VE DEPT), 24.7 (-CH-), 23.3 (-CH<sub>3</sub>), 21.5 (-CH<sub>3</sub>).

$^{19}\text{F}$  NMR (376 MHz, DMSO- $d_6$ ):  $\delta$  -58.33 - -58.41 (m), -62.09 - -62.20 (m).

### *N*-3,5-difluorobenzoyl-L-leucine-glycine nitrile **103**

*N*-3,5-difluorobenzoyl-L-leucine (2.3 g, 8.5 mmol) and glycine nitrile hydrochloride (0.79 g, 8.5 mmol) were used. Isolation by column chromatography and recrystallisation from ethyl acetate/hexane



furnished **103** as a white powder (0.62 g, 22%).

m.p. 150-153 °C.

$[\alpha]_D^{25} = -16.0^\circ$  (c, 2.1, EtOH).

Anal. calcd. for C<sub>15</sub>H<sub>17</sub>N<sub>3</sub>O<sub>2</sub>F<sub>2</sub>: C, 58.25; H, 5.54; N, 13.59.

Found C, 58.94; H, 5.37; N, 12.83.

IR (KBr):  $\nu$  3281, 2967, 2146, 1641, 1543, 1298, 1023, 754 cm<sup>-1</sup>.

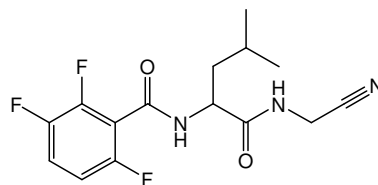
<sup>1</sup>H NMR (400 MHz, DMSO-*d*<sub>6</sub>):  $\delta$  8.78-8.80 (2H, m, -NH-), 7.64-7.67 (2H, m, -ArH 2 & 6), 7.53-7.45 (1H, m, -ArH 4), 4.47-4.53 (1H, m,  $\alpha$ -H), 4.14 (2H, d,  $J = 5.6$  Hz, -CH<sub>2</sub>-), 1.55-1.74 (3H, m, -CH<sub>2</sub>- & -CH-), 0.91 (3H, d,  $J = 6.4$  Hz, -CH<sub>3</sub>), 0.87 (3H, d,  $J = 6.4$  Hz, -CH<sub>3</sub>).

<sup>13</sup>C NMR (100 MHz, DMSO-*d*<sub>6</sub>):  $\delta$  172.99 (-CONH-), 164.27 (-ArCO-), 163.73 (d, -ArC 3), 161.27 (d, -ArC 5), 137.62 (t, -ArC 1), 117.94 (-CN), 111.35 (dd, -ArC 2 & 5), 107.22 (t, -ArC 4), 52.1 ( $\alpha$ -C), 40.2 (-CH<sub>2</sub>, -VE DEPT), 27.5 (-CH<sub>2</sub>, -VE DEPT), 24.7 (-CH-), 23.3 (-CH<sub>3</sub>), 21.5 (-CH<sub>3</sub>).

<sup>19</sup>F NMR (376 MHz, DMSO-*d*<sub>6</sub>):  $\delta$  -32.61 - -32.68 (m).

#### ***N*-2,3,6-trifluorobenzoyl-L-leucine-glycine nitrile 104**

*N*-2,3,6-trifluorobenzoyl-L-leucine (1.05 g, 3.63 mmol) and glycine nitrile hydrochloride (0.34 g, 3.63 mmol) were used. Isolation by column chromatography and recrystallisation from ethyl acetate/hexane furnished **104** as a white powder (0.28 g, 24%).



m.p. 157-160 °C.

$[\alpha]_D^{25} = -27.2^\circ$  (c, 2.1, EtOH).

Anal. calcd. for C<sub>15</sub>H<sub>16</sub>N<sub>3</sub>O<sub>2</sub>F<sub>3</sub>: C, 55.05; H, 4.93; N, 12.84.

Found C, 55.13; H, 4.98; N, 12.67.

IR (KBr):  $\nu$  3276, 2961, 2252, 1660, 1541, 1492, 1025, 814 cm<sup>-1</sup>.

<sup>1</sup>H NMR (400 MHz, DMSO-*d*<sub>6</sub>):  $\delta$  9.13-9.15 (1H, d,  $J = 8.2$  Hz, -NH-), 8.90-8.93 (1H, t,  $J = 11.8$  Hz, -NH-), 7.55-7.64 (1H, m, -ArH 4), 7.18-7.24 (1H, m, -ArH 5), 4.51-4.57 (1H, m,  $\alpha$ -H), 4.20 (2H, d,  $J = 3.2$  Hz, -CH<sub>2</sub>-), 1.41-1.78 (3H, m, -CH<sub>2</sub>- & -CH-), 0.91 (3H, d,  $J = 5.4$  Hz, -CH<sub>3</sub>), 0.89 (3H, d,  $J = 5.4$  Hz, -CH<sub>3</sub>).

<sup>13</sup>C NMR (100 MHz, DMSO-*d*<sub>6</sub>):  $\delta$  172.3 (-CONH-), 158.77 (-ArCO-), 154.5 (d, -ArC 2), 147.9 (d, -ArC 6), 145.4 (t, -ArC 3), 118.70 (dd, -ArC 4), 117.87 (-CN),

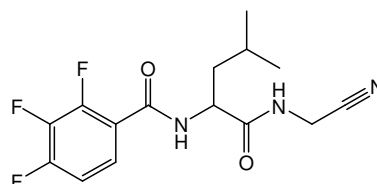


117.0 (t, -ArC 1), 112.4 (d, -ArC 5), 51.5 ( $\alpha$ -C), 40.8 (-CH<sub>2</sub>, -VE DEPT), 27.4 (-CH<sub>2</sub>, -VE DEPT), 24.5 (-CH-), 23.2 (-CH<sub>3</sub>), 21.6 (-CH<sub>3</sub>).

<sup>19</sup>F NMR (376 MHz, DMSO-*d*<sub>6</sub>):  $\delta$  -42.18 - -42.25 (m), -61.096- -61.18 (m), -66.48 - -66.62 (m).

### *N*-2,3,4-trifluorobenzoyl-L-leucine-glycine nitrile **105**

*N*-2,3,4-trifluorobenzoyl-L-leucine (1.17 g, 4 mmol) and glycine nitrile hydrochloride (0.37 g, 4 mmol) were used. Isolation by column chromatography and recrystallisation from ethyl acetate/hexane furnished **105** as a white powder (0.58 g, 44%).



m.p. 116-119 °C.

$[\alpha]_D^{25} = -4.2^\circ$  (c, 2.1, EtOH).

Anal. calcd. for C<sub>15</sub>H<sub>16</sub>N<sub>3</sub>O<sub>2</sub>F<sub>3</sub>: C, 55.05; H, 4.93; N, 12.84.

Found. C, 54.43; H, 5.95; N, 12.58.

IR (KBr):  $\nu$  3287, 2964, 2249, 1657, 1547, 1496, 1045, 828 cm<sup>-1</sup>.

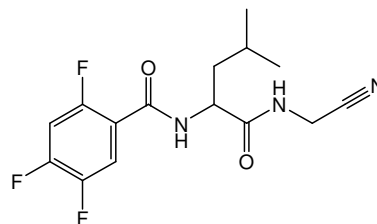
<sup>1</sup>H NMR (400 MHz, DMSO-*d*<sub>6</sub>):  $\delta$  8.85-8.87 (1H, t, *J* = 5.6 Hz, -NH-), 8.75-8.77 (1H, d, *J* = 8 Hz, -NH-), 7.41-7.55 (2H, m, -ArH 5 & 6), 4.52-4.56 (1H, m,  $\alpha$ -H), 4.21 (2H, d, *J* = 5.6 Hz, -CH<sub>2</sub>-), 1.51-1.75 (3H, m, -CH<sub>2</sub>- & -CH-), 0.96 (3H, d, *J* = 6.4 Hz, -CH<sub>3</sub>), 0.92 (3H, d, *J* = 6.4 Hz, -CH<sub>3</sub>).

<sup>13</sup>C NMR (100 MHz, DMSO-*d*<sub>6</sub>):  $\delta$  172.7 (-CONH-), 162.53 (-ArCO-), 150.46-153.02 (dd, -ArC 4), 147.46-150.09 (dd -ArC 2), 137.91-140.70 (dt, -ArC 3), 125.02 (dd, -ArC 5), 122.24 (t, -ArC 1), 117.89 (-CN), 113.02 (dd, -ArC 6), 51.8 ( $\alpha$ -C), 40.5 (-CH<sub>2</sub>, -VE DEPT), 27.5 (-CH<sub>2</sub>, -VE DEPT), 24.6 (-CH-), 23.3 (-CH<sub>3</sub>), 21.6 (-CH<sub>3</sub>).

<sup>19</sup>F NMR (376 MHz, DMSO-*d*<sub>6</sub>):  $\delta$  -55.67 - -55.79 (m), -58.916- -59.02 (m), -84.95 - -85.08 (m).

### *N*-2,4,5-trifluorobenzoyl-L-leucine-glycine nitrile **106**

*N*-2,4,5-trifluorobenzoyl-L-leucine (1.94 g, 6.7 mmol) and glycine nitrile hydrochloride (0.62 g, 6.7 mmol) were used. Isolation by column chromatography and recrystallisation from ethyl acetate/hexane furnished **106** as a white powder (1.20 g, 55%).



m.p. 104-108 °C.

$[\alpha]_D^{25} = -5.1^\circ$  (c, 2.1, EtOH).

Anal. calcd. for  $C_{15}H_{16}N_3O_2F_3$ : C, 55.05; H, 4.93; N, 12.84.

Found C, 54.75; H, 4.90, N, 12.63.

IR (KBr):  $\nu$  3282, 2959, 2261, 1657, 1537, 1465, 1031, 824  $cm^{-1}$ .

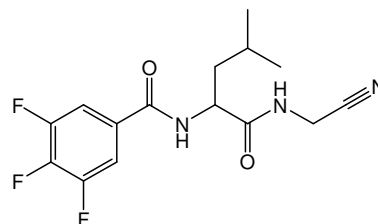
$^1H$  NMR (400 MHz, DMSO- $d_6$ ):  $\delta$  8.81-8.84 (1H, t,  $J = 5.4$  Hz, -NH-), 8.65-8.67 (1H, d,  $J = 8$  Hz, -NH-), 7.68-7.80 (2H, m, -ArH 3 & 6), 4.50-4.53 (1H, m,  $\alpha$ -H), 4.20 (2H, d,  $J = 5.6$  Hz, -CH<sub>2</sub>-), 1.55-1.73 (3H, m, -CH<sub>2</sub>- & -CH-), 0.95 (6H, t,  $J = 6.4$  Hz, -CH<sub>3</sub>).

$^{13}C$  NMR (100 MHz, DMSO- $d_6$ ):  $\delta$  172.7 (-CONH-), 162.3 (-ArCO-), 154.05-156.55 (dd, -ArC 2), 149.61-151.98 (dd -ArC 5), 144.85-147.22 (dd, -ArC 4), 120.85 (d, -ArC 1), 118.55 (d, -ArC 6), 117.90 (-CN), 107.20 (dd, -ArC 3), 51.9 ( $\alpha$ -C), 40.6 (-CH<sub>2</sub>, -VE DEPT), 27.5 (-CH<sub>2</sub>, -VE DEPT), 24.6 (-CH-), 23.3 (-CH<sub>3</sub>), 21.6 (-CH<sub>3</sub>).

$^{19}F$  NMR (376 MHz, DMSO- $d_6$ ):  $\delta$  -37.97 - -38.07 (m), -54.57- -54.70 (m), -66.76 - -66.90 (m).

### *N*-3,4,5-trifluorobenzoyl-L-leucine-glycine nitrile **107**

*N*-3,4,5-trifluorobenzoyl-L-leucine (2 g, 7 mmol) and glycine nitrile hydrochloride (0.65 g, 7 mmol) were used. Isolation by column chromatography and recrystallisation from ethyl acetate/hexane furnished **107** as a white powder (1.20 g, 52%).



m.p. 146-149 °C.

$[\alpha]_D^{25} = -0.2^\circ$  (c, 2.1, EtOH).

Anal. calcd. for  $C_{15}H_{16}N_3O_2F_3$ : C, 55.05; H, 4.93; N, 12.84.

Found C, 54.83; H, 4.87, N, 12.73.

IR (KBr):  $\nu$  3247, 2943, 2253, 1653, 1529, 1476, 1040, 794  $cm^{-1}$ .

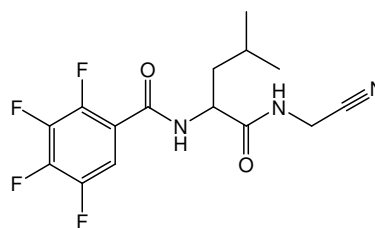
$^1H$  NMR (400 MHz, DMSO- $d_6$ ):  $\delta$  8.77-8.81 (2H, m, -NH-), 7.87-7.91 (2H, m, -ArH 2 & 6), 4.45-4.52 (1H, m,  $\alpha$ -H), 4.14 (2H, d,  $J = 6$  Hz, -CH<sub>2</sub>-), 1.53-1.73 (3H, m, -CH<sub>2</sub>- & -CH-), 0.91 (3H, d,  $J = 6.0$  Hz, -CH<sub>3</sub>), 0.87 (3H, d,  $J = 6.0$  Hz, -CH<sub>3</sub>).

$^{13}C$  NMR (100 MHz, DMSO- $d_6$ ):  $\delta$  172.9 (-CONH-), 163.6 (-ArCO-), 149.05-151.59 (dd, -ArC 3 & 6), 139.94-142.47 (dt -ArC 4), 130.43 (-ArC 1), 117.91 (-CN), 112.93-113.14 (dd, -ArC 2 & 6), 52.2 ( $\alpha$ -C), 40.3 (-CH<sub>2</sub>, -VE DEPT), 27.5 (-CH<sub>2</sub>, -VE DEPT), 24.7 (-CH-), 23.3 (-CH<sub>3</sub>), 21.5 (-CH<sub>3</sub>).

$^{19}\text{F}$  NMR (376 MHz,  $\text{DMSO-}d_6$ ):  $\delta$ -58.22 - -58.30 (m), -80.76 - -80.91 (m).

### *N*-2,3,4,5-tetrafluorobenzoyl-L-leucine-glycine nitrile **108**

*N*-2,3,4,5-tetrafluorobenzoyl-L-leucine (1.54 g, 5 mmol) and glycine nitrile hydrochloride (0.46 g, 5 mmol) were used. Isolation by column chromatography and recrystallisation from ethyl acetate/hexane furnished **108** as a white powder (0.72 g, 42%).



m.p. 97-101 °C.

$[\alpha]_D^{25} = -2.2^\circ$  (c, 2.1, EtOH).

Anal. calcd. for  $\text{C}_{15}\text{H}_{15}\text{N}_3\text{O}_2\text{F}_4$ : C, 52.18; H, 4.38; N, 12.17.

Found C, 52.02; H, 4.33, N, 12.06.

IR (KBr):  $\nu$  3294, 2962, 2252, 1648, 1521, 1482, 1361, 1238, 1031, 881  $\text{cm}^{-1}$ .

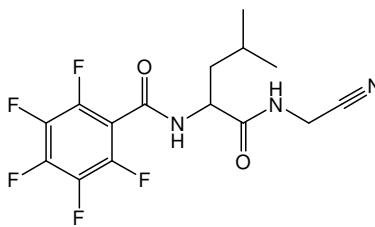
$^1\text{H}$  NMR (400 MHz,  $\text{DMSO-}d_6$ ):  $\delta$  8.80-8.84 (2H, m, -NH-), 7.61-7.63 (1H, m, -ArH 6), 4.44-4.50 (1H, m,  $\alpha$ -H), 4.17 (2H, d,  $J = 5.6$  Hz, - $\text{CH}_2$ -), 1.48-1.73 (3H, m, - $\text{CH}_2$ - & -CH-), 0.92 (3H, d,  $J = 6.4$  Hz, - $\text{CH}_3$ ), 0.89 (3H, d,  $J = 6.4$  Hz, - $\text{CH}_3$ ).

$^{13}\text{C}$  NMR (100 MHz,  $\text{DMSO-}d_6$ ):  $\delta$  172.5 (-CONH-), 161.5 (-ArCO-), 146.38-147.48 (d, -ArC 2), 144.00-145.00 (d, -ArC 5), 141.53-142.48 (d, -ArC 4), 138-91-139.95 (d, -ArC 3), 120.64 (-ArC 1), 117.87 (-CN), 112.13 (d, -ArC 6), 51.9 ( $\alpha$ -C), 40.6 (- $\text{CH}_2$ , -VE DEPT), 27.5 (- $\text{CH}_2$ , -VE DEPT), 24.6 (-CH-), 23.3 (- $\text{CH}_3$ ), 21.6 (- $\text{CH}_3$ ).

$^{19}\text{F}$  NMR (376 MHz,  $\text{DMSO-}d_6$ ):  $\delta$ -63.08 - -63.34 (2F m), -76.97 - -77.12 (1F m), -79.43 - -79.54 (1F t).

### *N*-2,3,4,5,6-pentafluorobenzoyl-L-leucine-glycine nitrile **109**

*N*-2,3,4,5,6-pentafluorobenzoyl-L-leucine (1.52 g, 6.6 mmol) and glycine nitrile hydrochloride (0.6 g, 6.6 mmol) were used. Isolation by column chromatography and recrystallisation from ethyl acetate/hexane furnished **109** as a white powder (1.20 g, 51%).



m.p. 131-133 °C.

$[\alpha]_D^{25} = -13.0^\circ$  (c, 2.1, EtOH).

Anal. calcd. for  $\text{C}_{15}\text{H}_{14}\text{N}_3\text{O}_2\text{F}_5$ : C, 49.60; H, 3.88; N, 11.57.

Found C, 49.70; H, 3.87, N, 11.40.

IR (KBr):  $\nu$  3265, 3077, 2962, 2252, 1654, 1554, 1521, 1343, 1115, 991  $\text{cm}^{-1}$ .

Mass Spectrum:  $\{M+\text{Na}^+\}$  found 386.1.

$\text{C}_{15}\text{H}_{14}\text{N}_3\text{O}_2\text{F}_5\text{Na}_1$  requires 386.29

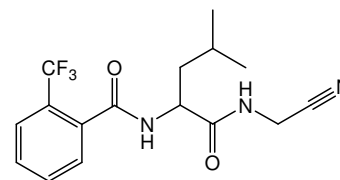
$^1\text{H}$  NMR (400 MHz,  $\text{DMSO}-d_6$ ):  $\delta$  9.26-9.28 (1H, d,  $J = 7.2$  Hz, -NH-), 8.96-8.99 (1H, t,  $J = 5.6$  Hz, -NH-), 4.51-4.57 (1H, m,  $\alpha$ -H), 4.20 (2H, d,  $J = 2.8$  Hz, -CH<sub>2</sub>-), 1.60-1.68 (3H, m, -CH<sub>2</sub>- & -CH-), 0.92 (6H, t,  $J = 6.8$  Hz, -CH<sub>3</sub>).

$^{13}\text{C}$  NMR (100 MHz,  $\text{DMSO}-d_6$ ):  $\delta$  172.1 (-CONH-), 156.9 (-ArCO-), 135.95, 138.41, 142.19, 142.72, 144.69 (m, -ArC 2,3,4,5,6), 117.81 (-CN), 112.6 (t, -ArC 1), 51.7 ( $\alpha$ -C), 40.8 (-CH<sub>2</sub>, -VE DEPT), 27.4 (-CH<sub>2</sub>, -VE DEPT), 24.5 (-CH-), 23.2 (-CH<sub>3</sub>), 21.5 (-CH<sub>3</sub>).

$^{19}\text{F}$  NMR (376 MHz,  $\text{DMSO}-d_6$ ):  $\delta$  -65.65 - -66.11 (2F, m), -76.99 - -77.11 (1F, m), -85.50 - -86.71 (2F, m).

### ***N*-2-trifluoromethylbenzoyl-L-leucine-glycine nitrile **110****

*N*-2-trifluoromethylbenzoyl-L-leucine (2.27 g, 7.5 mmol) and glycine nitrile hydrochloride (0.70 g, 7.5 mmol) were used. Isolation by column chromatography and recrystallisation from ethyl acetate/hexane furnished **110** as a white powder (1.30 g, 51%).



m.p. 163-166 °C.

$[\alpha]_D^{25} = -4.0^\circ$  (c, 2.1, EtOH).

Anal. calcd. for  $\text{C}_{16}\text{H}_{18}\text{N}_3\text{O}_2\text{F}_3$ : C, 56.30; H, 5.32; N, 12.31.

Found C, 56.07; H, 5.28; N, 12.17.

IR (KBr):  $\nu$  3292, 2958, 2247, 1642, 1547, 1341, 1283, 1173, 1121, 1068, 692  $\text{cm}^{-1}$ .

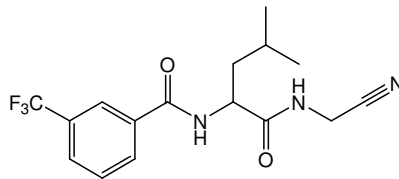
$^1\text{H}$  NMR (400 MHz,  $\text{DMSO}-d_6$ ):  $\delta$  8.79-8.81 (1H, d,  $J = 8$  Hz, -NH-), 8.75-8.77 (1H, t,  $J = 5.6$  Hz, -NH-), 7.73-7.79 (2H, m, -ArH 4 & 5), 7.66-7.68 (1H, d,  $J = 7.6$  Hz, -ArH 3), 7.58-7.60 (1H, d,  $J = 7.2$  Hz, -ArH 6), 4.41-4.55 (1H, m,  $\alpha$ -H), 4.19 (2H, d,  $J = 5.6$  Hz, -CH<sub>2</sub>-), 1.44-1.79 (3H, m, -CH<sub>2</sub>- & -CH-), 0.91 (3H, d,  $J = 2.8$  Hz, -CH<sub>3</sub>), 0.90 (3H, d,  $J = 2.8$  Hz, -CH<sub>3</sub>).

$^{13}\text{C}$  NMR (100 MHz,  $\text{DMSO}-d_6$ ):  $\delta$  172.9 (-CONH-), 167.5 (-ArCO-), 136.2 (-ArC 1) 132.6 (-ArC 6), 130.2 (-ArC 4), 129.2 (-ArC 3), 126.5 (t, -ArC 5), 125.4-126.2 (d, -ArC 2), 122.7 (d, -CF<sub>3</sub>), 117.9 (-CN), 51.6 ( $\alpha$ -C), 40.4 (-CH<sub>2</sub>, -VE DEPT), 27.5 (-CH<sub>2</sub>, -VE DEPT), 24.5 (-CH-), 23.3 (-CH<sub>3</sub>), 21.4 (-CH<sub>3</sub>).

$^{19}\text{F}$  NMR (376 MHz,  $\text{DMSO-}d_6$ ):  $\delta$  +18.08 (3F)

***N*-3-trifluoromethylbenzoyl-L-leucine-glycine nitrile 111**

*N*-3-trifluoromethylbenzoyl-L-leucine (2.27 g, 7.5 mmol) and glycine nitrile hydrochloride (0.70 g, 7.5 mmol) were used. Isolation by column chromatography and recrystallisation from ethyl acetate/hexane furnished **111** as a white powder (0.9 g, 36%).



m.p. 104-107 °C.

$[\alpha]_D^{25} = -33.5^\circ$  (c, 2.1, EtOH).

Anal. calcd. for  $\text{C}_{16}\text{H}_{18}\text{N}_3\text{O}_2\text{F}_3$ : C, 56.30; H, 5.32; N, 12.31.

Found C, 56.21; H, 5.34; N, 12.11.

IR (KBr):  $\nu$  3295, 2962, 2246, 1637, 1540, 1333, 1278, 1178, 1119, 1073, 696  $\text{cm}^{-1}$ .

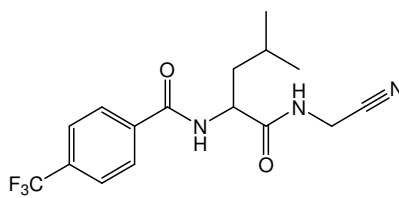
$^1\text{H}$  NMR (400 MHz,  $\text{DMSO-}d_6$ ):  $\delta$  8.94-8.96 (1H, d,  $J = 7.4$  Hz, -NH-), 8.82-8.85 (1H, t,  $J = 5.6$  Hz, -NH-), 8.33 (1H, -ArH 2), 8.26-8.27 (1H, d,  $J = 7.6$  Hz, -ArH 4), 7.94-7.96 (1H, d,  $J = 8$  Hz, -ArH 6), 7.75-7.79 (1H, t,  $J = 7.6$  Hz, -ArH 5), 4.55-4.62 (1H, m,  $\alpha$ -H), 4.19 (2H, d,  $J = 5.6$  Hz, - $\text{CH}_2$ -), 1.58-1.82 (3H, m, - $\text{CH}_2$ - & -CH-), 0.95 (3H, d,  $J = 6.4$  Hz, - $\text{CH}_3$ ), 0.91 (3H, d,  $J = 6.4$  Hz, - $\text{CH}_3$ ).

$^{13}\text{C}$  NMR (100 MHz,  $\text{DMSO-}d_6$ ):  $\delta$  173.1 (-CONH-), 165.4 (-ArCO-), 135.05(-ArC 1), 132.2 (-ArC 4), 129.9 (-ArC 5), 129.4 (d, -ArC 3), 128.3 (d, -ArC 6), 124.55 (d, -ArC 2), 123.0 (- $\text{CF}_3$ ), 117.9 (-CN), 52.0 ( $\alpha$ -C), 40.3 (- $\text{CH}_2$ , -VE DEPT), 27.5 (- $\text{CH}_2$ , -VE DEPT), 24.7 (-CH-), 23.3 (- $\text{CH}_3$ ), 21.5 (- $\text{CH}_3$ ).

$^{19}\text{F}$  NMR (376 MHz,  $\text{DMSO-}d_6$ ):  $\delta$  +14.94 (3F).

***N*-4-trifluoromethylbenzoyl-L-leucine-glycine nitrile 112**

*N*-4-trifluoromethylbenzoyl-L-leucine (1.52 g, 5 mmol) and glycine nitrile hydrochloride (0.46 g, 5 mmol) were used. Isolation by column chromatography and recrystallisation from ethyl acetate/hexane furnished **112** as a white powder (0.5 g, 28%).



m.p. 153-157 °C.

$[\alpha]_D^{25} = -26.0^\circ$  (c, 2.1, EtOH).

Anal. calcd. for C<sub>13</sub>H<sub>18</sub>N<sub>3</sub>O<sub>2</sub>S: C, 55.69; H, 6.47; N, 14.99.

Found C, 55.37; H, 6.09; N, 14.86.

IR (KBr):  $\nu$  3291, 2968, 2249, 1635, 1544, 1335, 1281, 1176, 1112, 1074, 691 cm<sup>-1</sup>.

<sup>1</sup>H NMR (400 MHz, DMSO-*d*<sub>6</sub>):  $\delta$  8.90-8.92 (1H, d, *J* = 8 Hz, -NH-), 8.82-8.85 (1H, t, *J* = 5.6 Hz, -NH-), 8.16 (2H, d, *J* = 8 Hz, -ArH 2 & 6), 7.91 (2H, d, *J* = 8.4 Hz, -ArH 3 & 5), 4.54-4.63 (1H, m,  $\alpha$ -H), 4.19 (2H, d, *J* = 5.6 Hz, -CH<sub>2</sub>-), 1.57-1.83 (3H, m, -CH<sub>2</sub>- & -CH-), 0.96 (3H, d, *J* = 6.4 & 17.2 Hz, -CH<sub>3</sub>), 0.92 (3H, d, *J* = 6.4 & 17.2 Hz, -CH<sub>3</sub>).

<sup>13</sup>C NMR (100 MHz, DMSO-*d*<sub>6</sub>):  $\delta$  173.1 (-CONH-), 165.7 (-ArCO-), 137.99 (-ArC 1), 131.62 (d, -ArC 4), 128.89 (-ArC 2 & 6), 125.6 (q, -ArC 3 & 5), 122.9 (-CF<sub>3</sub>), 117.9 (-CN), 52.0 ( $\alpha$ -C), 40.3 (-CH<sub>2</sub>, -VE DEPT), 27.5 (-CH<sub>2</sub>, -VE DEPT), 24.8 (-CH-), 23.3 (-CH<sub>3</sub>), 21.5 (-CH<sub>3</sub>).

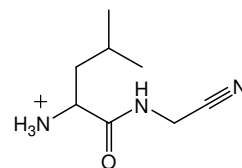
<sup>19</sup>F NMR (376 MHz, DMSO-*d*<sub>6</sub>):  $\delta$  +14.71 (3F)

#### **General procedure for the synthesis of *N*-substituted dipeptides:**

##### ***L*-leucine-glycine nitrile 114**

*N*-(9-Fluorenylmethoxycarbonyl)-*L*-leucine-glycine nitrile **130**

(2.0g, 4.76 mmol) was dissolved in anhydrous tetrahydrofuran (20mls). To this solution, 20mls of 10% piperidine in anhydrous THF was added under argon. The solution was



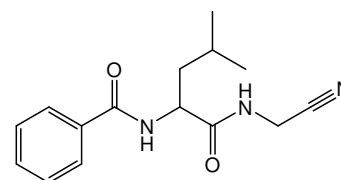
stirred for 2 hours with repeated TLC monitoring. The piperidine/THF solution was removed under vacuum to yield yellow and white residues. These residues were taken up in diethyl ether and repeatedly washed with hexane to remove white Fmoc by-product. Solvent was removed to yield **114**, as a yellow thick oil (0.74g, 90%).

<sup>1</sup>H NMR (400 MHz, CDCl<sub>3</sub>):  $\delta$  7.93 (1H, s, -NH-), 4.12-4.14 (2H, d, *J* = 6.14 Hz, -CH<sub>2</sub>-), 3.38-3.41 (1H, d, *J* = 12 Hz,  $\alpha$ -H), 1.65-1.69 (2H, m, -CH<sub>2</sub>-), 1.49 (2H, s, -NH<sub>2</sub>) 1.26-1.31 (1H, m, -CH-), 0.91 (3H, d, *J* = 3.1 Hz, -CH<sub>3</sub>), 0.87 (3H, d, *J* = 3.1 Hz, -CH<sub>3</sub>).

##### ***N*-benzoyl-*L*-leucine-glycine nitrile 115**

Benzoyl-*L*-leucine (1.57 g, 6.7 mmol) and glycine nitrile hydrochloride (0.6 g, 6.7 mmol) were used.

Isolation by column chromatography and recrystallisation from ethyl acetate/hexane furnished



**115** as a white powder (1.50 g, 82%).

m.p. = 165-167 °C

$[\alpha]_D^{25} = -2.2^\circ$  (c, 2.1, EtOH).

Anal. calcd. for C<sub>15</sub>H<sub>19</sub>N<sub>3</sub>O<sub>2</sub>: C, 65.91; H, 7.00; N, 15.37.

Found C, 65.89; H, 7.06; N, 15.23.

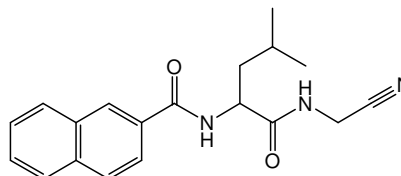
IR (KBr):  $\nu$  3283, 3190, 3046, 2957, 1157, 1657, 1635, 1540, 1253, 1039, 694, 657 cm<sup>-1</sup>.

<sup>1</sup>H NMR (400 MHz, DMSO-*d*<sub>6</sub>):  $\delta$  8.71-8.74 (1H, t, *J* = 5.5 Hz, -NH-), 8.58-8.60 (1H, d, *J* = 8 Hz, -NH-), 7.91-7.93 (2H, d, *J* = 8.4 Hz, -ArH 2 & 6), 7.53-7.55 (1H, t, *J* = 4 Hz, -ArH 4), 7.45-7.49 (2H, t, *J* = 7.8 Hz, -ArH 3 & 5) 4.48-4.55 (1H, m,  $\alpha$ -H), 4.13 (2H, d, *J* = 5.2 Hz, -CH<sub>2</sub>-), 1.53-1.76 (3H, m, -CH<sub>2</sub>- & -CH-), 0.92 (3H, d, *J* = 6.4 Hz, -CH<sub>3</sub>), 0.86 (3H, d, *J* = 6.4 Hz, -CH<sub>3</sub>).

<sup>13</sup>C NMR (100 MHz, DMSO-*d*<sub>6</sub>):  $\delta$  173.4 (-CONH-), 166.8 (-ArCO-), 134.2 (-ArC 1), 131.7 (-ArC 4), 128.5 (-ArC 2 & 6), 128.0 (-ArC 3 & 5), 118.0 (-CN), 51.8 ( $\alpha$ -C), 40.3 (-CH<sub>2</sub>, -VE DEPT), 27.5 (-CH<sub>2</sub>, -VE DEPT), 24.8 (-CH-), 22.4 (-CH<sub>3</sub>), 21.6 (-CH<sub>3</sub>).

### *N*-2-naphthoyl-*L*-leucine glycine nitrile **116**

*L*-leucine-glycine nitrile (0.75 g, 4.4 mmol) was dissolved in dichloromethane (40ml) with 2-naphthoic acid (0.42 g, 3 mmol). Isolation by column chromatography and recrystallisation from acetone/hexane furnished **116** as a white powder (0.65 g, 74%).



m.p. = 185-188 °C

$[\alpha]_D^{25} = -0.6^\circ$  (c, 2.1, EtOH).

Anal. calcd. for C<sub>19</sub>H<sub>21</sub>N<sub>3</sub>O<sub>2</sub> C, 70.27; H, 6.55; N, 12.99.

Found C, 70.27; H, 6.54; N, 12.84.

IR (KBr):  $\nu$  3341, 3238, 2957, 2241, 1648, 1642, 1537, 1315, 1302, 912, 839, 787, 681 cm<sup>-1</sup>.

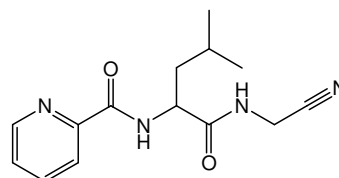
<sup>1</sup>H NMR (400 MHz, DMSO-*d*<sub>6</sub>):  $\delta$  8.76-8.81 (2H, m, -NH-), 8.55 (1H, s, -ArH 1), 7.98-8.06 (4H, m, -ArH 3,4,5 & 8), 7.59-7.65 (2H, m, -ArH 6 & 7), 4.56-4.62 (1H, m,  $\alpha$ -H), 4.16 (2H, d, *J* = 5.6 Hz, -CH<sub>2</sub>-), 1.56-1.82 (3H, m, -CH<sub>2</sub>- & -CH-), 0.95 (3H, d, *J* = 6.4 Hz, -CH<sub>3</sub>), 0.89 (3H, d, *J* = 6.4 Hz, -CH<sub>3</sub>).

$^{13}\text{C}$  NMR (100 MHz, DMSO- $d_6$ ):  $\delta$  173.0 (-CONH-), 166.5 (-ArCO-), 134.2 (-ArC 2), 132.0 & 131.2 (-ArC 9 & 10)\*, 128.8, 127.9, 127.6, 124.5 (-ArC 3,4,5 & 8)\*, 127.7 (-ArC 1), 127.6, 126.7 (-ArC 6 & 7)\*, 117.6 (-CN), 51.6 ( $\alpha$ -C), 40.0 (-CH<sub>2</sub>, -VE DEPT), 27.1 (-CH<sub>2</sub>, -VE DEPT), 24.4 (-CH-), 23.0 (-CH<sub>3</sub>), 21.2 (-CH<sub>3</sub>).

\*carbons individually unassignable

### ***N*-2-pyridinoyl-L-leucine-glycine nitrile 117**

L-leucine-glycine nitrile (0.9 g, 5.3 mmol) and 2-picolinic acid (0.65 g, 5.3 mmol) were used. Isolation by column chromatography and recrystallisation from ethyl acetate/hexane furnished **117** as a white powder (0.68 g, 47%).



m.p. = 109-112 °C

$[\alpha]_D^{25} = -1.4^\circ$  (c, 2.1, EtOH).

Anal. calcd. for C<sub>14</sub>H<sub>18</sub>N<sub>4</sub>O<sub>2</sub> C, 61.30; H, 6.61; N, 20.42.

Found C, 61.05; H, 6.58; N, 20.14.

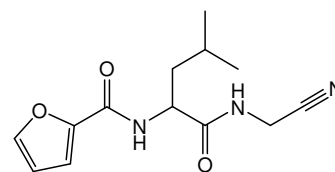
IR (KBr):  $\nu$  3406, 3391, 3294, 3054, 2983, 2957, 2931, 2875, 2243, 1684, 1667, 1509, 1465, 1483, 1349, 1000, 822, 751, 695 cm<sup>-1</sup>.

$^1\text{H}$  NMR (400 MHz, DMSO- $d_6$ ):  $\delta$  8.83-8.86 (1H, t,  $J = 5.6$  Hz, -NH-), 8.70-8.73 (1H, d,  $J = 8.8$  Hz, -NH-), 8.68-8.70 (2H, d, -ArH 6), 8.00-8.07 (2H, m, -ArH 3 & 4), 7.62-7.66 (1H, t, -ArH 5), 4.56-4.62 (1H, m,  $\alpha$ -H), 4.15 (2H, d,  $J = 5.6$  Hz, -CH<sub>2</sub>-), 1.56-1.76 (3H, m, -CH<sub>2</sub>- & -CH-), 0.90 (6H, t,  $J = 5.6$  Hz, -CH<sub>3</sub>).

$^{13}\text{C}$  NMR (100 MHz, DMSO- $d_6$ ):  $\delta$  172.4 (-CONH-), 163.6 (-ArCO-), 149.3 (-ArC 2), 148.5 (-ArC 6), 137.9 (-ArC 4), 126.8 (-ArC 5), 122.0 (-ArC 3), 117.5 (-CN), 51.0 ( $\alpha$ -C), 40.8 (-CH<sub>2</sub>, -VE DEPT), 27.1 (-CH<sub>2</sub>, -VE DEPT), 24.4 (-CH-), 22.9 (-CH<sub>3</sub>), 21.5 (-CH<sub>3</sub>).

### ***N*-2-furoyl-L-leucine glycine nitrile 118**

L-leucine-glycine nitrile (0.4 g, 2.4 mmol) was dissolved in dichloromethane (40ml) with 2-furoic acid (0.27 g, 2.4 mmol). Isolation by column chromatography and recrystallisation from acetone/hexane furnished **118** as a white powder (0.4 g, 60%).



m.p. = 107-109 °C



$[\alpha]_D^{25} = -13.6^\circ$  (c, 2.1, EtOH).

Anal. calcd. for  $C_{13}H_{17}N_3O_3$  C, 59.30; H, 6.51; N, 15.96.

Found C, 59.93; H, 6.84; N, 15.74.

IR (KBr):  $\nu$  3257, 3053, 2956, 2869, 2253, 1685, 1637, 1541, 1472, 1011, 938, 885, 763  $cm^{-1}$ .

$^1H$  NMR (400 MHz, DMSO- $d_6$ ):  $\delta$  8.74 (1H, t,  $J = 5.6$  Hz, -NH-), 8.46 (1H, d,  $J = 8.3$  Hz, -NH-), 7.86 (1H, d,  $J = 1.6$  Hz, -ArH 5), 7.21 (1H, d,  $J = 3.4$  Hz, -ArH 3), 7.21 (1H, t,  $J = 1.8$  Hz, -ArH 4), 4.43-4.49 (1H, m,  $\alpha$ -H), 4.12 (2H, d,  $J = 5.6$  Hz, -CH<sub>2</sub>-), 1.48-1.74 (3H, m, -CH<sub>2</sub>- & -CH-), 0.91 (3H, d,  $J = 6.4$  Hz, -CH<sub>3</sub>), 0.84 (3H, d,  $J = 6.4$  Hz, -CH<sub>3</sub>).

$^{13}C$  NMR (100 MHz, DMSO- $d_6$ ):  $\delta$  172.7 (-CONH-), 157.8 (-ArCO-), 147.3 (-ArC 2), 145.2 (-ArC 5), 117.6 (-CN), 113.9 (-ArC 3), 111.8 (-ArC 4), 50.6 ( $\alpha$ -C), 39.9 (-CH<sub>2</sub>, -VE DEPT), 27.1 (-CH<sub>2</sub>, -VE DEPT), 24.3 (-CH-), 23.0 (-CH<sub>3</sub>), 21.1 (-CH<sub>3</sub>).

#### *N*-thiophenoyl-L-leucine-glycine nitrile **119**

L-leucine-glycine nitrile (0.95 g, 5.6mmol) and thiophenecarboxylic acid (0.72 g, 5.6 mmol) was used.

Isolation by column chromatography and recrystallisation from ethyl acetate/hexane furnished

**119** as a white powder (0.91 g, 58%).

m.p. = 147-149 °C

$[\alpha]_D^{25} = -36.0^\circ$  (c, 2.1, EtOH).

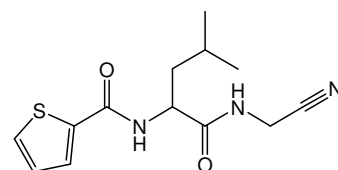
Anal. calcd. for  $C_{16}H_{18}N_3O_2F_3$ : C, 56.30; H, 5.32; N, 12.31.

Found C, 56.19; H, 5.32; N, 12.17.

IR (KBr):  $\nu$  3267, 3058, 2960, 2871, 2254, 1658, 1619, 1545, 1513, 1421, 1246, 1173, 1036, 864, 817, 717, 610  $cm^{-1}$ .

$^1H$  NMR (400 MHz, DMSO- $d_6$ ):  $\delta$  8.75-8.78 (1H, t,  $J = 5.5$  Hz, -NH-), 8.61-8.63 (1H, d,  $J = 8$  Hz, -NH-), 7.93 (1H, d,  $J = 3.7$  Hz, -ArH 5), 7.78 (1H, d,  $J = 4.9$  Hz, -ArH 3), 7.16 (1H, t, -ArH 4) 4.44-4.50 (1H, m,  $\alpha$ -H), 4.13 (2H, d,  $J = 5.6$  Hz, -CH<sub>2</sub>-), 1.53-1.72 (3H, m, -CH<sub>2</sub>- & -CH-), 0.92 (3H, d,  $J = 6.3$  Hz, -CH<sub>3</sub>), 0.86 (3H, d,  $J = 6.3$  Hz, -CH<sub>3</sub>).

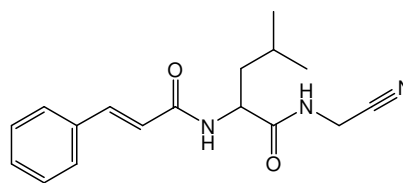
$^{13}C$  NMR (100 MHz, DMSO- $d_6$ ):  $\delta$  172.7 (-CONH-), 161.1 (-ArCO-), 139.29 (-ArC 1), 131.03 (-ArC 3), 128.71 (-ArC 5), 127.8 (-ArC 4), 117.5 (-CN), 51.2 ( $\alpha$ -C), 40.3 (-CH<sub>2</sub>, -VE DEPT), 27.1 (-CH<sub>2</sub>, -VE DEPT), 24.3 (-CH-), 22.9 (-CH<sub>3</sub>), 21.1 (-CH<sub>3</sub>).



***N-cinnamoyl-L-leucine-glycine nitrile 120***

L-leucine-glycine nitrile (0.2 g, 1.2 mmol) and cinnamic acid (0.18 g, 1.2 mmol) were used.

Isolation by column chromatography and



recrystallisation from ethyl acetate/hexane furnished **120** as a white powder (0.13 g, 35%).

m.p. = 155-159 °C

$[\alpha]_D^{25} = -18.2^\circ$  (c, 2.1, EtOH).

Anal. calcd. for  $C_{17}H_{21}N_3O_2$  C, 68.21; H, 7.07; N, 14.04.

Found C, 67.76; H, 6.98; N, 13.94.

IR (KBr):  $\nu$  3277, 3058, 2956, 2250, 1651, 1538, 1344, 1222, 973, 767, 724, 686  $cm^{-1}$ .

$^1H$  NMR (400 MHz, DMSO- $d_6$ ):  $\delta$  8.80-8.83 (1H, t,  $J = 5.6$  Hz, -NH-), 8.38-8.40 (1H, d,  $J = 8$  Hz, -NH-), 7.56-7.58 (2H, d, -ArH 2 & 6), 7.40-7.46 (4H, m, -ArH 3,4,5 & -ArCH-), 6.71-6.75 (1H, d,  $J = 16$  Hz, -CHCO-), 4.41-4.46 (1H, m,  $\alpha$ -H), 4.13 (2H, d,  $J = 5.6$  Hz, -CH<sub>2</sub>-), 1.48-1.64 (3H, m, -CH<sub>2</sub>- & -CH-), 0.91 (3H, d,  $J = 6.4$  Hz, -CH<sub>3</sub>), 0.86 (3H, d,  $J = 6.4$  Hz, -CH<sub>3</sub>).

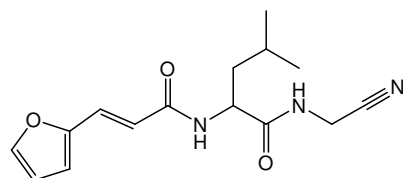
$^{13}C$  NMR (100 MHz, DMSO- $d_6$ ):  $\delta$  172.8 (-CONH-), 164.9 (-ArCO-), 139.1 (-COCH-), 134.8 (-ArC 1), 129.5 (-ArC 4), 129.0 (-ArC 2 & 6), 127.5 (-ArC 3 & 5), 121.8 (-ArCH-), 117.6 (-CN), 50.8 ( $\alpha$ -C), 40.7 (-CH<sub>2</sub>, -VE DEPT), 27.1 (-CH<sub>2</sub>, -VE DEPT), 24.3 (-CH-), 22.9 (-CH<sub>3</sub>), 21.4 (-CH<sub>3</sub>).

***N-2-furylacryloyl-L-leucine glycine nitrile 121***

L-leucine-glycine nitrile (0.5 g, 2.9 mmol) was

dissolved in dichloromethane (40ml) with 2-furylacrylic acid (0.4 g, 2.9 mmol). Isolation by

column chromatography and recrystallisation



from acetone/hexane furnished **121** as a white powder (0.66 g, 80%).

m.p. = 162-165 °C

$[\alpha]_D^{25} = -13.4^\circ$  (c, 2.1, EtOH).

Anal. calcd. for  $C_{15}H_{19}N_3O_3$  C, 62.27; H, 6.62; N, 14.52.

Found C, 61.97; H, 6.68; N, 14.23.

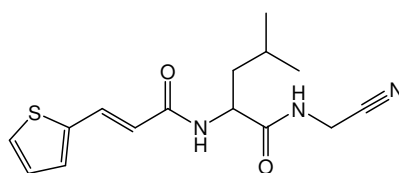
IR (KBr):  $\nu$  3255, 2958, 2872, 2246, 1655, 1627, 1536, 1340, 1232, 1030, 976, 769, 687  $cm^{-1}$ .

$^1\text{H}$  NMR (400 MHz,  $\text{DMSO-}d_6$ ):  $\delta$  8.80 (1H, t,  $J = 5.6$  Hz,  $-\text{NH}-$ ), 8.42 (1H, d,  $J = 8.1$  Hz,  $-\text{NH}-$ ), 7.80 (1H, d,  $J = 1.6$  Hz,  $-\text{ArH } 5$ ), 7.25 (1H, d,  $J = 15.6$  Hz,  $-\text{CH}-$ ), 6.78 (1H, d,  $J = 3.2$  Hz,  $-\text{ArH } 3$ ), 6.59 (1H, t,  $J = 1.6$  Hz,  $-\text{ArH } 4$ ), 6.51 (1H, d,  $J = 15.6$  Hz,  $-\text{CH}-$ ), 4.38-4.40 (1H, m,  $\alpha\text{-H}$ ), 4.13 (2H, d,  $J = 5.6$  Hz,  $-\text{CH}_2-$ ), 1.48-1.64 (3H, m,  $-\text{CH}_2-$  &  $-\text{CH}-$ ), 0.91 (3H, d,  $J = 6.4$  Hz,  $-\text{CH}_3$ ), 0.85 (3H, d,  $J = 6.4$  Hz,  $-\text{CH}_3$ ).

$^{13}\text{C}$  NMR (100 MHz,  $\text{DMSO-}d_6$ ):  $\delta$  172.8 ( $-\text{CONH}-$ ), 164.8 ( $-\text{ArCO}-$ ), 150.9 ( $-\text{ArC } 2$ ), 144.9 ( $-\text{ArC } 5$ ), 126.4 ( $-\text{CH}-$ ), 119.0 ( $-\text{CH}-$ ), 117.6 ( $-\text{CN}$ ), 113.9 ( $-\text{ArC } 3$ ), 112.4 ( $-\text{ArC } 4$ ), 50.8 ( $\alpha\text{-C}$ ), 40.6 ( $-\text{CH}_2$ ,  $-\text{VE DEPT}$ ), 27.0 ( $-\text{CH}_2$ ,  $-\text{VE DEPT}$ ), 24.2 ( $-\text{CH}-$ ), 22.9 ( $-\text{CH}_3$ ), 21.4 ( $-\text{CH}_3$ ).

### *N*-3-(2-thienyl)acryloyl-*L*-leucine-glycine nitrile **122**

*L*-leucine-glycine nitrile (1.04 g, 6.1 mmol) and 3-(2-thienyl)acrylic acid (0.95 g, 6.1 mmol) were used. Isolation by column chromatography and recrystallisation from ethyl acetate/hexane furnished **122** as a white powder (0.84 g, 45%).



m.p. = 173-176 °C

$[\alpha]_D^{25} = -2.8^\circ$  (c, 2.1, EtOH).

Anal. calcd. for  $\text{C}_{15}\text{H}_{19}\text{N}_3\text{O}_2\text{S}_1$  C, 58.99; H, 6.27; N, 13.76.

Found C, 58.72; H, 6.26; N, 13.46.

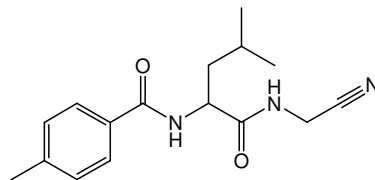
IR (KBr):  $\nu$  3276, 3061, 2957, 2251, 1668, 1645, 1615, 1538, 1230, 1207, 961, 706  $\text{cm}^{-1}$ .

$^1\text{H}$  NMR (400 MHz,  $\text{DMSO-}d_6$ ):  $\delta$  8.78-8.84 (1H, t,  $J = 5.6$  Hz,  $-\text{NH}-$ ), 8.36-8.38 (1H, d,  $J = 8$  Hz,  $-\text{NH}-$ ), 7.61-7.63 (1H, d,  $J = 5.6$  Hz,  $-\text{ArH } 4$ ), 7.57-7.61 (1H, d,  $J = 15.6$  Hz,  $-\text{ArCH}-$ ), 7.38-7.39 (1H, d,  $J = 3.2$  Hz,  $-\text{ArH } 2$ ), 7.10-7.13 (1H, t,  $J = 5.6$  Hz,  $-\text{ArH } 3$ ), 6.47-6.51 (1H, d,  $J = 15.6$  Hz,  $-\text{CHCO}-$ ), 4.35-4.42 (1H, m,  $\alpha\text{-H}$ ), 4.13 (2H, d,  $J = 5.6$  Hz,  $-\text{CH}_2-$ ), 1.47-1.63 (3H, m,  $-\text{CH}_2-$  &  $-\text{CH}-$ ), 0.91 (3H, d,  $J = 6.4$  & 17.6 Hz,  $-\text{CH}_3$ ), 0.85 (3H, d,  $J = 6.4$  & 17.6 Hz,  $-\text{CH}_3$ ).

$^{13}\text{C}$  NMR (100 MHz,  $\text{DMSO-}d_6$ ):  $\delta$  172.8 ( $-\text{CONH}-$ ), 164.7 ( $-\text{ArCO}-$ ), 149.0 ( $-\text{ArC } 2$ ), 132.1 ( $-\text{ArCH}-$ ), 130.7 ( $-\text{ArC } 2$ ), 128.3 ( $-\text{ArC } 3$ ), 128.0 ( $-\text{ArC } 4$ ), 120.5 ( $-\text{CHCO}-$ ), 117.5 ( $-\text{CN}$ ), 50.9 ( $\alpha\text{-C}$ ), 40.6 ( $-\text{CH}_2$ ,  $-\text{VE DEPT}$ ), 27.1 ( $-\text{CH}_2$ ,  $-\text{VE DEPT}$ ), 24.2 ( $-\text{CH}-$ ), 22.9 ( $-\text{CH}_3$ ), 21.4 ( $-\text{CH}_3$ ).

### *N*-4-methylbenzoyl-*L*-leucine glycine nitrile **123**

L-leucine-glycine nitrile (0.5 g, 3 mmol) was dissolved in dichloromethane (40ml) with 4-methylbenzoic acid (0.42 g, 3 mmol). Isolation by column chromatography and recrystallisation from acetone/hexane furnished **123** as a white powder (0.65 g, 74%).



m.p. = 172-176 °C

$[\alpha]_D^{25} = -23.8^\circ$  (c, 2.1, EtOH).

Anal. calcd. for  $C_{16}H_{21}N_3O_2$  C, 66.88; H, 7.37; N, 14.62.

Found C, 67.01; H, 7.49; N, 14.33.

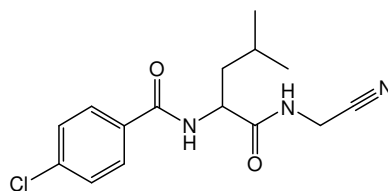
IR (KBr):  $\nu$  3308, 3055, 2954, 2870, 2250, 1662, 1636, 1545, 1504, 1329, 1280, 1038, 836, 753  $cm^{-1}$ .

$^1H$  NMR (400 MHz, DMSO- $d_6$ ):  $\delta$  8.71 (1H, t,  $J = 5.6$  Hz, -NH-), 8.41 (1H, d,  $J = 8$  Hz, -NH-), 7.83 (2H, d,  $J = 8$  Hz, -ArH 2 & 6), 7.28 (2H, d,  $J = 8$  Hz, -ArH 3 & 5), 4.47-4.53 (1H, m,  $\alpha$ -H), 4.13 (2H, d,  $J = 5.6$  Hz, -CH<sub>2</sub>-), 2.36 (3H, s, -CH<sub>3</sub>) 1.49-1.76 (3H, m, -CH<sub>2</sub>- & -CH-), 0.92 (3H, d,  $J = 6.4$  Hz, -CH<sub>3</sub>), 0.85 (3H, d,  $J = 6.4$  Hz, -CH<sub>3</sub>).

$^{13}C$  NMR (100 MHz, DMSO- $d_6$ ):  $\delta$  173.0 (-CONH-), 166.2 (-ArCO-), 141.2 (-ArC 1), 131.0 (-ArC 4), 128.6 (-ArC 2 & 6), 127.5 (-ArC 3 & 5), 117.6 (-CN), 51.3 ( $\alpha$ -C), 39.9 (-CH<sub>2</sub>-), 27.0 (-CH<sub>2</sub>, -VE DEPT), 24.3 (-CH, -VE DEPT), 22.9 (-CH<sub>3</sub>), 21.1 (-CH<sub>3</sub>), 20.9 (-CH<sub>3</sub>).

#### ***N*-4-chlorobenzoyl-L-leucine glycine nitrile 124**

L-leucine-glycine nitrile (0.5 g, 3 mmol) was dissolved in dichloromethane (40ml) with 4-chlorobenzoic acid (0.46 g, 3 mmol). Isolation by column chromatography and recrystallisation from acetone/hexane furnished **124** as a white powder (0.49 g, 54%).



m.p. = 184-187 °C

$[\alpha]_D^{25} = -19.2^\circ$  (c, 2.1, EtOH).

Anal. calcd. for  $C_{15}H_{18}N_3O_2Cl$  C, 58.54; H, 5.89; N, 13.65.

Found C, 58.48; H, 5.99; N, 13.38.

IR (KBr):  $\nu$  3277, 3054, 2958, 2246, 1675, 1634, 1535, 1330, 844, 684  $cm^{-1}$ .

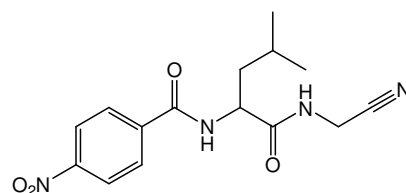
$^1H$  NMR (400 MHz, DMSO- $d_6$ ):  $\delta$  8.75 (1H, t,  $J = 5.6$  Hz, -NH-), 8.69 (1H, d,  $J = 8$  Hz, -NH-), 7.94 (2H, d,  $J = 8.8$  Hz, -ArH 2 & 6), 7.56 (2H, d,  $J = 8.8$  Hz, -ArH 3 &

5), 4.47-4.53 (1H, m,  $\alpha$ -H), 4.13 (2H, d,  $J = 5.6$  Hz,  $-\text{CH}_2-$ ), 1.51-1.76 (3H, m,  $-\text{CH}_2-$  &  $-\text{CH}-$ ), 0.92 (3H, d,  $J = 6.4$  Hz,  $-\text{CH}_3$ ), 0.86 (3H, d,  $J = 6.4$  Hz,  $-\text{CH}_3$ ).

$^{13}\text{C}$  NMR (100 MHz, DMSO- $d_6$ ):  $\delta$  172.8 ( $-\text{CONH}-$ ), 165.3 ( $-\text{ArCO}-$ ), 136.1 ( $-\text{ArC}$  1), 132.5 ( $-\text{ArC}$  4), 129.5 ( $-\text{ArC}$  2 & 6), 128.2 ( $-\text{ArC}$  3 & 5), 117.5 ( $-\text{CN}$ ), 51.5 ( $\alpha$ -C), 39.9 ( $-\text{CH}_2$ , -VE DEPT), 27.1 ( $-\text{CH}_2$ , -VE DEPT), 24.4 ( $-\text{CH}-$ ), 23.0 ( $-\text{CH}_3$ ), 21.2 ( $-\text{CH}_3$ ).

#### ***N*-4-nitrobenzoyl-*L*-leucine-glycine nitrile **125****

*L*-leucine-glycine nitrile (0.8 g, 4.7 mmol) was dissolved in dichloromethane (40ml) with 4-nitrobenzoic acid (0.31 g, 4.7 mmol), 1-hydroxybenzotriazole (0.63 g, 4.7 mmol) and triethylamine (0.65 ml, 4.7 mmol). The mixture was cooled to 0 °C, and *N*-(3-Dimethylaminopropyl)-*N'*-ethylcarbodiimide hydrochloride (0.9 g, 4.7 mmol) was added. After 30 min. the solution was raised to room temperature and the reaction was allowed to proceed for 48 hrs. The precipitated *N*, *N*-dicyclohexylurea was removed by filtration and the filtrate was washed with brine, sat. potassium hydrogen carbonate, 10% citric acid and dried over sodium sulphate. The solvent was evaporated *in vacuo* and isolation by column chromatography and recrystallisation from ethyl acetate/hexane furnished **125** as a white powder (0.96 g, 65%).



m.p. = 161-165 °C  
[ $\alpha$ ]<sub>D</sub><sup>25</sup> = -4.0° (c, 2.1, EtOH).  
Anal. calcd. for C<sub>15</sub>H<sub>18</sub>N<sub>4</sub>O<sub>4</sub> C, 56.60; H, 5.70; N, 17.60.  
Found C, 56.33; H, 5.69; N, 17.30.

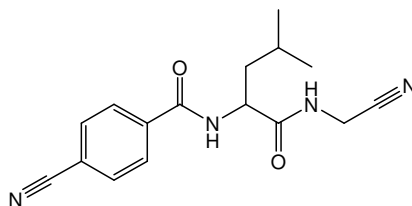
IR (KBr):  $\nu$  3279, 3053, 2955, 2873, 2254, 1167, 1639, 1602, 1535, 1436, 1353, 1273, 1214, 1154, 1169, 1015, 873, 845, 787, 704, 633  $\text{cm}^{-1}$ .

$^1\text{H}$  NMR (400 MHz, DMSO- $d_6$ ):  $\delta$  8.96-8.98 (1H, d,  $J = 8$  Hz,  $-\text{NH}-$ ), 8.79-8.81 (1H, t,  $J = 5.2$  Hz,  $-\text{NH}-$ ), 8.33-8.35 (2H, d,  $-\text{ArH}$  3 & 5), 8.13-8.15 (2H, d,  $-\text{ArH}$  2 & 6), 4.50-4.55 (1H, m,  $\alpha$ -H), 4.15 (2H, d,  $J = 5.6$  Hz,  $-\text{CH}_2-$ ), 1.55-1.74 (3H, m,  $-\text{CH}_2-$  &  $-\text{CH}-$ ), 0.93 (3H, d,  $J = 6.4$  Hz,  $-\text{CH}_3$ ), 0.87 (3H, d,  $J = 6.4$  Hz,  $-\text{CH}_3$ ).

$^{13}\text{C}$  NMR (100 MHz, DMSO- $d_6$ ):  $\delta$  172.5 ( $-\text{CONH}-$ ), 164.8 ( $-\text{ArCO}-$ ), 149.0 ( $-\text{ArC}$  4), 139.4 ( $-\text{ArC}$  1), 129.0 ( $-\text{ArC}$  3 & 5), 123.3 ( $-\text{ArC}$  2 & 6), 117.5 ( $-\text{CN}$ ), 51.6 ( $\alpha$ -C), 40.2 ( $-\text{CH}_2$ , -VE DEPT), 27.1 ( $-\text{CH}_2$ , -VE DEPT), 24.4 ( $-\text{CH}-$ ), 23.0 ( $-\text{CH}_3$ ), 21.2 ( $-\text{CH}_3$ ).

***N*-4-cyanobenzoyl-L-leucine glycine nitrile **126****

L-leucine-glycine nitrile (0.62 g, 3.7 mmol) and 4-cyanobenzoic acid (0.54 g, 3.7 mmol) were used. Isolation by column chromatography and recrystallisation from ethyl acetate/petroleum ether (40:60) furnished **126** as a white powder (0.75 g, 69%).



m.p. = 147-151 °C

$[\alpha]_D^{25} = -10.4^\circ$  (c, 2.1, EtOH).

Anal. calcd. for  $C_{16}H_{18}N_4O_2$  C, 64.41; H, 6.08; N, 18.78.

Found C, 64.15; H, 6.26; N, 118.49

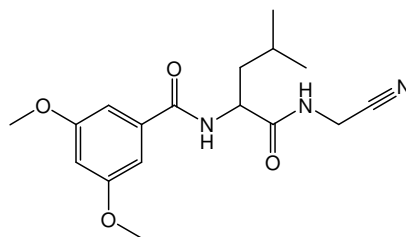
IR (KBr):  $\nu$  3273, 3068, 2961, 2933, 2231, 1672, 1640, 1548, 1500, 1327, 1247, 864, 768  $cm^{-1}$ .

$^1H$  NMR (400 MHz, DMSO- $d_6$ ):  $\delta$  8.89 (1H, d,  $J = 7.9$  Hz, -NH-), 8.80 (1H, t,  $J = 5.5$  Hz, -NH-), 8.07 (2H, d,  $J = 8.4$  Hz, -ArH 2 & 6), 7.99 (2H, d,  $J = 8.4$  Hz, -ArH 3 & 5), 4.48-4.55 (1H, m,  $\alpha$ -H), 4.15 (2H, d,  $J = 5.6$  Hz, -CH<sub>2</sub>-), 1.52-1.77 (3H, m, -CH<sub>2</sub>-, -CH-), 0.89 (3H, d,  $J = 6.3$  Hz, -CH<sub>3</sub>), 0.92 (3H, d,  $J = 6.3$  Hz, -CH<sub>3</sub>).

$^{13}C$  NMR (100 MHz, DMSO- $d_6$ ):  $\delta$  172.6 (-CONH-), 165.1 (-ArCON-), 137.8 (-ArC 1), 132.3 (-ArC 2,6), 128.5 (-ArC 3,5), 118.3 (-ArCN), 117.6 (-CH<sub>2</sub>CN), 113.7 (-ArC 4), 51.6 ( $\alpha$ -C), 40.1 (-CH<sub>2</sub>, -VE DEPT), 27.1 (-CH<sub>2</sub>, -VE DEPT), 24.4 (-CH-), 23.0 (-CH<sub>3</sub>), 21.2 (-CH<sub>3</sub>).

***N*-3,5-dimethoxybenzoyl-L-leucine-glycine nitrile **127****

3,5-dimethoxybenzoyl-L-leucine (2.59 g, 8.75mmol) and glycine nitrile hydrochloride (0.8 g, 8.8 mmol) were used. Isolation by column chromatography and recrystallisation from ethyl acetate/hexane furnished **127** as a white powder (1.62 g, 55%).



m.p. = 153-156 °C

$[\alpha]_D^{25} = -2.8^\circ$  (c, 2.1, EtOH).

Anal. calcd. for  $C_{17}H_{23}N_3O_4$  C, 61.25; H, 6.95; N, 12.60.

Found C, 61.21; H, 6.92; N, 12.49.

IR (KBr):  $\nu$  3243, 3057, 2959, 2230, 1673, 1629, 1595, 1548, 1461, 1343, 1240, 1195, 1158, 1063, 859, 762, 678  $\text{cm}^{-1}$ .

$^1\text{H}$  NMR (400 MHz,  $\text{DMSO-}d_6$ ):  $\delta$  8.69-8.72 (1H, t,  $J = 5.6$  Hz, -NH-), 8.55-8.57 (1H, d,  $J = 8$  Hz, -NH-), 7.09 (2H, -ArH 2 & 6), 6.67 (1H, -ArH 4), 4.47-4.54 (1H, m,  $\alpha$ -H), 4.13 (2H, d,  $J = 5.2$  Hz, - $\text{CH}_2$ -), 3.8 (6H, - $\text{OCH}_3$ ), 1.52-1.73 (3H, m, - $\text{CH}_2$ - & -CH-), 0.92 (3H, d,  $J = 6.4$  Hz, - $\text{CH}_3$ ), 0.87 (3H, d,  $J = 6.4$  Hz, - $\text{CH}_3$ ).

$^{13}\text{C}$  NMR (100 MHz,  $\text{DMSO-}d_6$ ):  $\delta$  172.9 (-CONH-), 165.9 (-ArCO-), 160.2 (-ArC 3 & 5), 135.9 (-ArC 1), 117.6 (-CN), 105.5 (-ArC 2 & 6), 103.3 (-ArC 4), 55.4 (- $\text{OCH}_3$ ), 51.5 ( $\alpha$ -C), 40.1 (- $\text{CH}_2$ , -VE DEPT), 27.1 (- $\text{CH}_2$ , -VE DEPT), 24.4 (-CH-), 23.0 (- $\text{CH}_3$ ), 21.3 (- $\text{CH}_3$ ).

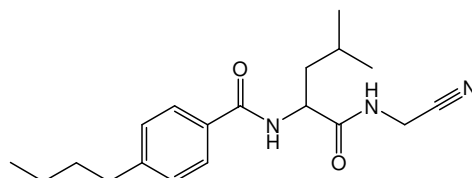
#### *N*-4-butylbenzoyl-L-leucine glycine nitrile **128**

L-leucine-glycine nitrile (0.56 g, 3.4 mmol)

was dissolved in dichloromethane (40ml)

with 4-butylbenzoic acid (0.60 g, 3.4

mmol). Isolation by column



chromatography and recrystallisation from ethyl acetate/petroleum ether (40:60)

furnished **128** as a white powder (0.69 g, 63%).

m.p. = 101-104  $^{\circ}\text{C}$

$[\alpha]_D^{25} = -16.6^{\circ}$  (c, 2.1, EtOH).

Anal. calcd. for  $\text{C}_{19}\text{H}_{27}\text{N}_3\text{O}_2$  C, 69.27; H, 8.26; N, 12.75.

Found C, 69.08; H, 8.27; N, 12.61.

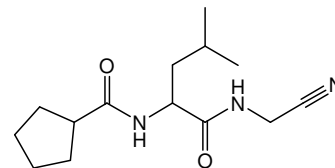
IR (KBr):  $\nu$  3290, 3059, 2955, 2930, 2870, 2248, 1657, 1633, 1544, 1504, 1242, 849, 761, 626  $\text{cm}^{-1}$ .

$^1\text{H}$  NMR (400 MHz,  $\text{DMSO-}d_6$ ):  $\delta$  8.70 (1H, t,  $J = 5.6$  Hz, -NH-), 8.51 (1H, d,  $J = 8$  Hz, -NH-), 7.85 (2H, d,  $J = 8$  Hz, -ArH 2 & 6), 7.29 (2H, d,  $J = 8$  Hz, -ArH 3 & 5), 4.49-4.55 (1H, m,  $\alpha$ -H), 4.13 (2H, d,  $J = 5.6$  Hz, - $\text{CH}_2$ -), 2.63 (2H, t,  $J = 7.6$  Hz, - $\text{CH}_2\text{CH}_2$ -), 1.51-1.77 (5H, m, - $\text{CH}_2\text{CH}_2$ -, - $\text{CH}_2$ - & -CH-), 1.25-1.34 (2H, sex,  $J = 7.6$ , - $\text{CH}_2\text{CH}_3$ ), 0.88-0.92 (9H, m, - $\text{CH}_3$ ).

$^{13}\text{C}$  NMR (100 MHz,  $\text{DMSO-}d_6$ ):  $\delta$  173.1 (-CONH-), 166.3 (-ArCO-), 146.0 (-ArC 1), 131.3 (-ArC 4), 128.0 (-ArC 2 & 6), 127.7 (-ArC 3 & 5), 117.6 (-CN), 51.4 ( $\alpha$ -C), 39.9 (- $\text{CH}_2$ , -VE DEPT), 34.6 (- $\text{CH}_2$ , -VE DEPT), 32.9 (- $\text{CH}_2$ , -VE DEPT), 27.1 (- $\text{CH}_2$ , -VE DEPT), 24.4 (-CH-), 23.0 (- $\text{CH}_3$ ), 21.7 (- $\text{CH}_2$ , -VE DEPT), 21.2 (- $\text{CH}_3$ ), 13.7 (- $\text{CH}_3$ ).

### *N-cyclopentanoyl-L-leucine-glycine nitrile 129*

L-leucine-glycine nitrile (0.84 g, 5 mmol) and cyclopentane carboxylic acid (0.54 g, 5 mmol) were used. Isolation by column chromatography and recrystallisation from ethyl acetate/hexane furnished **129** as a white powder (0.76 g, 58%).



m.p. = 143-145 °C

$[\alpha]_D^{25} = -40.2^\circ$  (c, 2.1, EtOH).

Anal. calcd. for  $C_{14}H_{23}N_3O_2$ : C, 63.37; H, 8.74; N, 15.84.

Found C, 63.08; H, 8.59; N, 15.73.

IR (KBr):  $\nu$  3272, 3066, 2957, 2870, 2242, 1668, 1641, 1543, 1228, 1039, 904, 691  $cm^{-1}$ .

Mass Spectrum:  $\{M+Na^+\}$  found 288.2.

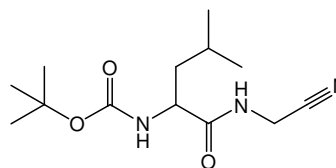
$C_{14}H_{23}N_3O_2Na_1$  requires 288.34.

$^1H$  NMR (400 MHz,  $CDCl_3$ ):  $\delta$  8.59-8.62 (1H, t,  $J = 5.5$  Hz, -NH-), 6.98-7.00 (1H, d,  $J = 8$  Hz, -NH-), 4.56-4.62 (1H, m,  $\alpha$ -H), 4.05 (2H, d,  $J = 5.2$  Hz, - $CH_2$ -), 2.51-2.60 (1H, p, -CHCO-) 1.46-1.78 (11H, m, - $CH_2$ -, -CH- & -cyclo $CH_2$ -), 0.88 (3H, d,  $J = 6.1$  Hz, - $CH_3$ ), 0.82 (3H, d,  $J = 6.1$  Hz, - $CH_3$ ).

$^{13}C$  NMR (100 MHz,  $DMSO-d_6$ ):  $\delta$  177.3 (-cycloCO-), 173.8 (-CONH-), 116.1 (-CN), 51.4 ( $\alpha$ -C), 45.1 (-CHCO-), 41.0 (- $CH_2$ -, -VE DEPT), 31.0, 30.0, 26.1 & 26.0 (-cyclo $CH_2$ -, -VE DEPT), 27.5 (- $CH_2$ -, -VE DEPT), 24.8 (-CH), 22.7 (- $CH_3$ ), 22.1 (- $CH_3$ ).

### *N-tert-butoxycarbonyl-L-leucine-glycine nitrile 130*

BOC-L-leucine (1 g, 4.3mmol) and glycine nitrile hydrochloride (0.4 g, 4.3 mmol) were used. Recrystallisation from ethyl acetate/hexane furnished **130** as a white powder (0.96 g, 82%).



m.p. = 116-119 °C

$[\alpha]_D^{25} = -33.0^\circ$  (c, 2.1, EtOH).

IR (KBr):  $\nu$  3335, 3311, 2963, 2240, 1671, 1523, 1274, 1164, 1051, 896, 850, 644  $cm^{-1}$ .

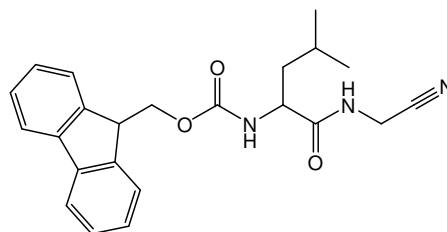


$^1\text{H}$  NMR (400 MHz,  $\text{DMSO-}d_6$ ):  $\delta$  8.55-8.58 (1H, t,  $J = 5.4$  Hz,  $-\text{NH}-$ ), 7.01 (2H, d,  $J = 8$  Hz,  $-\text{NH}-$ ), 4.11 (2H, d,  $J = 5.8$  Hz,  $-\text{CH}_2-$ ), 3.95 (1H, m,  $\alpha\text{-H}$ ), 1.37-1.63 (12H, m,  $-\text{CH}_2-$ ,  $-\text{CH}-$  & t- $\text{CH}_3$ ), 0.88 (3H, d,  $J = 6.6$  Hz,  $-\text{CH}_3$ ), 0.84 (3H, d,  $J = 6.6$  Hz,  $-\text{CH}_3$ ).

$^{13}\text{C}$  NMR (100 MHz,  $\text{DMSO-}d_6$ ):  $\delta$  173.3 ( $-\text{CONH}-$ ), 155.4 ( $-\text{OCO}-$ ), 117.6 ( $-\text{CN}$ ), 78.1 ( $-\text{C}(\text{CH}_3)_3-$ ), 52.4 ( $\alpha\text{-C}$ ), 40.3 ( $-\text{CH}_2-$ , -VE DEPT), 28.1 ( $-\text{CH}_3$ ), 27.0 ( $-\text{CH}_2-$ , -VE DEPT), 24.2 ( $-\text{CH}-$ ), 22.9 ( $-\text{CH}_3$ ), 21.3 ( $-\text{CH}_3$ ).

***N*-(9-fluorenylmethoxycarbonyl)-L-leucine-glycine nitrile **131****

FMOC-L-leucine (10.6 g, 30mmol) and glycine nitrile hydrochloride (2.78 g, 30 mmol) were used. Recrystallisation from ethyl acetate/hexane furnished **131** as a white powder (12.24 g, 95%).



m.p. = 160-163 °C

$[\alpha]_D^{25} = -38.8^\circ$  (c, 2.1, EtOH).

Anal. calcd. for  $\text{C}_{22}\text{H}_{23}\text{N}_3\text{O}_3$  C, 70.01; H, 6.14; N, 11.13.

Found C, 70.14; H, 6.39; N, 10.36.

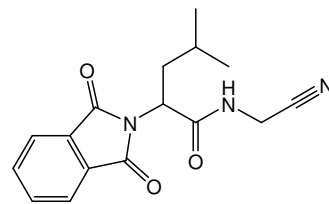
IR (KBr):  $\nu$  2963, 2588, 2273, 1720, 1566, 1508, 1428, 1357, 1256, 1223, 1106, 1055, 1028, 884, 861, 758, 739, 728, 656  $\text{cm}^{-1}$ .

$^1\text{H}$  NMR (400 MHz,  $\text{DMSO-}d_6$ ):  $\delta$  8.73-8.76 (1H, t,  $J = 5.6$  Hz,  $-\text{NH}-$ ), 7.90 (2H, d,  $J = 7.5$  Hz, - ArH 5-), 7.75 (2H, t,  $J = 5.4$  Hz, -ArH 3), 7.67 (1H, d,  $J = 8.2$  Hz,  $-\text{NH}-$ ), 7.43 (2H, t,  $J = 14.7$  Hz, -ArH 4), 7.31-7.36 (2H, m, -ArH 2), 4.15-4.37 (3H, m,  $-\text{CHCH}_2\text{O}-$ ), 4.15 (2H, d,  $J = 5.6$  Hz,  $-\text{CH}_2-$ ), 4.06 (1H, m,  $\alpha\text{-H}$ ), 1.39-1.67 (3H, m,  $-\text{CH}_2-$  &  $-\text{CH}-$ ), 0.91 (3H, d,  $J = 6.5$  Hz,  $-\text{CH}_3$ ), 0.86 (3H, d,  $J = 6.5$  Hz,  $-\text{CH}_3$ ).

$^{13}\text{C}$  NMR (100 MHz,  $\text{DMSO-}d_6$ ):  $\delta$  173.1 ( $-\text{CONH}-$ ), 156.0 ( $-\text{OCO}-$ ), 143.7 (d, -ArC 1), 140.7 (d, -ArC 6), 127.6 (-ArC 4), 127.0 (-ArC 2), 125.3 (-ArC 3), 120.1 (-ArC 5), 117.6 ( $-\text{CN}$ ), 65.6 ( $-\text{CHCH}_2\text{O}$ , -VE DEPT), 52.7 ( $\alpha\text{-C}$ ), 46.7 ( $-\text{CHCH}_2\text{O}-$ ), 40.3 ( $-\text{CH}_2-$ , -VE DEPT), 27.1 ( $-\text{CH}_2-$ , -VE DEPT), 24.3 ( $-\text{CH}-$ ), 22.9 ( $-\text{CH}_3$ ), 21.3 ( $-\text{CH}_3$ ).

### *N-phthalimide-L-leucine-glycine nitrile 132*

N-phthalimide-L-leucine (1.93 g, 7.4 mmol) and glycine nitrile hydrochloride (0.7 g, 7.4 mmol) were used. Isolation by column chromatography and recrystallisation from ethyl acetate/hexane furnished **132** as a red powder (1.38 g, 62%).



m.p. = 217-220 °C

$[\alpha]_D^{25} = -38.8^\circ$  (c, 2.1, EtOH).

Anal. calcd. for  $C_{16}H_{17}N_3O_2$  C, 67.83; H, 6.05; N, 14.83.

Found C, 64.02; H, 5.78; N, 13.96.

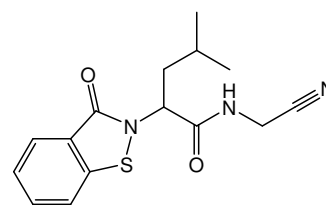
IR (KBr):  $\nu$  3325, 2928, 2851, 2267, 1625, 1577, 1536, 1437, 1312, 1244, 1089, 893, 641  $cm^{-1}$ .

$^1H$  NMR (400 MHz, DMSO- $d_6$ ):  $\delta$  8.88-8.90 (1H, t,  $J = 5.2$  Hz, -NH-), 7.93-7.99 (4H, m, -ArH), 4.78-4.82 (1H, m,  $\alpha$ -H), 4.17 (2H, d,  $J = 5.2$  Hz, -CH $_2$ -), 2.17 (1H, t, -CH $_2$ -), 1.94 (1H, t, -CH $_2$ -), 1.38 (1H, m, -CH-), 0.91 (6H, t,  $J = 6.4$  Hz, -CH $_3$ ).

$^{13}C$  NMR (100 MHz, DMSO- $d_6$ ):  $\delta$  169.3 (-CONH-), 167.5 (-ArCO-), 134.7 (-ArC 2 & 5), 131.4 (-ArC 1 & 6), 123.3 (-ArC 3 & 4), 117.4 (-CN), 50.9 ( $\alpha$ -C), 36.4 (-CH $_2$ , -VE DEPT), 27.4 (-CH $_2$ , -VE DEPT), 24.5 (-CH-), 23.1 (-CH $_3$ ), 20.8 (-CH $_3$ ).

### *N-1,2-benzisothiazolin-3-one-L-leucine-glycine nitrile 133*

L-leucine-glycine nitrile (0.7 g, 4.12 mmol) and thiosalyicyclic acid (0.64 g, 4.12 mmol) were used. Isolation by column chromatography and recrystallisation from ethyl acetate/hexane furnished **133** as a white powder (0.15 g, 12%).



m.p. = 122-125 °C

$[\alpha]_D^{25} = -8.8^\circ$  (c, 2.1, EtOH).

IR (KBr):  $\nu$  3209, 3045, 2955, 2920, 2252, 1681, 1622, 1550, 1446, 1329, 1243, 1032, 736, 673  $cm^{-1}$ .

Mass Spectrum:  $\{M+Na^+\}$  found 326.09.

$C_{15}H_{17}N_3O_2S_1Na_1$  requires 326.1.

$^1H$  NMR (400 MHz, ACN- $d_3$ ):  $\delta$  7.94 (1H, d,  $J = 8$  Hz, -ArH 6-), 7.79 (1H, d, -ArH 3), 7.68 (1H, t, -ArH 5), 7.54 (1H, t,  $J = 5.6$  Hz, -NH-), 7.45 (1H, t, -ArH 4), 5.34-5.38

(1H, dd,  $J = 5.0$  &  $9.6$  Hz  $\alpha$ -H), 4.08 (2H, d,  $J = 2$  Hz, -CH<sub>2</sub>-), 1.82-1.98 (2H, m, -CH<sub>2</sub>-), 1.34-1.47 (1H, m, -CH-), 0.93 (6H, d,  $J = 7.3$  Hz, -CH<sub>3</sub>).

<sup>13</sup>C NMR (100 MHz, ACN-*d*<sub>3</sub>):  $\delta$  171.1 (-CONH-), 166.3 (-ArCON-), 142.2 (-ArC 1), 133.2 (-ArC 6), 126.9 (-ArC 3), 126.5 (-ArC 5), 124.6 (-ArC 2), 121.9 (-ArC 4), 117.5 (-CN), 55.1 ( $\alpha$ -C), 40.6 (-CH<sub>2</sub>, -VE DEPT), 28.2 (-CH<sub>2</sub>, -VE DEPT), 25.3 (-CH-), 23.0 (-CH<sub>3</sub>), 21.5 (-CH<sub>3</sub>).

# **Section B**

## *Resveratrol Analogues*

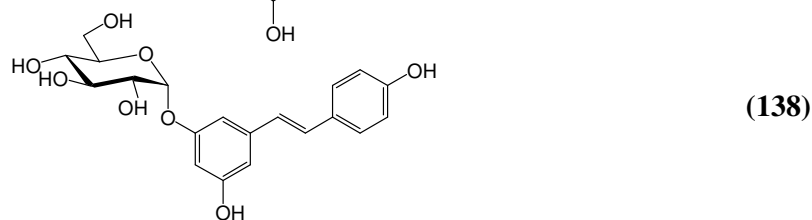
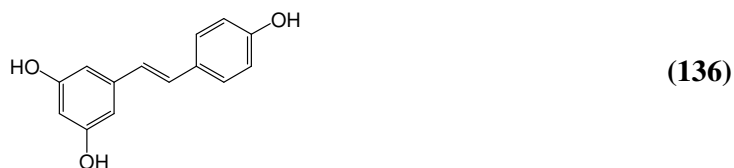
## 6.0 Resveratrol

### 6.1 Introduction

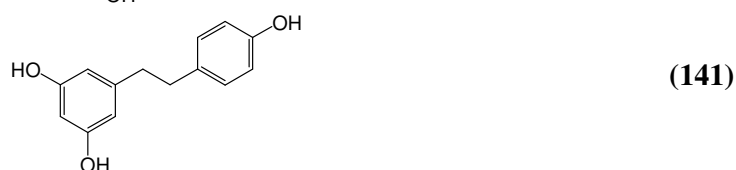
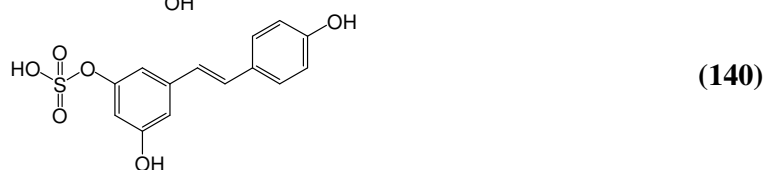
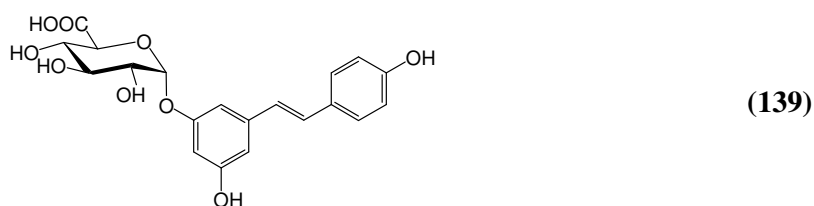
*“Resveratrol, found in nuts, ahh.....grapes and, ah.....stuff!”*

Quote taken from Oral Presentation,  
60<sup>th</sup> Irish Universities Chemistry Research Colloquium,  
UCC, 11<sup>th</sup>-13<sup>th</sup> June 2008.

Resveratrol **136** (3, 4', 5-trihydroxy-*trans*-stilbene) was first isolated from the roots of white hellebore (*Veratrum grandiflorum*) in 1940. This natural polyphenolic compound is found in several plant species, including mulberries, peanuts, grapes, pines, and legumes. A phytoalexin, or plant antibiotic, resveratrol is produced in response to stress, such as fungal infection, UV radiation, and temperature changes. Resveratrol is present in high concentrations in fresh grape skin, and its concentration in specific types of red wine can reach up to 14 mg/L. Research over the past several decades has revealed that resveratrol exerts a multitude of biological effects, including potent antioxidant, anti-inflammatory, anti-platelet, and anti-proliferative effects<sup>1</sup>.



In addition to *trans*-resveratrol, naturally occurring analogues are the *cis*-isomer **137** and resveratrol-3-*O*- $\beta$ -D-glucoside derivative (piceid) **138**. Resveratrol-3-sulphate **139**, resveratrol-3-*O*-glucuronide **140** and dihydroresveratrol **141** are known metabolites of resveratrol<sup>1</sup>.



As a result of research into a commonly known phenomenon, the “French Paradox”, resveratrol has come to prominence. Epidemiological studies have revealed an inverse correlation between red wine consumption and the incidence of cardiovascular disease. This is in relation to the fact that the incidence of heart infarction in France is about 40% lower than the rest of Europe, despite a diet being traditionally high in saturated fat<sup>2</sup>. This led to the discovery of resveratrol in red wine and a possible link to this phenomenon. Indeed, resveratrol protects the cardiovascular system by a large number of mechanisms including defence against ischemic-reperfusion injury, promotion of vasorelaxation, promotion and maintenance of intact endothelium, anti-atherosclerotic properties, inhibition of low-density lipoprotein oxidation, suppression of platelet aggregation and oestrogen-like actions<sup>3</sup>.

The effects of resveratrol are pleiotropic, besides its effects on the cardiovascular system resveratrol exhibits a remarkable inhibitory potential in various stages of tumour development. The antitumour activity of resveratrol was first revealed by its

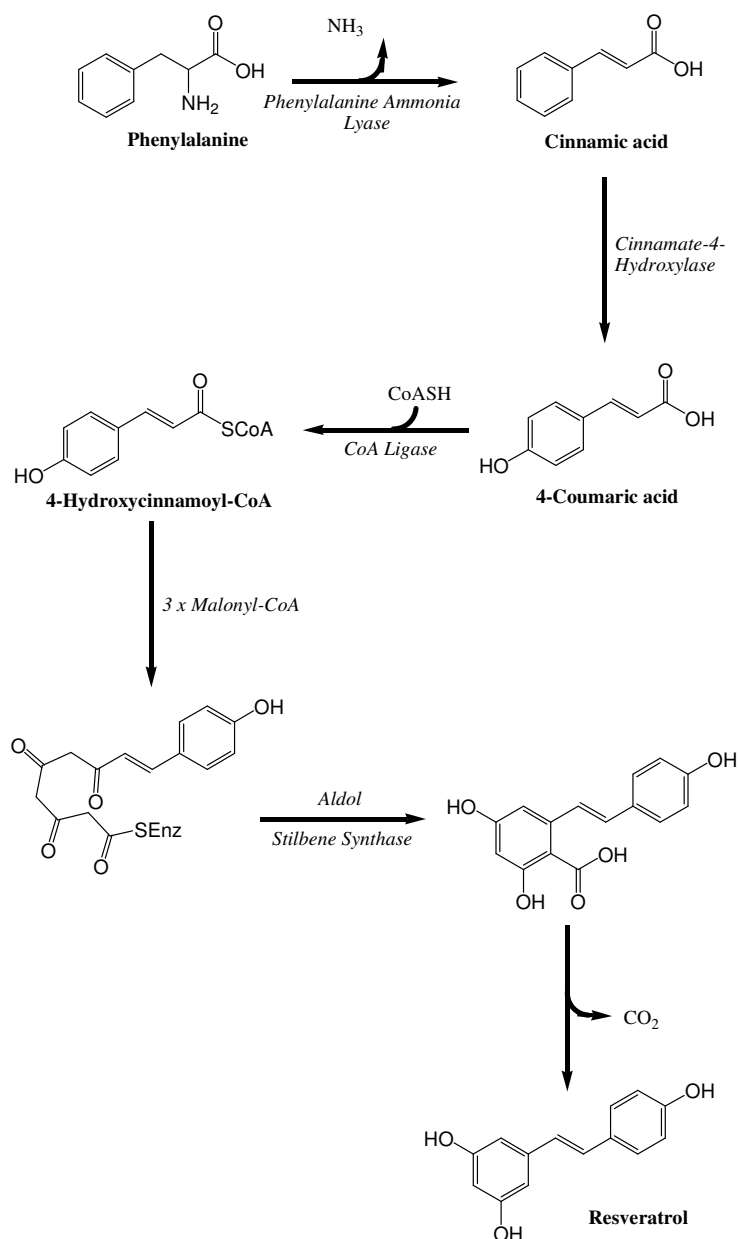
ability to reduce the incidence of carcinogen-induced development of cancers in experimental animals<sup>4</sup>. Resveratrol causes an arrest at the S/G2 phase transition of the cell cycle and is capable of inducing differentiation and apoptosis in a multitude of human tumour cell lines, such as leukaemia, colon, breast, prostate, and oesophageal cells. Resveratrol was also identified as an effective inhibitor of ribonucleotide reductase (RR). Ribonucleotide reductase catalyzes the rate-limiting step of *de novo* DNA synthesis, namely the reduction of ribonucleotides into the corresponding deoxyribonucleoside triphosphates (dNTPs)<sup>5</sup>. The importance of all these targets for cancer development is well known and therefore resveratrol can beneficially contribute to cancer prevention.

Furthermore, resveratrol has been shown to have neuroprotective effects. Neural dysfunction and metabolic imbalances underlie many progressive neurodegenerative maladies such as Alzheimer's, Huntington's, and Parkinson's diseases. Resveratrol induces a multitude of effects that depend on the cell type (e.g. NF- $\kappa$ B modulation in cancer cells vs. neural cells), cellular condition (normal, stressed or malignant) and concentration (proliferative vs. growth arrest) and can have opposing activities. Resveratrol targets whole pathways and sets of intracellular events rather than a single enzyme and therefore offers a less specific but more gentle (fewer side effects) and possibly more effective strategy for therapy to restore homeostasis.

Due to its striking inhibitory effects on cellular events associated with cancer initiation, promotion and progression, resveratrol has been suggested as a potential cancer chemopreventative agent<sup>6</sup>. This triphenolic stilbene has also displayed *in vitro* growth inhibition in a number of human cells<sup>7</sup>. The mechanistic basis for the whole wide range of biological activity of resveratrol remains unknown. Numerous studies point to its ability to function as a cellular antioxidant while others have demonstrated the inhibition of signalling kinases as its key function.

## 6.2 Biosynthetic pathway of resveratrol

The resveratrol biosynthetic pathway consists of four enzymes: phenylalanine ammonia lyase (PAL), cinnamic acid 4-hydroxylase (C4H), 4-coumarate:CoA ligase (4CL) and stilbene synthase (STS)<sup>8</sup>. Using three molecules of malonyl CoA as a chain extension, the stilbene resveratrol is derived from a *p*-coumaroyl CoA starter unit.



**Scheme 6.1:** The biosynthetic pathway of resveratrol



The starter unit, *p*-coumaroyl CoA is derived from phenylalanine while malonyl CoA is derived from the elongation of acetyl CoA units. Through oxidative deamination, phenylalanine loses the amino moiety with the enzyme phenylalanine ammonia lyase (PAL) acting as catalyst. This results in the production of cinnamic acid which is then converted to *p*-coumaric acid via C4H enzymatic hydroxylation. *P*-coumaric acid is then transformed to *p*-coumaroyl CoA after treatment with the free co-enzyme of a specific CoA ligase (4CL). The next step in the biosynthetic pathway of resveratrol involves the condensation of three malonyl CoA units with 4-hydroxycinnamoyl-CoA or *p*-coumaroyl CoA. This reaction forms a polyketide which further undergoes an enzymatic induced (stilbene synthase) Aldol condensation to yield a carboxylated stilbene. This stilbene is then decarboxylated to form resveratrol. For every mole of resveratrol formed, four moles of carbon dioxide are released<sup>9</sup>. Stilbene synthase (STS) is a member of the type III polyketide synthases and has extensive homology to chalcone synthase (CHS). Chalcone synthase is responsible for the formation of chalcones in many higher plants – chalcones are starting molecules for all flavonoid compounds. Although chalcone synthase is ubiquitous in plants, stilbene synthase is only found in species that accumulate resveratrol and related compounds. Therefore, stilbene synthase is essential for the bioengineering of resveratrol. It exists as a soluble homodimer with a molecular weight of ~40 kDa (**Figure 6.1**)<sup>10</sup>. Similar to chalcone synthase, the internal active site has a conserved Cys-His-Asn catalytic triad. Both enzymes synthesize the same long-chain polyketide intermediate. Structure–function analysis suggests that STS uses an Aldol-switch mechanism to regiospecifically carry out a C2–C7 cyclisation, instead of the C6–C1 cyclisation of chalcone synthase<sup>10</sup>. This reaction is followed by thioester hydrolysis to produce resveratrol.

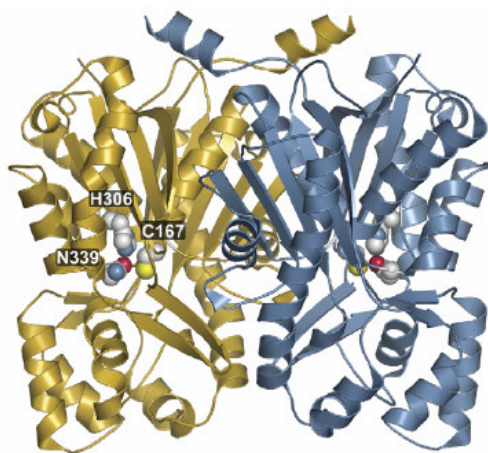
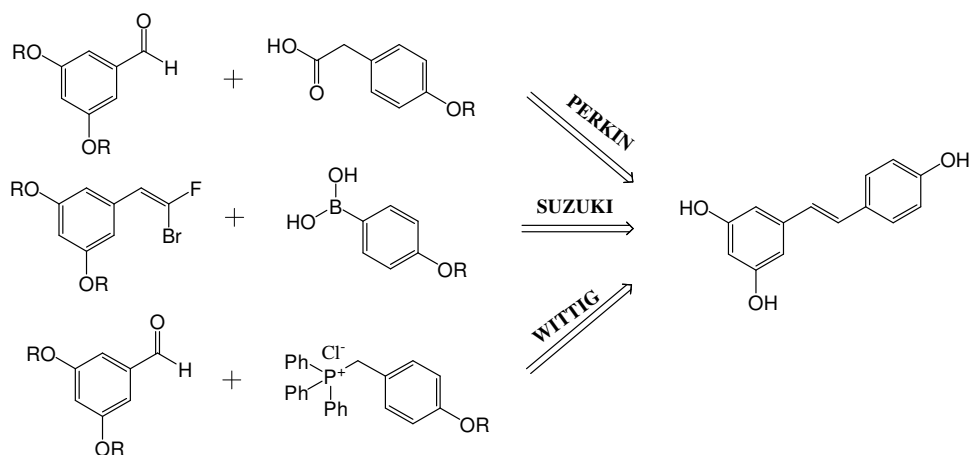


**Figure 6.1:** Structure of stilbene synthase (STS)

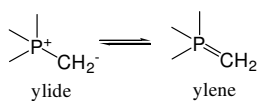
### 6.3 Synthesis of resveratrol

Although resveratrol is a natural product, it is only found in very small quantities in nature. It is found in many plant sources but its quantity depends on the stress situation of the plant. For this reason, isolation from natural sources is not viable. Levels of resveratrol in dried roots of *Cassia q. Rich* (30 mg/kg)<sup>11</sup> and dried grape skins (92 mg/kg)<sup>12</sup> have been reported. Because of these low levels, reliable and efficient synthetic routes to resveratrol are therefore highly desirable. The first synthetic preparation of the stilbene resveratrol was carried out by Späth and Kromp in 1941 via a Perkins type condensation with *p*-anisyl acetic acid sodium salt and 1,3-dimethoxy benzaldehyde as starting materials<sup>13</sup>. The synthesis of carbon-carbon double bonds can be achieved by various reactions including the Perkin and Suzuki reactions but it was not until the Wittig reaction in 1953 that research in this area of chemistry grew rapidly. The majority of published routes for the synthesis of resveratrol are based on the Wittig or Wittig-like reactions.



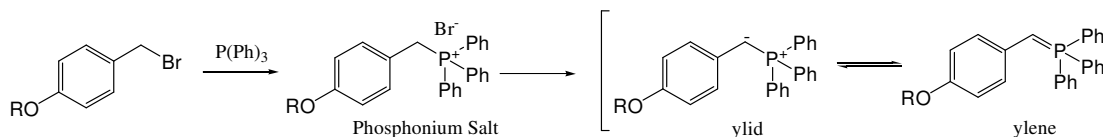
**Scheme 6.2:** Retrosynthetic analysis of resveratrol

The Perkin-type condensation reaction involves combining an arylacetic acid and a substituted benzaldehyde, followed by a decarboxylation reaction to form the basic stilbene structure. The Suzuki-type reaction employs an ethenyl halide and a substituted boronic acid in the presence of a palladium catalyst to produce substituted stilbenes. The Wittig reaction involves phosphorous ylides as nucleophilic carbon species. A ylide is a molecule that has a contributing Lewis structure with opposite charges on adjacent atoms. Phosphorous ylides are stable, but usually quite reactive compounds. They can be represented by two limiting resonance structures, which are sometimes referred to as the ylide and ylene forms (**Scheme 6.3**). The ylene form is pentavalent at phosphorous and implies involvement of phosphorous *3d* orbitals. Using trimethylphosphonium methylene as an example, the two forms are



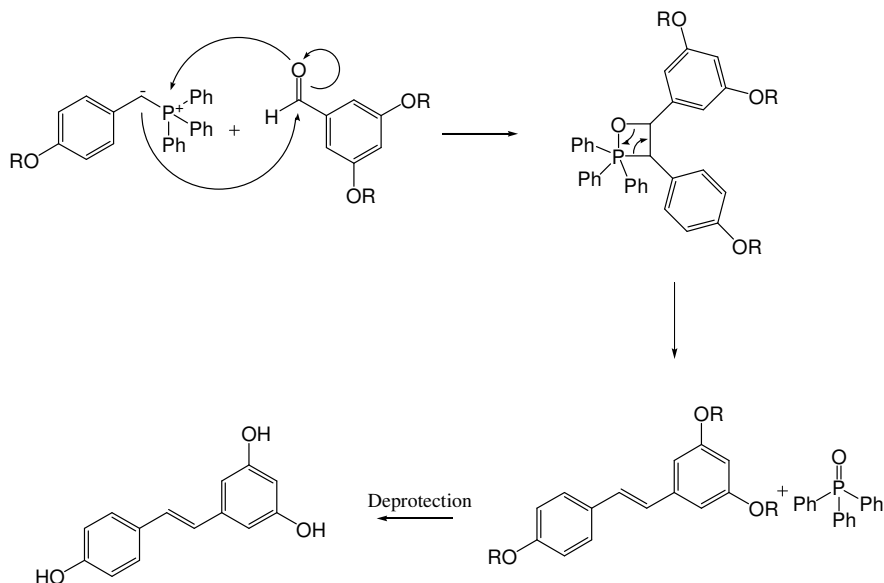
**Scheme 6.3:** Resonance structures of trimethylphosphonium methylene

Phosphorous ylides are usually prepared by deprotonation of phosphonium salts. The phosphonium salts most often used are alkyltriphenylphosphonium halides, which can be prepared by the reaction of triphenylphosphine with an alkyl halide.



**Scheme 6.4:** Formation of ylide

The alkyl halide must be one that is reactive toward  $S_N2$  displacement. Alkyltriphenylphosphonium halides are only weakly acidic, so strong bases are used for deprotonation. The ylides are not normally isolated so the reaction is carried out either with the carbonyl compound present or it may be added immediately after ylide formation. The reaction of a phosphorous ylide with an aldehyde or ketone introduces a carbon-carbon double bond in place of the carbonyl bond. The mechanism proposed is an addition of the nucleophilic ylide carbon to the carbonyl group to yield a dipolar intermediate, followed by elimination of phosphine oxide. The elimination is presumed to occur after formation of a four-membered oxaphosphetane intermediate.

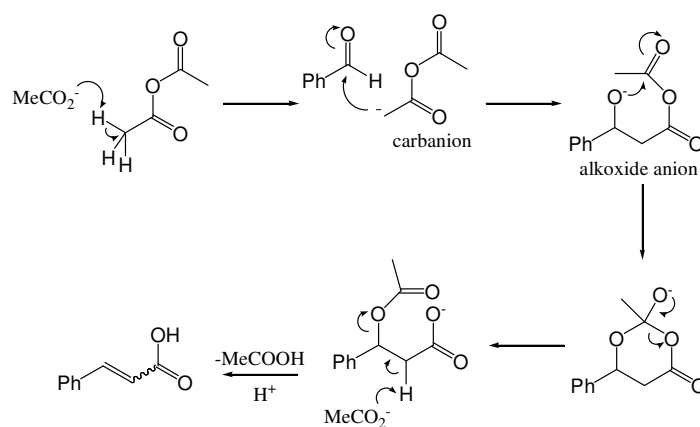


**Scheme 6.5:** Synthesis of resveratrol via the Wittig reaction

The synthesis of resveratrol via this method has been reported by Pettit *et al*<sup>6</sup>. In order for this reaction to proceed, the hydroxyl groups of the starting materials must be protected. Successful protection and deprotection of the hydroxyl moieties has been achieved with a wide range of substituents but mainly methyl, acetyl and more

recently *tert*-butyldimethylsilyl groups<sup>14</sup>. The main disadvantage of the Wittig reaction is the lack of stereoselectivity in relation to the formation of the new vinylic double bond. The lack of stereoselectivity of the Wittig reaction is believed to be the result of steric effects which develop as the ylide and carbonyl compound approach one another. The three phenyl substituents on phosphorous impose large steric demands which govern the formation of the diastereomeric adducts. Stereoselectivity has been improved with the use of trialkyl phosphines, a change in solvent or by the addition of salts. The *E*- and *Z*- resveratrol isomers formed by the Wittig reaction were separated by column chromatography<sup>6</sup>.

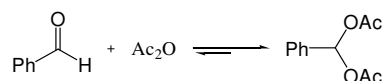
The condensation of non-enolisable aromatic aldehydes with anhydride is called the Perkin reaction. When the anhydride has two  $\alpha$ -hydrogens present, dehydration always occurs giving an aromatic alkenyl carboxylic acid derivative. Usually the salt of the acid is used so that nucleophilic attack on the anhydride regenerates the anhydride. This compound can then be decarboxylated using a variety of reagents to furnish a mixture of *Z*- and *E*- isomers with the *cis* isomer generally being the most abundant.



**Scheme 6.6:** Mechanism of the Perkin reaction

In this condensation reaction, the carbanion is obtained by the removal of an  $\alpha$ -hydrogen from a molecule of an anhydride, the anion of the corresponding acid acting as the necessary base. The carbonyl acceptor is generally confined to aromatic anhydrides. The carbanion attacks the carbonyl carbon of the aldehyde in the usual

way to yield the alkoxide anion. Internal transfer of the acetyl group in this anion is believed to take place from the carboxyl oxygen atom to the alkoxy oxygen atom via a cyclic intermediate, thereby forming a more stable species. Removal of an  $\alpha$ -H from this anion by  $\text{MeCO}_2^-$  results in loss of the good leaving group  $\text{MeCO}_2^-$  from the adjacent  $\beta$ -position to yield the anion of the  $\alpha\beta$ -unsaturated acid, which readily hydrolyses on work up with weak acid to form cinnamic acid. Some support for this mechanism is provided by the observation that on reaction with anhydrides of the form  $(\text{R}_2\text{CHCO})_2\text{O}$ , where there would be no  $\alpha$ -hydrogen to remove in the intermediate following opening of the cyclic structure, it is possible to isolate the analogue of the intermediate as the end product of the reaction<sup>15</sup>. Although this mechanism has been accepted for years, recent investigations into the Perkin condensation by Chandraekhar *et al* has resulted in a revised mechanism and new methodology for the reaction<sup>16</sup>.

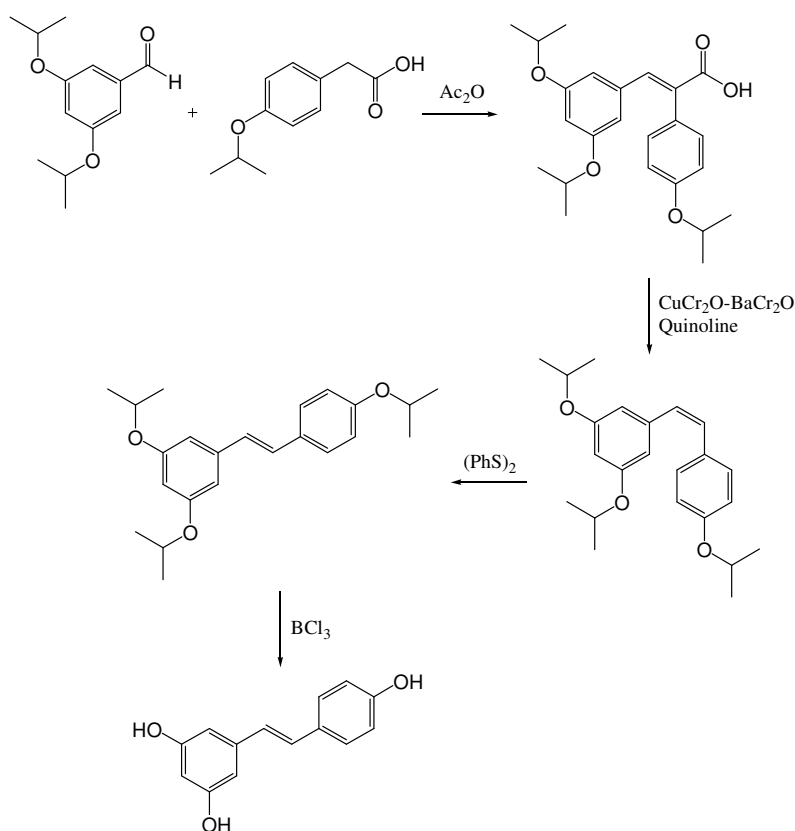


**Scheme 6.7:** *Gem*-diacetate formation from aldehyde

This proposed mechanism is based around the derivitisation of the enolate of the *gem*-diacetate (from the aromatic aldehyde and acetic anhydride, **Scheme 6.7**). This is in contrast to the enolate formation of acetic anhydride itself in the original mechanism, both of which are involved in the addition to the aldehyde in the key step of the mechanism. The deprotonation of the diacetate to the enolate appears to be electrophilically assisted by the neighbouring acetate group.

The synthesis of resveratrol using the Perkin condensation has been reported by Solladié *et al*<sup>17</sup>. This synthesis was carried out using 3,5-diisopropoxybenzaldehyde and 4-isopropoxyphenylacetic acid in the presence of acetic acid. Isopropyl ethers were used as the protecting groups as they can be easily removed at lower temperatures than that of their methyl counterparts thus avoiding isomerisation of the product. Decarboxylation was carried out using copper chromate yielding the protected resveratrol analogue in a ratio of 79:21 *cis:trans*. Isomerisation from *cis* to *trans* was achieved by refluxing the mixture with phenyl disulphide in THF. This step

was followed by deprotection of the isopropyl ethers using boron trichloride at  $-78^{\circ}\text{C}$ , resulting in a final resveratrol yield of 85%.



**Scheme 6.8:** Synthesis of resveratrol via the Perkin Reaction

The third of the three recognised synthetic pathways outlined in **Scheme 6.2**, involves palladium cross-coupling of boronic acids with organic halides. This cross coupling reaction is known as the Suzuki reaction. The cross-coupling reaction of organoboron reagents with organic halides or related electrophiles represents one of the most straightforward methods for carbon-carbon bond formation. The reaction proceeds under mild conditions, being largely unaffected by the presence of water, tolerating a broad range of functionalities, and yielding non-toxic byproducts.

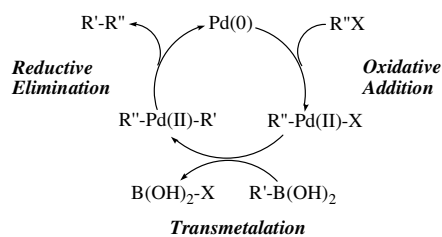
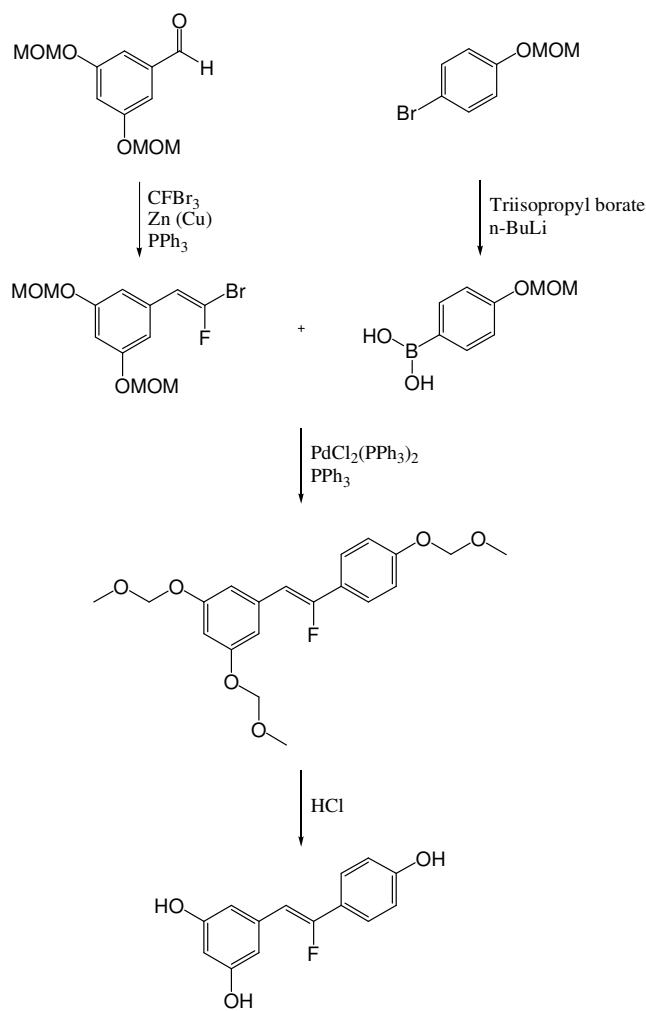


**Figure 6.2:** General catalytic cycle for cross-coupling reactions of organometallics

A general catalytic cycle for the cross-coupling reaction of organometallics, which involves oxidative addition-transmetalation-reductive elimination sequences, is depicted in **Figure 6.2**. Although each step involves further complex processes including ligand exchanges, there is no doubt about the presence of those intermediates ( $R''\text{-Pd(II)-R}'$  and  $R''\text{-Pd(II)-X}$ ) which have been characterised by isolation and spectroscopic analysis<sup>18</sup>. Oxidative addition is often the rate-determining step in a catalytic cycle. The relative reactivity decreases in the order of  $I > \text{OTf} > \text{Br} \gg \text{Cl}$ . A very wide range of palladium(0) catalysts or precursors can be used for cross-coupling reactions.  $\text{Pd(PPh}_3)_4$  is most commonly used, but  $\text{PdCl}_2(\text{PPh}_3)_2$  and  $\text{Pd(OAc)}_2$  plus  $\text{PPh}_3$  or other phosphine ligands are also efficient since they are stable in air and readily reduce to the active Pd(0) complexes with organometallics or phosphines used for the cross-couplings<sup>19-21</sup>. Reductive elimination of organic partners from  $R''\text{-Pd(II)-R}'$  reproduces the palladium(0) complex<sup>22</sup>. Although the mechanism of oxidative addition and reductive elimination sequences are reasonably well reported and are fundamentally common for all cross-coupling reactions of organometallics, little is known about the transmetalation step. This is because the mechanism is highly dependent on organometallics or reaction conditions used for the couplings.

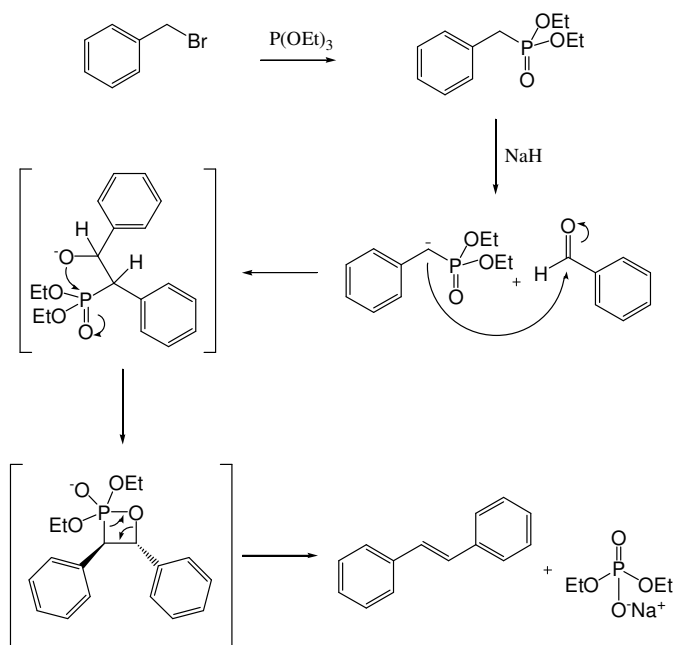
This reaction has been utilised by Eddarir *et al* in the preparation of fluorinated analogues of the resveratrol stilbene<sup>23</sup>. The initial step in this synthetic pathway involved the synthesis of a bromofluoroolefin from the reaction of tribromofluoromethane with an aldehyde in the presence of a tertiary phosphine and zinc dust activated by cupric sulphate. Protection of the hydroxyl groups was achieved using the methoxymethyl ether protecting group. The Suzuki cross-coupling step was carried out using the bromofluoroolefin and a MOM-protected hydroxyphenylboronic acid, catalysed by a palladium species. This reaction is most likely to occur via oxidative addition of Pd(0) to a carbon-boron bond. The boronic acid was prepared from 4-(OMOM)phenyl bromide using triisopropyl borate as the trapping agent. Deprotection of the hydroxyl groups was achieved by weak acid hydrolysis.





**Scheme 6.9:** Synthesis of fluorinated resveratrol derivative using the Suzuki coupling method

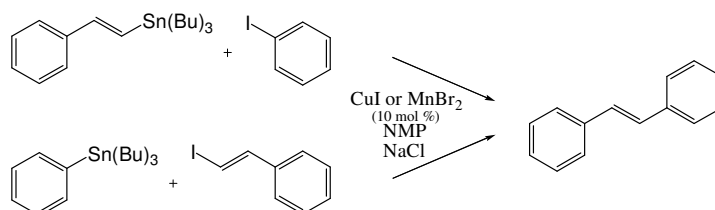
Resveratrol has been prepared using a variety of synthetic methodologies. The discovery of the Wittig reaction has been instrumental in the synthesis of resveratrol and its analogues. To date the majority of synthetic routes available for the synthesis of stilbenes are based loosely on the Wittig reaction with deviations such as the Wadsworth-Emmons and Wittig-Horner the main examples. The widespread use of these reactions is largely due to the commercial availability of starting materials. The main disadvantage of this type of reaction is lack of stereoselectivity leading to low yields.



**Scheme 6.10:** Mechanism of the Wadsworth-Emmons reaction

The Wadsworth-Emmons reaction is a deviation of the classic Wittig reaction. In 1958, Horner *et al* published a modified Wittig reaction using phosphonate-stabilized carbanions<sup>24</sup>, and this was further altered by William Wadsworth and William Emmons<sup>25</sup>. In contrast to phosphonium ylides used in the Wittig reaction, phosphonate-stabilized carbanions are more nucleophilic and more basic. Likewise, phosphonate-stabilized carbanions can be alkylated, unlike phosphonium ylides. Other advantages of the Wadsworth-Emmons variation over the Wittig reaction include the fact that the dialkylphosphate salt byproduct is water soluble and therefore easily removed by aqueous extraction. Also, the reaction is stereospecific therefore the yield of the *trans*- isomer is greatly increased. Under strongly basic conditions at elevated temperatures the isomerisation of *cis*-stilbene to *trans*-stilbene occurs, which is contrary to the initial reports of Wadsworth and Emmons who believed that the reaction was like its predecessor in being non-stereospecific<sup>26</sup>. The phosphonate esters can be produced via the Michaelis-Arbuzov reaction by reacting benzyl bromide with triethyl phosphite. The Wadsworth-Emmons reaction combines this phosphonate ester with benzaldehyde, in the presence of a strong base such as sodium hydride to yield a *trans*-stilbene as the product. **Scheme 6.10** shows the mechanism of the reaction for the synthesis of a stilbene. The phosphoryl- stabilized carbanion attacks the carbonyl in a stepwise manner, to give an oxyanion intermediate, which then decomposes via a

transient four-centred intermediate, to yield an olefin. Although direct observation of intermediates in the reaction has not been generally possible, there are several kinetic and spectroscopic studies that shed light on the course of this process<sup>27</sup>. Synthesis of resveratrol and a fluorinated derivative have been reported using the Horner-Wadsworth-Emmons methodology. An isotopically labelled fluorinated version was also synthesised for positron emission tomography (PET) studies via this method<sup>28</sup>.

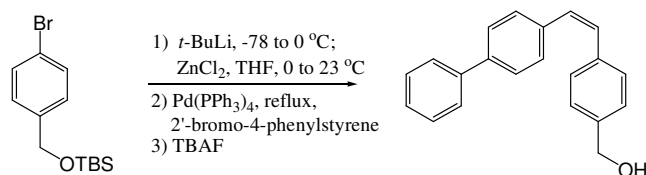


**Scheme 6.11:** Copper- and manganese-catalysed cross-couplings of organostannanes with organic iodides

In recent years, new synthetic routes for stilbene production have become more prevalent, such as the Stille, Negishi and Heck reactions<sup>29</sup>. These methodologies offer a stereospecific synthesis of stilbenes. The major advantage of these reactions is due to the increased stereospecificity and as a result, a much higher yield of a particular isomer is achieved. The other key component in the synthesis of resveratrol analogues is the protection of the hydroxyl groups with stable but easily removable protecting groups.

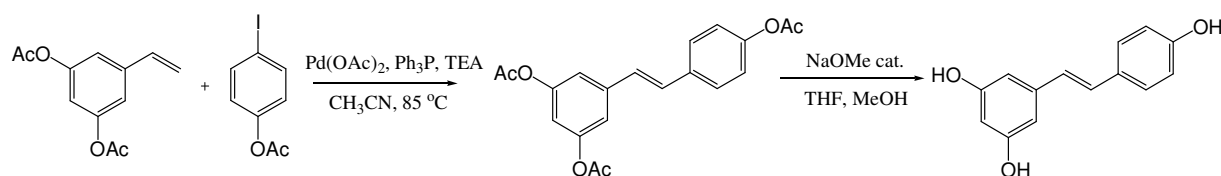
The palladium-catalysed coupling of organotin reagents with organic electrophiles such as aryl and vinyl halides or triflates is known as the Stille reaction. In comparison to Suzuki coupling, the Stille reaction does not require the addition of a base and is applicable to a wider spectrum of electrophiles, including saturated aliphatic halides and some alcohol derivatives. However, although organostannanes are extremely valuable synthetic intermediates because of their compatibility with most functional groups and mildness of their reaction conditions, few syntheses of stilbene derivatives via Stille vinylation have been reported in the literature. Kang *et al* have reported copper and manganese-catalysed cross-couplings of organostannanes with organic iodides affording stilbenes in good yields (**Scheme 6.11**)<sup>30</sup>.

In order to obtain a *Z*-configuration of the double bond in stilbenes, Bosanac and Wilcox have utilised a variant of the Negishi reaction. In this palladium-catalysed reaction, an organozinc reagent was coupled with an organohalide to yield the *Z*-adduct, as shown in **Scheme 6.12**<sup>31</sup>.



**Scheme 6.12:** *Z*-stilbene synthesis using modified Negishi reaction

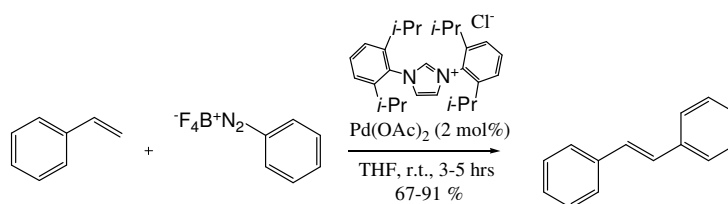
The palladium-catalysed olefination of aryl halides is known as the Heck reaction (or Mizoroki-Heck reaction). Because it is highly stereoselective and amenable to a large variety of starting materials, it has become one of the most commonly used pathways for the synthesis of stilbenes. The reaction is catalysed by either Pd(0) or Pd(II) complexes in solution, usually in the presence of a stoichiometric amount of a base. A coordinating ligand, most often a phosphine, is added. In this synthetic pathway, stilbenes may be afforded by coupling a styrene with an aryl halide. Three possible products may be formed, both *E*- and *Z*- isomers, and 1,1-diphenylethylene, however careful choice of reaction conditions can control the regioselectivity of the addition. The Heck reaction has provided ready access to the synthesis of oligomeric styrylpyrroles<sup>32</sup>, oligo(phenylenevinylene) derivatives<sup>33</sup>, stilbenoid dendrimers<sup>34</sup>, and non linear optical electron donor-acceptor substituted stilbene derivatives<sup>35</sup>. The synthetic preparation of resveratrol has been published by Guiso *et al* using the Heck reaction with an overall yield of 70%<sup>36</sup>.



**Scheme 6.13:** Synthesis of resveratrol via Heck reaction

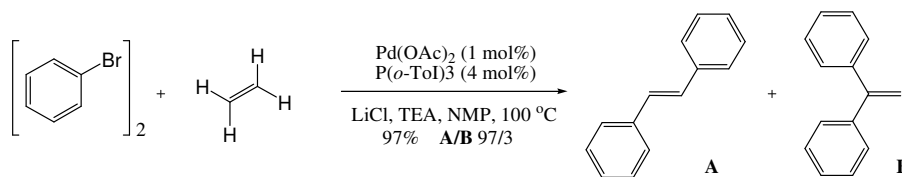
The classic Heck reaction afforded new carbon-carbon bonds using aryl halides as electrophiles. This reaction has severe drawbacks associated with it resulting from oxidative degradation and other side reactions observed with phosphines, hence the importance of investigating non phosphine-based complexes as catalytic precursors.

Indeed, nitrogen-, oxygen-, and sulphur-containing palladacycles can provide excellent alternatives to their phosphorus-based counterparts. Many variations of the Heck reaction has been successfully utilised in stilbene synthesis over the years. Besides halides, other electrophiles have been tested in Heck-type reactions. For example, aryldiazonium salts are even more reactive than aryl iodides and do not require the presence of a base nor phosphine ligands. Indeed, coupling reactions with diazonium salts are fast and proceed smoothly, but usually require a relatively large amount of palladium (1-2 mol%). However, the coupling products are generally obtained in lower yields<sup>37</sup>



**Scheme 6.14:** Stilbene synthesis using aryldiazonium salt species

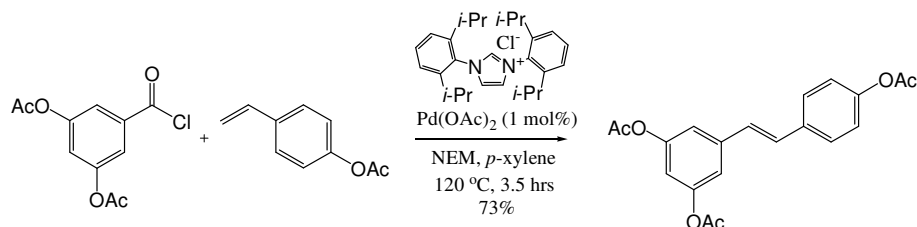
Symmetrical *trans*-stilbenes may be formed by a two-fold coupling of ethylene with two equivalents of bromoarene. The ratio of stilbene to byproducts (styrene and 1,1-substituted adducts) depends on the solvent, the ethylene pressure, and the bromoarene concentration. Addition of lithium chloride increases the regioselectivity. This approach leads to the formation of small amounts of oligomers and polymers of poly(*p*-phenylenevinylene). The optimum conditions for the palladium-catalysed coupling of bromobenzene with ethylene are summarized in **Scheme 6.15**<sup>38</sup>.



**Scheme 6.15:** Synthesis of symmetrical stilbenes with ethylene

One of the most commonly used synthetic pathways for the production of resveratrol and its derivatives is the decarbonylative Heck reaction. This version of the Heck reaction has been known since the beginning of the eighties. Spencer *et al* first reported the palladium-catalysed coupling of alkenes to aryl chlorides in the

presence of a tertiary amine<sup>39</sup>. The arylation of ethylene to styrene and stilbene derivatives was also described by Spencer *et al*<sup>40</sup>. The reaction involves a highly efficient decarbonylation of the aroyl chloride. The reaction is not particularly sensitive to substituents on the aroyl chloride although strongly electron-donating moieties have been shown to be advantageous. With mono-substituted alkenes the *trans*-isomer is formed with total isomeric specificity.

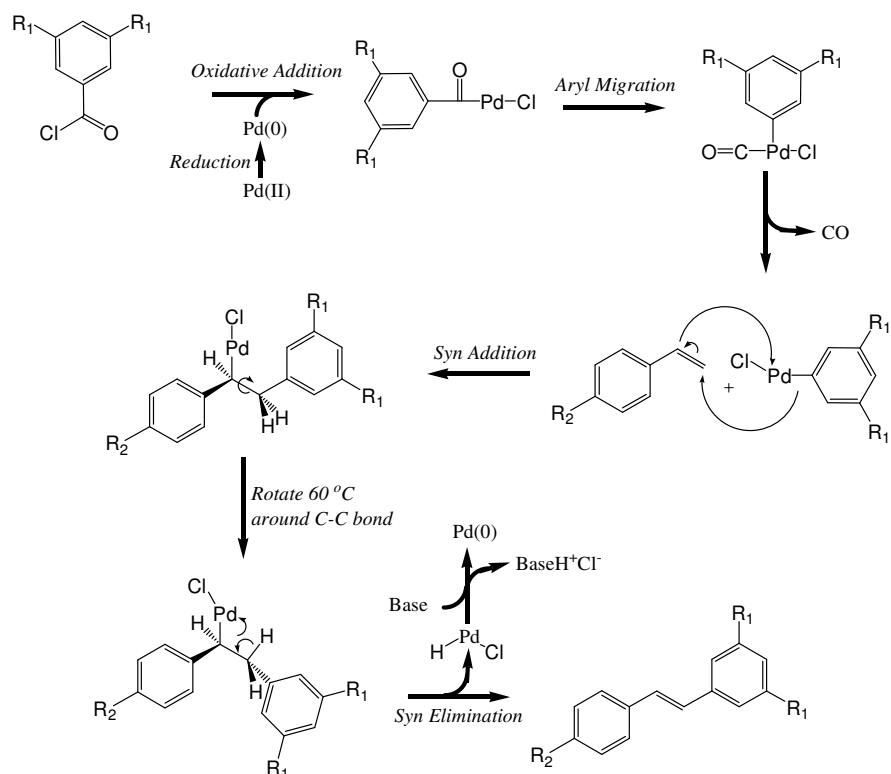


**Scheme 6.16:** The decarbonylative Heck reaction

The best results from the decarbonylative Heck reaction have been obtained using tertiary bases with  $pK_a$  values in the range 7.5 to 11. Weak bases were shown to facilitate a slower reaction whereas strong bases would react with the aroyl chloride<sup>41</sup>. *N*-Ethylmorpholine was shown to be the most effective base as it did not react with aroyl chlorides nor did it cleave the bond between strongly electron-withdrawing groups and the aroyl chloride. The solvent used was *p*-xylene as optimisation of the reaction showed that the best results were achieved at 120-130 °C.

In the initial publication of this version of the Heck reaction, Blaser and Spencer proposed a mechanism<sup>41</sup>. Only the reacting groups are shown as little is known about the ligands occupying the vacant coordination sites. The first step is believed to involve oxidative addition of the aroyl chloride to a palladium (0) species. The Pd(0) moiety is believed to be the product of a preliminary reduction of palladium acetate perhaps caused by the alkene or base. If there are no strongly bound ligands occupying the other coordination sites, aryl migration to the metal should be facilitated. The release of carbon monoxide is expected as there are no ligands present capable of stabilising a palladium (0) carbonyl at high temperature. Alkene coordination is proposed as the next step although it is quite probable that the alkene is present as a ligand throughout the reaction. *Syn* addition of the alkene gives an intermediate that undergoes internal rotation about the central carbon-carbon bond to

place H and H-Pd-Cl *syn* to each other. Following this the palladium is cleaved, and the double bond is formed with the regeneration of Pd(0). It has been shown that the cumulative effect of multiple electron-withdrawing groups has a detrimental effect on the yield of the reaction. The decarbonylative Heck reaction gives almost complete specificity for the formation of *E*-isomers with mono-substituted alkenes. There are no sterically bulky ligands present so this steric specificity must be due to electronic factors.



**Scheme 6.17:** Proposed mechanism of the decarbonylative Heck reaction

The expense of this reaction is somewhat reduced due to the regeneration of a palladium adduct, however this is not always easy to recover. More recently this procedure has been used in the preparation of the phytoalexin resveratrol and provides a very efficient stereospecific method to yield *trans*-stilbenes<sup>42</sup>. With an overall yield of 53%, the decarbonylative Heck approach requires only four steps from the commercially inexpensive  $\alpha$ -resorcylic acid (3,5-dihydroxybenzoic acid) to produce resveratrol.

## 6.4 Bioactivity of Resveratrol

A primary impetus for research on resveratrol was initiated from the paradoxical observation that a low incidence of cardiovascular diseases may co-exist with a high-fat diet intake and moderate consumption of red wine, a phenomenon known as the “French Paradox”<sup>2</sup>. Resveratrol has been identified as an effective candidate for cancer chemoprevention due its ability to block each step in the carcinogenesis process by inhibiting several molecular targets. Examples of these molecular targets include kinases, cyclooxygenases, ribonucleotide reductase, and DNA polymerases. In addition, resveratrol protects the cardiovascular system by a large number of mechanisms, including defence against ischemic reperfusion injury, promotion of vasorelaxation mediated by NO (nitric oxide) release, protection and maintenance of intact endothelium, anti-atherosclerotic properties, inhibition of low-density lipoprotein oxidation, and suppression of platelet aggregation, thereby strongly supporting its role in the prevention of coronary disease. Promising data regarding progressive neurodegenerative maladies such as Alzheimer’s, Huntington’s, and Parkinson’s diseases has been reported in recent years<sup>5</sup>. Some of these effects may be due in part to resveratrol being a phytoestrogen, i.e. a plant compound that has biologically similar properties to those of oestrogens<sup>43</sup>. More recent results provide interesting insights into the effect of this compound on the lifespan of yeasts and flies, implicating its potential as an anti-aging agent in treating age-related human diseases<sup>44</sup>.



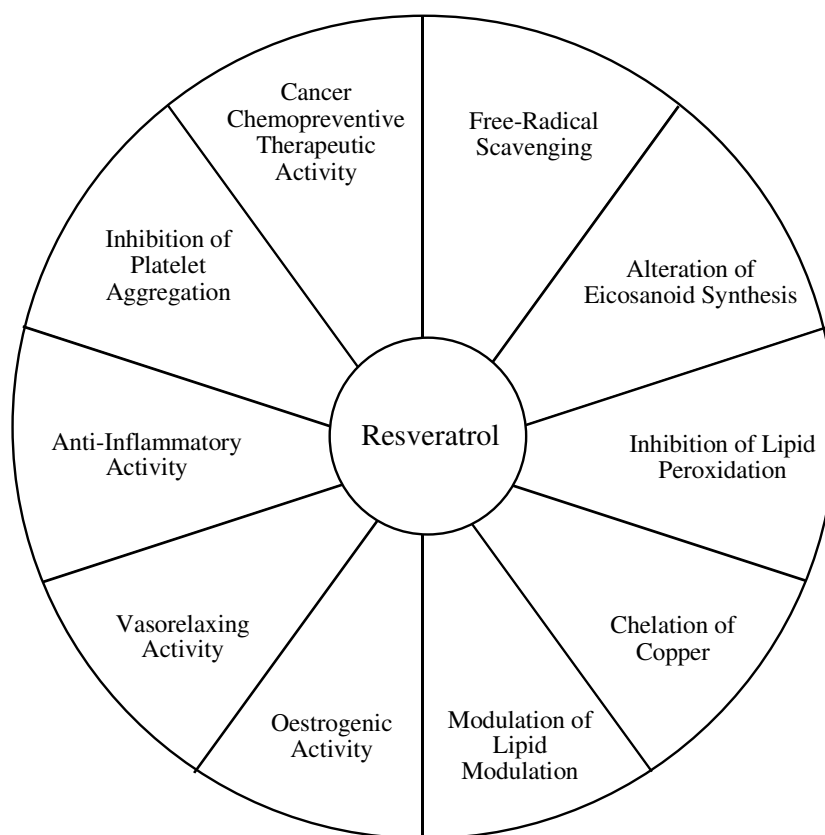


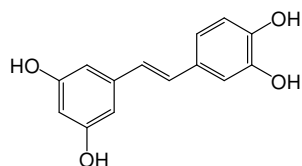
**Figure 6.3:** Major biological activities of resveratrol

#### 6.4.1 Anticancer activity

One of the most intensely investigated biological properties of resveratrol has been its cancer-chemopreventative or anticancer properties. This was first demonstrated by Jang *et al* who showed that resveratrol possesses cancer-chemopreventative and cytostatic properties in each of the three major stages of carcinogenesis, i.e. initiation, promotion and progression<sup>11</sup>. Since this discovery, there has been a flurry of papers and reviews reporting the implication of resveratrol in cancer chemoprevention through a wide range of actions that are not necessarily fully understood. From published reports, resveratrol has been shown to appear to help detoxify carcinogens, to reduce the synthesis of various cancer related compounds and to interfere with cell survival programmes. For example, resveratrol has been shown to promote apoptosis in cancer cells by blocking anti-apoptotic protein expression or by inhibiting signal transduction through the phosphoinositide 3-kinase (PI3K), mitogen-activated protein kinase (MAPK) or NF- $\kappa$ B pathways<sup>44</sup>.

Most of the scientific evidence that demonstrate the bioactivity of resveratrol is based on *in vitro* studies in which the *cis/trans* diastereomers have been tested. However, from *in vivo* studies we know that the predominant isomer that is orally ingested with foods is *trans*-resveratrol glucoside (piceid) **138**, which is biotransformed and rapidly eliminated<sup>12</sup>. In addition, these derivatives might be less biologically active due to their esterified hydroxyl groups. However, the chemopreventive activity of orally administered *trans*-resveratrol has been demonstrated in cancer-induced animal models<sup>45</sup>.

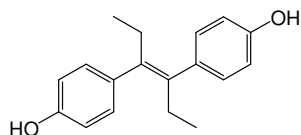
Skin cancer is one of the most common types of human malignancy. It can be split into 2 groups, melanoma and non-melanoma skin cancer. As with most cancers, many studies have concentrated on the biological effect of resveratrol on both types. As non-melanoma skin cancer is the most frequent, the majority of skin cancer studies have concentrated on this. Much of the work regarding skin tumourigenesis has focused on the effects of UVB radiation, whereas much less is known about UVA-induced signalling pathways and their role in tumour promotion. Jang *et al* assessed the chemopreventive effects of resveratrol, employing UVB-mediated skin tumourigenesis in the SKH-1 hairless mouse model<sup>11</sup>. Topical application of resveratrol either pre- or post-UVB significantly inhibited tumour incidence and delayed the onset of new tumour development. Similarly in a standard chemical carcinogenesis mouse tumour protocol using a two stage, DMBA (7,12-dimethylbenz(*a*)anthracene)-initiated and TPA (12-*O*-tetradecanoylphorbol-13-acetate)-promoted murine skin cancer model showed a 98% reduction in skin tumours<sup>11</sup>. Orally administered resveratrol was also shown to inhibit DMBA/croton oil-induced mouse skin papillomas, correlated with prolonging the latent period of tumour occurrence and inhibiting croton oil-induced enhancement of epidermal ODC activities<sup>46</sup>.



(142)

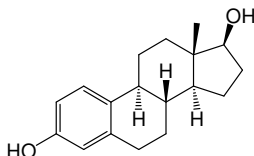
Niles *et al* displayed the inhibition of growth and induction of apoptosis in melanoma cells lines by resveratrol<sup>47</sup>. However, in a human melanoma xenograft model, they

reported that resveratrol did not have a statistically significant effect on melanoma growth, and it might even stimulate tumour growth at high dose levels. In addition piceatannol **142**, a major resveratrol metabolite, did not effect the *in vitro* growth of a murine melanoma cell line, but significantly stimulated the number of lung metastases<sup>48</sup>.



(143)

Resveratrol is structurally similar to the synthetic oestrogen diethylstilbestrol (DES) **143**. It can bind to oestrogen receptors (agonism) in the low micromolar range and can act as a weak competitor or antagonist to DES. However, despite low receptor binding affinity it can activate hormone receptor-mediated gene transcription (superagonism). Furthermore, resveratrol can prevent oestrogen-induced processes by modulating parallel pathways with opposing effects, for example proliferation, transformation and progression<sup>49</sup>. Resveratrol promotes proliferation at low doses but at higher dose levels it is apoptotic. Resveratrol can bind to both  $\alpha$ - and  $\beta$ -oestrogen receptors, and activates oestrogen receptor-dependent transcription in human cancer cells. Although numerous studies have been performed on breast cancer cells, using both hormone-sensitive and hormone-resistant strains, the oestrogen-modulatory effects of resveratrol remain debatable. In some cell types, such as oestrogen receptor (ER)-positive MCF-7 and T47D cells, resveratrol is seen to act as a superagonist, whereas in other cell types it produces activation levels equal to or less than that of the hormone oestradiol **144**.



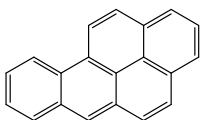
(144)

By antagonising the growth-stimulatory effect of oestradiol in a dose-dependent manner, resveratrol (>1  $\mu$ M) inhibited the growth of MCF-7 cells<sup>50</sup>. It has also been reported that resveratrol inhibited the highly invasive MDA-MB-435 cells<sup>51</sup>. In a study by Bhat *et al*, resveratrol was observed to carry out mixed oestrogen agonist/antagonist activities in some breast cancer cell lines in the absence of oestradiol

**144.** However when oestradiol was present resveratrol was shown to act as an anti-oestrogen<sup>52</sup>. By inhibiting the levels of autocrine growth stimulators, transforming growth factor- $\alpha$  (TGF- $\alpha$ ), PC cell-derived growth factor, insulin-like growth factor I receptor and increasing the growth factor inhibitor TGF- $\beta$ 2, resveratrol was also shown to inhibit the proliferation of the oestrogen-receptor negative human mammary carcinoma cell line, MDA-MB-468<sup>50</sup>. Along with these studies, research has shown that resveratrol also promotes the accumulation of growth inhibitory/pro-apoptotic ceramide, the induction of quinine reductase (a phase II detoxification enzyme) and induces caspase-independent apoptosis through Bcl-2 downregulation. It has also been shown to suppress Src tyrosine kinase activity, nitric oxide generation and the NF $\kappa$ B pathway<sup>5</sup>. From these examples of *in vitro* results on mammary cell lines, it is clear the chemopreventative effects of resveratrol are very complex and not yet fully understood.

The main causes for gastric cancer are believed to be exposure to chemical carcinogens and/or chronic infection with *Helicobacter pylori*. Resveratrol has been shown to be effective in inhibiting the replication of this bacterium, therefore intervention studies into the use of resveratrol for combating gastric cancer are ongoing<sup>53</sup>. In colon cancer cells, resveratrol activates various caspases and triggers apoptosis. This involves the accumulation of the pro-apoptotic proteins Bax and Bak and redistribution of the death receptor FasR in membrane rafts. Relatively high concentrations also substantially downregulate telomerase activity<sup>54</sup>. The *in vivo* efficiency of resveratrol has been assessed in two different animal models of colorectal cancer, dimethylhydrazine-induced AOM and mutant *min* mice, by Tessitore *et al*<sup>55</sup> and Schneider *et al*<sup>56</sup>, respectively. Resveratrol was found to significantly reduce the number of AOM-induced aberrant crypt foci (ACF, the earliest stages of colon cancer) associated with Bax and p21 expression<sup>55</sup>. In the case of the mutant *min* mice, a 70% reduction in the formation of small intestinal tumours and prevention of colon tumour development was observed after receiving resveratrol. Treatment led to the downregulation of genes that are directly involved in cell cycle progression or cell proliferation and the upregulation of genes that are involved in the recruitment and activation of immune cells. It also showed inhibition of the carcinogenic process and tumour expansion suggesting the multiplicity of the

molecular targets and signalling cascades<sup>56</sup>. An inhibitory effect was also observed in experiments conducted in the xenograft gastric tumour model.



(145)

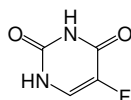
In human bronchial epithelial cells, resveratrol alters the expression of PAH (polycyclic aromatic hydrocarbons)-metabolising genes (e.g. cytochrome P450 1A1), microsomal epoxide hydrolase (*mEH*) and glutathione S-transferase P1 (*GSTP1*) genes. This results in the altered formation of carcinogenic benzo[*a*]pyrene **145** (BaP) metabolites<sup>57</sup>. BaP is universal environmental pollutant and is also present in cigarette smoke. Cigarette smoke contains many carcinogens that are likely to be involved in the mechanism of this tumour type. BaP metabolism requires the induction of the cytochrome P450 1A1 through the activation of the aryl hydrocarbon receptor (AhR). At various doses of resveratrol, significant reduction in tumour volume (42%), tumour weight (44%) and metastatic potential (56%) in mice bearing metastatic Lewis lung carcinomas (LLCs) was noted, through the inhibition of DNA synthesis and LLC-induced neovascularisation and tube formation of human umbilical vein endothelial cells (HUVEC)<sup>58</sup>.

With exposure to benzo[*a*]pyrene **145** being a known major risk factor to oesophageal cancer, resveratrol has been shown to have suppressive growth effects on oesophageal cancer cell lines such as EC-9706. The *in vivo* effects were evaluated in *N*-nitrosomethylbenzylamine (NMBA)-induced oesophageal tumorigenesis in rats. Resveratrol suppressed both the number and size of NMBA-induced oesophageal tumours per rat, by targeting COX enzymes and the prostaglandin E synthase, PGE(2)<sup>59</sup>.

For prostate cancer, the growth inhibitory effect of resveratrol has been demonstrated in various cultured cells, both hormone-sensitive and hormone-refractory. These mimic the initial and advanced stages of prostate carcinoma, respectively. It is reported that resveratrol modulates the growth of these cells and alters the expression of multiple sets of functionally related molecular targets. Resveratrol can repress

different classes of androgen-responsive genes, such as prostate-specific antigen (PSA), human glandular kallikrein-2, androgen receptor-specific coactivator (ARA70), and p21WAF1/CIP1 in hormone-responsive cells. It also activates p53-responsive genes such as PIG7, p300/CBP and Apaf-1, inhibits PI3K/AKT activation and increases Bax, Bak, Bid, and Bad<sup>60</sup>. To date no preclinical studies have been reported on prostate carcinogenesis.

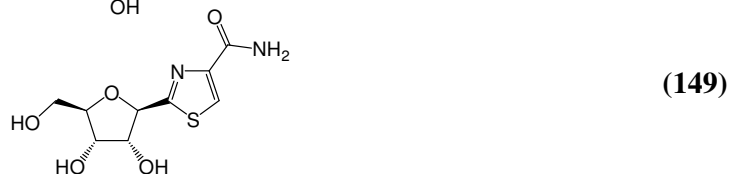
Oxidative stress has been implicated in the pathogenesis of liver cancer and, therefore, the use of antioxidants as therapeutic or preventative agents has been recommended. The blockage of the ROS-potentiated invasion of the hepatoma cells<sup>61</sup> and inducing of apoptosis<sup>62</sup> by resveratrol has been shown through *in vitro* studies. In an *in vivo* study carried out by Carbo *et al*, resveratrol was shown to enhance the anti-tumour effect of 5-fluorouracil (5-FU) **146**, suggesting that resveratrol could act as a biochemical modulator to enhance the therapeutic activity of 5-FU on hepatocellular carcinomas<sup>63</sup>. It caused a marked decrease of 25% in tumour cell content by inducing apoptosis. In this study by Carbo *et al*, it was reported that resveratrol treatment also induces an accumulation of cells in the G2/M phase in rats inoculated with a fast-growing tumour.



(146)

Resveratrol has been shown to inhibit caspase-7 activation in neuronal-like cells, such as the human neuroblastoma SH-SY5Y. It has also displayed degradation of poly-(ADP-ribose)-polymerase, which occurs in cells exposed to paclitaxel (Taxol<sup>TM</sup>), a known anticancer drug<sup>64</sup>. The mechanism of resveratrol as a neuroprotective agent is believed to occur through modulation of the signal pathways, committing these neuronal-like cells to apoptosis. Paclitaxel **147** (Taxol<sup>TM</sup>) exerts its activity in the mitosis phase of the cell cycle, which is where resveratrol is known to induce S phase arrest, preventing SH-SY5Y from entering the phase<sup>64</sup>.

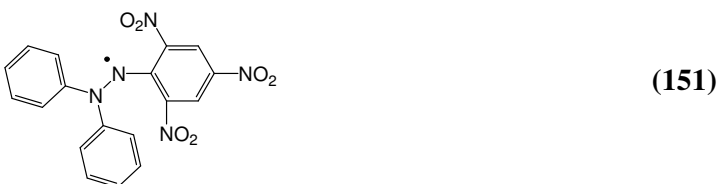
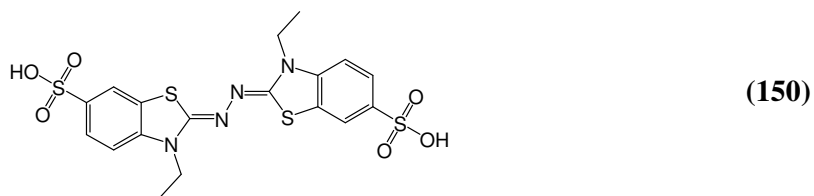




The combined effects of resveratrol have been tested with both cytarabine **148** (Ara-C) and tiazofurin **149**, both chemotherapeutic antimetabolites. The results showed synergistic growth inhibition and apoptosis induction in HL-60 cells<sup>70</sup>. However, *in vivo* research shows resveratrol to have weak anti-leukemic activity. This is despite the strong anti-proliferative and pro-apoptotic activities of resveratrol against these cells *in vitro*<sup>71</sup>.

#### 6.4.2 Antioxidant activity

Many compounds with aromatic groups are able to function as antioxidants by forming stable radicals via resonance structures, thereby preventing continued oxidation. Resveratrol contains two phenyl groups and is highly conjugated, and it has been shown to have a higher scavenging capacity for ABTS **150** (2,2'-azinobis(3-ethylbenzthiazoline-6-sulfonic acid)), DPPH **151** (1,1-diphenyl-2-picrylhydrazyl), and hydroxyl radicals, than propyl gallate, vitamin C, and vitamin E<sup>72</sup>.





Resveratrol may delay and/or prevent oxidative stress-induced cellular damage and disease, in its role as an antioxidant. Cell apoptosis can be induced by oxidative stress due to excessive damage. Resveratrol has been shown to inhibit oxidative-induced apoptosis in a variety of cell lines including Swiss 3T3 mouse fibroblasts, rat pheochromocytoma (PC12), human peripheral blood mononuclear (PBM), and human retinal pigment epithelium (RPE) cells<sup>73</sup>. The reduced incidence of age-related macular degeneration (AMD), a leading cause of blindness in the elderly, can be associated with reduced oxidative stress in RPE cells by resveratrol.

The antioxidant activity of resveratrol may also be associated with protection against the progression of atherosclerosis. The oxidation of low-density lipoproteins (LDL) is an important event in the development of this disease. From *in vivo* studies, Frankel *et al* has shown resveratrol to inhibit copper-catalysed LDL oxidation in two healthy human subjects by 81 and 70%<sup>74</sup>. Blood platelets can also be found at the site of early atherosclerosis lesions. Activation of these platelets can generate reactive oxygen species (ROS). Resveratrol has been shown to inhibit ROS production and lower lipid peroxidation of blood platelets, although not to vitamin C levels. Resveratrol was capable of reducing the prooxidant effect of vitamin C, even though there was no synergism between them<sup>75</sup>.

Excessive accumulation of reactive oxygen species may induce the oxidative modification of cellular macromolecules (lipid, proteins and nucleic acids) with detrimental effects. In fact, DNA damage by ROS has been implicated in mutagenesis, oncogenesis and aging. Resveratrol prevents initial DNA damage by two different pathways: (i) acting as an antimutagen through the induction of Phase II enzymes, such as quinone reductase and (ii) acting as an antioxidant through inhibition of DNA damage by ROS. When acting as an antimutagen resveratrol is capable of metabolically detoxifying carcinogens by inhibiting COX and cytochrome P450. It has been proposed that ROS derived from lipopolysaccharides may function as tumour initiators. Leonard *et al* have demonstrated that resveratrol exhibits a protective effect against lipopolysaccharides in cell membranes and DNA damage caused by reactive oxygen species<sup>76</sup>.

Apart from its antioxidant effects, there are two other biological properties of resveratrol that support its coronary disease prevention. Firstly, resveratrol has been demonstrated to modulate the production of nitric oxide (NO) from vascular endothelium. This nitrogen species is known to be involved in inflammatory responses<sup>77</sup>. The development of atheromatous plaque is linked to vascular damage which in turn can be caused by increased levels of nitric acid. The second biological effect that supports the notion of resveratrol preventing coronary disease is its oestrogenic activity. Resveratrol inhibits the oestrogen-metabolising phase I enzymes and also suppresses the induction of the carcinogen activator cytochrome P450 1A1. It does this by interfering with the binding site of the aryl hydrocarbon receptor (AhR) to the promoter of the gene<sup>78</sup>.

Huntington's disease is a genetic neurological disorder that can occur through a large range of ages around a mean occurrence of late forties/early fifties. Huntington's disease's most obvious symptoms are abnormal body movements and a lack of coordination, but it also affects a number of mental abilities and some aspects of behaviour. The Huntington disease gene, also called Huntingtin gene codes for a 348 kDa protein called huntingtin protein. The exact function of this protein is not known, but it plays an important role in nerve cells. Within cells, huntingtin may be involved in signalling, transporting materials, binding proteins and other structures, and protecting against programmed cell death (apoptosis)<sup>79</sup>. Mutant huntingtin is toxic to cells, leading to mitochondrial dysfunction and oxidative stress, and subsequently to neuronal dysfunction and cell death. A recent study by Parker *et al* has emphasised the neuroprotective roles of the human homologue of Sir2, sirtuin 1 (SIRT1) in Huntington's disease. Resveratrol-induced SIRT1 and Sir2 in neurons of Huntington's disease models prevented neuronal dysfunction caused by polyQ toxicity<sup>80</sup>.

Alzheimer's disease is a degenerative and terminal disease for which there is currently no known cure. In its most common form, it occurs in people over 65 years old although a less-prevalent early-onset form also exists. It is a complex disorder leading to the most common mental illness characterised by the loss of memory and multiple cognitive degenerations. It is associated with the presence of intercellular neurofibrillary tangles, extracellular  $\beta$ -amyloid ( $A\beta$ ) peptides, synaptic failure and mitochondrial dysfunction. Resveratrol markedly lowers the levels of secreted or

intracellular  $\beta$ -amyloid peptides produced by different cell lines. Resveratrol does not inhibit  $\beta$ -amyloid peptide production, but acts by promoting the intracellular degradation of  $\beta$ -amyloid peptides via a mechanism that implicates the proteasome<sup>81</sup>. Similar to Huntington's disease neurons, Alzheimer's disease neurons may be protected by the over-expression of SIRT1, however the precise connection between over-expression of SIRT1 and protection of neurons from Alzheimer's disease is not clearly understood.

Parkinson's disease is a degenerative disorder of the central nervous system that often impairs the sufferer's motor skills and speech, as well as other functions. The primary symptoms are the results of decreased stimulation of the motor cortex by the basal ganglia, as well as from degenerative changes in the brain stem. Depletion of dopamine results in an imbalance between cholinergic and dopaminergic neurons in the extrapyramidal system. A study carried out at Lund University, Sweden by Karlsson *et al* determined that resveratrol was found to protect embryonic mesenchymal cells of the rat from *tert*-butyl hydroperoxide through a radical scavenging mechanism that was detected by electron paramagnetic resonance (EPR) spectroscopy in conjunction with the nitron spin trap 5,5-dimethyl-1-pyrroline-N-oxide (DMPO)<sup>82</sup>.

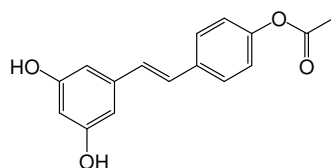
When considering resveratrol as an anticancer agent, it has primarily been associated with growth and death regulatory pathways. In recent years emerging information shows that, under physiological conditions, resveratrol additionally contributes to maintaining genome stability. Therefore, resveratrol protects the genome as an antioxidant via the inhibition of inflammation, suppression of metabolic carcinogen activation, *de novo* expression of genes that encode detoxifying proteins and possibly even via radical scavenging properties, all at the stage of DNA damage formation<sup>83</sup>.

The bioactivity of resveratrol is highly complex and there are many proposed mechanisms for resveratrol interaction. A proposed mode of action of resveratrol and its interaction with DNA has been suggested<sup>84</sup>. Although resveratrol itself does not intercalate with DNA, it has been shown to revert DNA intercalation through stabilisation of double-stranded DNA structure, resulting in a protective effect. An alternative mechanism of resveratrol interaction giving access to reactive oxygen

molecules such as hydrogen peroxide, is in transition metal interactions {*e.g.* copper(II)}, as was reported for various flavonoids by Snyder *et al*<sup>85</sup>. It is also proposed that through blockage of enzymatic interaction sites on DNA, resveratrol may counteract DNA-metabolising processes. Therefore, mere DNA bonding by resveratrol could be the basis for resveratrol induced replication stress and downstream ATM and ATR signalling<sup>86</sup>. Adding further to the complexity of the effect resveratrol has on the genome structure, it is reported that it may also contribute to chromatin remodelling through upregulation of the transcription coactivator gene, p300 and activation of SIRT1<sup>87</sup>.

## 6.5 Resveratrol derivatives

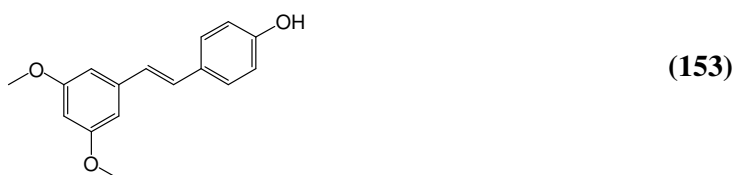
Based on the 3,5,4'-trihydroxystilbene structure, many derivatives of resveratrol have been synthesised in an effort to improve bioactivity. With so many synthetic routes available for stilbene production, the main limitations to synthesis of derivatives are the availability of starting materials. Andrus *et al*, who first published the synthesis of resveratrol via the stereoselective decarbonylative Heck reaction, have subsequently published ester analogues via this method<sup>88</sup>. These ester analogues were tested on human leukaemia HL-60 cells to determine anti-cancer potential in comparison to resveratrol. Of the compounds tested in this report, only one of the ester analogues showed a better ED<sub>50</sub> value than that of resveratrol. A 4'-acetoxy derivative **152** was found to have increased anti-cancer activity with an ED<sub>50</sub> value of 17  $\mu$ M (resveratrol, ED<sub>50</sub> 23  $\mu$ M).



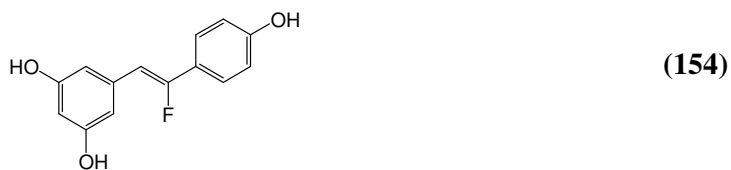
(152)

The addition of fluorine atoms into a drug molecule has been a fundamental element in the search for increased biological activity over the years. There are generally two consequences of introducing fluorine into a drug molecule<sup>89</sup>. Firstly there are the physiochemical properties. Fluorine has the ability to modulate electronic, lipophilic

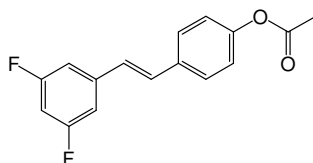
and steric parameters that can critically influence the pharmacological properties of a drug molecule. The introduction of a fluorine atom will generally increase lipophilicity, decrease basicity and alter the hydrogen bonding interactions of a molecule. Secondly, there is the influence of fluorine substitution on the biological stability of a drug molecule, *e.g.* through altering the metabolism of the drug<sup>90</sup>. In 2001, Eddarir *et al* reported the synthesis of fluorinated derivatives of both resveratrol and pterostilbene **153** (3,5-dimethoxy-4'-hydroxystilbene)<sup>23</sup>. Analogues containing fluorine substituents on the central vinylic double bond were prepared, such as **154**, however the biological activity of these compounds was not reported.



The replacement of the hydroxyl groups of the resveratrol structure with halogens was reported in 2005 by French researchers<sup>91</sup>. A series of chlorinated and fluorinated derivatives were synthesised to investigate the chemical modification of resveratrol in order to obtain specific antagonists of dioxins with a higher affinity for the aryl hydrocarbon receptor (AhR) but devoid of affinity for oestrogen receptor (ER) binding. All substituted *trans*-isomers showed a higher affinity for the AhR than resveratrol with little affinity to ER.



Andrus *et al* reported the synthesis fluorinated analogues aimed at ascertaining their chemotherapeutic potency<sup>88</sup>. A fluorinated series of derivatives was reported containing mono-, di- and trifluoro substituted resveratrol, in replacement of the hydroxyl groups. However in this report it is stated that they were unable to assess toxicity profiles in leukaemia cell lines for these fluorinated analogues.



(155)

Unpublished data from this laboratory showed that the fluorinated derivatives of resveratrol possess a broad array of cytotoxicity<sup>92</sup>. Preliminary biological results have indicated that various fluorinated analogues exhibited anticancer activity against a variety of tumour cell lines. Fluorinated analogues such as the 4'-acetoxy derivative **155**, have been shown to possess bioactive potency in the same region as resveratrol. When assayed with the lung carcinoma cell line DLKP, **155** has an  $IC_{50}$  of  $7 \pm 1 \mu M$  and  $10 \pm 3 \mu M$  against the DLKP-A cell line. These, compared to the resveratrol  $IC_{50}$  control of  $10 \pm 2 \mu M$  and  $15 \pm 3 \mu M$ , respectively, demonstrated the potential of fluorinated analogues. Herein, we report studies in the synthesis of molecules with increased bioactivity, utilising a known hydroxyl moiety chemical-isostere, the amino group.

## 6.6 Conclusion and Aims

Resveratrol (3,5,4'-trihydroxystilbene) **136**, isolated from a plant used in traditional Chinese and Japanese medicine was initially characterized as a phytoalexin. Resveratrol attracted little interest until 1992, when it was postulated to explain some of the cardioprotective effects of red wine. Since then, over 6000 letters and reviews have been published in a variety of journals around the world. There have been many synthetic routes devised to produce resveratrol, using a variety of reactions and methods, each with their own advantages and disadvantages. Recent reaction modifications are tending to produce isomerically pure stilbenes.

However, the greatest flourish in research activity it has been in the biological realm. The reason for the intensity in research into resveratrol and its analogues is due to the vast array of biological properties displayed by this hydroxylated *trans*-stilbene. The screening of resveratrol and its derivatives is ongoing and investigation into its modes

of action is continuing. However, the complete biological activity of resveratrol is not yet fully understood.

Resveratrol is often referred to as a 'dirty' molecule in the pharmaceutical industry, meaning that it seems to interact with many different proteins. Thus, its activity cannot be presumed in a unique mechanism of action but likely results from various complementary actions of different biochemical pathways

Could resveratrol and similar molecules form the next class of wonder-drugs? Although it has shown remarkable promise, as a potent chemopreventative agent in several bioassay systems, there is a long way to go when it could be developed as an agent for chemoprevention/treatment of cancer. In the meantime, we might all do well to follow the advice of Antonio Todde, once the world's oldest man: "Just love your brother and drink a good glass of red wine everyday".

The aim of this research was to investigate the substitution of the hydroxyl groups of resveratrol with fluorine and the bioisotere, the amino group. Substituted amines with acetyl and trifluoroacetyl derivatives were also synthesised. A tertiary amine was also prepared. The potential of a prodrug delivery system was investigated by synthesising a series of amino acid derivatives. Comparative analogues with fluorine substitution on one aromatic ring and nitrogen substitution on the other were synthesised, maintaining the 3,4',5- substitution pattern of resveratrol.

## 6.7 References

1. Baur J.A, Sinclair D.A.; *Nat. Rev., Drug Discov.* **2006**, *5*, 493.
2. Renaud S., de Lorgeril M.; *Lancet* **1992**, *339*, 8808, 1523.
3. Hao, H.D., He, L.R.; *J. Med. Food* **2004**, *7*, 3, 290.
4. Dong Z.; *Mutat. Res.* **2003**, *145*, 523.
5. Saiko, P., Szakmary, A., Jaeger, W., Szekeres, T.; *Mutat. Res.* **2008**, *658*, 68.
6. Pettit, G.R., Grealish, M.P., Jung, M.K., Hamel, E., Pettit, R.K., Chapuis, J.C., Schmidt, J.M.; *J. Med. Chem.* **2002**, *45*, 2534.
7. Botella, L., Nájera, C.; *Tetrahedron* **2004**, *60*, 5563.
8. Halls, C., Yu, O.; *Trends in Biotechnology* **2008**, *26*, 2, 77.
9. Dewick, P.M.; “*Medicinal Natural Products, A Biosynthetic Approach*”, Wiley and Sons, **2003**, 2nd edition.
10. Austin, M.B., Bowman, M.E., Ferrer, J.L., Schröder, J., Noell, J.P.; *Chem. Bio.* **2004**, *11*, 1179.
11. Jang, M., Cai, L., Udeani, G.O., Slowing, K.V., Thomas, C.F., Beecher, C.W.W., Fong, H.H.S., Farnsworth, N.R., Kinghorn, A.D., Mehta, R.G., Moon, R.C., Pezzuto, J.M.; *Science (Washington, D. C.)* **1997**, *275*, 5297, 218.
12. Romero-Pérez, A.I., Lamuela-Raventós, R.M., Andrés-Lacueva, C, de la Torre-Boronat, M.C.; *J. Agric. Food Chem.* **2001**, *49*, 210.
13. Späth, E., Kromp, K.; *Chem. Ber.* **1941**, *74*, 189.
14. Roberti, M., Pizzirani, D., Simoni, D., Rondanin, R, Baruchello, R., C. Bonora, Buscemi, F., Grimaudo, S., Tolomeo, M.; *J. Med. Chem.* **2003**, *46*, 3546.
15. McMurry, J.; “*Organic Chemistry*”, **2000**, Brooks/Cole, 5th edition.
16. Chandrasekhar, S., Karri, P.; *Tet. Lett.* **2006**, *47*, 2249.
17. Solladié, G., Pasturel-Jacopé, Y., Maignan, J.; *Tetrahedron* **2003**, *59*, 3315.
18. Aliprantis, A.O., Canary, J.W., *JACS* **1994**, *116*, 6985.
19. Amatore C., Jutand, A., M'Barki, M.A.; *Organomet.* **1992**, *11*, 3009.
20. Amatore, C., Jutand, A., Suarez, A.; *JACS* **1993**, *115*, 9531.
21. Amatore, C., Carre, E., Jutand, A., M'Barki, M.A.; *Organomet.* **1995**, *14*, 1818.



22. Farina, V., Krishnan, B.; *JACS* **1991**, *113*, 9585.
23. Eddarir, S., Abdelhadi, Z., Rolando, C.; *Tet. Lett.* **2001**, *42*, 9127.
24. Horner, L., Hoffmann, H., Wippel, H.G.; *Chem. Berichte* **1958**, *91*, 61.
25. Wadsworth, W. S., Jr., Emmons, W. D.; *JACS* **1961**, *83*, 1733.
26. Maryanoff, B.E., Reitz, A.B.; *Chem. Rev.* **1989**, *89*, 863.
27. Brandt, P., Norrby, P.-O., Martin, I., Rein, T.; *J. Org. Chem.* **1998**, *63*, 1280.
28. Gester, S., Wuest, F., Pawelke, B., Bergmann, R., Pietzsch, J.; *Amino Acids* **2005**, *29*, 415.
29. Ferré-Filmon, K., Delaude, L., Demonceau, A., Noels, A.F.; *Coord. Chem. Rev.* **2004**, *248*, 2323.
30. Kang, S.K., Kim, J.-S., Choi, S.-C.; *J. Org. Chem.* **1997**, *62*, 4208.
31. Bosanac, T., Wilcox, C.S.; *Tet. Lett.* **2001**, *42*, 4309.
32. Tietze, L.F., Nordmann, G.; *Synlett* **2001**, *3*, 337.
33. Maddux, T., Li, W., Yu, L.; *JACS* **1997**, *119*, 844.
34. Sengupta, S., Kumar, S., Rajkumar, S., Singh, S., Pal, N.; *Tet. Lett.* **2002**, *43*, 1117.
35. Belfield, K.D., Chinna, C., Schafer, K.J.; *Tet. Lett.* **1997**, *38*, 6131.
36. Guiso, M., Marra, C., Farina, A.; *Tet. Lett.* **2002**, *43*, 597.
37. Andrus, M.B., Song, C., Zhang, J.; *Org. Lett.* **2002**, *4*, 12, 2079.
38. Klingelhofer, S., Schellenberg, C., Pommerehne, J., Bassler, H., Greiner, A., Heitz, W.; *Macromol. Chem. Phys.* **1997**, *198*, 5, 1511.
39. Spencer, A.; *J. Organomet. Chem.* **1984**, *265*, 3, 323.
40. Spencer, A.; *J. Organomet. Chem.* **1983**, *247*, 1, 117.
41. Blaser, H.U., Spencer, A.; *J. Organomet. Chem.* **1982**, *233*, 2, 267.
42. Andrus, M.B., Liu, J., Meredith, E.L., Nartey, E.; *Tet Lett.* **2003**, *44*, 4819.
43. Delmas, D., Jannin, B., Latruffe, N.; *Mol. Nutr. Food Res.* **2005**, *49*, 377.
44. Holme, A.L., Pervaiz, S.; *J. Bioenerg. Biomembr.* **2007**, *39*, 59.
45. Somoza, V.; *Mol. Nutr. Food Res.* **2005**, *49*, 373.
46. Fu Z.D., Cao Y., Wang K.F., Xu S.F., Han R. *Aizheng (Chinese J. Cancer)*, **2004**, *23*, 8, 869.
47. Niles, R.M., McFarland, M., Weimer, M.B., Redkar, A., Fu, Y.-F., Meadows, G.G.; *Cancer Lett.* **2003**, *190*, 157.
48. Niles, R.M., Cook, C.P., Meadows, G.G., Fu, Y.-M., McLaughlin, J.L., Rankin, G.O., *J. Nutr.* **2006**, *136*, 2542.

49. Basly, J.P., Lavier, M.C.; *Planta Med.* **2005**, *71*, 4, 287.
50. Lu, R., Serrero, G.; *J. Cell. Physiol.* **1999**, *179*, 297.
51. Hsieh, T.-C., Wu, J.M.; *Exp. Cell Res.* **1999**, *249*, 109.
52. Bhat, K.P.L., Lantvit, D., Christov, K., Mehta, R.G., Moon, R.C., Pezzuto, J.M.; *Cancer Res.* **2001**, *61*, 7456.
53. Atten, M.J., Godoy-Romero, E., Attar, B.M., Milson, T., Zopel, M., Holian, O.; *Invest. New Drugs* **2005**, *23*, 111.
54. Delmas, D., Rébé, C., Lacour, S., Filomenko, R., Athias, A., Gambert, P., Cherkaoui-Malki, M., Jannin, B., Dubrez-Daloz, L., Latruffe, N., Solary, E.; *J. Bio. Chem.* **2003**, *278*, 42, 41482.
55. Tessitore, L., Davit, A., Sarotto, I., Caderni, G.; *Carcinogenesis* **2000**, *21*, 8, 1619.
56. Schneider, Y., Durantou, B., Gossé, F., Schleiffer, R., Seiler, N., Raul, F.; *Nutr. Cancer* **2001**, *39*, 1, 102.
57. Mollerup, S., Øverbø, S., Haugen, A.; *Int. J. Cancer* **2001**, *92*, 18.
58. Kimura, Y., Okuda, H.; *J. Nutr.* **2001**, *131*, 1844.
59. Li, Z.G., Hong, T., Shimada, Y., Komoto, I., Kawabe, A., Ding, Y., Kaganoi, J., Hashimoto, Y., Imamura, M.; *Carcinogenesis* **2002**, *23*, 9, 1531.
60. Aziz, M.H., Nihal, M., Fu, V.X., Jarrard, D.F., Ahmad, N.; *Mol. Cancer Ther.* **2006**, *5*, 5, 1335.
61. Miura, D., Miura, Y., Yagasaki, K.; *Clin. Exp. Met.* **2004**, *21*, 445.
62. Michels, G., Wätjen, W., Weber, N., Niering, P., Chovolou, Y., Kampkötter, A., Proksch, P., Kahl, R.; *Toxicology* **2006**, *225*, 173.
63. Carbó, N., Costelli, P., Baccino, F.M., López-Soriano, F.J., Argilés, J.M.; *Biochem. Biophys. Res. Comm.* **1999**, *254*, 739.
64. Rigolio, R., Miloso, M., Nicolini, G., Villa, D., Scuteri, A., Simone, M., Tredici, G.; *Neurochem. International.* **2005**, *46*, 205.
65. Fulda, S., Debatin, K.-M.; *Cancer Res.* **2004**, *64*, 337.
66. Kotha, A., Sekharam, M., Cilenti, L., Siddiquee, K., Khaled, A., Zervos, A.S., Carter, B., Turkson, J., Jove, R.; *Mol. Cancer Ther.* **2006**, *5*, 3, 621.
67. Dörrie, J., Gerauer, H., Wachter, Y., Zunino, S.J.; *Cancer Res.* **2001**, *61*, 4731.
68. Estrov, Z., Shishodia, S., Faderl, S., Harris, D., Van, Q., Kantarjian, H.M., Talpaz, M., Aggarwal, B.B.; *Blood* **2003**, *102*, 3, 987.

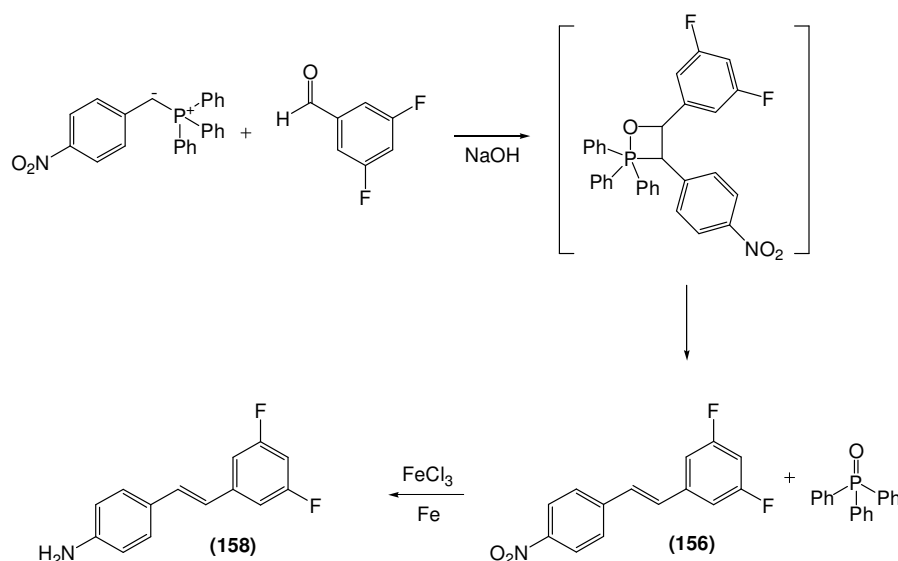
69. Ahmad, K.A., Clement, M.V., Hanif, I.M., Pervaiz, S.; *Cancer Res.* **2004**, *64*, 1452.
70. Horvath, Z., Saiko, P., Illmer, C., Madlener, S., Hoechtl, T., Bauer, W., Erker, T., Jaeger, W., Fritzer-Szekeres, M., Szekeres, T.; *Exp. Hematology* **2005**, *33*, 329.
71. Gao, X., Xu, Y.X., Divine, G., Janakiraman, N., Chapman, R.A., Gautam, S.C.; *J. Nutr.* **2002**, *132*, 2076.
72. Soares, D., Andrezza, A.C., Salvador, M.; *J. Agric. Food Chem.* **2003**, *51*, 1077.
73. Losa, G.A.; *Eur. J. Clin. Invest.*, **2003**, *33*, 818.
74. Frankel, E.N., Waterhouse, A.L., Kinsella, J.E.; *Lancet* **1993**, *341*, 8852, 1103.
75. Olas, B., Wachowicz, B., *Throm. Res.* **2002**, *106*, 143.
76. Leonard, S.S., Xia, C., Jiang, B.-H., Stinefelt, B., Klandorf, H., Harris, G.K., Shi, X., *Biochem. Biophys. Res. Comm.* **2003**, *309*, 1017.
77. Hattori, R., Otani, H., Maulik, N., Das, D.K.; *Am. J. Physiol. Heart Circ. Physiol.* **2002**, *282*, H1988.
78. Ciolino, H.P., Yeh, G.C.; *Molecular Pharmacol.* **1999**, *56*, 760.
79. Bates, G.; *Lancet* **2003**, *361*, 1642.
80. Parker, J.A., Arango, M., Abderrahmane, S., Lambert, E., Tourette, C., Catoire, H., Néri, C.; *Nat. Genetics* **2005**, *37*, 4, 349.
81. Marambaud, P., Zhao, H., Davies, P.; *J. Bio. Chem.* **2005**, *280*, 45, 37377.
82. Karlsson, J., Emgård, M., Brundin, P., Burkitt, M.J.; *J. Neurochem.* **2000**, *75*, 141.
83. Gatz, S.A., Wiesmüller, L.; *Carcinogenesis* **2008**, *29*, 2, 321.
84. Usha, S., Johnson, I.M., Malathi, R.; *J. Biochem. Mol. Bio.* **2005**, *38*, 2, 198.
85. Snyder, R.D., Gillies, P.J.; *Environ. Mol. Mutagen* **2002**, *40*, 266.
86. Heiss, E.H., Schilder, Y.D.C., Dirsch, V.M.; *J. Bio. Chem.* **2007**, *282*, 37, 26759.
87. Signorelli, P., Ghidoni, R.; *J. Nutr. Biochem.* **2005**, *16*, 449.
88. Andrus, M.B., Liu, J.; *Tet. Lett.* **2006**, *47*, 5811.
89. Emeléus, H.J.; *“The Chemistry of Fluorine and its Compounds”*, Academic Press, New York, London, **1969**.
90. Park, B.K., Kitteringham, N.R., O’Neill, P.M., *Annu. Rev. Pharamcol. Toxicol.* **2001**, *41*, 443

91. De Medina, P., Casper, R., Savouret, J.F, Poirot, M.; *J. Med. Chem.* **2005**, *48*, 287.
92. Anderson, F.P.; “*The synthesis, structural characterisation and biological evaluation of potential chemotherapeutic agents*”, Dublin City University, *PhD Thesis*, **2005**.

## 7.0 Synthesis and characterisation of novel fluoro-amino stilbenes

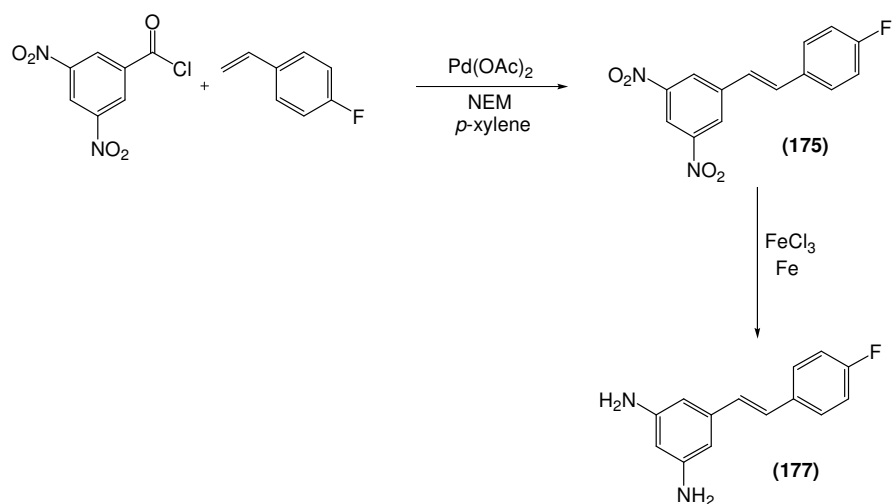
### 7.1 Introduction

A series of fluorinated amino stilbenes were synthesised in an attempt to create a novel compound with greater bioactivity than that of resveratrol **136**. Previous work carried out in this laboratory has shown that substitution of the hydroxyl moieties of resveratrol by fluorine has a minimal effect on the potency. By maintaining this fluorine substitution, a novel series of compounds containing the known hydroxyl chemical isostere, the amino group, was generated. As described in the previous section, there are many methods for the production of stilbenes. The selection of synthetic route was based on factors such as, commercial availability of starting materials, cost of starting materials and stereospecificity of each reaction. The first series of analogues created had fluorines at the 3 and 5 positions while the amino group replaced the 4'-hydroxyl. These amino derivatives were synthesised from the reduction of the corresponding nitro analogue. The classic Wittig reaction was chosen for the carbon-carbon bond forming synthesis of the basic nitro stilbene. This synthesis of (*E*)-3,5-difluoro-4'-nitrostilbene **156** is outlined in *Scheme 7.1*.



*Scheme 7.1:* Synthesis of (*E*)-3,5-difluoro-4'-amino stilbene **158**

The second series of novel derivatives concentrated on synthesising the reverse of those prepared in the first series. In contrast to the first series, stilbene analogues with amino groups at the 3 and 5 positions and a fluorine atom at the 4' position were synthesised. Using the stereoselective decarbonylative Heck reaction, the *trans*-dinitro-isomer was synthesised. By reacting 3,5-dinitrobenzoyl chloride with 4-fluorostyrene, *trans*-3,5-dinitro-4'-fluorostilbene **175** was synthesised. **Scheme 7.2** shows the reaction steps used for the synthesis of the diamino analogue.



**Scheme 7.2:** Synthesis of (*E*)-3,5-diamino-4'-fluoro stilbene **177**

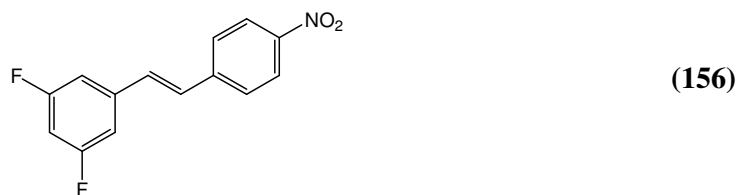
For comparison purposes, the *cis*-isomer **176** was synthesised via the Wittig reaction. All nitro compounds were reduced to yield the amino derivatives and these were utilised for further derivatisation.

## 7.2 Synthesis of 3,5-difluoro resveratrol analogues

### 7.2.1 Synthesis of 3,5-difluoro-4'-nitro stilbene

The synthesis of 3,5-difluoro-4'-amino stilbene derivatives was successfully achieved using the Wittig reaction. This reaction involves the combining of phosphonium ylide with an aldehyde to form a stilbene. These phosphonium ylides were prepared by stirring the corresponding benzyl chloride in toluene with an excess of triphenylphosphine<sup>1</sup>. Both 3,5-difluoro and 4-nitrobenzyl(triphenylphosphonium)

bromide were synthesised. Depending on reaction times, the yield of these phosphonium salts ranged from 70 % to quantitative values. From these salts, the main starting material for the 4'-amino derivatives was made. Reaction of the triphenyl phosphonium bromide compounds with the appropriate substituted benzaldehyde in the presence of sodium hydroxide yielded the nitro stilbenes isomers **156** and **157**.



This Wittig reaction yielded a mixture of isomers as a yellow powder. The isomers were formed in equal quantities. Fractional crystallisation from ethanol was used to separate the *cis* and *trans* isomers. Yields of both isomers ranged from 40-50%. Quantitative yields of the isomeric mixture were achieved. Separation of the isomers initially proved very difficult. Column chromatography was not possible as the isomers would not separate sufficiently. Recrystallisation of the isomeric mixture was attempted as a method of isolation of the isomers. Many solvent mixtures were tried before recrystallisation from ethanol proved successful. Fractional crystallisation was identified as the most efficient method of separation. On addition of warm ethanol, the *trans* product was found to be largely insoluble, and when isolated was a dark yellow solid. The *Z*-isomer was found to be much paler yellow in colour.

#### 7.2.1.1 Determination of isomeric orientation

Once the isomers were separated, determination of the orientation of each compound was necessary. The easiest and most common method of determining the stereochemistry of the double bond is from the vinylic proton splitting in the  $^1\text{H}$  NMR. By calculating the coupling constants of the protons of the central double bond,

it can be demonstrated which isomer is the *E*- and which is the *Z*-derivative. Generally the vinylic protons of a *trans*-isomer would have a coupling constant of approximately 16 Hz while the *cis*-isomer would have a vinylic *J* value closer to 10 Hz. However, in the case of 3,5-difluoro-4'-nitrostilbene, the vinylic signals of the *cis* product appear at the same chemical shift as the *ortho* protons on the fluorinated phenyl ring, at approximately  $\delta$  6.9. For this reason, further confirmation was required to guarantee the stereochemical configuration. Crystals of the *trans*-isomer were grown from toluene for X-ray crystallography. The following crystal structure has been deposited at the Cambridge Crystallographic Data Centre and allocated the deposition number CCDC 685944. This proved beyond doubt the orientation of the double bond and that the insoluble isomer was *trans*-3,5-difluoro-4'-nitrostilbene **156**. The monoclinic unit cell of stilbene **156** is shown in *Figure 7.1*.

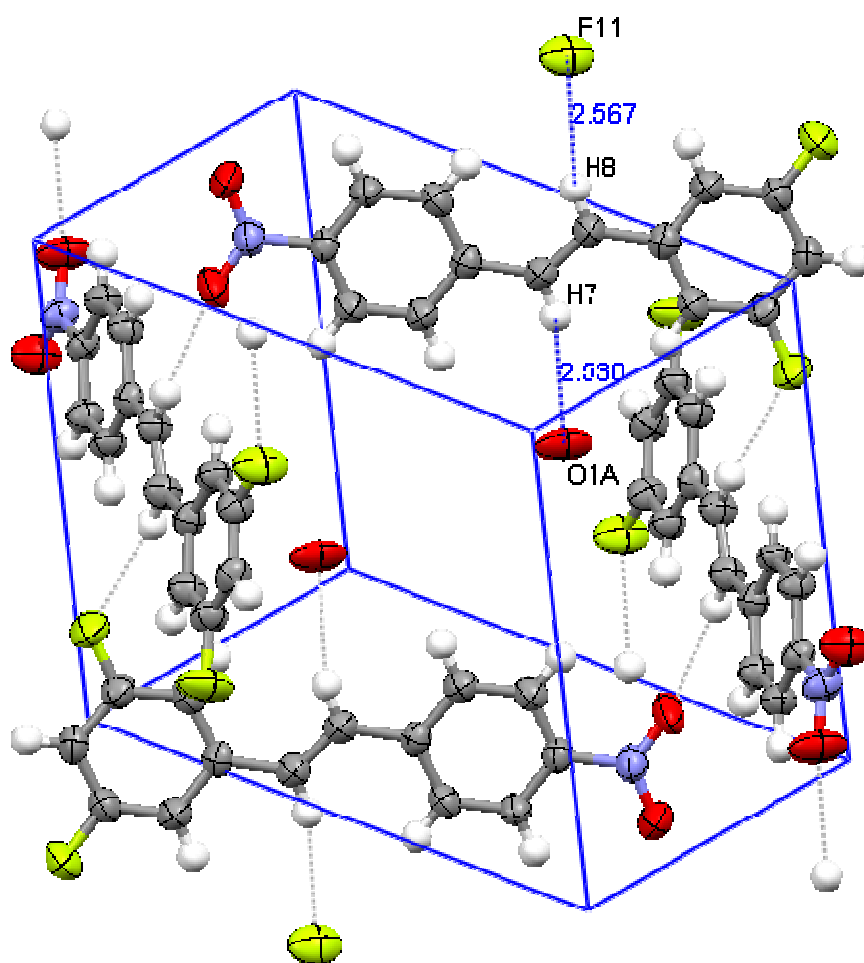


**Figure 7.1:** X-ray crystal structure and unit cell of (*E*)-3,5-difluoro-4'-nitrostilbene **156**



<b>Empirical formula</b>	C <sub>14</sub> H <sub>9</sub> F <sub>2</sub> NO <sub>2</sub>
<b>M<sub>r</sub></b>	261.22
<b>Crystal colour</b>	Yellow, block
<b>Crystal system</b>	Monoclinic
<b>Space group</b>	P2 <sub>1</sub> /n
<b>a/Å</b>	8.566(4)
<b>b/Å</b>	12.003(5)
<b>c/Å</b>	11.885(5)
<b>α/°</b>	90
<b>β/°</b>	103.945(10)
<b>γ/°</b>	90.00
<b>V/Å<sup>3</sup></b>	1186.0(9)
<b>Z</b>	4
<b>Temperature/K</b>	273(2)
<b>D<sub>calc</sub>/gcm<sup>-3</sup></b>	1.463
<b>F<sub>(000)</sub></b>	536
<b>μ/mm<sup>-1</sup></b>	0.199
<b>Crystal dimensions/mm</b>	0.27 x 0.19 x 0.14
<b>Index ranges</b>	<i>h</i> , -10 - 10; <i>k</i> , -14 - 14; <i>l</i> , -14 - 14
<b>Max. to min. transmission</b>	0.9685 – 0.9835
<b>Refinement method</b>	Full matrix on F <sup>2</sup>
<b>Reflections</b>	2093
<b>Parameters</b>	172
<b>Goodness of fit</b>	1.030
<b>Final R indices (I&gt;2σ(I))</b>	0.0450 (R <sub>1</sub> ), 0.1171 (R <sub>w</sub> )

**Table 7.1:** Crystal data and structure refinement of (*E*)-3,5-difluoro-4'-nitrostilbene **156**

<b>Bond distances (Å)</b>			
<i>O(1A)</i> - <i>N1</i>	1.224	<i>C(8)</i> - <i>H(8)</i>	0.930
<i>O(1B)</i> - <i>N1</i>	1.222	<i>C(8)</i> - <i>C(9)</i>	1.467

<i>C1-N1</i>	1.465	<i>C(9)-C(10)</i>	1.392
<i>C(1)-C(2)</i>	1.376	<i>C(10)-C(11)</i>	1.368
<i>C(2)-C(3)</i>	1.376	<i>C(11)-C(12)</i>	1.374
<i>C(3)-C(4)</i>	1.393	<i>C(12)-C(13)</i>	1.365
<i>C(4)-C(5)</i>	1.396	<i>C(13)-C(14)</i>	1.165
<i>C(5)-C(6)</i>	1.376	<i>C(9)-C(14)</i>	1.388
<i>C(1)-C(6)</i>	1.380	<i>C(11)-F(11)</i>	1.355
<i>C(4)-C(7)</i>	1.465	<i>C(13)-F(13)</i>	1.359
<i>C(7)-C(8)</i>	1.314		
<b>Bond angles (°)</b>			
<i>O(1A)-N1-O(1B)</i>	122.84	<i>C(7)-C(8)-C(9)</i>	127.00
<i>O(1A)-N1-C(1)</i>	118.68	<i>H(8)-C(8)-C(9)</i>	116.53
<i>C(4)-C(7)-H(7)</i>	116.71	<i>F(11)-C(11)-C(10)</i>	118.48
<i>C(4)-C(7)-C(8)</i>	126.49	<i>C(10)-C(11)-C(12)</i>	123.78
<i>H(7)-C(7)-C(8)</i>	116.80	<i>F(11)-C(11)-C(12)</i>	117.74
<i>C(7)-C(8)-H(8)</i>	116.47		

**Table 7.2:** Selected bond distances (Å) and angles (°) **156**

From the X-ray crystal structure the bond distances and angles of the stilbene **156** can be measured. These are displayed in **Table 7.2**. The nitrostilbene **156** crystallises in the monoclinic space group  $P2_1/n$  with four independent molecules per asymmetric unit. The phenyl C-C bond distances range from 1.365 Å to 1.396 Å. The carbon-nitrogen bond measures 1.459 Å while the carbon fluorine bonds are 1.355 and 1.359 Å. The central double bond of the molecule (*C(7)-C(8)*) is 1.314 Å. The hydrogen bonding of compound **156** is also displayed. The intramolecular contacts occur between hydrogen and oxygen, and hydrogen and fluorine. The hydrogen bonding to the fluorine atoms is 2.567 Å. The distances of the hydrogen bonding to oxygen atoms varies slightly. Distances of 2.530 Å for *H(7)-O(1A)*, 2.650 & 2.661 Å for *O(1A)* and *O(1B)* to *H(12)*, respectively, and for *H(2)-O(1B)* is 2.678 Å were measured. These are clearly displayed in **Figure 7.2**.

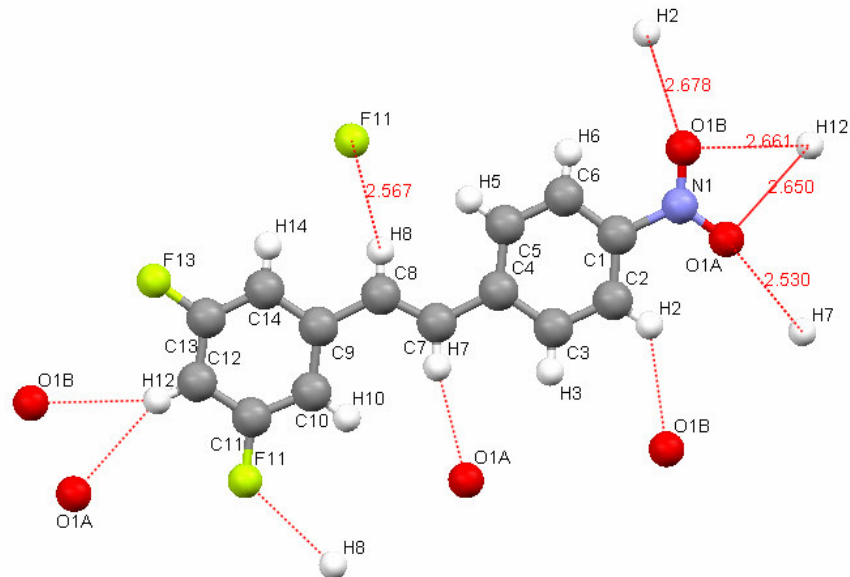


**Figure 7.2:** Hydrogen-bonding of stilbene **156**

Molecular modelling was carried out on the nitrostilbene isomers. The calculations were performed at the HF/3-21G level. Energy optimisation of the structure led to the *cis* form **157**. This was then forced into the *trans* form with the difference in energies between the two isomers being 13.77 J/mol (please note **Figure 7.3** not drawn to scale, energy difference between isomeric levels is minute compared to the energy required for transition).

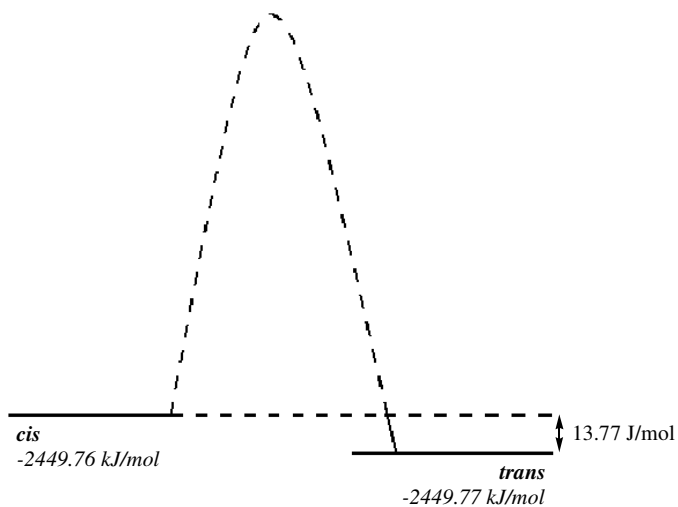


**Figure 7.3:** Energy level diagram of *cis-trans* isomerisation between **156** & **157**

The intraspatial distances were calculated using molecular modelling. The distance between hydrogens 6 and 14 for the *trans* isomer was found to be 6.94 Å. The distance between H(3)-H(7) and H(7)-H(10) is 2.43 Å and 2.29 Å, respectively. Molecular modelling was employed in order to use NMR 2-D experiments to prove the orientation of the central double bond. Nuclear overhauser effect spectroscopy (NOESY) shows intraspatial correlations between atoms of a molecule within 5 Å. It was hoped that this technique could be exploited to determine either the *cis* or *trans* isomers. The distances from H(7) to the aromatic protons of the second ring were selected due to their clarity in the <sup>1</sup>H NMR spectra. The signals of these protons do not overlap with the signals of other protons of the molecule, such as the 2,6-hydrogens with the vinylic protons in the *cis* isomer **157** ( $\delta$  ~6.9). Molecular modelling determined the proton at the 4 position {H(12)} and the aromatic hydrogens on the nitrophenyl ring. They ranged from 7.8 to 10.5 Å for the *trans* isomer **156**. The *cis* orientation gave shorter distances as anticipated, however they were not within the maximum NOESY distance of 5 Å. The distances ranged from 5.3 to 8.7 Å which was not close enough for NOESY correlation.

The UV-vis spectra of both isomers (**156** and **157**) show very different UV absorbances. The  $\lambda_{\text{max}}$  of (*E*)-3,5-difluoro-4'-nitrostilbene **156** was present at 337 nm while the maximum absorbance of the *cis* isomer occurs at 314-315 nm. This is due to the absorbance of the carbon-carbon double bond and its orientation in the respective compounds. This was believed to be another possible way of distinguishing the isomers and proving the configuration.

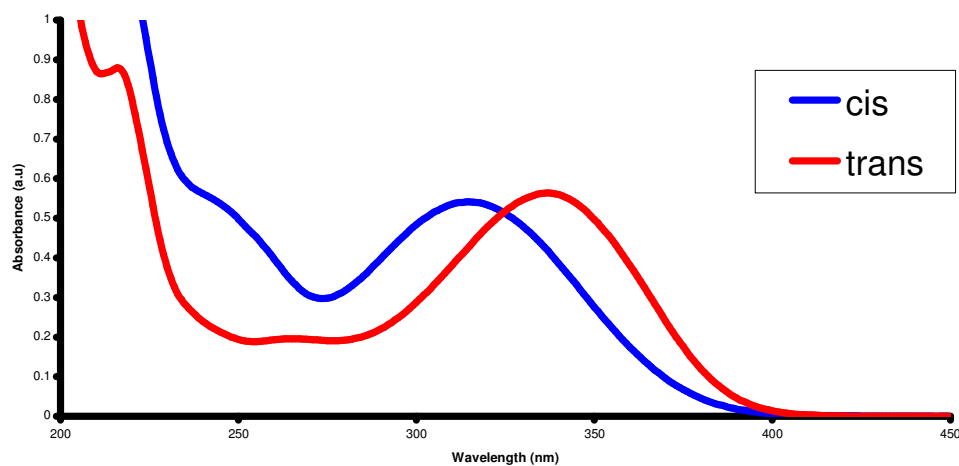
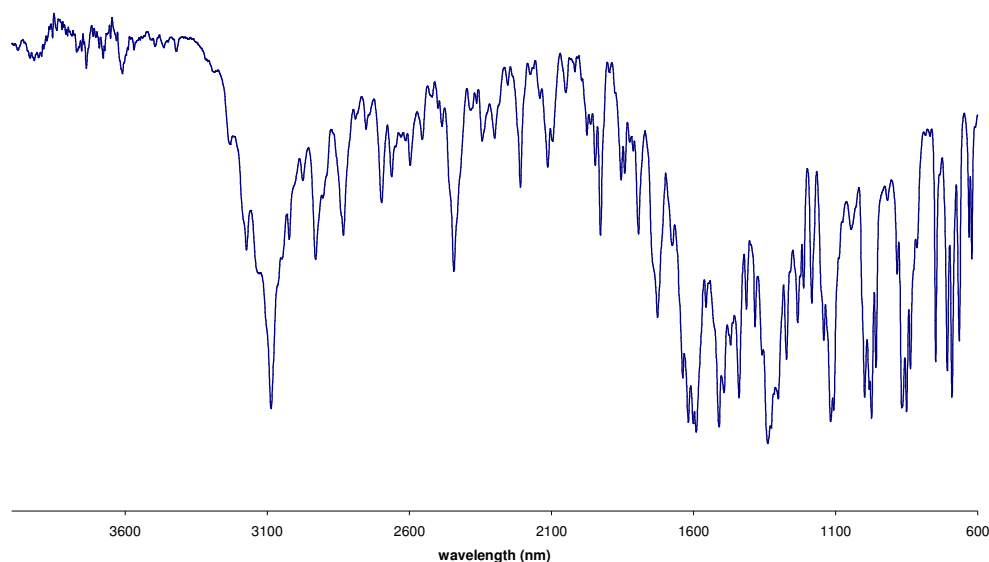


Figure 7.4: UV spectra of *cis/trans* isomers **156** & **157**

### 7.2.1.2 IR study of (E/Z)-3,5-difluoro-4'-nitro stilbene

The infrared spectra for all of the synthesised fluorinated analogues show very complex absorptions, mainly in the fingerprint region. This is largely due to the C-F stretching mode which couples strongly with other vibrational modes, especially the C-C stretching<sup>2</sup>. Carbon-fluorine bands can occur in the region of 1400 to 900  $\text{cm}^{-1}$ . Vinylic carbon stretching generally occurs about 1630  $\text{cm}^{-1}$  and is highly dependent on the substituents. A vinylic C=C stretch of a planar molecule generally occurs in the region of 1640-1610  $\text{cm}^{-1}$  in infrared spectra. Due to the planarity of the *trans* isomer **156**, absorption is visible at 1618  $\text{cm}^{-1}$ . The *cis* isomer **157** is in a forced non-planar configuration of as a result of steric hindrance, leading to reduced conjugation between the vinyl and phenyl groups. As a consequence, the C=C stretching band is present at 1660-1630  $\text{cm}^{-1}$ . In the spectrum of **157**, there is an absorption peak at 1640  $\text{cm}^{-1}$ .



**Figure 7.5:** Infrared spectrum of (*E*)-3,5-difluoro-4'-nitrostilbene **156**

In general, the characteristic  $\text{NO}_2$  stretching frequencies appear in the region of 1550-1475  $\text{cm}^{-1}$  for the asymmetric and 1360-1315  $\text{cm}^{-1}$  for the symmetric  $\text{NO}_2$  stretch. Such frequency lowering, in both of these stretching modes, is attributed to the conjunction of  $\text{NO}_2$  with the aromatic ring. The intensity of symmetric  $\text{NO}_2$  stretching is enhanced by conjugation, and the asymmetric and symmetric stretching bands are found to be very similar in peak intensity. The nitro stretching frequencies of nitrobenzene occur at 1548  $\text{cm}^{-1}$  and 1360  $\text{cm}^{-1}$  for the asymmetric and symmetric

modes, respectively<sup>3</sup>. For isomers **156** and **157**, the NO<sub>2</sub> asymmetrical stretch can be seen at 1509 and 1503 cm<sup>-1</sup>, while the symmetrical stretches appear at 1336 and 1340 cm<sup>-1</sup>, respectively. Because of the coupling between the C-N vibrational mode and other ring vibrations, carbon-nitrogen stretching frequencies of aromatic nitro compounds occur in the 1180-860 cm<sup>-1</sup> region. The NO<sub>2</sub> deformation vibrations, which include NO<sub>2</sub> scissoring (in-plane), NO<sub>2</sub> wagging (out-of-plane), and NO<sub>2</sub> rocking (in-plane), usually occur at frequencies lower than 900 cm<sup>-1</sup>. For the majority of compounds, the scissoring mode possesses the higher vibrational frequency of the three deformations, and it is by far the most characteristic deformation mode. The NO<sub>2</sub> rocking mode, on the other hand has the lowest frequency of these deformations. The intense absorptions at approximately 3100 cm<sup>-1</sup> are as a result of the carbon-hydrogen stretching of the phenyl rings, while the aromatic carbon-carbon double bonds stretch is weak in intensity and occurs about 1600 cm<sup>-1</sup>. Monosubstituted C-H bending occurs in the range 690-710 cm<sup>-1</sup> and 730-770 cm<sup>-1</sup>, while *meta*-disubstituted bending can be found in the range 680-725 cm<sup>-1</sup> and 750-810 cm<sup>-1</sup>. Although these absorptions are strong, the IR spectra of compounds **156** and **157** are complex with many peaks present in the fingerprint region. Definitive identification of exact peaks is all but impossible but absorptions are present in all the relevant ranges mentioned.

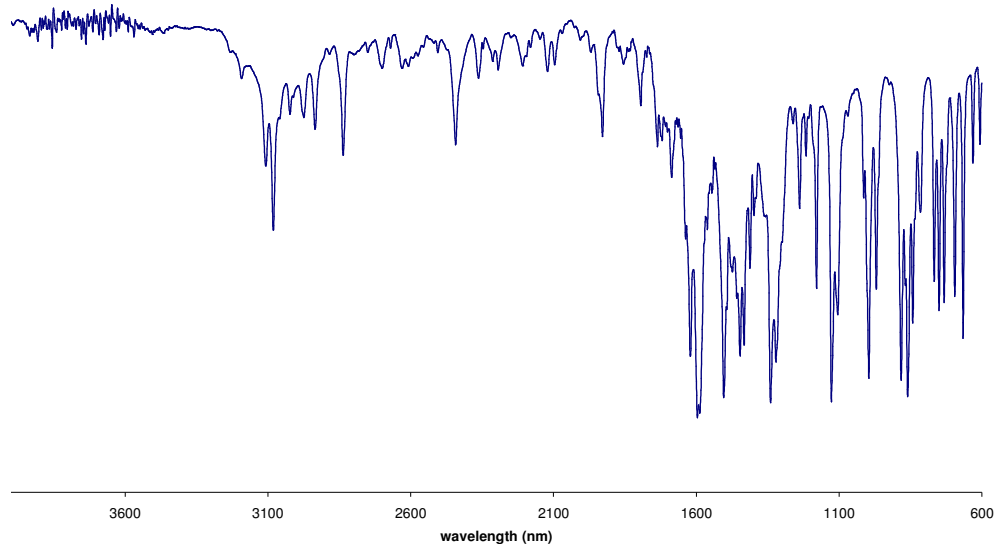


**Figure 7.6:** Infrared spectrum of (*Z*)-3,5-difluoro-4'-nitrostilbene **157**

### 7.2.1.3 NMR study of (E/Z)-3,5-difluoro-4'-nitrostilbene

The  $^1\text{H}$  NMR of the *trans*-stilbene **156** is shown in **Figure 7.7**. The unsaturated unit appears as two doublets  $\delta$  7.59 and 7.51 with coupling constants of 16.4 Hz. In the case of the *cis* isomer **157**, they should also appear as doublets; however in the proton NMR they occur at the same chemical shift as the *ortho*-protons of the fluorinated ring so the coupling constant cannot be calculated. The main difference between *E*- and *Z*- isomers in  $^1\text{H}$  NMR is the size of the coupling constant. *Z*-isomers generally record coupling constants between 7 and 11 Hz whereas *E*-isomers generally are in the range of 15-18 Hz<sup>4</sup>.

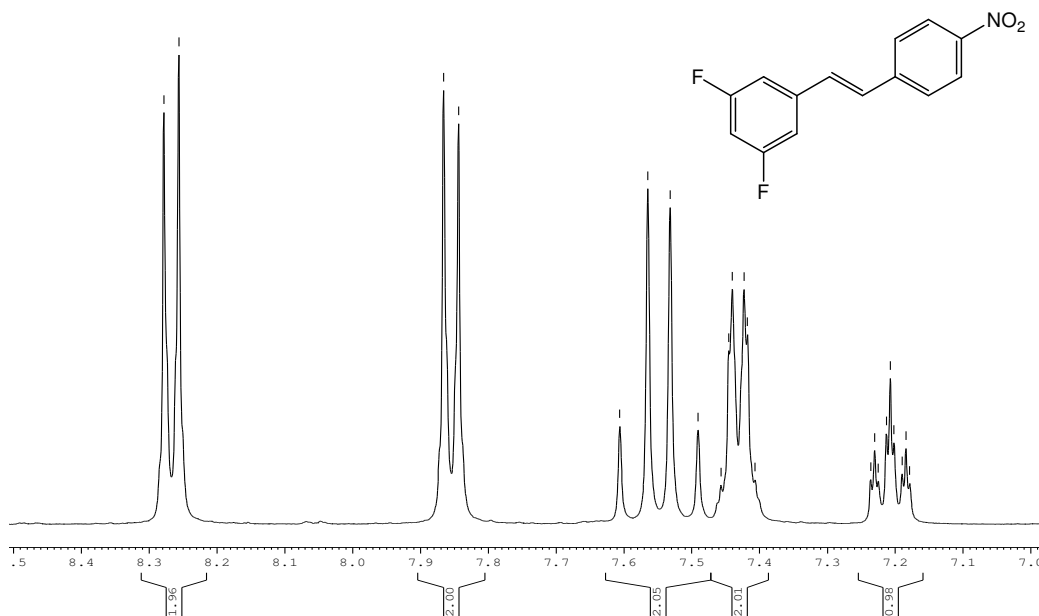


**Figure 7.7:**  $^1\text{H}$  NMR spectrum of (*E*)-3,5-difluoro-4'-nitrostilbene **156**

In the case of both isomers, the aromatic protons of the nitro substituted ring appear as doublets as is standard with a *para*-substituted phenyl ring. These have coupling constants in the region of 8-9 Hz. The two hydrogens  $\alpha$  to the nitro group are shifted the furthest downfield due to the electronic effects of the nitro group. For the *trans*-isomer the protons in the 3' and 5' positions appear at  $\delta$  8.27, while for the *cis*-isomer at  $\delta$  8.17. The protons in the 2' and 6' positions appear at  $\delta$  7.86 and 7.48 for **156** and **157**, respectively.

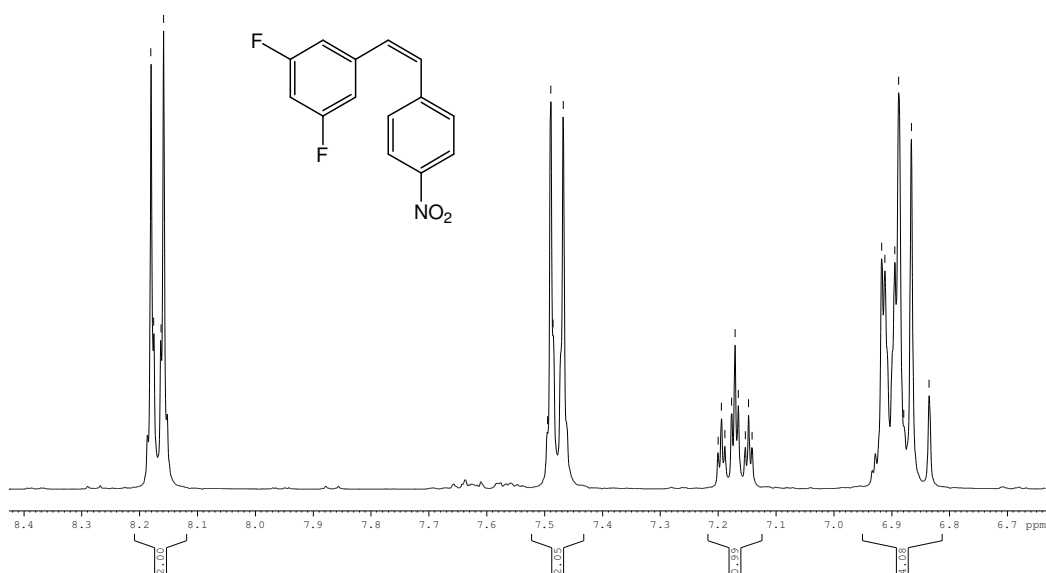


**Figure 7.8:**  $^1\text{H}$  NMR spectrum of (*Z*)-3,5-difluoro-4'-nitrostilbene **157**

Fluorine has a spin number of  $\frac{1}{2}$ , therefore coupling between fluorine and hydrogen occurs. The equivalent protons in the *ortho*-position of the fluorinated ring are therefore split by fluorine coupling. However, because fluorine exerts strong long range coupling effects, the proton signal is not split into a simple doublet but a multiplet. For the (*E*)-isomer this multiplet is found in the range of  $\delta$  7.39-7.48 while for the (*Z*)-isomer it shifts to a range of  $\delta$  6.82-6.94. The *para*-proton of this ring shows an interesting splitting pattern, caused by adjacent fluorine atoms. At a chemical shift of  $\delta$  7.21 and 7.17 for *trans* **156** and *cis* **157** respectively, the signal for the 4-H is split into a triplet of triplets in the  $^1\text{H}$  NMR spectra. This triplet of triplets has coupling constants of 2.9 and 9.2 Hz for the *trans* and 2.4 and 9.4 Hz for the *cis*.

The effect of fluorine coupling is also evident in the  $^{13}\text{C}$  NMR spectra. As can be seen in the  $^{13}\text{C}$  NMR spectrum of (*E*)-3,5-difluoro-4'-nitrostilbene **156**, the *meta*-carbons attached to fluorine are split into doublets because of  $^{13}\text{C}$ - $^{19}\text{F}$  coupling, and appear at  $\delta$  162.8 and  $\delta$  162.6 with *J* values of 244.2 and 244.0 Hz, respectively. In the case of the *cis*-isomer, the *meta*-carbons are present at  $\delta$  162.4 and  $\delta$  162.3, with *J* values of 245.0 and 244.7 Hz, respectively. The quaternary carbon at position 1 in both isomers is also affected by  $^{13}\text{C}$ - $^{19}\text{F}$  coupling, being split into a triplet due to coupling to both fluorine atoms. This triplet has a coupling constant of 9.9 Hz and occurs at a chemical shift of  $\delta$  140.2 and  $\delta$  139.6 for **156** and **157**, respectively. The other carbons in the fluorine-substituted phenyl ring also display fluorine-carbon coupling induced



splitting. The *ortho*-carbons, at positions 2 and 6 are split into doublets while the *para*-carbon at position 4 is split into a triplet. In the case of the *trans*-isomer **156**, the doublet from 2,6-C appears at  $\delta$  109.9 ( $J = 25.6$  Hz) and the 4-C triplet at  $\delta$  103.64 ( $J = 25.9$  Hz). For the *cis*-nitrostilbene **157**, the doublet has a chemical shift of  $\delta$  111.60 and a coupling constant of 25.5 Hz, while the triplet of the *para*-carbon is further upfield at  $\delta$  103.30 and has a coupling constant of 25.8 Hz.

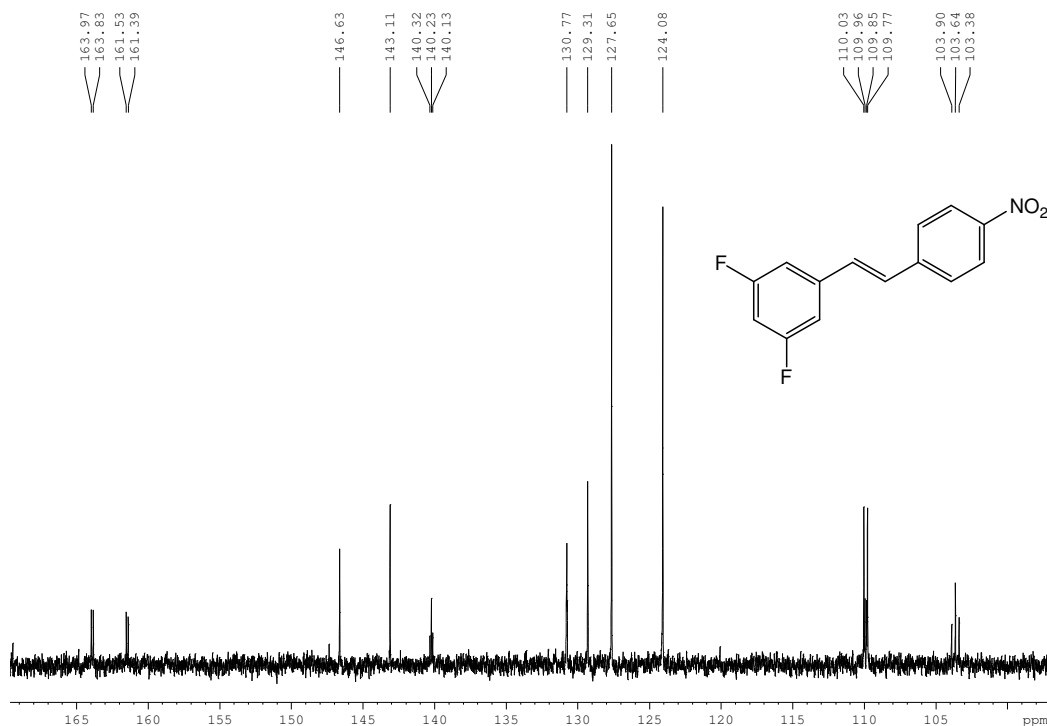


**Figure 7.9:**  $^{13}\text{C}$  NMR spectrum of *(E)*-3,5-difluoro-4'-nitrostilbene **156**

NMR evidence of fluorine coupling to hydrogen and carbon atoms, is not solely confined to just  $^1\text{H}$  and  $^{13}\text{C}$  NMR spectra. Signal splitting due to coupling is also seen in the  $^{19}\text{F}$  NMR, where in the case of the isomers of 3,5-difluoro-4'-nitrostilbene, the signal associated with the fluorine atoms is split into a triplet. This is due to the strong coupling to the two adjacent protons. For the *(E)*-stilbene **156**, the triplet has a chemical shift of  $\delta$  -109.81 with a coupling constant of 9.4 Hz. For compound **157**, it has a chemical shift of -109.57 and this signal has a coupling constant of 8.0 Hz.

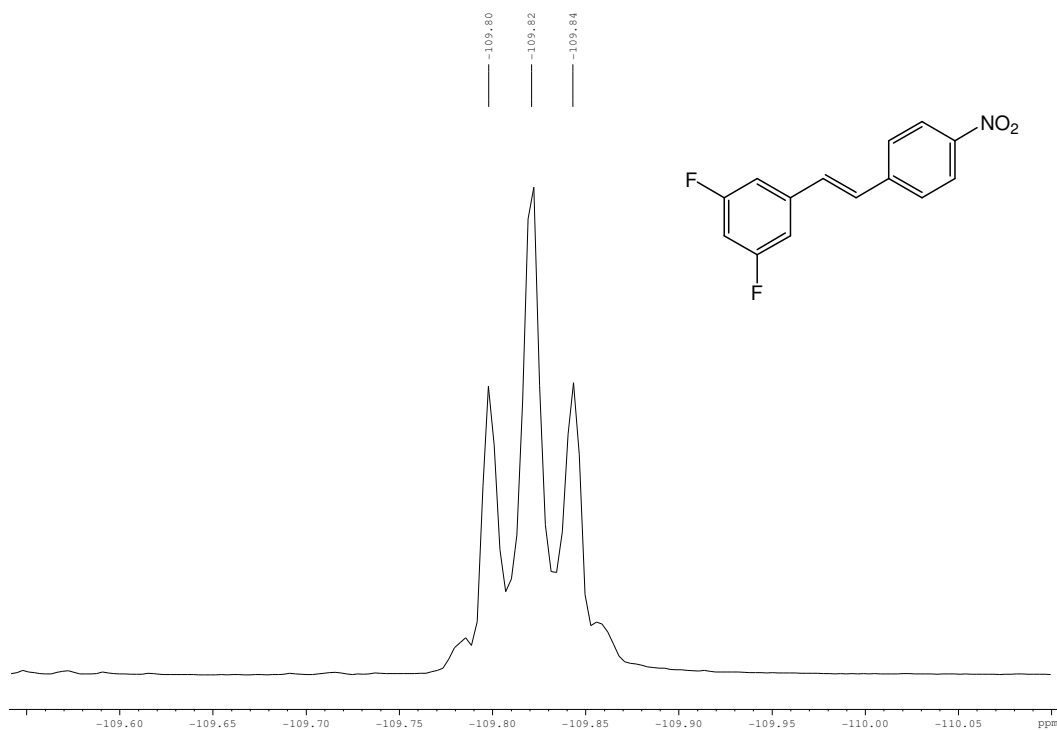
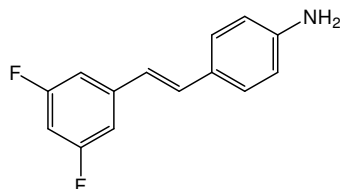


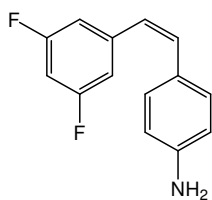
**Figure 7.10:**  $^{19}\text{F}$  NMR spectrum of (*E*)-3,5-difluoro-4'-nitrostilbene **156**

### 7.2.2 Synthesis of 4'-amino derivatives

In order to synthesis the targeted amino derivatives, the reduction of the nitro isomers was attempted. The initial effort to reduce stilbene **156** was carried out using poly(methylhydrosiloxane) (PMHS)<sup>5</sup>. A combination of palladium (II) acetate, aqueous potassium fluoride, and polymethylhydrosiloxane (PMHS) facilitates the room-temperature reduction of aromatic nitro compounds to anilines. Although the reaction did reduce the nitro group as expected, it also reduced the central double bond and yielded the diphenylethane derivative **171**.

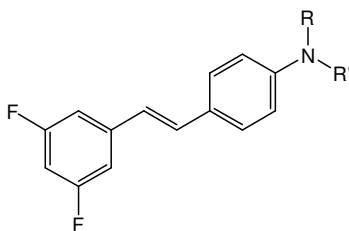


**(158)**



(159)

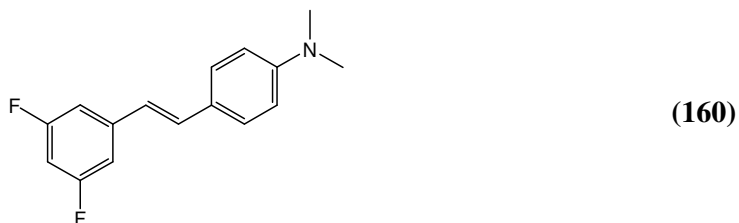
Further attempts at the reduction of the nitro group were tried under milder conditions, for example using zinc in conjunction with ammonium chloride. Tin chloride and hydrochloric acid proved unsuccessful as did sodium dithionite, in an effort to produce the 4'-amine **158**. The specific reduction of the nitro group to an amine was achieved using iron and iron (III) chloride<sup>6</sup>. Both the *trans* and *cis* isomers (**156** and **157**) were reduced by this method yielding (*E*)-3,5-difluoro-4'-aminostilbene **158** and (*Z*)-3,5-difluoro-4'-aminostilbene **159** in quantitative yields. The reduction was carried out in a mixture of ethanol and acetic acid. Care was required on addition of the iron (pindust) as attraction to the magnetic stirrer often caused the reaction not to proceed as anticipated. Vigorous stirring by a large stirrer bar was required to maintain the stirring motion during reflux. Although the reaction was very efficient, the reaction was very messy producing a dark brown residue. Hot filtration was required to remove unused iron and insoluble by-products. Generally the product was isolated pure and did not require further purification.



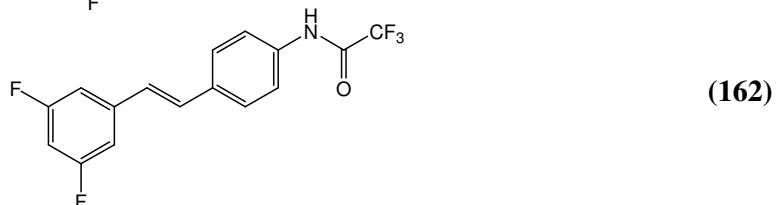
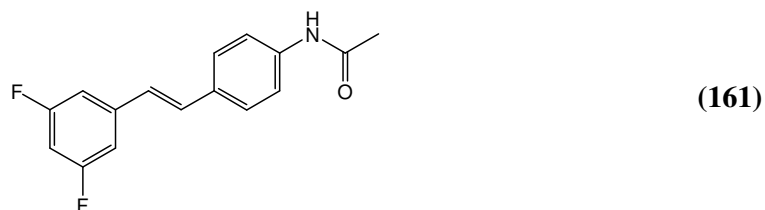
<i>Compound</i>	<i>Isomer</i>	<i>R</i>	<i>R'</i>	<i>% Yield</i>
<b>158</b>	<i>trans</i>	H	H	80
<b>159</b>	<i>cis</i>	H	H	88
<b>160</b>	<i>trans</i>	CH <sub>3</sub>	CH <sub>3</sub>	32
<b>161</b>	<i>trans</i>	H	COCH <sub>3</sub>	70
<b>162</b>	<i>trans</i>	H	COCF <sub>3</sub>	62
<b>163</b>	<i>cis</i>	H	CON(CH <sub>3</sub> ) <sub>2</sub>	20
<b>164</b>	<i>cis</i>	H	CON(CH <sub>2</sub> CH <sub>2</sub> ) <sub>2</sub> O	29

Table 7.3: 4'-Amino derivatives **158-164**

A stilbene containing a tertiary amine was prepared via the classical Wittig reaction. Reaction of a difluorinated phosphonium ylide with 4-(dimethylamino)benzaldehyde in the presence of sodium hydroxide yielded a mixture of isomers. However, the *cis*-isomer was found to be in excess, in a ratio of 3:1. Separation of isomers was achieved by fractional crystallisation as described for the nitro stilbenes. The *trans*-isomer, (*E*)-3,5-difluoro-4'-(dimethylamino)stilbene **160** was separated in an overall reaction yield of approximately 16%.

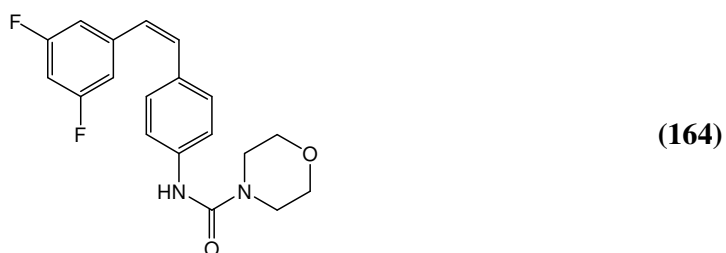
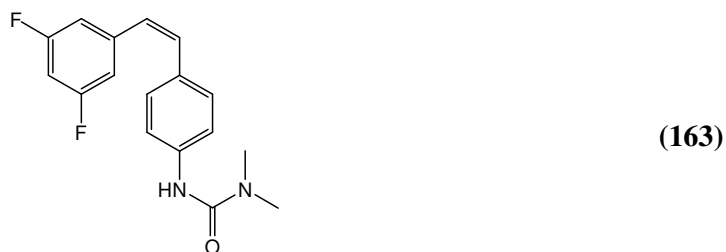


Resveratrol analogues containing a secondary amide at the 4' position were synthesised. Starting with the *trans*-aminostilbene derivative **158**, two acetyl analogues were prepared. By reacting the free amino group with excess acetic anhydride in the presence of a catalytic amount of pyridine (1 drop), the aminoacetyl derivative **161** was prepared in a yield of 70%. (*E*)-3,5-Difluoro-4'-trifluoroacetylaminostilbene **162** was prepared using trifluoroacetic anhydride. Recrystallisation from ethyl acetate of the crude reaction mixture gave the desired product **162** in a yield of 62%.

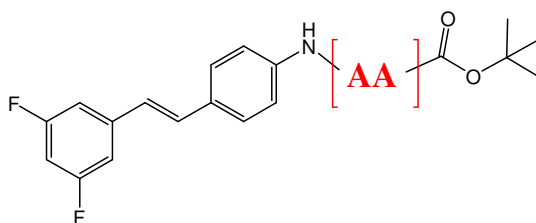


Two *cis* derivatives **163** and **164**, were synthesised containing a carbamyl moiety (-C(O)NH-). The *cis*-stilbenes **163** and **164** were prepared by reacting carbamyl chloride with (*Z*)-3,5-difluoro-4'-aminostilbene **159** in the presence of a molar equivalent of triethylamine. (*Z*)-3,5-difluoro-4'-amino(dimethylcarbamyl) stilbene **163** was isolated as a white powder in low yield (~19 %) by column chromatography.

(*Z*)-3,5-difluoro-4'-(carbamyl-4-morpholine) stilbene **164** was also synthesised in a similar fashion employing 4-morpholinecarbonyl chloride. This was purified by column chromatography furnishing a white solid with yield of 29 %.



Four BOC-protected amino acid derivatives were synthesised to investigate a possible prodrug delivery system, as displayed in **Table 7.3**. These analogues were synthesised using (*E*)-3,5-difluoro-4'-aminostilbene **158** as starting material. Using the standard EDC coupling reaction, the BOC-protected amino acid was coupled to the free amine with *N*-(3-dimethylaminopropyl)-*N'*-ethylcarbodiimide hydrochloride (EDC) **113** as activation agent. Chiral integrity is preserved in this reaction by the use of 1-hydroxybenzotriazole (HOBt) **95**.

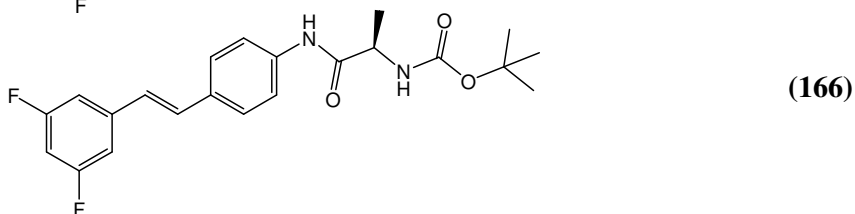
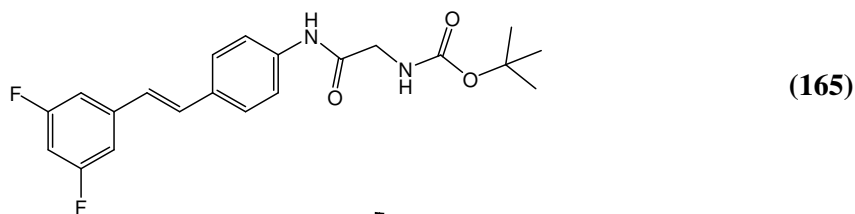


<i>Compound</i>	<i>Isomer</i>	<i>Amino Acid</i>	<i>% Yield</i>
<b>165</b>	<i>trans</i>	glycine	17
<b>166</b>	<i>trans</i>	L-alanine	18
<b>167</b>	<i>trans</i>	β-alanine	12
<b>168</b>	<i>trans</i>	L-valine	11

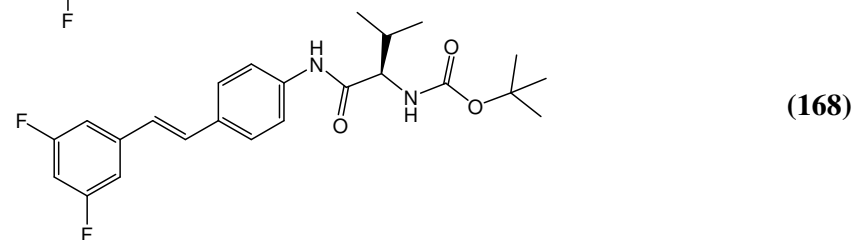
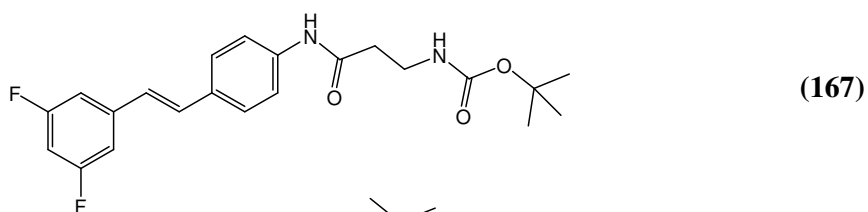
**Table 7.4:** BOC-protected amino acid derivatives of (*E*)-3,5-difluoro-4'-aminostilbene

158

(*E*)-3,5-difluoro-4'-*N*-(*tert*-butoxycarbonyl-glycine)aminostilbene **165** was synthesised using the protected amino acid, BOC-glycine. (*E*)-3,5-difluoro-4'-*N*-(*tert*-butoxycarbonyl-L-alanine)aminostilbene **166** was synthesised from EDC coupling with *N*-BOC-protected L-alanine. Filtration from ethyl acetate yielded the desired stilbene **166** (yield 4 %) a white solid. A further yield of 14 % of the L-alanine analogue **166** was purified by column chromatography using hexane/ethyl acetate as eluant.

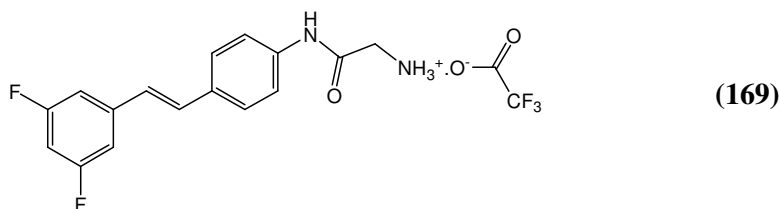


Compounds **167** and **168** were again synthesised via the EDC activated peptide coupling from the *trans*-aminostilbene **158**. The substituted stilbene **167** was prepared using BOC- $\beta$ -alanine while BOC-L-valine was used to prepare product **168**.



Deprotection of an amino acid derivative was attempted using the glycine analogue **165**. (*E*)-3,5-difluoro-4'-*N*-(*tert*-butoxycarbonyl-glycine)aminostilbene **165** was stirred in a 50 % solution of trifluoroacetic acid in dichloromethane, resulting in

complete deprotection. Care was taken due to previous experience from *Section A*, when TFA deprotection destroyed the peptide by not only cleaving protection group but also extracting the  $\alpha$ -proton from the chiral centre. The crude product isolated on evaporation of solvent and excess TFA was found to be highly hydrophilic. From the NMR spectra taken of the crude reaction product, it is clear that a salt was formed, namely (*E*)-3,5-difluoro-4'-aminoglycine stilbene trifluoroacetate salt **169**, and complete removal of the butoxycarbonyl group was achieved.



#### 7.2.2.1 IR study of (*E/Z*)-3,5-difluoro-4'-aminostilbene

The infrared spectrum of (*E*)-3,5-difluoro-4'-aminostilbene **158** confirmed the reduction of the nitro group to the amine. The  $\text{NO}_2$  stretching frequencies, both asymmetric ( $1509\text{ cm}^{-1}$ ) and symmetric ( $1336\text{ cm}^{-1}$ ) present in the IR spectrum of stilbene **156**, have disappeared in the IR spectrum of **158**. Asymmetrical and symmetrical stretching of a primary amine generally occurs between  $3500$  and  $3300\text{ cm}^{-1}$ , with the former having the higher wavenumber.

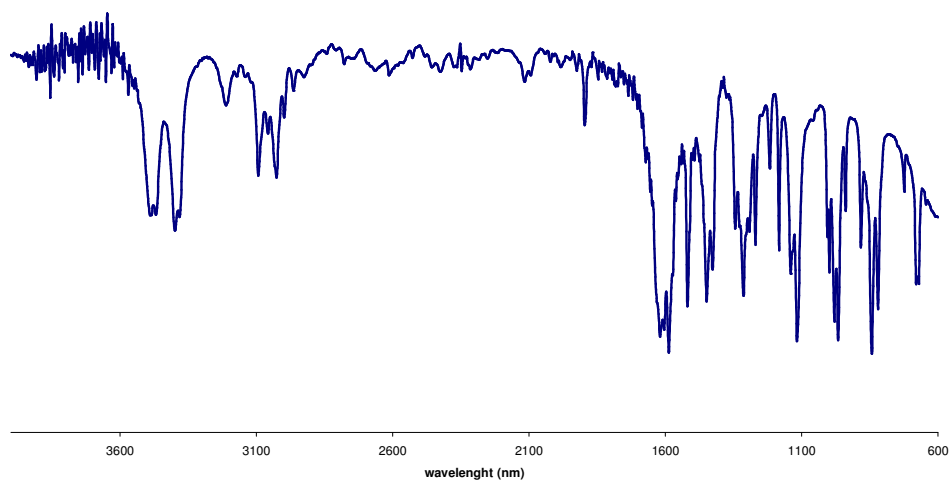


**Figure 7.11:** Infrared spectrum of (*E*)-3,5-difluoro-4'-aminostilbene **158**

In the spectrum of **158**, two main stretches are evident at 3483 and 3396  $\text{cm}^{-1}$ , representing these stretchings. A shoulder band usually appears on the lower wavenumber side in primary and secondary amines arising from the overtone of the N-H bending band. This can be seen in the spectrum at 3206  $\text{cm}^{-1}$ . The N-H bending vibration of primary amines is observed in the region 1650-1580  $\text{cm}^{-1}$ . This bending vibration may be one of two peaks observed at 1617 and 1586  $\text{cm}^{-1}$ . Another band attributed to amines is observed in the region 910-665  $\text{cm}^{-1}$ . This strong, broad band is due to N-H wag and can be seen in the infrared spectrum of the *trans*-amino stilbene **158** at 839  $\text{cm}^{-1}$ . All appropriate amine stretching, bending and wagging frequencies can also be seen for the *cis*-isomer **159**. The two stretches appear at 3461 and 3372  $\text{cm}^{-1}$ , with the overtone shoulder band appearing at 3214  $\text{cm}^{-1}$ . The bending vibration is observed at 1616 or 1583  $\text{cm}^{-1}$  while the amine wagging is prominent at 830  $\text{cm}^{-1}$ .

#### 7.2.2.2 NMR study of 4'-amino analogues

The proton NMR of (*E*)-3,5-difluoro-4'-aminostilbene **158** shows large differences in chemical shifts compared to the starting material **156**. The hydrogens adjacent to the nitro group, at *meta*-positions 3' and 5' have moved from  $\delta$  8.27 in the nitro compound to  $\delta$  6.57 in the amino compound **158**. The doublet corresponding to the *ortho*-protons at positions 2' and 6' have a chemical shift of  $\sim \delta$  7.3 compared to  $\delta$  7.86 for the nitro stilbene **156**. The protons of the fluorinated ring have also shifted upfield following the reduction of the nitro group. The multiplet from the 2,6-H appear as part of a larger multiplet ( $\sim \delta$  7.25) integrating for 5 protons, containing the 2'6'-H, the 2,6-H and a vinylic proton. The *para*-proton, located between the fluorine atoms is present as a triplet of triplets and shifted upfield to  $\delta$  7.17. The proton nearest the fluorinated ring has only moved upfield slightly, to approximately  $\delta$  7.2, and is one of the protons included in the multiplet in the region  $\delta$  7.20-7.30. However, it's the other hydrogen of the double bond that shows the greatest difference. On reduction of the nitro group to an amine group, the proton signal has migrated upfield from  $\sim \delta$  7.6 (**156**) to a chemical shift of  $\delta$  6.89 for the *trans*-difluoroamino derivative **158**. The coupling constants for these vinylic doublets are 16.4 Hz. The amino group appears as a singlet, integrating for 2 hydrogens at  $\delta$  5.45.



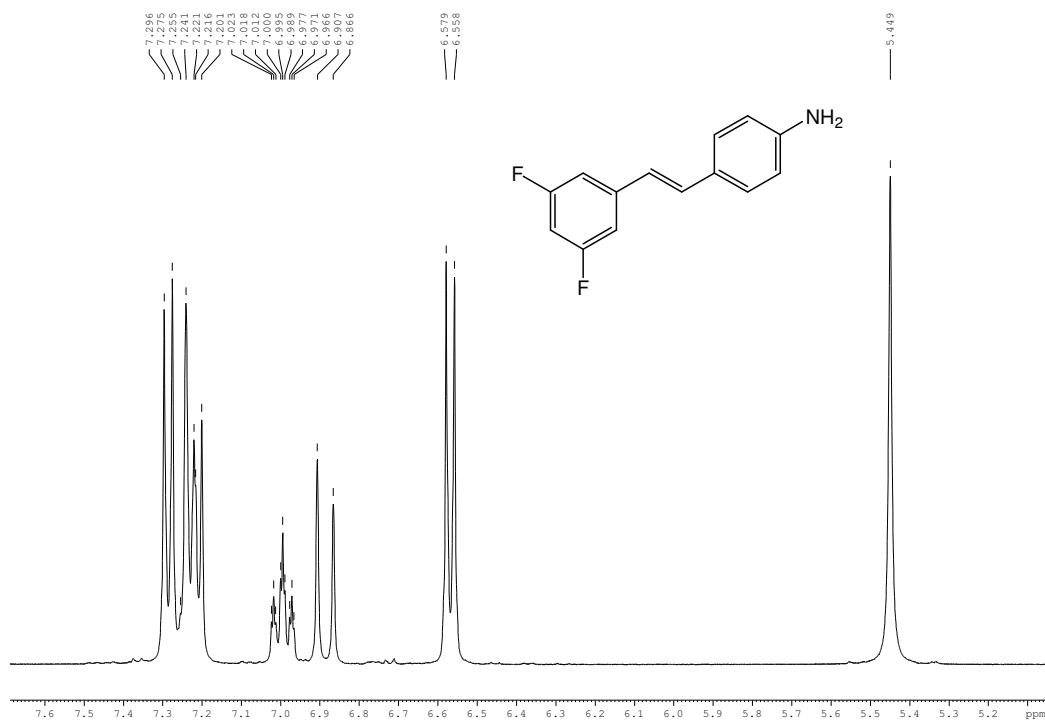


**Figure 7.12:** <sup>1</sup>H NMR spectrum of (*E*)-3,5-difluoro-4'-aminostilbene **158**

The triplet of triplets at  $\delta$  7.05 in the <sup>1</sup>H NMR of the *cis*-isomer **159** is due to the *para*-hydrogen. A doublet at  $\delta$  6.93, which integrates for 4 is due to the aromatic protons positioned at 2 and 6 on fluorinated ring, and 2' and 6' on the amino-substituted phenyl ring. The final 2 aromatic protons occur at  $\delta$  6.46 and are the 3' and 5' hydrogens. The doublets of the vinylic protons have a chemical shift of  $\delta$  6.65 and  $\delta$  6.29, and have a *J* value of 12.4 Hz. The amino group appears as a broad singlet at  $\delta$  5.34.

The aromatic protons of the amino-substituted phenyl ring appear as doublets at  $\delta$  7.43 and  $\delta$  6.72 with *J* values of 8.8 Hz, in the <sup>1</sup>H NMR spectrum of the dimethyl amino compound **160**. Although the vinylic protons signals appear at the same approximate chemical shifts of the protons of the fluorinated phenyl ring, their intensity is strong enough, compared to the aromatic protons, to estimate the coupling constants. One vinylic proton appears with the 2,6-hydrogens in the region of  $\delta$  7.24-7.31. The other vinylic proton appears as a multiplet with the triplet of triplets from the *para*-proton, in the region of  $\delta$  6.93-7.03. The coupling constants for this *trans*-isomer can be calculated as 16.4 Hz. The two methyl groups of the tertiary amine appear at  $\delta$  2.94.

For (*E*)-3,5-difluoro-4'-aminoacetyl stilbene **161**, the amide singlet is present at  $\delta$  10.07 in the  $^1\text{H}$  NMR spectrum. The aromatic protons of the amide ring appear close together with chemical shifts of  $\delta$  7.62 and  $\delta$  7.53, and with coupling constants of 8.8 and 8.4 Hz, respectively. The vinylic protons appear in the same region as the fluorinated ring aromatic protons. A multiplet resulting from a vinylic proton and the protons in positions 2 and 6 is present at  $\delta$  7.30-7.38. The other vinylic proton occurs with the *para*-aromatic proton in the range  $\delta$  7.06-7.16. The three protons of the acetyl group have a chemical shift of  $\delta$  2.06.

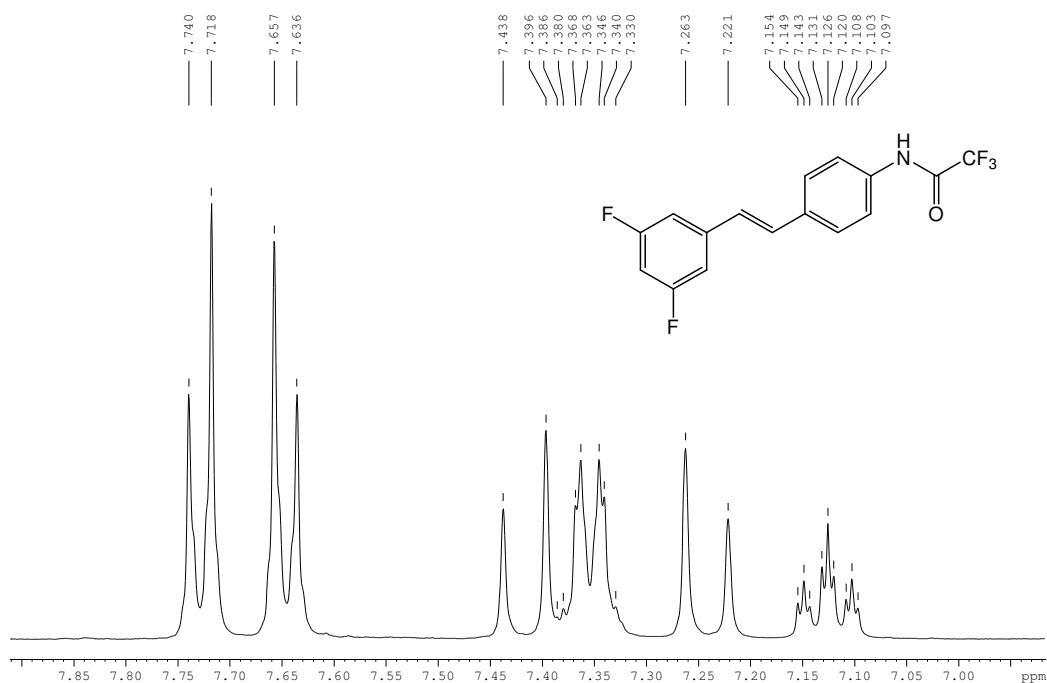


**Figure 7.13:**  $^1\text{H}$  NMR spectrum of (*E*)-3,5-difluoro-4'-(trifluoroacetyl)aminostilbene **162**

The secondary amide singlet is present at  $\delta$  11.38 in the  $^1\text{H}$  NMR spectrum of the trifluoroacetyl derivative **162**, while the aromatic protons of the amide-substituted phenyl ring have chemical shifts of  $\delta$  7.73 and  $\delta$  7.66 with coupling constants of 8.8 and 8.4 Hz. The doublets of the vinylic double bond occur at  $\delta$  7.42 and  $\delta$  7.24 and both have coupling constants of 16.8 Hz. The doublet of the 2,6-protons has a chemical shift of 7.35 while the *para*-proton appears at  $\delta$  7.13. The addition of further fluorine atoms to the molecule increases the occurrence of splitting with the trifluoroacetyl moiety showing a very distinctive pattern in the  $^{13}\text{C}$  NMR. The splitting of carbons due to the 3,5-difluorine substitution is consistent with that

described compounds **156-161**, with splitting of the carbons directly attached to the fluorine into a doublet with coupling constants of 243.7 and 243.6 Hz. These doublets both appear at approximately  $\delta$  162. The triplet of carbon at position 1 has a chemical shift of  $\delta$  141.13 and a  $J$  value of 9.8 Hz. The *ortho*-carbons are present as a doublet at  $\delta$  109.17 while the triplet of the *para*-carbon appears at a chemical shift of 102.56, with coupling constants of 25.4 and 26.0 Hz, respectively.

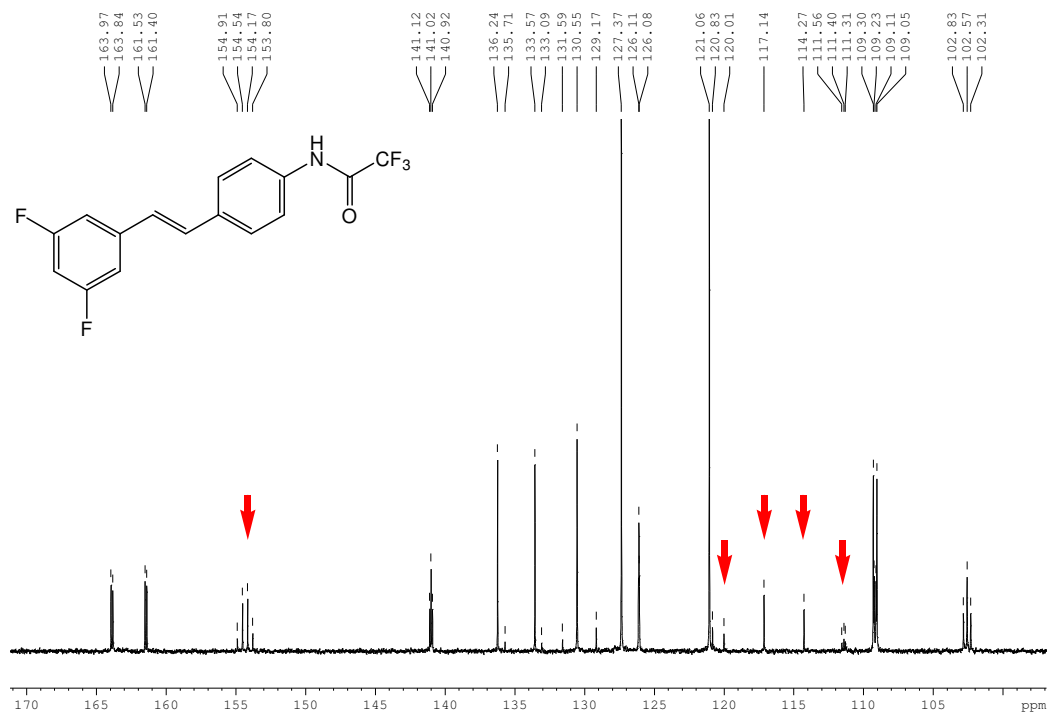


**Figure 7.14:**  $^{13}\text{C}$  NMR spectrum of (E)-3,5-difluoro-4'-(trifluoroacetyl)aminostilbene **162**

**Figure 7.14** shows the  $^{13}\text{C}$  NMR of stilbene **162**, with the carbon signals of the trifluoroacetyl group identified by the red arrows. The carbonyl carbon has a chemical shift of  $\delta$  154.4 and is split by carbon-fluorine coupling with the adjacent trifluoromethyl group. It is split into a quartet with a coupling constant of 36.8 Hz. The trifluoromethyl group itself is also split into a quartet spread over a range of 10 ppm. This quartet appears in the region of  $\delta$  111.4-120.0. Due to the fact that this carbon has three fluorines directly attached, the coupling constant is large, calculated to be as 266.9 Hz. In the  $^{19}\text{F}$  NMR both peaks are present with the singlet at  $\delta$  -73.83, integrating for 3 fluorines, the trifluoromethyl group and the triplet at  $\delta$  -110.14 due to the *meta*-fluorines. This triplet has a coupling constant of 7.5 Hz.

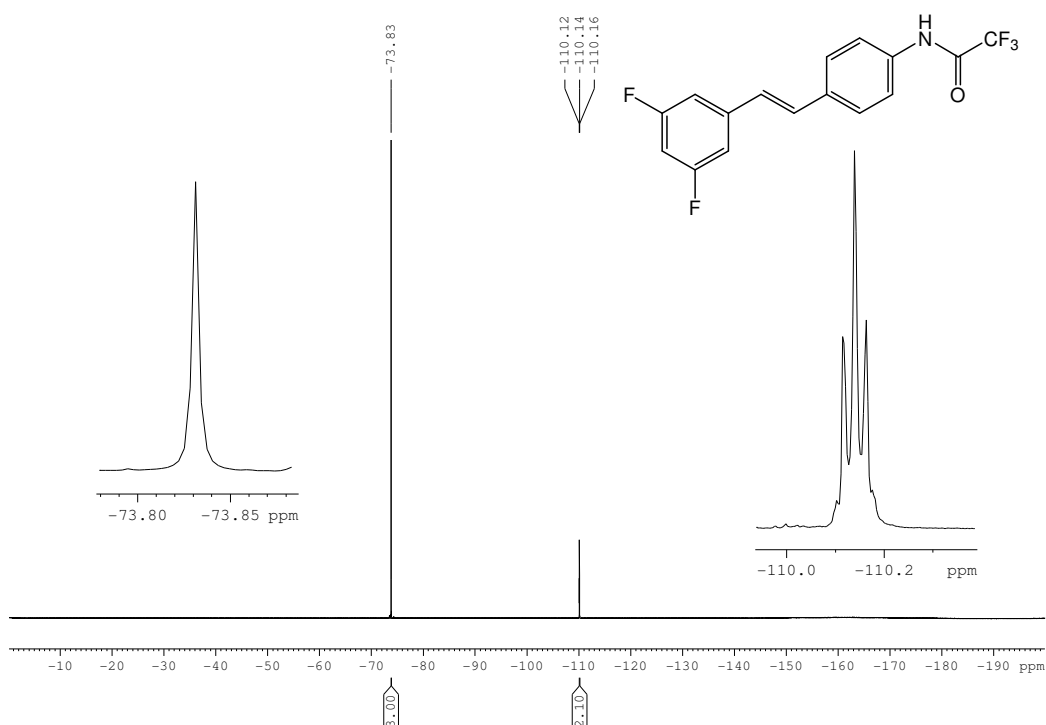


**Figure 7.15:**  $^{19}\text{F}$  NMR spectrum of *(E)*-3,5-difluoro-4'-(trifluoroacetyl)aminostilbene **162**

In the  $^1\text{H}$  NMR spectrum of the *cis*-derivative **163**, the amide proton appears as a singlet at  $\delta$  8.36. The aromatic protons of the *para*-substituted phenyl ring appear as doublets at  $\delta$  7.40 and as part of a multiplet in the range  $\delta$  7.06-7.11. The coupling constant of the doublet at  $\delta$  7.4 is 9.2 Hz. The *ortho*-protons of the fluorinated ring have a chemical shift of  $\delta$  6.9. The two doublets at  $\delta$  6.68 and  $\delta$  6.49 with coupling constants of 12.4 and 12 Hz are due to the vinylic protons. The singlet of the methyl groups on the terminal tertiary amine is present at  $\delta$  2.92.

The amide proton of the *cis*-morpholine analogue **164** appears as a singlet at  $\delta$  8.64. The vinylic protons appear as doublets at  $\delta$  6.69 and  $\delta$  6.50 with  $J$  values of 12.4 Hz. The methylene protons of the morpholine ring appear as two distinct multiplets with chemical shifts of  $\delta$  3.60 and  $\delta$  3.42, with the latter signal, due to the protons adjacent to the nitrogen.

The  $^1\text{H}$  NMR spectra of the amino acid derivatives **165-168** shows all the signals expected of the difluorostilbenes with the extra peaks of the *N*-protected amino acid. In the spectrum of the BOC-glycine analogue **165**, the amide attached to the stilbene

appears with a chemical shift of  $\delta$  10.05 while the glycine amide triplet is part of a multiplet present at approximately  $\delta$  7.10, also in this multiplet is the triplet of triplet due to the *para*-proton of the fluorinated phenyl ring. The aromatic doublets of the *para*-substituted ring have chemical shifts of  $\delta$  7.62 and  $\delta$  7.55 with coupling constants of 8.4 and 8.8 Hz. One of the vinylic doublets makes up part of a multiplet with the *ortho*-protons of the fluorinated ring, occurring at a chemical shift of  $\delta$  7.34. The second doublet of the central double bond protons is found at  $\delta$  7.15 and has a coupling constant of 16.4 Hz. The methylene hydrogens of glycine have a chemical shift of  $\delta$  3.73 and are split into a doublet by the neighbouring amide, with a coupling constant of 6.0 Hz. The singlet at  $\delta$  1.4, integrating for 9 H is due to the *tert*-butyl moiety of the protection group. In the  $^1\text{H}$  NMR spectrum of the glycine analogue **165** (Figure 7.16), a second smaller singlet can be seen at  $\delta$  1.33. This is due to isomerisation of the *trans*-isomer when in solution. When in solution, pure stilbene isomers can isomerise with light. This can be observed in the  $^1\text{H}$  NMR spectra of the glycine analogue. Isomerisation from this *trans* isomer **165** to the *cis* isomer results can be noted by a peak from the BOC group of the *cis* derivative. Integration of this peak is 0.2 compared to the *trans*-peak of 9; therefore the ration of *trans* to *cis* is 45:1.

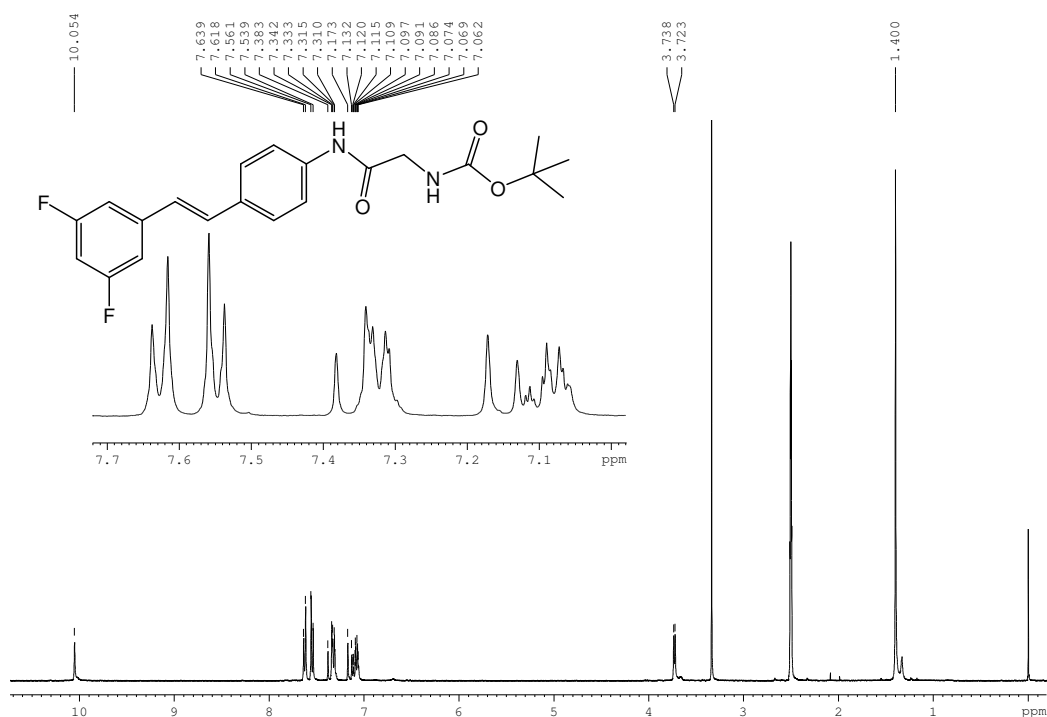


**Figure 7.16:**  $^1\text{H}$  NMR spectrum of (*E*)-3,5-difluoro-4'-(BOC-Gly)aminostilbene **165**

In the  $^1\text{H}$  NMR of (*E*)-3,5-difluoro-4'-(BOC-L-Ala)amino stilbene **166**, the *para*-substituted amide appears as a singlet at  $\delta$  10.08 while the amide of the amino acid appears at the same chemical shift as the triplet of triplets, at  $\delta$  7.1. Adjacent to this multiplet is one of the vinylic doublets, at  $\delta$  7.16 which has a coupling constant of 16.0 Hz. The  $\alpha$ -H at the chiral centre of L-alanine splits into a quintet due to the adjacent amide and methyl group. This signal has a chemical shift of  $\delta$  4.13 and a coupling constant of 7.2 Hz. The *t*-butyl moiety of the protection group appears as a very intense singlet at  $\delta$  1.39, while the methyl group of the alanine is split by the  $\alpha$ -H into a doublet with chemical shift of  $\delta$  1.27 and *J* value of 7.2 Hz.

The  $^1\text{H}$  NMR spectra of the  $\beta$ -alanine and L-valine compounds (**167** and **168**) shows slight differences between the compounds, with the amide attached to the stilbene having a chemical shift of  $\delta$  10.07 for the  $\beta$ -Ala analogue **167** and  $\delta$  10.13 for the L-Val derivative **168**. When compared to the previous two amino acid derivatives (**165** and **166**), the amide of  $\beta$ -alanine and L-valine can be seen at independent chemical shifts, to that of the rest of the molecule. The *N*-terminal hydrogen of  $\beta$ -alanine is split into a triplet in the  $^1\text{H}$  spectrum at  $\delta$  6.90 with a coupling constant of 5.6 Hz, due to H-H coupling with the protons in the  $\alpha$ -position of the amino acid. This  $\alpha$ -methylene has a chemical shift of  $\delta$  2.49 but the triplet is partially masked by the signal of the deuterated NMR solvent dimethylsulphoxide (DMSO-*d*<sub>6</sub>) at  $\delta$  2.51. The  $\beta$ -methylene of compound **167** is present as a quartet, due to splitting by the  $\alpha$ -CH<sub>2</sub> and the *N*-terminal amide and appears at  $\delta$  3.22 with a *J* value of 6.4 Hz. The singlet of the *t*-butyl group has a chemical shift of  $\delta$  1.38. For the L-valine derivative **168**, the amino acid amide couples with the proton of the  $\alpha$ -carbon at the chiral centre and is therefore split into a doublet. It has a chemical shift of  $\delta$  6.94 and a coupling constant of 8.8 Hz. The  $\alpha$ -proton of this compound **168** can be found at  $\delta$  3.92 as a triplet, with a coupling constant of 7.8 Hz. The proton next to the  $\alpha$ -hydrogen, at the centre of the isopropyl side chain is split into a multiplet with a chemical shift of  $\delta$  1.99 while the two equivalent methyl groups of the isopropyl side chain are split into a doublet by it, and can be seen at  $\delta$  0.90 and with a coupling constant of 6.4 Hz. The vinylic coupling constants for (*E*)-3,5-difluoro-4'-*N*-(*tert*-butoxycarbonyl- $\beta$ -alanine)aminostilbene **167** and (*E*)-3,5-difluoro-4'-*N*-(*tert*-butoxycarbonyl-L-valine)aminostilbene **168** are 16.0 and 16.4 Hz, respectively.

The deprotected glycine stilbene **169** shows some subtle changes to the chemical shifts of the main stilbene components compared to the protected stilbene **165**, but as expected there are more significant changes to the chemical shifts of the glycine signals. The amide attached to the stilbene has a chemical shift of  $\delta$  10.70 while the methylene protons of glycine appear at  $\delta$  3.84. However this signal is no longer a doublet as in **165**, but now exists as a singlet. This is somehow due to the fact that the protons that previously coupled to it are now part of a charged amino species and not the neutral primary amine. Following on from this, the glycine amide triplet that appeared at  $\delta$  7.10 for product **165** can now be found as a broad singlet, characteristic of a charged amine, at  $\delta$  8.25. Further evidence of a charged amine is that this singlet integrates for 3 protons. Proof of the trifluoroacetate salt can be seen in the  $^{19}\text{F}$  NMR with 2 signals present, an intense singlet at  $\delta$  -73.61 and the known triplet of the *meta*-substituted fluorines, occurring at  $\delta$  -110.20. The carbons of trifluoroacetic acid appear as a similar pattern to that described for the trifluoroacetyl derivative **162**, with the carbonyl carbon split into a quartet at  $\delta$  158.26 ( $J = 52.1$  Hz). However the carbon of the trifluoromethyl group is split into a doublet in the range  $\delta$  115-118 with a coupling constant of 298.0 Hz. This is perhaps due to the equivalency of the fluorines and is split by the  $^{13}\text{C}$ - $^{19}\text{F}$ .

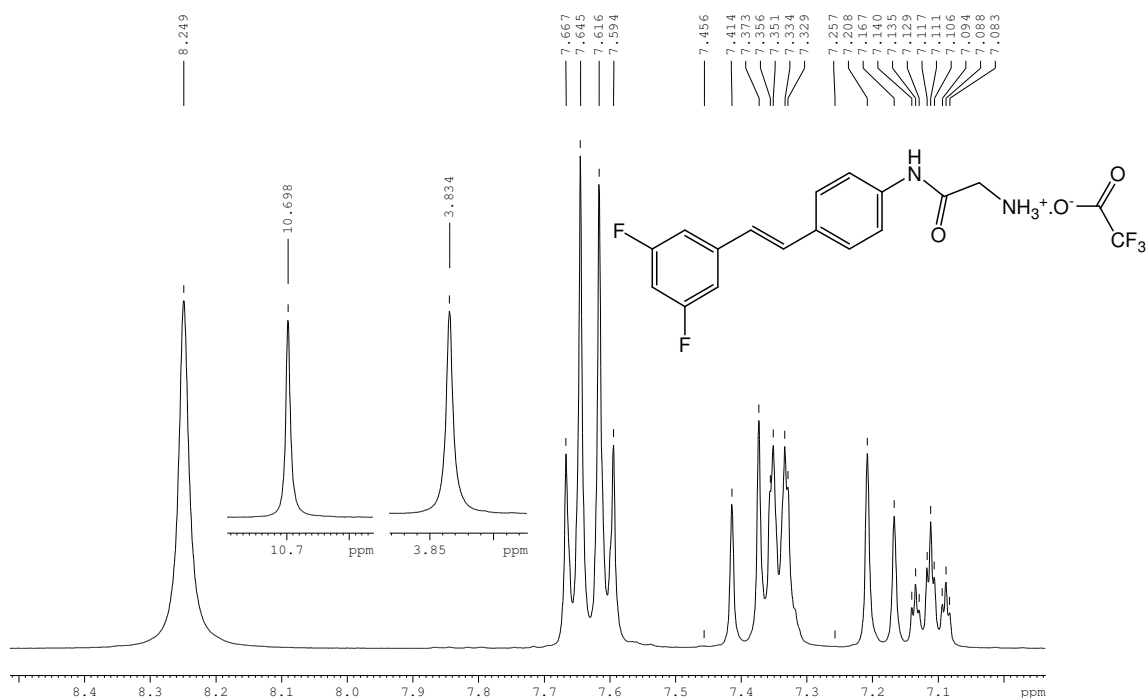
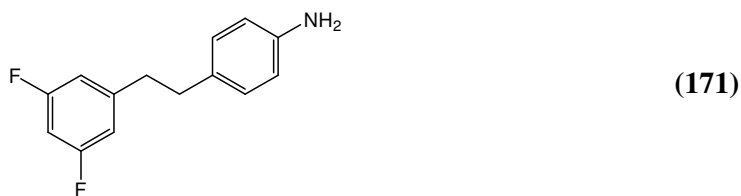
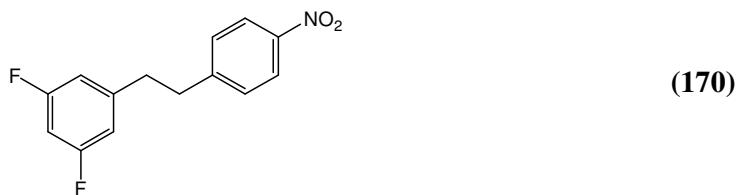


**Figure 7.17:**  $^1\text{H}$  NMR spectrum of (*E*)-3,5-difluoro-4'-aminoglycine stilbene trifluoroacetate salt **169**

### 7.2.3 Basic resveratrol structure investigation

The importance of the substitution pattern of resveratrol was investigated. Research previously carried out in this laboratory, showed that the activity of resveratrol remained after the hydroxyl groups were replaced with fluorine atoms<sup>7</sup>. The importance of the central double bond of the stilbene structure and the significance of the 3,5-aromatic substitution pattern was investigated by synthesising analogues **170-173**. The bioactivity was determined using lung cell carcinoma assays. These derivatives were prepared without some of the basic components of the resveratrol backbone, while maintaining the 4'-nitro group and its corresponding amino moiety. As a by-product of one of the reduction reactions, the central vinyl double bond was reduced. This was synthesised using palladium (II) acetate, aqueous potassium fluoride and poly(methylhydrosiloxane). By varying the molar equivalents, both the reduced nitro and amino compounds were isolated. 1-(3,5-Difluorophenylethyl)-4'-nitrobenzene **170** was isolated as a beige powder.



In the proton NMR of this reduced nitro compound, the aromatic protons of the nitro-substituted ring appear at  $\delta$  8.02 and  $\delta$  7.39, with the *meta*-hydrogens the further downfield. The three aromatic protons of the fluorinated ring occur as a multiplet in the region of  $\delta$  6.85-6.92. The methylene protons appear as symmetrical multiplets at  $\delta$  2.91 and  $\delta$  2.83. Confirmation of these as methylenes is clear from the DEPT 135 NMR, with negative signals at  $\delta$  35.76 and  $\delta$  35.61.



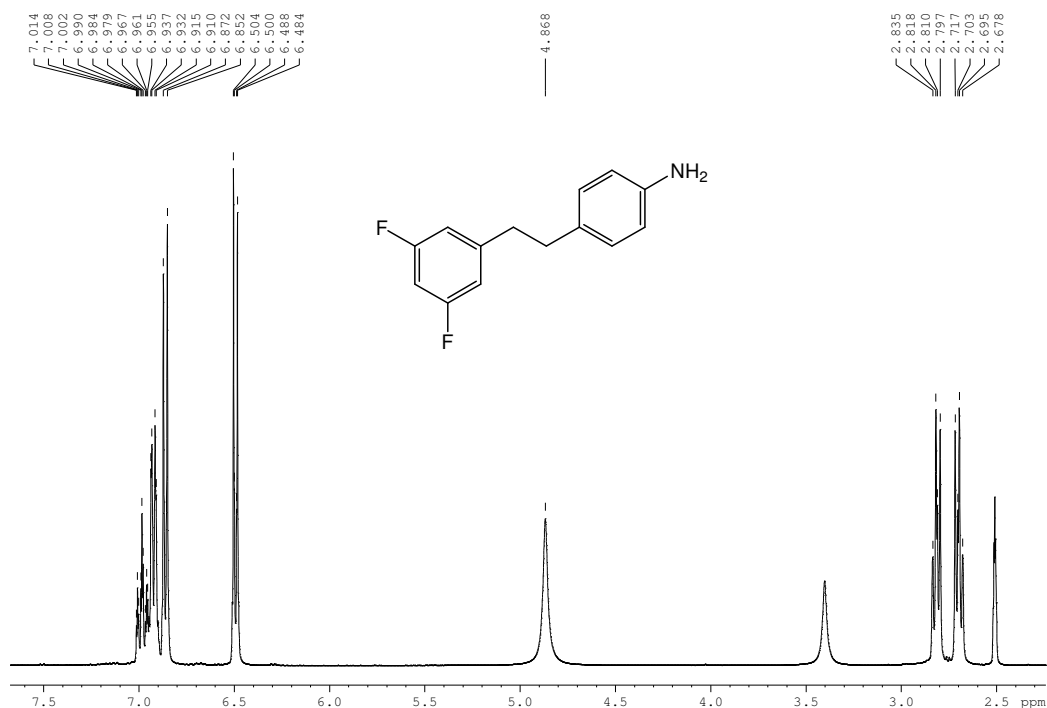
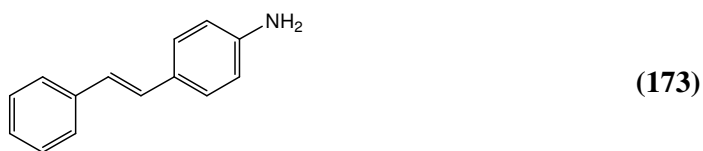
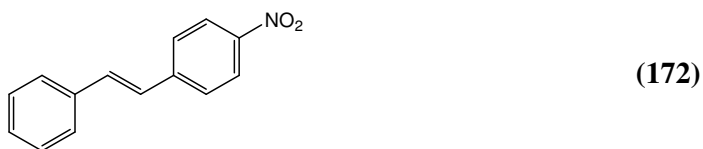


**Figure 7.18:** <sup>1</sup>H NMR spectrum of 1-(3,5-difluorophenylethyl)-4'-aminobenzene **171**

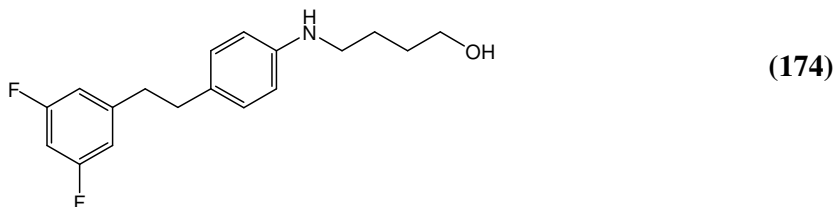
The amino derivative **171** was isolated as a dark brown liquid with a boiling point of approximately 194°C. The triplet of triplets from the hydrogen at position 4 and the 2, 6 protons of 1-(3,5-difluorophenylethyl)-4'-aminobenzene **171** are present at  $\delta$  6.98 and  $\delta$  6.92 respectively, in the <sup>1</sup>H NMR spectrum. Due to the reduction of the nitro group to the amine, the protons of the *para*-substituted ring have moved upfield with the doublet of the *ortho* protons at  $\delta$  6.86, while the *meta* protons appear at  $\delta$  6.49. The broad amine signal appears at  $\delta$  4.87. As in the <sup>1</sup>H NMR spectrum of the nitro compound **170**, two multiplets are seen as a result of the methylene units at  $\delta$  2.81 and  $\delta$  2.70. The <sup>1</sup>H NMR of the amino-diphenylethyl analogue is shown in **Figure 7.18**. The methylene group carbon atoms of the amino analogue **171** are present at  $\delta$  37.02 and  $\delta$  35.01.



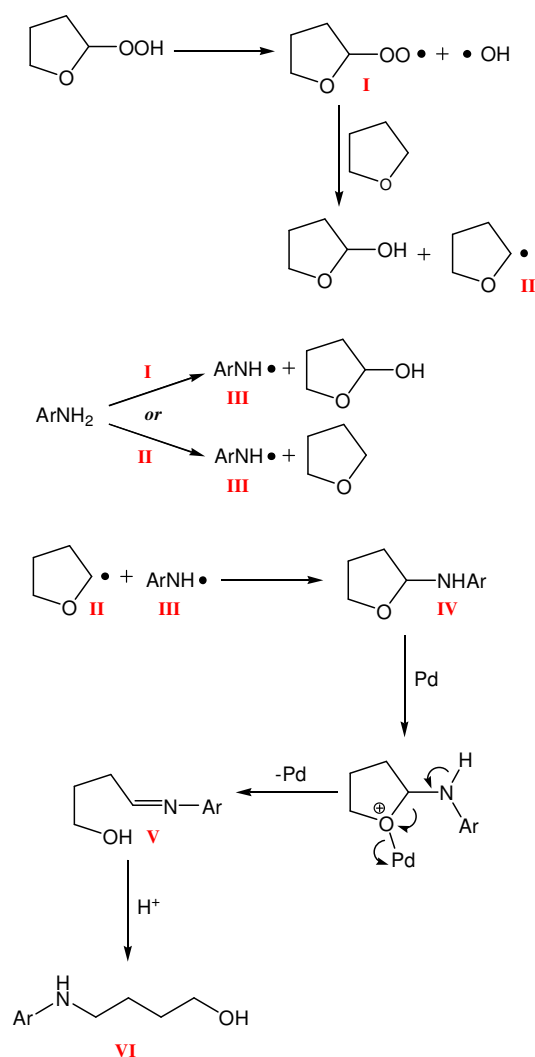
The importance of the 3,5-substitution pattern was assessed by the preparation of nitrostilbene **172** (commercially available, *Sigma Aldrich*) via the Wittig reaction. In an attempt to increase the yield of *trans*-isomer over the *cis*, the normal procedure using sodium hydroxide was not used; instead a procedure described by Miljanić *et al* was used<sup>8</sup>. This procedure uses a weaker base, potassium carbonate in conjunction with a few crystals of dibenzo-18-crown-6. After work-up, a crude <sup>1</sup>H NMR showed a mixture of isomers in the ratio of 1.6:1 (*trans*:*cis*). Separation of the isomers was achieved by fractional recrystallisation from ethanol. The pure *trans*-isomer was isolated as yellow needle-shaped crystals in a yield of 59%. These crystals were identified as the *trans*-isomer **172** by <sup>1</sup>H NMR, with vinylic coupling constants of 16.4 Hz. This *trans*-nitrostilbene **172** was then reduced using the iron and iron (III) chloride procedure, yielding 4-aminostilbene **173**. The vinylic doublets ( $\delta$  7.07 and  $\delta$  6.90) for the amino derivative had *J* values of 16.4 Hz. The primary amine formed appeared as a singlet at  $\delta$  5.32.

#### 7.2.4 Synthesis of 4-aminobutan-1-ol derivative

In an attempt to reduce the nitro group of the stilbene **156**, it has been shown that the procedure using the siloxane (PMHS) and aqueous potassium fluoride produced the completely reduced diphenylethyl compound **171**. However, on a few occasions when the reaction was allowed proceed for 4 hours, an interesting byproduct was formed. On work up of the reaction, TLC analysis showed the formation of two products. Column chromatography was used to separate the two products with the less polar product being confirmed as the diphenylethyl compound **171**. The second product was isolated for analysis. NMR data showed that this second product was the *n*-butan-1-ol derivative of the diphenylethyl compound. This product has been fully characterised and shown to be 4-(4-(3,5-difluorophenylethyl)phenylamino)butan-1-ol **174**.



Reports of the synthesis of n-substituted 4-amino-1-butanols by various two- and three-step reaction methods have been published over the years<sup>10,11</sup>. Recently a one-step method hydrogenation reaction using palladium on carbon (1 atm) has been published<sup>12</sup>. The procedure using PMHS outlined in this thesis requires approximately 4 hours compared to 24-36 hours for the hydrogenation reaction reported by Russell *et al*. Although the ring opening of tetrahydrofuran by amines has been reported over the years, it normally involves the complexing of the THF with cationic metal compounds such as uranium amide compounds<sup>13</sup> and zirconium complexes<sup>14</sup>.



**Scheme 7.3:** Proposed mechanism for the palladium-mediated tetrahydrofuran ring opening<sup>12</sup>.

However in the recent publication by Russell *et al*, a free-radical-based mechanism is proposed, as shown in **Scheme 7.3**. This mechanism is based the use of unstabilised

THF, allowing for a potential build up of THF hydroperoxide. The cleavage of the hydrogen-oxygen bond of the hydroperoxide results in the formation of a peroxide free radical **I**, which can then abstract a hydrogen from the 2-position of THF forming radical **II**. Either radical (**I** or **II**) can then remove a hydrogen from the amine to form the aminyl radical **III** which is the resonance stabilized. This in turn could couple to radical **II** to form the intermediate 2-amino-THF **IV**. Complexing of the palladium to the intermediate **IV** may occur at this point which in turn forces ring opening to form the imine **V** with loss of the palladium, Reduction of the imine double bond can then take place to yield the final amino-butanol product **VI**. The reaction mechanism is plausible for the reaction being described in the synthesis of the 4-amino-butan-1-ol compound **174**. The THF used in this reaction was of anhydrous grade and free of inhibitor/stabilizer. It was also a relatively old bottle of solvent (~1 year old), which makes the likelihood of hydroperoxide formation a real possibility. A test for peroxide was carried out on the THF solvent used in these reactions, using Quantofix<sup>®</sup> peroxide test sticks (Sigma Aldrich). The result of this starch/iodide test proved positive for the present of peroxides in the solvent.

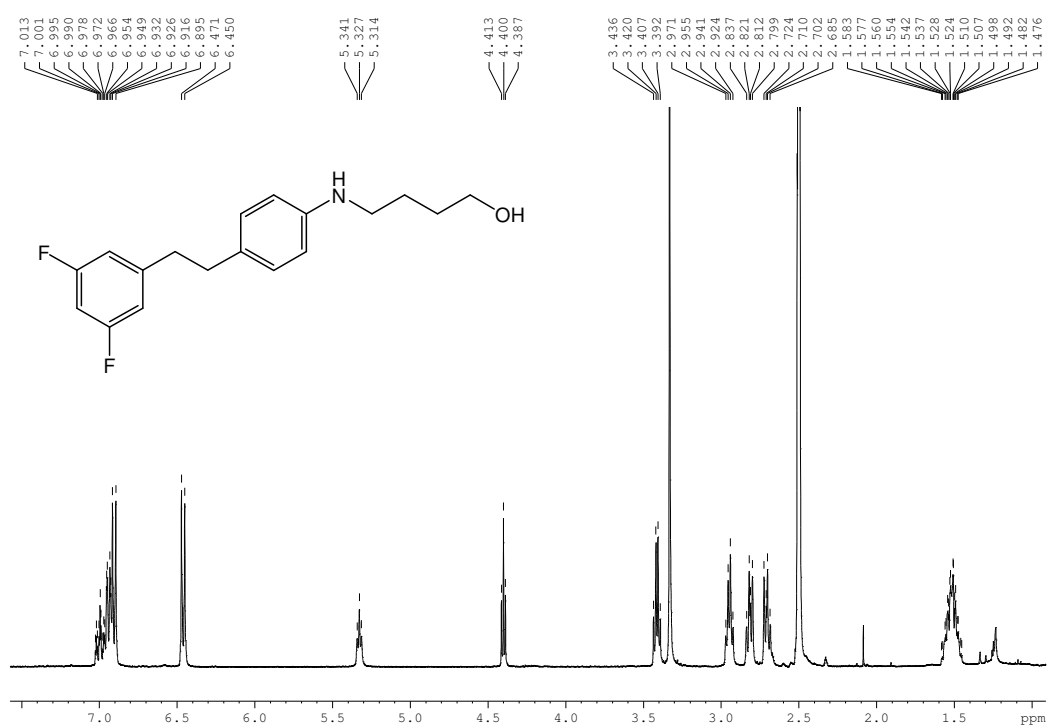


**Figure 7.19:** <sup>1</sup>H NMR spectrum of 4-(4-(3,5-difluorophenylethyl)phenylamino)butan-1-ol **174**.

The  $^1\text{H}$  NMR of the 4-amino-1-butanol compound **174** maintains all the fluorine coupling characteristics discussed for the 4'-amino compounds. The aromatic protons of the fluorinated ring can be seen as a multiplet, which also contain the doublet from the protons in the 3' and 5' positions of the second phenyl ring. The remaining aromatic protons have a chemical shift of  $\delta$  6.46 and this doublet has a coupling constant of 8.4 Hz. In a similar pattern to that reported for compound **171**, the central double bond, now reduced to two methylene groups appears as two multiplets. They have chemical shifts in the ranges  $\delta$  2.80-2.84 and  $\delta$  2.69-2.72. The protons of the amino-butanol side chain are present in the spectrum from approximately  $\delta$  1.4-5.5. The most downfield signal of these is from the amide proton, which is split into a triplet by the adjacent methylene, it has a chemical shift of  $\delta$  5.33 and a coupling constant of 5.4 Hz. The hydroxyl proton is also split into a triplet by an adjacent methylene and can be seen at  $\delta$  4.40. This signal has a coupling constant of 5.2 Hz. Of the butanol methylene groups, the  $\text{CH}_2$  in the 1 position (**b**) beside the hydroxyl is the most downfield. This quartet has a coupling constant of  $\delta$  3.42 and a coupling constant of 6.2 Hz. At a chemical shift of  $\delta$  2.95, the  $\text{CH}_2$  (**e**) beside the amine is split into a quartet with a coupling constant of 6.6 Hz. The remaining protons of the butanol side chain, at C-2 (**c**) and C-3 (**d**), form a multiplet in the region  $\delta$  1.45-1.58. The 2D COSY NMR spectrum is shown in *Figure 7.20*. A labelling system will be employed for the 4'-amino-butan-1-ol, giving a letter to each proton signal.

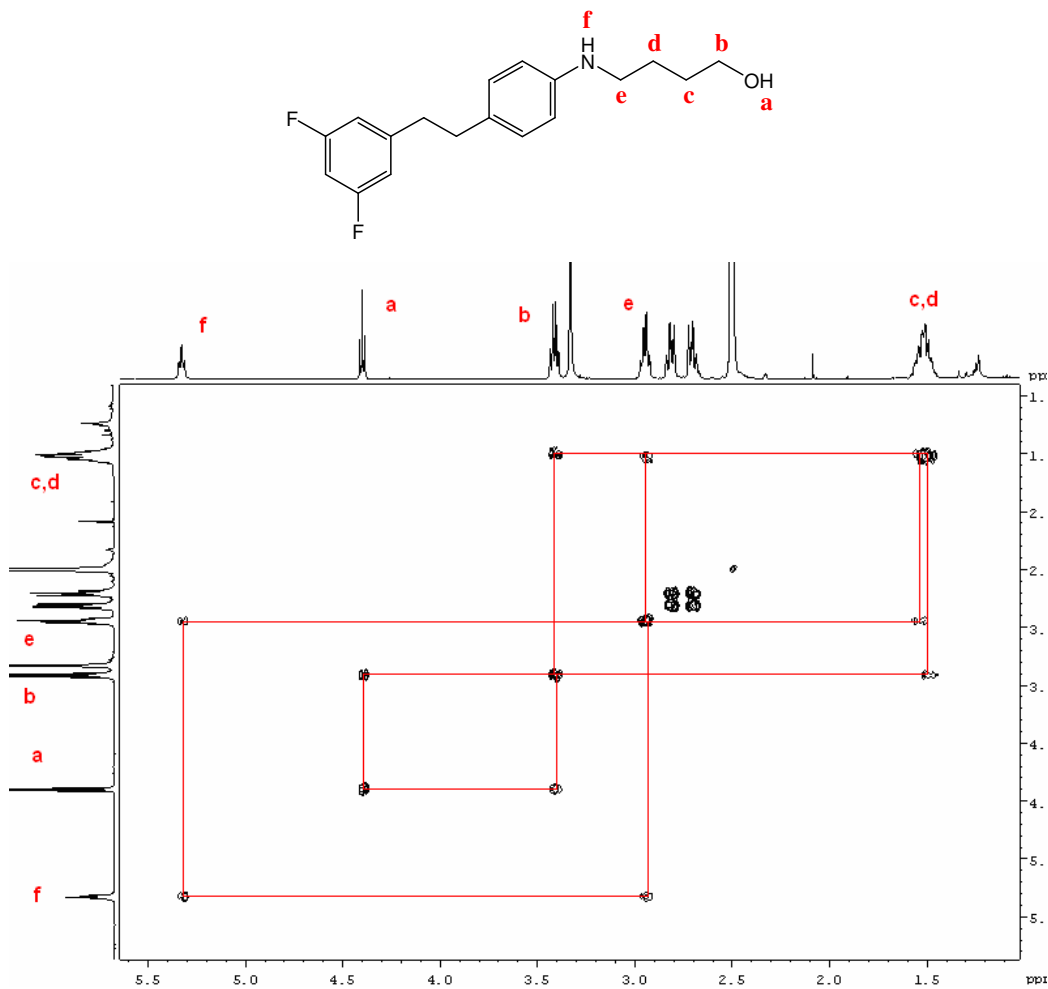


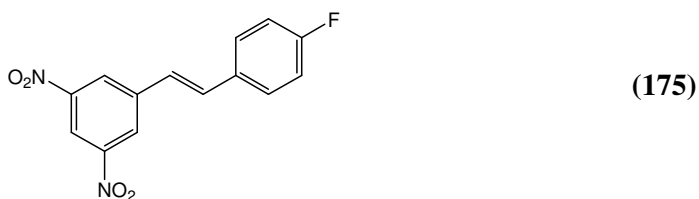
**Figure 7.20:** 2D COSY NMR spectrum of 4-(4-(3,5-difluorophenylethyl)phenylamino)butan-1-ol **174**.

In the COSY NMR of compound **174**, the correlation between adjacent protons can be clearly seen. For the hydroxyl proton signal at  $\delta$  4.40, a correlation can be seen by the box to the **b** proton (C-1'') at  $\delta$  3.42. From this proton, the chain can be followed to the multiplet of the central methylenes (C-2'' and C-3'') **c** and **d**. Obviously a box cannot be drawn for the correlation between protons **c** and **d** ( $\delta$  1.52) but can for the interaction between **e** ( $\delta$  2.95). An interesting note that can be observed from this 2D spectrum is that, although comprising of a multiplet, the protons of C-2'' and C-3'' have slightly different chemical shifts. From the signals in the spectrum, it can be seen the proton the correlates to **b** ( $\delta$  3.42) is very slightly more downfield than the correlation signal to that of **e** ( $\delta$  2.95). This indicates that the methylene at C-2'' comprises of the left hand side (downfield-side) of the multiplet at  $\delta$  1.52. Completing the amino-butanol chain, a final box can be drawn between the C-4'' protons **e** and the amide triplet **f** at  $\delta$  5.33.

## 7.3 Synthesis of 4'-fluoro resveratrol analogues

### 7.3.1 Synthesis of 3,5-dinitro-4'-fluoro stilbene

The second series of fluorinated amino derivatives of resveratrol contains nitrogen moieties at the 3 and 5 positions and a fluorine atom at the 4' position of the stilbene structure. Synthesis of (*E*)-3,5-dinitro-4'-fluorostilbene **175** was carried out via the decarbonylative Heck reaction. The major benefit of using this procedure over the Wittig reaction employed for first series is the stereoselectivity of the reaction. The decarbonylative Heck reaction solely produces the *trans*-isomer which as already mentioned is the bioactive isomer of resveratrol **136**. The procedure was carried out as published for the Andrus *et al* synthesis of resveratrol<sup>9</sup>. Using 3,5-dinitrobenzoyl chloride and 4'-fluorostyreneas starting materials, the (*E*)-isomer **175** was isolated. The reaction was performed in the presence of a molar equivalent of *N*-ethylmorpholine and a catalytic amount of palladium (II) acetate. The solvent used was *p*-xylene as reports have shown the reaction to proceed optimally at 120°C. The resulting crude brown solid residue was recrystallised from ethanol to furnish the desired product **175** as a mustard yellow powder. Yields of the dinitro compound were generally in the range of 60-70 %.



The *cis*-isomer, (*Z*)-3,5-dinitro-4'-fluorostilbene **176** was prepared for comparative purposes. This was synthesised in an isomeric mixture via the classical Wittig reaction. 3,5-Dinitrobenzyl(triphenylphosphonium) bromide was prepared from benzyl bromide and triphenylphosphine. This was reacted via the ylide, with 4'-

fluorobenzaldehyde under strong basic conditions, to form an isomeric (*E/Z*)-mixture of compounds **175** and **176**. As described for the 4'-nitro compounds (**156** and **157**), separation was achieved by fractional recrystallisation from ethanol. The *trans*-isomer **175** was far less soluble than the *cis*-isomer **176**.

### 7.3.1.1 IR study of (*E/Z*)-3,5-dinitro-4'-fluorostilbene

The infra red spectra of isomers **175** and **176** appear very similar. The major structural difference, the orientation of the central double bond has very little influence on the spectra. Although the vinylic stretching is clearly visible in the IR spectra of both 3,5-difluoro-4'-nitrostilbenes (**156** and **157**), they are not as obvious in the reverse compounds **175** and **176**. Carbon stretching of the vinylic bond generally occurs about  $1630\text{ cm}^{-1}$  however it is strongly dependent on the substituents. For *trans*-isomers, due the planar orientation of the bond and substituents, the absorption is in the region of  $1640\text{-}1610\text{ cm}^{-1}$  while the forced non-planar configuration of the *cis*-isomer absorbs at a higher wavenumber, generally  $1660\text{-}1630\text{ cm}^{-1}$ . This is as a result of steric hindrance, leading to reduced conjugation between the vinyl and phenyl groups. Both 3,5-dinitro-4'-nitrostilbene isomers (**175** and **176**) have two *meta*-substituted nitro groups and this may well be the reason for not being able see these vinylic stretchings. As previously mentioned, the nitro group has two main stretches, which are generally equal in intensity as each other and are strong absorptions. Asymmetrical stretching of the nitro group occurs in the region of  $1550\text{-}1475\text{ cm}^{-1}$  while symmetrical stretching in the section of  $1360\text{-}1315\text{ cm}^{-1}$ . In the IR spectra of these isomers, strong absorptions are present at  $1533, 1506$  and  $1343\text{ cm}^{-1}$  for the *trans* **175** and at  $1535, 1506$  and  $1342\text{ cm}^{-1}$  for the *cis* **176**. The presence of these strong absorptions, particularly the asymmetrical mode may be over shadowing the C=C stretching of the vinylic double bond. However, an absorption at  $1592$  and  $1600\text{ cm}^{-1}$  for the *trans* and *cis* respectively, may be the vinylic stretch and have been shifted from the general range by the aromatic substituents present in these molecules.

As with previous molecules discussed, identification of peak absorptions in the fingerprint region is very difficult for fluorinated compounds. This is largely due to the C-F stretching mode which couples strongly with other vibrational modes, especially the C-C stretching. Carbon-fluorine bands can occur anywhere from  $1400$  to  $900\text{ cm}^{-1}$ . Also specific bands can be seen for mono-substituted and *meta*-



disubstituted aromatic compounds, both of which are present in these compounds. All these factors lead to a very complex and crowded fingerprint region from approximately 600 to 1600  $\text{cm}^{-1}$  and makes definite identification of individual absorptions very difficult.

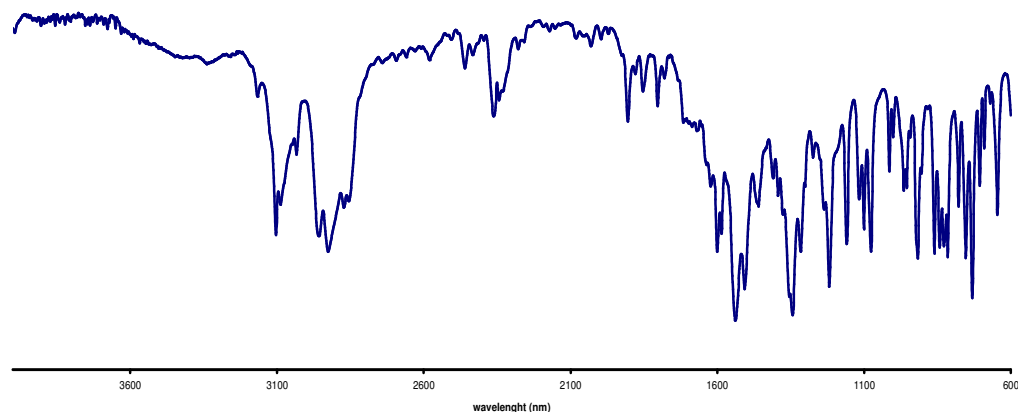


**Figure 7.21:** Infra red spectrum of (*Z*)-3,5-dinitro-4'-fluorostilbene **176**

#### 7.3.1.2 $^1\text{H}$ NMR study of (*E/Z*)-3,5-dinitro-4'-fluorostilbene

In the  $^1\text{H}$  NMR spectrum of compound **175** the vinylic protons appear as doublets as expected, however the vinylic proton nearest the nitro-substituted ring appears at the same chemical shift as the aromatic protons in the 2' and 6' positions of the fluorinated ring. This results in a multiplet at an approximate chemical shift of  $\delta$  7.73. The vinylic proton adjacent to the fluorinated ring is present at  $\delta$  7.51 with a coupling constant of 16.4 Hz, proving *trans* orientation of the stilbene double bond, and can be seen in **Figure 7.22**. Due to long range coupling across a phenyl ring, splitting can be seen for the protons of the dinitrophenyl ring, but with small coupling constants. The *ortho*-protons of this ring appear as a doublet at a chemical shift of  $\delta$  8.81 and with a coupling constant of 2.0 Hz. The *para*-proton, situated between the two nitro groups is split into a triplet with a *J* value of 1.8 Hz and a chemical shift of  $\delta$  8.66. The most upfield protons are observed as a triplet at  $\delta$  7.28 and have a coupling constant of 8.8 Hz. This signal is from the *meta*-protons beside the fluorine, and is a triplet due to  $^1\text{H}$ - $^1\text{H}$  and  $^1\text{H}$ - $^{19}\text{F}$  coupling.

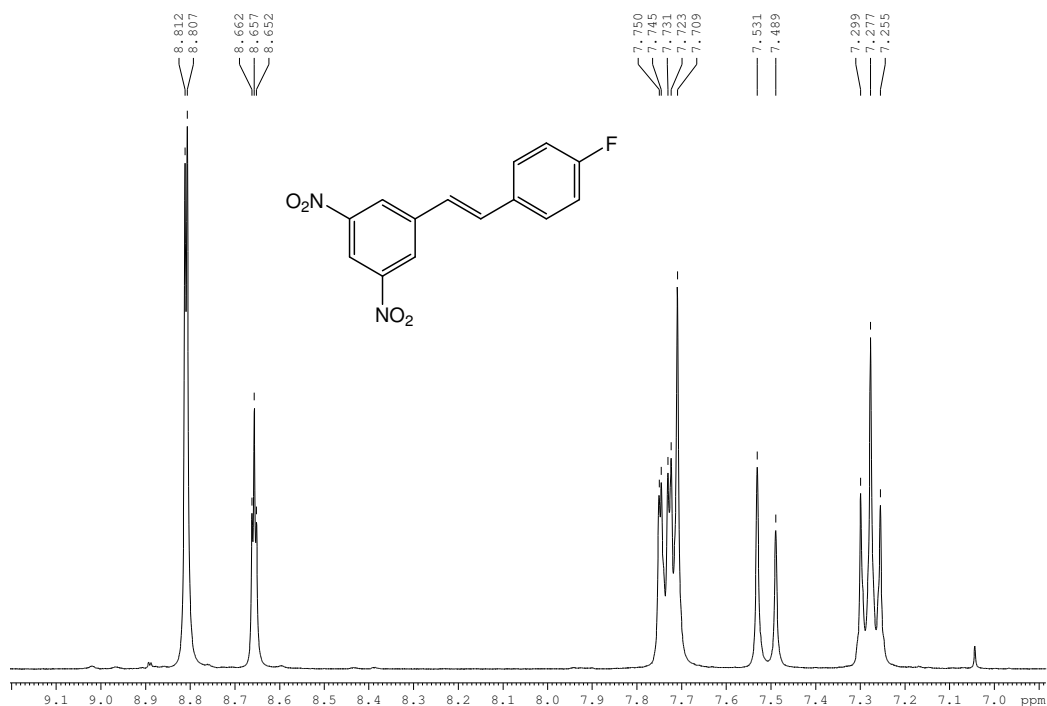


**Figure 7.22:**  $^1\text{H}$  NMR spectrum of (*E*)-3,5-dinitro-4'-fluorostilbene **175**

As with the 4'-nitro analogues described previously, fluorine coupling affects not only the  $^1\text{H}$  NMR but also the  $^{13}\text{C}$  NMR spectra of the 3,5-dinitro derivatives. Due to  $^{13}\text{C}$ - $^{19}\text{F}$  coupling, signal splitting is observed to the aromatic carbons of the fluorinated phenyl ring. The largest coupling constant observed is for the aromatic carbon directly attached to the fluorine atom at the 4' position. This signal is split into a doublet with a chemical shift of  $\delta$  162.32 and a coupling constant of 245.0 Hz. The other aromatic carbons of the ring are also split into doublets, with varying coupling constants in relation to their proximity to the fluorine atom. The carbons in the 2' and 6' positions have a chemical shift of  $\delta$  129.1 and a coupling constant of 8.2 Hz, while the carbons in the 3' and 5' positions appear further upfield at  $\delta$  115.8 and with a coupling constant of 21.5 Hz. The quaternary carbon at position 1' has a chemical shift of  $\delta$  132.6 and a coupling constant of 3.3 Hz. The *ortho*-carbons (3,5) of the nitro ring can be seen at  $\delta$  148.5 and the carbon between the nitro groups is at  $\delta$  140.9. The quaternary carbon at position 1 has a chemical shift of  $\delta$  140.9. The vinylic carbons appear at  $\delta$  132.6 and  $\delta$  124.4. The latter carbon is split by long range fluorine coupling and has a coupling constant of 2.3 Hz. The remaining aromatic carbons appear at  $\delta$  125.9 and  $\delta$  116.4 for positions 2 and 6 and for position 4, respectively.

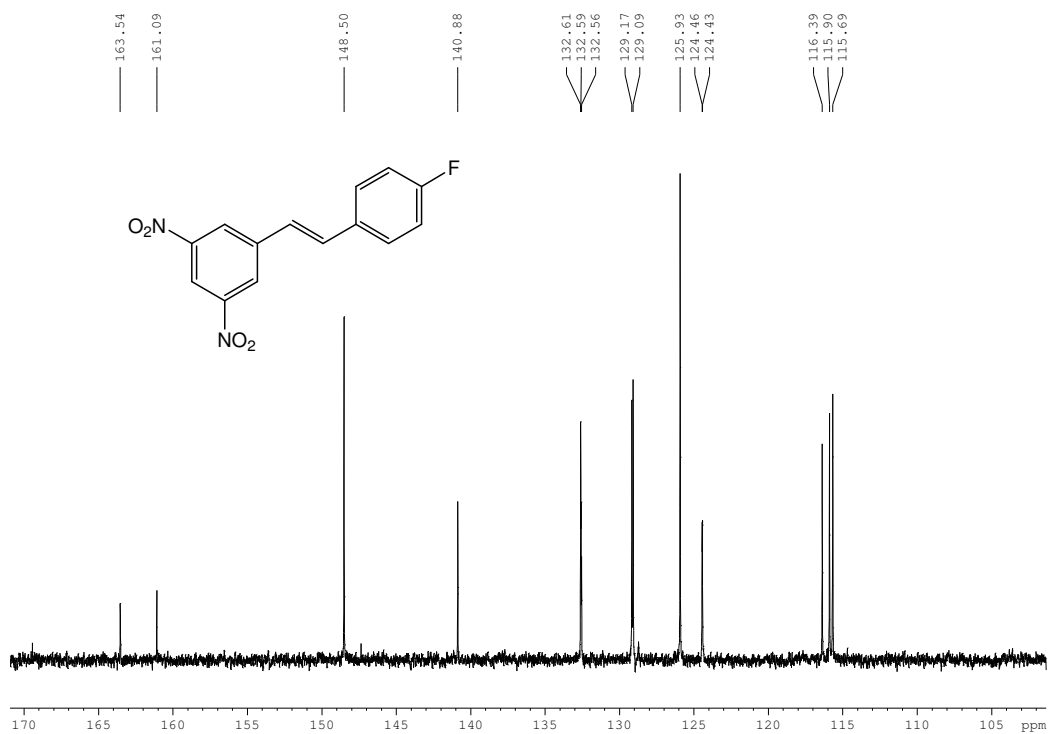


**Figure 7.23:**  $^{13}\text{C}$  NMR spectrum of *(E)*-3,5-dinitro-4'-fluorostilbene **175**

The  $^{19}\text{F}$  NMR of this *para*-substituted stilbene **175** shows one signal at a chemical shift of -112.30.  $^{19}\text{F}$  coupling to both hydrogen and carbon affects the fluorine NMR spectra. In the case of this compound **175** and other *para*-fluorinated stilbene analogues discussed later, the signal of the fluorine atom is split into a multiplet.

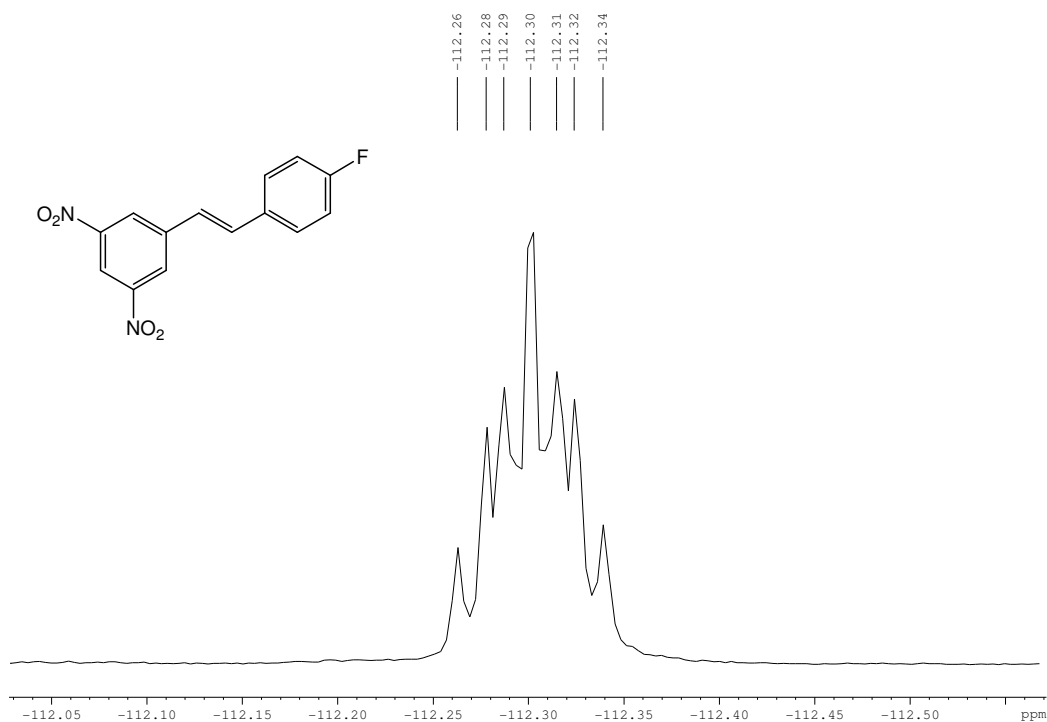


**Figure 7.24:**  $^{19}\text{F}$  NMR spectrum of (*E*)-3,5-dinitro-4'-fluorostilbene **175**

The vinylic protons appear as doublets at  $\delta$  6.99 and  $\delta$  6.87 in the  $^1\text{H}$  NMR of the (*Z*)-isomer **176**, and have coupling constants of 12.0 and 12.4 Hz, confirming *cis* orientation. The proton situated between nitro groups is the furthest downfield due the presence of the very strong electron withdrawing groups flanking it. It has a chemical shift  $\delta$  8.66 and is split into a fine triplet with a coupling constant 2.2 Hz. The equivalent protons at the other side of the nitro groups, at positions 2 and 6, are split into a doublet at  $\delta$  8.40 and with a coupling constant 2.0 Hz. The hydrogens in the corresponding position of the fluorinated ring is a multiplet at  $\delta$  7.33 while the protons adjacent to the fluorine form a triplet with a coupling constant 8.8 Hz at  $\delta$  7.17.

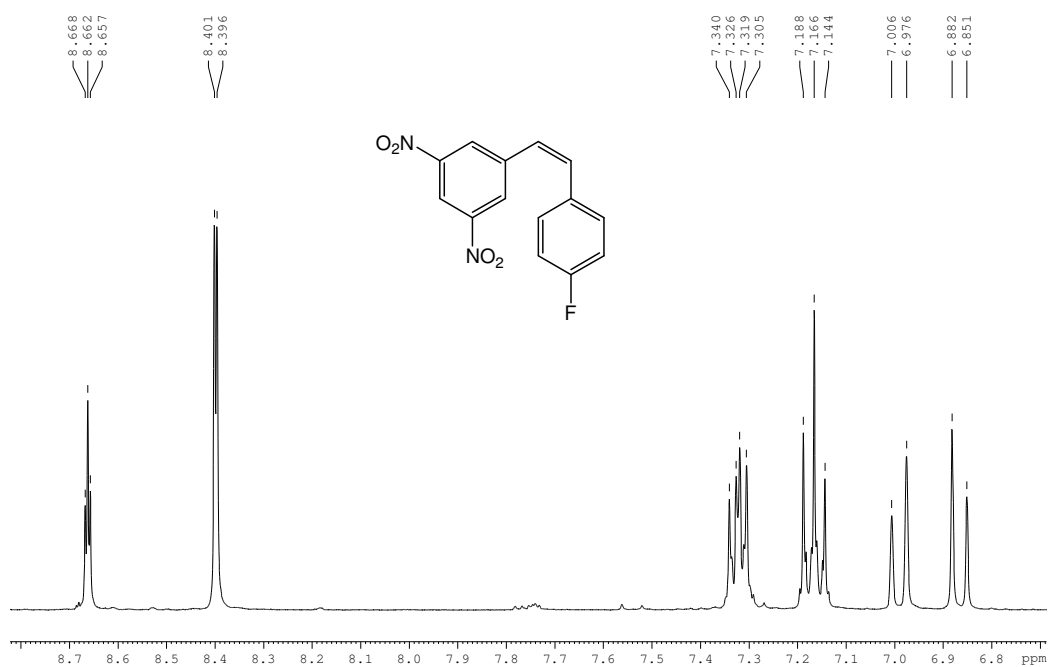
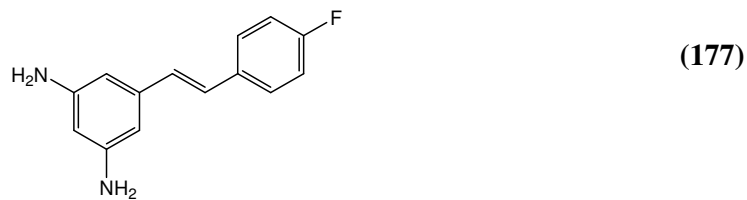


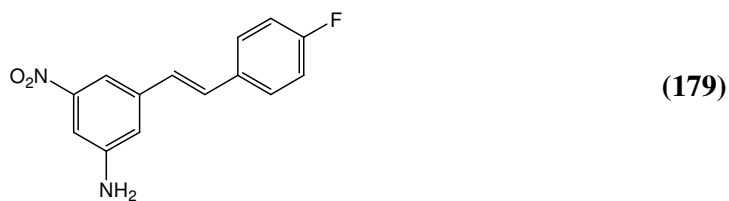
**Figure 7.25:** <sup>1</sup>H NMR spectrum of (Z)-3,5-dinitro-4'-fluorostilbene **176**

Although the vinylic hydrogens of the isomers showed an obvious change in chemical shift and coupling constant in the <sup>1</sup>H NMR, the difference is not as noticeable for the carbon atoms in the <sup>13</sup>C NMR spectra. The vinylic carbon adjacent to the dinitro phenyl ring has a chemical shift of  $\delta$  133.3 whereas the other vinylic carbon beside the fluorinated ring is further upfield at  $\delta$  126.1. When compared to the vinylic chemical shifts of the *trans*-isomer ( $\delta$  132.6 and  $\delta$  124.4), the difference is negligible. The carbon attached to the fluorine is again split with a coupling constant of 244.4 Hz and is present at  $\delta$  161.6. The carbons of the fluorinated ring also are split, with carbon 1' ( $\delta$  131.5), carbons 2' and 6' ( $\delta$  130.5), and the carbons at the 3' and 5' positions ( $\delta$  115.7) having a coupling constants of 3.5, 8.1 and 21.3 Hz respectively. The multiplet signal in the <sup>19</sup>F NMR spectrum of (Z)-3,5-dinitro-4'-fluorostilbene **176** occurs at  $\delta$  -113.02

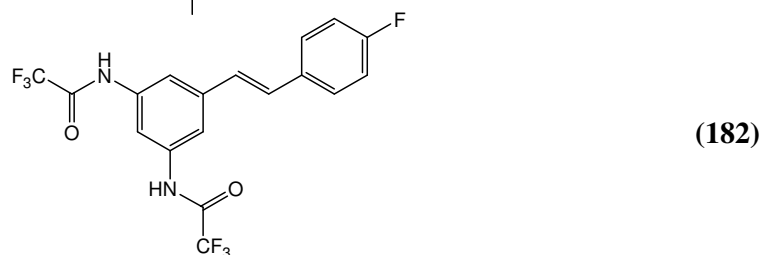
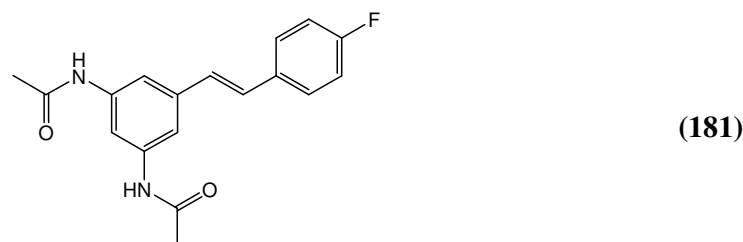
### 7.3.2 Synthesis of (E/Z)-3,5-diamino derivatives



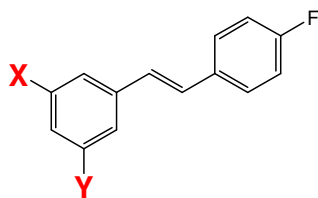
The next step in the synthesis of the 3,5-diamino resveratrol derivatives was the reduction of the nitro groups to amino groups. The *trans* **177** and *cis* **178** diamino isomers were synthesised by the iron and iron (III) chloride reduction procedure. The *trans*-isomer was isolated as a brown powder whereas the *cis*-isomer was a brown viscous oil when pure. By increasing the stated equivalents used for the mono-substituted nitro compounds, complete nitro reduction was achieved. It was found that upwards of 3 times the equivalents used for the 4'-nitro compounds was required to quantitatively reduce both nitro groups. Each 3,5-dinitro-4'-fluoro isomer was individually reduced and the desired product, be it *cis* or *trans* was isolated in quantitative yields and in 100 % isomeric purity equal to that of the initial starting material.



By controlling the equivalents of reducing agents used in the reaction, it was possible to isolate stilbenes with only one nitro group reduced, and therefore producing 3-nitro-5-amino-4'-fluorostilbene. This was carried out using both *trans* **175** and *cis* dinitro-isomers **176** as starting materials, thereby producing (*E*)-3-nitro-5-amino-4'-fluorostilbene **179** and (*Z*)-3-nitro-5-amino-4'-fluorostilbene **180** as orange powders. These mono reduced compounds were synthesised in a 1:1 ratio to the diamino compounds (**177** & **178**) previously described. These were purified by column chromatography using ethyl acetate and hexane as mobile phase.



As for the case of the 3,5-difluoro-4'-amino derivatives, the acetyl derivatives of the 3,5-diamino-4'-fluoro series were synthesised. These compounds were produced as described for the 4' series using the anhydride with catalytic amounts of pyridine. Both the diacetyl analogue **181** and the di(trifluoroacetyl) derivative **182** were purified in good yields and recrystallised from ethyl acetate.



<i>Compound</i>	<i>Isomer</i>	<i>X</i>	<i>Y</i>	<i>% Yield</i>
<b>177</b>	<i>trans</i>	-NH <sub>2</sub>	-NH <sub>2</sub>	77
<b>178</b>	<i>cis</i>	-NH <sub>2</sub>	-NH <sub>2</sub>	65

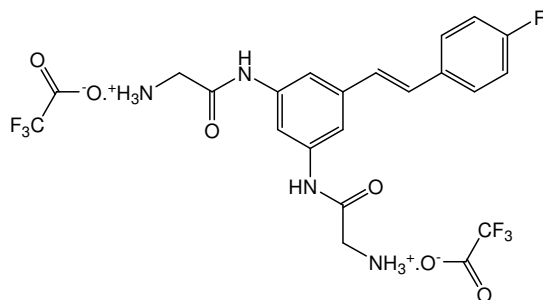
<b>179</b>	<i>trans</i>	-NO <sub>2</sub>	-NH <sub>2</sub>	17
<b>180</b>	<i>cis</i>	-NO <sub>2</sub>	-NH <sub>2</sub>	23
<b>181</b>	<i>trans</i>	-NH-CO(CH <sub>3</sub> )	-NH-CO(CH <sub>3</sub> )	78
<b>182</b>	<i>trans</i>	-NH-CO(CF <sub>3</sub> )	-NH-CO(CF <sub>3</sub> )	56
<b>183</b>	<i>trans</i>	-NH-Gly-BOC	-NH-Gly-BOC	56
<b>184</b>	<i>trans</i>	-NH-L-Ala-BOC	-NH-L-Ala-BOC	38
<b>185</b>	<i>trans</i>	-NH-β-Ala-BOC	-NH-β-Ala-BOC	60
<b>186</b>	<i>trans</i>	-NH-L-Val-BOC	-NH-L-Val-BOC	12
<b>187</b>	<i>trans</i>	-NH-L-Val-BOC	-NH <sub>2</sub>	81

**Table 7.5:** 3,5-Diamino derivatives **177-187**

Compounds **183-187** were synthesised using (*E*)-3,5-diamino-4'-fluorostilbene **177** as starting material. By utilising the classic peptide coupling reaction using EDC as activating agent, the stilbenes **183-187** were isolated. Using the *N*-butoxycarbonyl protected amino acids in excess, reasonably good yields were achieved (**Table 7.5**). In all cases for the preparation of the amino acid derivatives, approximately three equivalents of reagents were used, relative to the diamino starting material. All products were purified by column chromatography and obtained as white powders, with the exception of the L-valine derivative **186**. In the case of the valine analogue, the disubstituted product was isolated after chromatography as a brown wax. This was formed in a relatively low yield, when compared to the other amino acid derivatives.

A major byproduct was isolated in the preparation of the valine stilbene analogue **186**. This byproduct was separated by column chromatography and from the NMR spectra recorded, it was shown to be the monosubstituted product, (*E*)-3-amino(BOC-L-valine)-5-amino-4'-fluorostilbene **187**. The deprotection of the 3,5-di(amino acid) derivatives was attempted on the glycine analogue **183**. It was carried out using trifluoroacetic acid in dichloromethane with stirring at room temperature for one hour. After evaporation of the solvent and excess acid using a nitrogen stream, the solid residue was recrystallised from ethyl acetate. NMR spectra showed that the product formed is the trifluoroacetate salt of (*E*)-3,5-diaminoglycine-4'-fluoro stilbene **188**. The deprotection was achieved in a quantitative yield. The salt was dried to yield a beige powder with a melting point of approximately 205°C.





(188)

### 7.3.2.1 IR NMR study of (E)-3,5-diamino derivatives

Evidence of the nitro reduction can be seen from the IR spectra of the diamine-isomers. Although some of the peaks proposed earlier as nitro based are present in the IR spectra of the diamino derivatives. Nitro stretching, asymmetrical and symmetrical occur in the general region around  $1500\text{ cm}^{-1}$  and  $1340\text{ cm}^{-1}$ . The main peaks in these areas mentioned in the IR discussion of compound **175** have mostly disappeared in the corresponding IR spectrum of amine **177**. However one absorption in particular,  $1509\text{ cm}^{-1}$ , which was identified in the 4'-nitro compound **156** as an asymmetrical nitro stretch is also seen in the IR spectrum of the dinitrostilbene **175** ( $1506\text{ cm}^{-1}$ ) and is still present in the reduce diaminstilbene **177** ( $1507\text{ cm}^{-1}$ ). Stretching of an amine is normally observed between  $3500$  and  $3300\text{ cm}^{-1}$ , with the asymmetrical having a higher frequency to that of the symmetrical stretch. The *trans*-isomer **177** shows four absorptions within this region where as just two are observed in this area for the *cis*, with absorptions at  $3424$  and  $3339\text{ cm}^{-1}$ . A shoulder band is normally seen on the lower wavenumber side of these stretchings and can be seen for both isomers at  $3193\text{ cm}^{-1}$  (*trans*) and  $3208\text{ cm}^{-1}$  (*cis*). This is due to the overtone of the N-H bending band. The N-H bending vibration of primary amines is observed in the spectral region of  $1650$ - $1580\text{ cm}^{-1}$ , and accounts for the strong absorptions at  $1593$  and  $1585\text{ cm}^{-1}$  for *trans* and *cis*, respectively. The N-H wag is usually a strong broad band at approximately  $910$ - $665\text{ cm}^{-1}$  and is most likely the absorption at  $834\text{ cm}^{-1}$  in the IR spectra of both isomers.

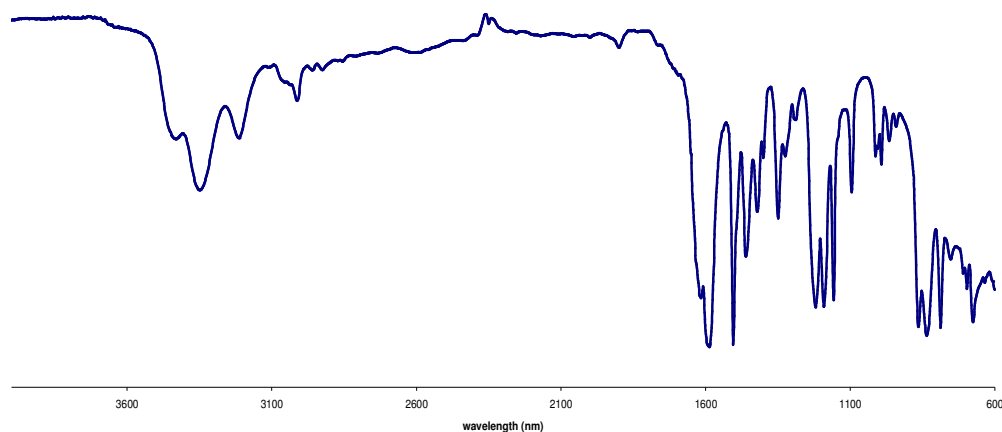


**Figure 7.26:** Infra red spectrum of (*Z*)-3,5-diamino-4'-fluorostilbene **178**

The IR spectrum of the *trans*-nitro-amino stilbene **179** is shown in **Figure 7.27** is. All the relevant stretchings of a nitro and amino substituted *trans*-stilbene are present in this spectrum. The three absorptions seen at the highest frequencies are representative of the presence of a primary amine. The asymmetrical amine stretch can be seen at  $3472\text{ cm}^{-1}$  while the symmetrical stretch at  $3373\text{ cm}^{-1}$ . The broad shoulder absorption seen at  $3224\text{ cm}^{-1}$  is as an overtone of the N-H bending band. The stretch of a *trans*-orientated central stilbene double bond generally appears in the range  $1640\text{-}1610\text{ cm}^{-1}$ , and for compound **177** can be found at  $1620\text{ cm}^{-1}$ . The intense broad bands of the nitro stretches are also clearly visible. The asymmetrical stretching of the nitro group for this compound can be seen at  $1531$  and  $1509\text{ cm}^{-1}$  while the symmetrical stretch is present at  $1352$  and  $1333\text{ cm}^{-1}$ . The same clarity of absorptions can be seen in the IR of the *cis*-isomer **180**, with the  $\text{C}=\text{C}$  stretch at  $1635\text{ cm}^{-1}$ .

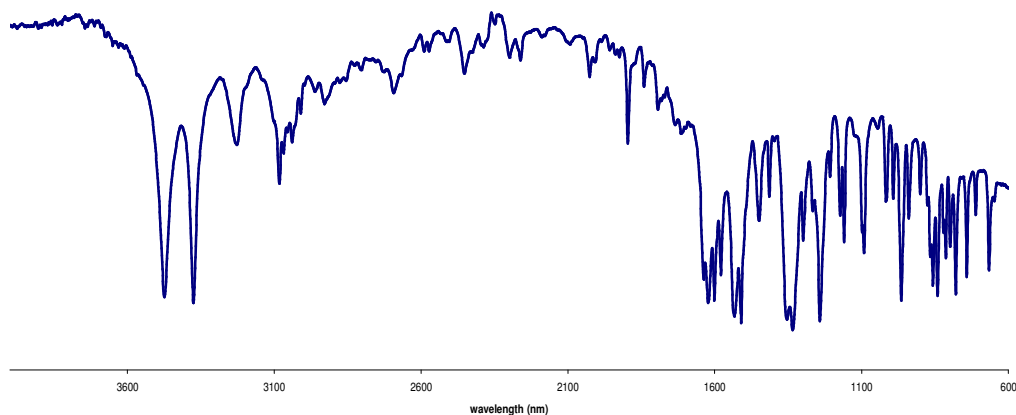


**Figure 7.27:** Infra red spectrum of (*E*)-3-nitro-5-amino-4'-fluorostilbene **179**

### 7.3.2.2 $^1\text{H}$ NMR study of (*E*)-3,5-diamino derivatives

In the  $^1\text{H}$  NMR of the *trans* isomer, (*E*)-3,5-diamino-4'-fluorostilbene **177**, a major chemical shift can be seen in the location of the aromatic protons of the amino-substituted phenyl ring. The central *para*-proton in the 4 position has moved from  $\delta$  8.66 to  $\delta$  5.80, while the protons at 3 and 5 have moved from  $\delta$  8.81 to  $\delta$  6.04, on reduction to the amine. Both signals maintained their coupling constants of 1.8 Hz and 2.0 for the latter. The aromatic protons of the fluorinated ring appear as a multiplet at a chemical shift of  $\delta$  7.59 for the 2' and 6' hydrogens and at  $\delta$  7.17 for the 3', 5' triplet ( $J = 8.8$  Hz). On reduction of the nitro groups to amines, the two doublets of the central vinylic bonds have merged into a doublet with a coupling constant of 2.0 Hz and a chemical shift of  $\delta$  6.89 shown in **Figure 7.28**. However, outlining peaks at either side of this doublet which look like shadow peaks can be seen. The coupling constants between these small peaks and the main doublet are 16.8 Hz, within the anticipated coupling constant region for a *trans*-isomer. This may be due to a similarity in the electron-withdrawing effect of an electronegative fluorine versus two free amines. The free amines appear as a broad singlet with a chemical shift of  $\delta$  4.76.

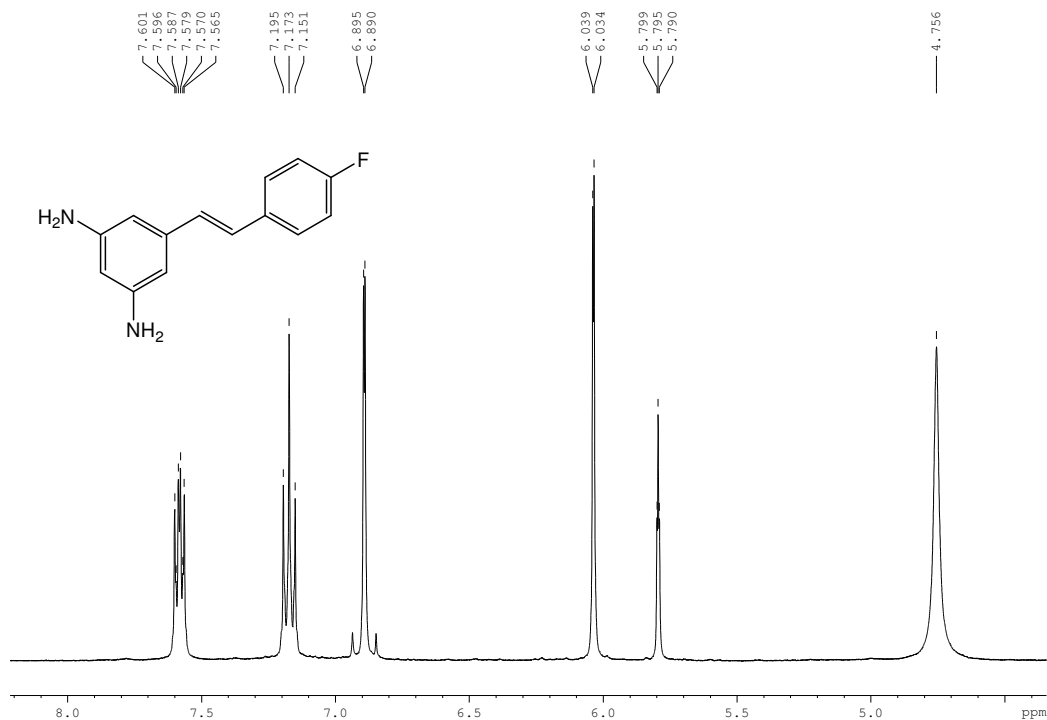


**Figure 7.28:**  $^1\text{H}$  NMR spectrum of (*E*)-3,5-diamino-4'-fluorostilbene **177**

The  $^{13}\text{C}$  NMR spectrum of the diamino stilbene **177**, shown in **Figure 7.29**, shows small variations from that of the dinitro compound **175**. The most noticeable shifts occur around the central double bond and adjoining aromatic quaternary carbons at positions 1 and 1'. After the reduction, the carbon at position 1 has moved slightly upfield to  $\delta$  137.5 while the doublet of the corresponding carbon on the other phenyl ring (1') has moved down to  $\delta$  133.9, maintaining a small coupling constant of 3.0 Hz. The vinylic carbon nearest the fluorinated ring has migrated downfield to  $\delta$  130.0 with a coupling constant of 2.1 Hz, while on the amino side of the molecule, the vinylic carbon, like carbon 1 has shifted upfield by approximately 7 ppm to a chemical shift of  $\delta$  125.1. Large movement in the signals of the aromatic carbon of the amino phenyl ring can be seen, however the carbons directly attached to the amines hardly shifted at all and are present at  $\delta$  149.3. The protonated carbons of this ring show the most dramatic effect of reduction with the *ortho*-carbons moving from  $\delta$  125.9 for the dinitro compound **175** to  $\delta$  101.7 for the compound **177**. The *para*-carbon, between the reduced amines also moved upfield to a chemical shift of  $\delta$  100.1. The remaining carbons of the fluorinated ring, *ortho*-, *meta*- and *para*-carbons retained almost identical chemical shifts on reduction. The location of the fluorine multiplet in the  $^{19}\text{F}$  NMR can be observed at a chemical shift of  $\delta$  -114.97.

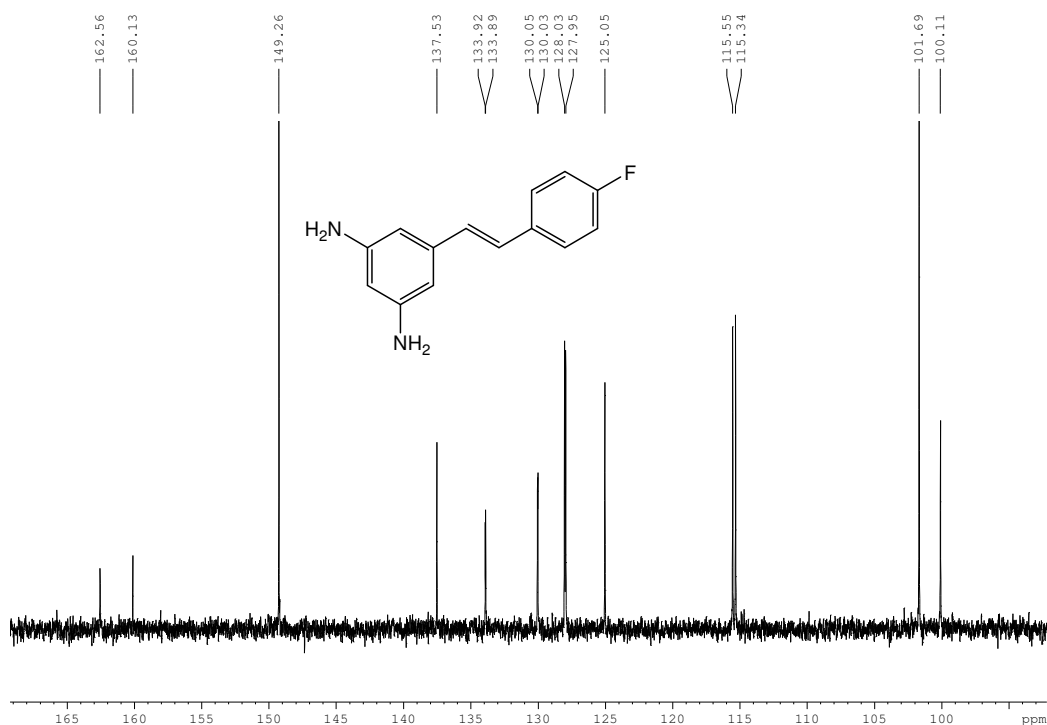


**Figure 7.29:**  $^{13}\text{C}$  NMR spectrum of (*E*)-3,5-diamino-4'-fluorostilbene **177**

A similar signal due to the vinylic protons of (*Z*)-3,5-diamino-4'-fluorostilbene **178** is seen in the  $^1\text{H}$  NMR spectrum, compared to that of the *trans*-isomer **177**. These protons appear as a doublet with what appears to be shadow peaks surrounding it. This signal is present at  $\delta$  6.38 and has a coupling constant of 3.2 Hz while the coupling constant between shadow peaks and doublet is 12.4 Hz. The signals of the protons of the fluorinated ring are split due to coupling to the fluorine, with the *ortho*-protons split into a multiplet at  $\delta$  7.32 and the *meta*-protons, a triplet at  $\delta$  7.05 with a *J* value of 9.0 Hz. The three protons of the aminated ring appear as a multiplet at  $\delta$  5.71, and the broad amine singlet has a chemical shift of  $\delta$  4.68.

The  $^1\text{H}$  NMR spectrum of the *trans*-isomer **179** shows the *ortho*-proton, adjacent to the nitro group as a singlet with a chemical shift of  $\delta$  7.58. The other *ortho*-proton of this molecule at position 6, beside the amine also appears as a singlet at  $\delta$  7.14. The *para*-proton of this compound, situated between the nitro and amino groups is part of the multiplet present in the range  $\delta$  7.15-7.35. Also included in this multiplet, which integrates for 5, are the vinylic protons and the aromatic hydrogens at positions 3' and 5' on the fluorinated ring. The 2' and 6' protons have a chemical shift of  $\delta$  7.69 and maintain their multiplet splitting. An intense broad singlet, integrating for 2 can be observed at  $\delta$  5.86 and corresponds to the newly formed amino group.

The  $^1\text{H}$  NMR of the *cis*-nitro-amino-stilbene derivative **180** shows an upshift in the chemical shifts of most of the proton signals. The *ortho*-proton has moved upfield to  $\delta$  6.80 while the vinylic protons appear at  $\delta$  6.68 and  $\delta$  6.59 with coupling constants of 12.4 and 12.0 Hz, respectively. The remaining six aromatic protons form two multiplets in the regions  $\delta$  7.23-7.28 and  $\delta$  7.10-7.14. The singlet due to the amine has is present at  $\delta$  5.80.

The  $^{13}\text{C}$  NMR spectra of isomers **179** and **180** show interesting differences when compared to each other. The nitro and amine substituted carbons appear at  $\delta$  150.1 and  $\delta$  149.2 (**179**) and  $\delta$  148.8 and  $\delta$  147.4 (**180**). The aromatic quaternary carbons in the primary positions (1 and 1') show the biggest difference in chemical shift. They appear at  $\delta$  138.9 and  $\delta$  133.1 with the 1' proton having a coupling constant of 3.3 Hz, for the *trans*- compound. For the *cis*-isomer, they can be observed at  $\delta$  150.1 and  $\delta$  138.5. However the 1' carbon is only seen to have one peak in this spectrum. The

vinyl carbons can be found at  $\delta$  128.9 and  $\delta$  127.0 for the *trans*-isomer and at  $\delta$  130.3 and  $\delta$  128.7 for the *cis*.

The vinylic coupling constant of the diacetylamino stilbene **181** was calculated as 16.4 Hz from the doublets at  $\delta$  7.14 and  $\delta$  7.03. The amide protons appear as a singlet with a chemical shift of  $\delta$  9.99 while the protons of the acetyl groups have a chemical shift of  $\delta$  2.05, integrating for 2 and 6 respectively. In the  $^1\text{H}$  NMR of (*E*)-3,5-di(trifluoroacetyl)amino-4'-fluorostilbene **182**, the amide has a chemical shift of  $\delta$  11.47. One of the vinylic doublets is obscured by the 3' and 5' protons signals forming a multiplet at  $\delta$  7.24 but the more upfield doublet is seen at a chemical shift of  $\delta$  7.18. This doublet has a coupling constant of 16.0 Hz, proving *trans* orientation. The  $^{19}\text{F}$  NMR of compound **182** shows 2 independent signals, integrating for 6 and 1. The trifluoroacetyl fluorines have a chemical shift of  $\delta$  -73.87 and due to their equivalency appear as a singlet. The multiplet of the 4'-*para*-fluorine appears at  $\delta$  -113.53.

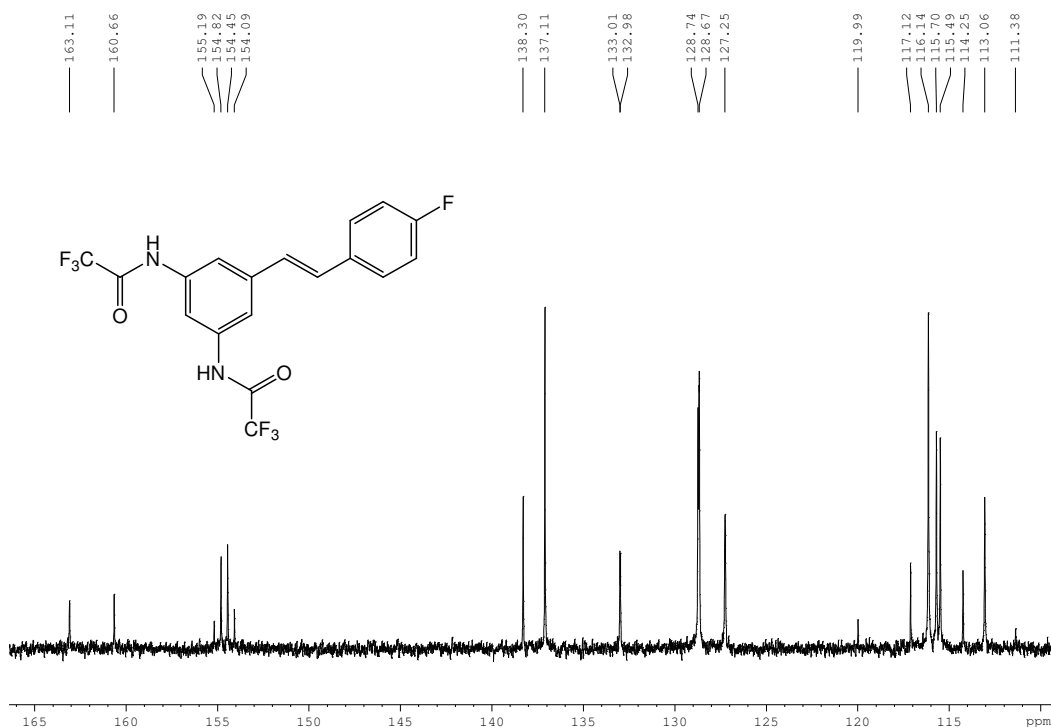
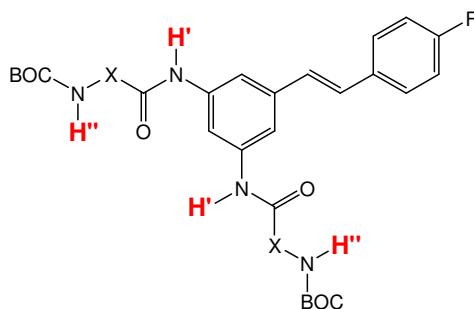


**Figure 7.30:**  $^{13}\text{C}$  NMR spectrum of (*E*)-3,5-di(trifluoroacetyl)amino-4'-fluorostilbene **182**

As with the 4'-trifluoroacetylamino analogue **162**, the  $^{13}\text{C}$  NMR spectrum (**Figure 7.30**) shows extremely large splitting due to  $^{13}\text{C}$ - $^{19}\text{F}$  coupling. As for all the

compounds synthesised with a 4'-fluorine, the 4'-carbon is split into a doublet with a chemical shift of  $\delta$  161.90 and a coupling constant of 243.8 Hz. The carbonyl of the trifluoroacetyl moiety is split into a quartet at  $\delta$  154.65 with a coupling constant of 36.9 Hz. The trifluoro group of this moiety has a carbon signal also split into a quartet, but at a chemical shift of  $\delta$  115.69 with a coupling constant of 286.9 Hz.



	<i>Amide Chemical Shift (<math>\delta</math>)</i>		
	<b>X</b>	<b>H'</b>	<b>H''</b>
<b>183</b>	-CH <sub>2</sub> -	9.99 (s)	7.06* (m)
<b>184</b>	-CH(CH <sub>3</sub> )-	9.98 (s)	7.06* (m)
<b>185</b>	-CH <sub>2</sub> CH <sub>2</sub> -	10.00 (s)	6.85 (t)
<b>186</b>	-CH( <i>i</i> Pr)-	10.07 (s)	6.89 (d)
<b>187</b> <sup>†</sup>	-CH( <i>i</i> Pr)-	9.69 (s)	6.81 (d)

**Table 7.6:** <sup>1</sup>H NMR chemical shifts of amide protons of amino acid derivatives **183-187**

\*amide signal forms part of multiplet, stated chemical shift is central point of multiplet

<sup>†</sup> mono-amino substituted compound

The <sup>1</sup>H NMR of the diaminoglycine derivative **183** shows the methylene protons of the glycine moiety as a doublet with a chemical shift of  $\delta$  3.74 and a coupling constant of 6.4 Hz. The methyl groups of the BOC protection group appear as a very intense singlet, integrating for 18 and at a chemical shift of  $\delta$  1.41. The doublets of the vinylic protons appear as part of the multiplets at  $\delta$  7.19 and  $\delta$  7.06. The fluorine NMR shows the 4'-multiplet at a chemical shift of  $\delta$  -114.02.

In the proton NMR spectrum of the di(amino-L-alanine) derivative **184**, as in the case of the glycine analogue, the proton doublets of the central double bond appear at a similar chemical shift to that of other protons. In this case, one doublet makes up a

multiplet with the aromatic protons of the 3' and 5' positions while the other doublet is part of a multiplet with the alanine amide protons, in the region of  $\delta$  7.00-7.25. The  $\alpha$ -H at the chiral centre of L-alanine is present at a chemical shift of  $\delta$  4.14. This signal is split into a quintet due to the adjacent methyl group and amide, and has a coupling constant of 7.2 Hz. The alanine methyl group appears as a doublet and is present at  $\delta$  1.27. This doublet has a coupling constant of 7.2 Hz, due to the coupling with the  $\alpha$ -proton. The protons of the BOC group have a chemical shift of  $\delta$  1.39.

The vinylic protons of the  $\beta$ -alanine analogue **185** appear independently as doublets and not as part of multiplets as was the case for the previous amino acid derivatives, **183** and **184**. The doublets have a chemical shift of  $\delta$  7.13 and  $\delta$  7.03 and coupling constants of 16.4 and 16.0 Hz. In the amino acid moiety, the methylene protons beside the carbonyl are split into a quartet with chemical shift of  $\delta$  3.23 and coupling constant of 6.8 Hz. The other methylene unit, adjacent to the  $\beta$ -alanine amine appears at a chemical shift similar to that of the deuterated solvent, dimethylsulphoxide (DMSO), at approximately  $\delta$  2.5. The BOC methyl groups for this compound have a chemical shift of  $\delta$  1.38.

Confirmation of the *trans*-orientation of compound **186** is achieved from calculation of a coupling constant of 16.4 Hz from the vinylic doublet seen at a chemical shift of  $\delta$  7.08. The other doublet from the stilbene central double bond forms a multiplet with the aromatic protons in the 3' and 5' positions. The  $\alpha$ -proton at the chiral centre of the valine unit has a chemical shift of  $\delta$  3.98 and is split into a triplet with coupling constant of 7.8 Hz. The C-H in the centre of the isopropyl valine side chain is split into a multiplet at  $\delta$  2.02 while the methyl groups of this side chain is present as a doublet at  $\delta$  0.94 with a coupling constant of 6.0 Hz. The protons of the protecting groups appear at a chemical shift of  $\delta$  1.41.

The vinylic protons of (*E*)-3-amino-BOC-L-valine-5-amino-4'-fluoro stilbene **187** appear in the same region as the proton in the 2 position, beside the amino acid substituent. They form a multiplet, integrating as 3 at a chemical shift of  $\delta$  6.99. A broad singlet due to the free amine appears at a chemical shift of  $\delta$  5.17 and integrates for 2 protons. The  $\alpha$ -proton at the chiral centre is split into a triplet with coupling constant of 10.0 Hz and at a chemical shift of  $\delta$  3.91. The central proton of the



isopropyl side chain forms a multiplet at approximately  $\delta$  2.00 and the methyl groups of this side chain a doublet at  $\delta$  0.92 with a coupling constant of 2.0 Hz. The BOC protons are present at  $\delta$  1.40.

In the  $^1\text{H}$  NMR (**Figure 7.31**), we can see evidence of the salt formation of the glycine stilbene **188**. The *N*-terminus of the glycine unit appears a broad singlet which often indicates that it is a charged amine. Also the fact that this singlet integrates for 6 protons is further evidence of its charged nature. The methylene unit of glycine is present at  $\delta$  3.84 and also occurs as a broad singlet, instead of a doublet as seen in the BOC protected compound **183**. The amide that links the stilbene structure to the glycine is the most downfield signal seen in the  $^1\text{H}$  NMR. It can be observed as an intense singlet with a chemical shift of  $\delta$  10.67. The aromatic protons of the aminoglycine substituents appear as a singlet and doublet. The proton between the substituents, in the *para* position has a chemical shift of  $\delta$  7.89 while the *ortho*-protons at  $\delta$  7.58 are split into a doublet with a coupling constant of 1.2 Hz. The hydrogens of the *para*-substituted fluorine ring are both found to be or be part of, a multiplet with the 2' and 6' protons forming a multiplet at  $\delta$  7.70 and the 3' and 5' protons make up a multiplet with one of the vinylic signals. This has a chemical shift of  $\delta$  7.22. The second vinylic proton is split into the normal doublet at  $\delta$  7.08 and has a coupling constant of 16.0 Hz, indicating the *trans* orientation.

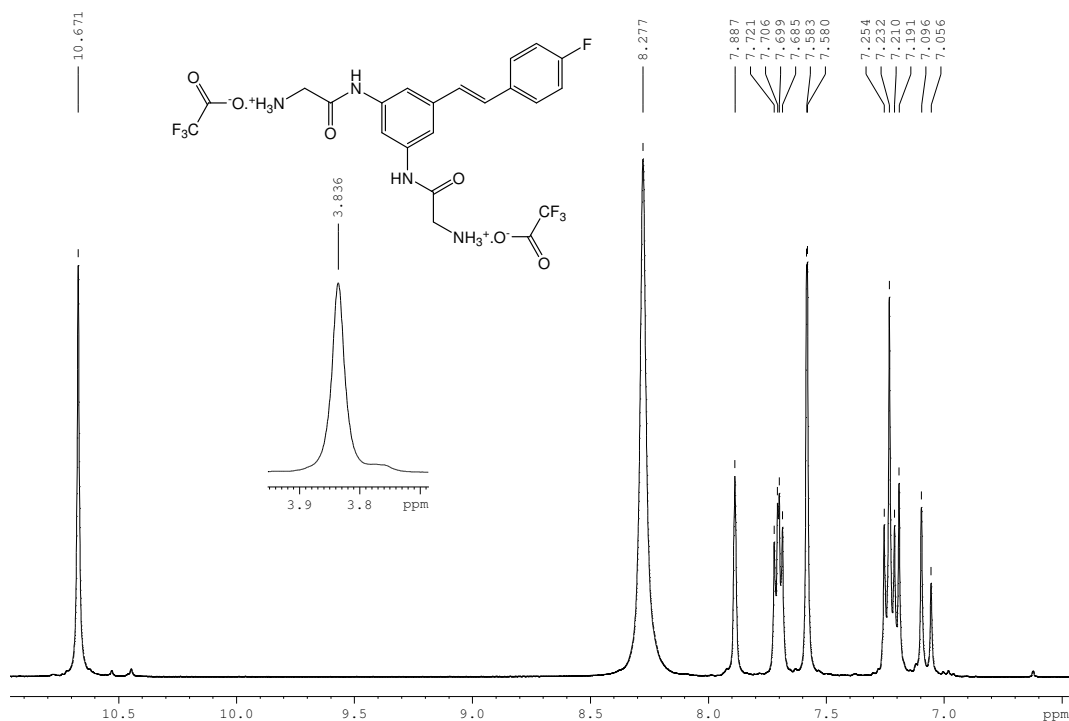


**Figure 7.31:**  $^1\text{H}$  NMR spectrum of (*E*)-3,5-di(aminoglycine)-4'-fluorostilbene trifluoroacetate salt **188**

Evidence of the trifluoroacetate salt can be clearly seen from the  $^{19}\text{F}$  NMR spectrum. This spectrum shows two signals, integrating as 6 and 1 (**Figure 7.32**). The large singlet at  $\delta$  -73.84 integrates for 6 and is due to the trifluoromethyl group of the salt. There are two trifluoroacetate salt moieties in compound **188**, each with 3 fluorines. The much less intense multiplet is from the *para*-substituted fluorine. This signal has a chemical shift of -113.76.

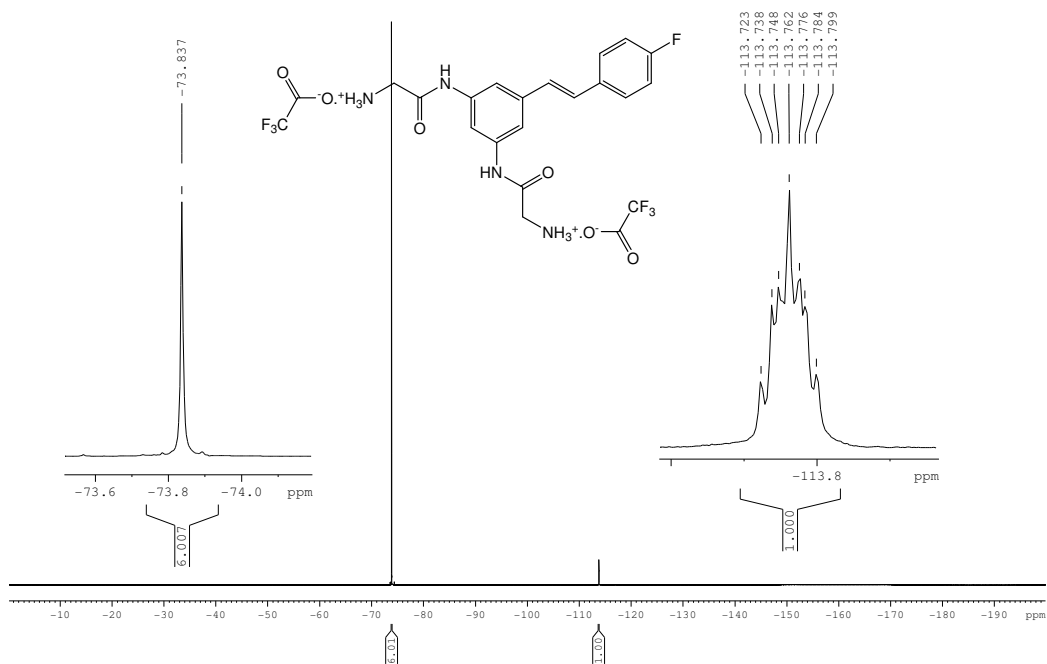


**Figure 7.32:**  $^{19}\text{F}$  NMR spectrum of  $(E)$ -3,5-di(aminoglycine)-4'-fluorostilbene trifluoroacetate salt **188**

Evidence of the salt can also be seen in the carbon NMR. At a chemical shift of  $\delta$  158.4, the quartet of the salt carbonyl can be seen with a coupling constant of 129.7 Hz. Also the quartet of the trifluoromethyl group is visible, in the approximate range of  $\delta$  110-120.

## 7.4 References

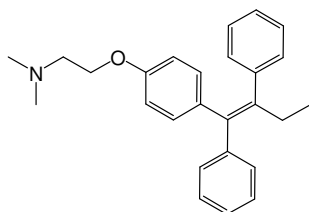
1. Pettit, G.R., Grealish, M.P., Jung, M.K., Hamel, E., Pettit, R.K., Chapuis, J.C., Schmidt, J.M.; *J. Med. Chem.* **2002**, *45*, 2534.
2. Günzler, H., Gremlich, H.-U.; “*IR Spectroscopy, An Introduction*”, Wiley-VCH, **2002**.
3. Lin-Vien, D., Colthup, N.B., Fateley, W.G., Grasselli, J.G.; “*The Handbook of Infrared and Raman Characteristic Frequencies of Organic Molecules*”, Academic Press, **1991**.
4. Williams, D.H., Fleming, I.; “*Spectroscopic Methods in Organic Chemistry*”, McGraw-Hill publishers, **1995**, 5th edition.
5. Rahaim, R.J., Jr., Maleczka, R.E., Jr.; *Synthesis* **2006**, *19*, 3316.
6. McCarroll, A.; *Synthetic Pages* **2007**, 261.  
<http://www.syntheticpages.org/search.php?&action=1&page=1&id=261>
7. Anderson, F.P.; “*The synthesis, structural characterisation and biological evaluation of potential chemotherapeutic agents*”, Dublin City University, *PhD Thesis*, **2005**.
8. Miljanić, S., Frkanec, L., Meić, Z., Žinić, M.; *Eur. J. Org. Chem.* **2006**, *5*, 1323.
9. Andrus, M.B., Liu, J.; *Tet. Lett.* **2006**, *47*, 5811.
10. Lunsford, C.D., Murphy, R.S., Rose, E.K.; *J. Org. Chem.*, **1957**, *22*, 1225.
11. Flaniken, J.M., Collins, C.J., Lanz, M., Singaram, B.; *Org. Lett.* **1999**, *1*, 5, 799.
12. Russell, H.F., Bremner, J.B., Bushelle-Edghill, J., Lewis, M.R., Thomas, S.R., Bates II, F.; *Tet. Lett.* **2007**, *48*, 1637.
13. Boisson, B., Berthet, J.C., Lance, M., Nierlich, M., Ephritikhine, M.; *Chem. Commun.* **1996**, 2129
14. Borkowsky, S.L., Jordan, R.F., Hinch, G.D.; *Organometallics* **1991**, *10*, 1268.

## 8.0 Biological activity of novel resveratrol analogues

### 8.1 Introduction

Resveratrol **136** has been shown to prevent and slow the progression of a wide variety of illnesses, including cancer, cardiovascular disease and ischaemic injuries, as well as enhance stress resistance and extend the lifespans of various organisms from yeast to vertebrates. The mechanism by which resveratrol exerts such a range of beneficial effects across species and disease models is not yet clear. Cancer prevention is one of the mostly widely researched areas today. Resveratrol has been identified as an effective candidate for cancer chemoprevention due to its availability to block each step in the carcinogenesis process by inhibiting several molecular targets<sup>1</sup>. It has been shown to inhibit the growth of various cancers cell lines. Resveratrol has also been shown to provide cancer chemopreventative effects in different systems based on its potent inhibition of diverse cellular events associated with tumour initiation, promotion and progression<sup>2</sup>.

The term cancer is used for diseases which are characterised by uncontrolled, abnormal cell division and are capable of spreading and invading other tissues<sup>3</sup>. Cancer cells can spread through the blood and lymph systems to other parts of the body. It is not just one disease but many diseases. There are more than 100 different types of cancer. Most cancers are named for the organ or type of cell in which they start, for example basal cell carcinoma is a cancer that originates in the basal cells of the skin. There is much reported evidence that resveratrol can act on the carcinogenesis process by affecting the three phases: tumour initiation, promotion and progression phases. It appears that resveratrol can prevent metabolic activation, ROS production, adduct formation and stimulate metabolic inactivation. Resveratrol is also able to act against the chemical carcinogens and other various stimuli by several mechanisms such as activation of apoptosis, arrest of the cell cycle or inhibition of kinase pathways<sup>4</sup>. Resveratrol can suppress the later steps of carcinogenesis, namely angiogenesis and metastasis. Ideally chemopreventive agents act at safe doses effectively affecting the carcinogenic process without toxicity.



(189)

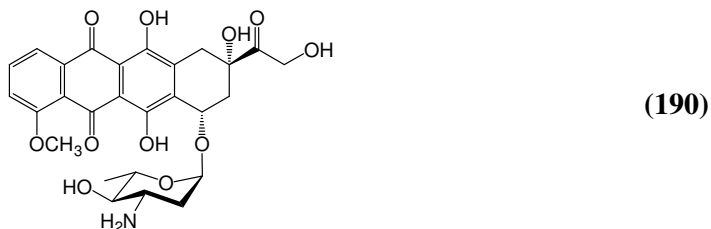
Chemoprevention can be defined as the prevention or reduction of cancer risk by the ingestion of natural or synthetic compounds with low toxicity that are able to suppress, delay or reverse carcinogenesis. The use of tamoxifen **189** in breast cancer is one of the best examples of chemoprevention<sup>5</sup>. This stilbene derivative is administered for five years following surgery for breast cancer and it has been found to reduce the risk of tumour recurrence. The cancer chemopreventative activity of resveratrol **136** is believed to be due to its ability to activate apoptosis. Apoptosis is a type of cell death in which a series of molecular steps in a cell leads to its death. This is the body's normal way of eliminating unneeded or abnormal cells. Commonly used chemotherapeutic drugs can induce this programmed cell death. Apoptosis is therefore a common mechanism for the removal of unrepairable genetic lesions from cells. The enhancement of apoptosis in pancreatic cells by resveratrol has been reported for *in vitro* studies and is associated with mitochondrial depolarization and cytochrome *c* release followed by caspase-3 activation<sup>6</sup>. It has been reported that resveratrol has the ability to selectively induce apoptosis in leukemic cells lines but not in normal haematopoietic cells<sup>7</sup>. The p53 gene is one of the most important tumour suppressor genes, and mutation or loss of this gene is believed to be responsible for more than half of human cancers<sup>8</sup>. The p53 gene is critical for apoptosis and lack of p53 expression or function is associated with an increased risk of tumour formation. Resveratrol induces p53 dependent transcriptional activation. Resveratrol triggered apoptosis occurs in cells expressing p53 but not in p53 deficient cells. This resveratrol-induced activation of p53 is also partly due to the activities of extracellular signal regulated protein kinases and p38 kinase and their phosphorylation of p53 at serine 15 that plays a critical role in the stabilization, up-regulation and functional activation of p53<sup>9</sup>.

The biological evaluation of resveratrol derivatives has focussed on assessing the inhibition against leukemic cell lines<sup>10</sup>. Protection of the hydroxyl groups by esters and ethers has provided potent cell growth inhibitors of leukaemia. Few published inhibitors have reached the levels of bioactivity of resveratrol, with the 4'-acetyl derivative **152** showing slightly better potency than that of resveratrol. This analogue was part of a series synthesised and tested against human leukaemia HL-60 cells<sup>10</sup>. 3,5-Dihydroxy-4'-acetoxystilbene prepared by Andrus *et al* had an ED<sub>50</sub> of 17 µM, which when compared to that of resveratrol (23 µM), shows a slight improvement. The introduction of a fluorine atom often brings about an improvement in bioactivity mainly due to the alteration of metabolism and increased lipophilicity. Fluorination of the resveratrol structure has also been reported over the past few years, with fluorine substitution on the central vinyl double bond being reported in 2001<sup>11</sup>. Andrus *et al* have also synthesised fluorinated stilbene derivatives, maintaining the resveratrol substitution pattern and replacing the hydroxyl groups with fluorine atoms. However in this report it is stated that they were unable to assess toxicity profiles in leukaemia cell lines for these fluorinated analogues<sup>10</sup>. Contrary to this statement, identical analogues of resveratrol were prepared at the same time in our laboratory<sup>12</sup>. Testing of these derivatives was carried out on non-small cell lung carcinoma cell lines. Results generated in our laboratory have shown that these fluorinated analogues possess levels of bioactivity comparable to the parent compound resveratrol **136**, and in some cases increased potency was found. Preliminary biological assays carried out by the National Cancer Institute (NCI) have indicated that various fluorinated analogues synthesised in our laboratory exhibited anticancer activity against a variety of tumour cell lines<sup>12</sup>.

It is hoped that by maintaining the resveratrol substitution pattern and utilising fluorine substitution, the production of potent selective drugs with anticancer activity can be achieved. Also by way of a further modification, an alteration of the resveratrol structure, utilising a known hydroxyl chemical-isostere, the amino group, greater chemotherapeutic effects can be observed.

## 8.2 Lung cell carcinoma assays

For the purpose of this project, the bioactivity of resveratrol derivatives was assessed by assaying against non-small cell lung carcinoma cell lines. The *in vitro* model chosen for investigating the potential of the resveratrol compounds was the DLKP-A cell line. The DLKP-A cell line is a daughter cell line of DLKP, a poorly differentiated squamous cell lung carcinoma. DLKP-A's main mechanism of multidrug resistance (MDR) is via the P-glycoprotein (P-gp) membrane pump. It highly expresses P-gp, while expressing very low levels of multidrug resistance protein 1 (MRP1). Derivatives that showed inhibitory potency against the lung cell lines were then subjected to further investigations into their bioactivity when combined with a known chemotherapeutic agent. The known active agent used for combination studies was epirubicin **190**.



Multidrug resistance (MDR) is a major cause of failure of cancer chemotherapy. MDR is a phenomenon whereby tumour cells *in vitro* that have been exposed to one cytotoxic agent develop cross-resistance to a range of structurally and functionally unrelated compounds. This resistance is often due to the elevation in the expression of particular proteins, such as cell membrane transporters, which can result in an increased efflux of cytotoxic drugs from the cancer cells<sup>13</sup>. The protein of interest in this report is P-glycoprotein (P-gp). It is a member of the ATP-binding cassette (ABC) family. The protein binds ATP and uses the energy to drive the transport of various molecules across all cell membranes. P-gp is a transmembrane protein with a very broad specificity to the substrates it pumps out of the cells. One effective way of overcome P-gp-mediated drug resistance is either to block its drug pump function or to inhibit its expression. Many agents that modulate the function of P-gp have been identified, including calcium channel blockers, calmodulin antagonists, steroidal



agents, protein kinase C inhibitors, immunosuppressive drugs, antibiotics, and surfactants<sup>14</sup>.

A cross section of some 13 compounds synthesised were selected for biological investigation. A commercially purchased sample of resveratrol **136** (Sigma Aldrich, *R5010*) was used as a control in all assays performed. These compounds were firstly selected on their solubility properties in aqueous solutions. Dimethylsulphoxide was used to solubilise the compounds in question, before solubility of the solution was tested in media. A minimum concentration of 0.5 mg/ml in the media was required for a compound to undergo biological evaluation. This is due to the adverse effects of DMSO on the cells. Of the resveratrol derivatives reported in this thesis, thirteen analogues passed the preliminary solubility test and were subsequently assessed for bioactivity.

### 8.3 Biological Results

As a control and for comparison purposes assays on both cell lines, DLKP and DLKP-A, were performed with resveratrol **136**. Combination assays with the chemo drug epirubicin **190** were also carried out. An  $IC_{50}$  value of  $10 \pm 2 \mu\text{M}$  was calculated for resveratrol with DLKP while a value of  $15 \pm 3 \mu\text{M}$  was found when assayed against the daughter cell line DLKP-A. The bar charts shown in *Figure 8.1* and *8.2* demonstrate the increase in activity when **136** is combined with the P-glycoprotein substrate, epirubicin.

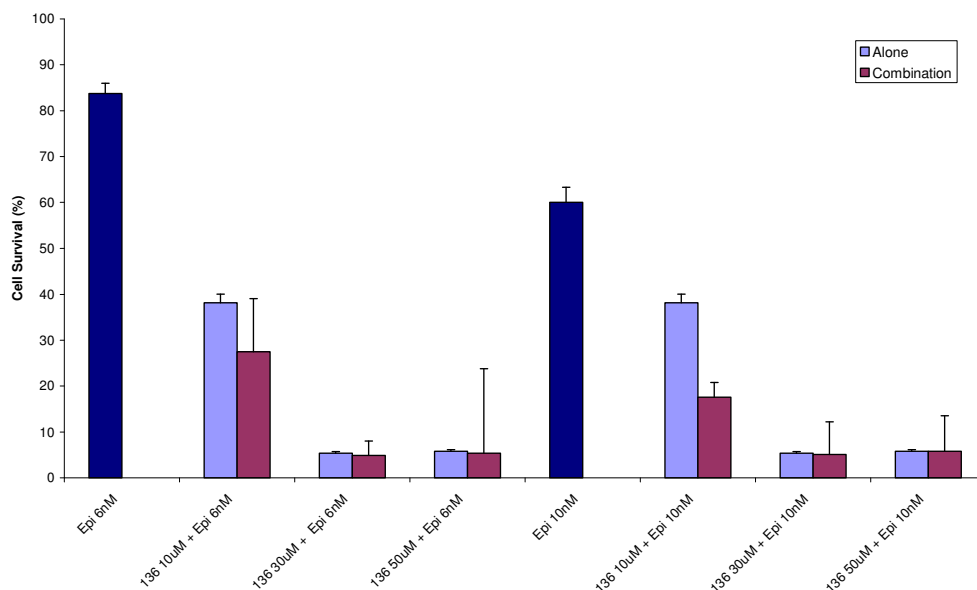


**Figure 8.1:** Combination assay of **136** with epirubicin on the DLKP cell line.

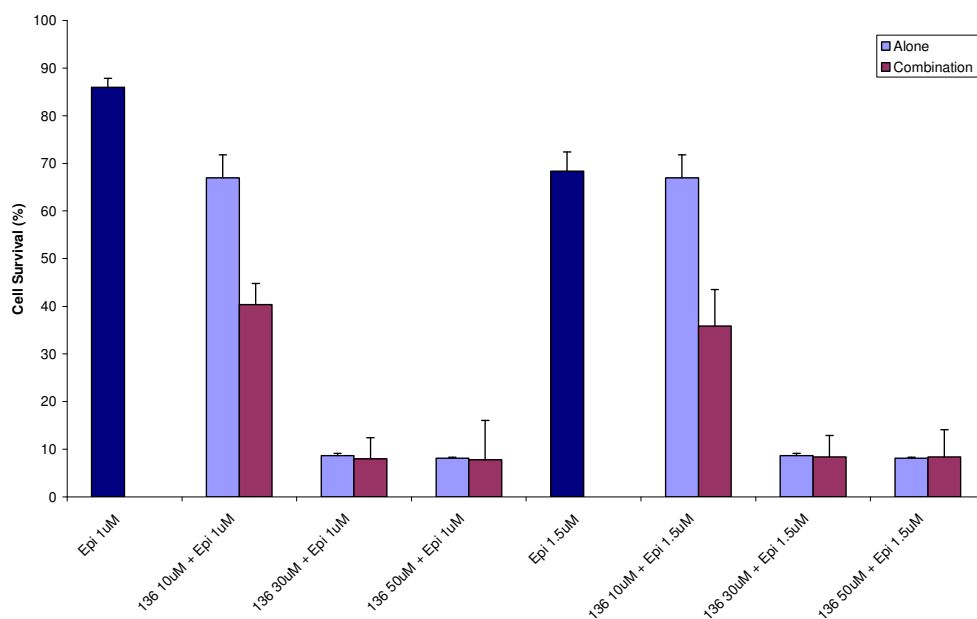


**Figure 8.2:** Combination assay of **136** with epirubicin on the DLKP-A cell line.

In the DLKP assay, resveratrol inhibits growth by over 60% at the lowest concentration used. Some synergy is noted with this combination (Epi 10 nM and Res 10 µM). In the assay of cell line DLKP-A, resveratrol causes a 50% growth inhibition at 15 ± 3 µM. In combination with epirubicin synergy is consistently observed in this P-glycoprotein rich cell line.

The *trans*-fluorinated nitrostilbenes (**156** & **175**), were tested for bioactivity and also for their effect when in combination with the drug, epirubicin. Solubility was an issue with these *trans*-derivatives, with the 4'-nitro remaining in solution only at 1 mg/ml and the 3,5-nitro only just remaining soluble at the limit of 0.5 mg/ml. However, as with the reduced stilbene structure **171** these *trans*-nitro compounds, both 4'-NO<sub>2</sub> and 3,5-NO<sub>2</sub>, showed no cell kill when assayed with the lung cancer cell line. (*E*)-3,5-Difluoro-4'-nitrostilbene **156** showed no alteration in the bioactivity levels in the combination tests while the (*E*)-3,5-dinitro analogue **175** was found to be slightly antagonist in combination with epirubicin. The *cis*-isomers (**157** & **176**) of the respective nitro compounds both failed the solubility pretest so biological activity could not be assessed.

The amino derivatives were then subjected to testing. The *trans*-amino-isomers (**158** & **177**) and the *cis*-amino analogue **159**, were subjected to biological investigation. (*E*)-3,5-Difluoro-4'-aminostilbene **158** was readily soluble although when tested, results indicated that the presence of this potential inhibitor had an adverse effect and actually increased cell growth. No effect was seen for the drug interaction study with epirubicin. (*Z*)-3,5-Difluoro-4'-aminostilbene **159** showed identical results to the corresponding *trans*-isomer, increasing DLKP-A growth and showing no effect in combination assays. However, the *trans*-diamino compound **177** showed positive results in the DLKP and DLKP-A assays, albeit with weak potency. The calculated IC<sub>50</sub> for this compound, with respect to both cell lines was outside the parameters of the experiment design (> 50 μM). At 50 μM, analogue **177** caused 22 ± 3 % and 10 ± 3 % cell kill in the DLKP and DLKP-A cell lines, respectively. Compound **177** shows minimal growth inhibition at 50 μM. When in combination with epirubicin an increase in activity was observed, as can be seen in **Figure 8.3**. This suggests that the alteration made to the structure had no effect on toxicity but may enhance the effects of epirubicin.

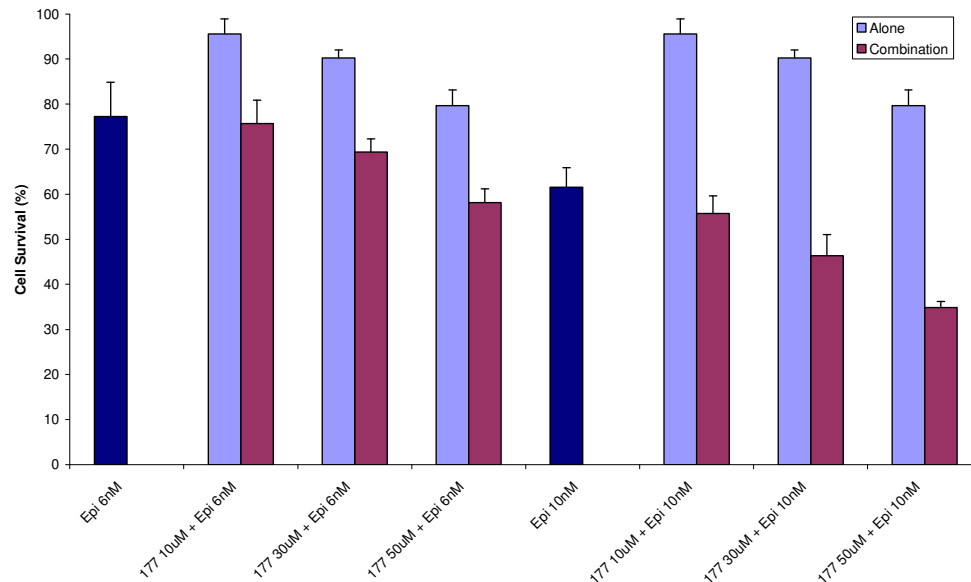


**Figure 8.3:** Combination assay of **177** with epirubicin on the DLKP cell line.

Both of the *cis*-carbamyl derivatives (**163** & **164**) proved soluble enough for determination of biological potency with the lung cancer cell lines. The dimethylcarbamoyl derivative **163** displayed an increase in the cell growth after assay incubation and was shown to have an antagonistic effect when combined with the known P-gp substrate, epirubicin. The morpholine analogue **164** showed no effect in either assay, by itself or in combination. These results along with the results of other *cis*-isomers tested shows that the *trans*-orientation is indeed necessary for activity.

	<b>136</b>	<b>161</b>	<b>169</b>	<b>177</b>	<b>181</b>	<b>182</b>	<b>188</b>
<b>DLKP</b>	10 ± 2	39 ± 2	unknown	> 50	> 50	28 ± 4	unknown
<b>DLKP-A</b>	15 ± 3	n/a*	20 ± 10	> 50	> 50	n/a*	> 50

**Table 8.1:** IC<sub>50</sub> values (µM) of selected resveratrol derivatives on the non-small lung cell carcinoma cell lines, DLKP and DLKP-A.

\*Due to DMSO effects, IC<sub>50</sub> calculations not possible

Of the *trans*-amino-substituted compounds tested, both acetyl (**161** & **181**) and the ditrifluoroacetyl compound **182** were viable candidates for potency analysis. The 4'-trifluoroacetyl derivative **162** failed to remain fully in solution when added to media.

The three soluble compounds were subjected to assays with both DLKP and its daughter cell line, DLKP-A. From the results of the biological tests on the DLKP cell line, the calculated  $IC_{50}$  of the 4'-acetyl derivative **161** was found to lie above 30  $\mu\text{M}$ . The corresponding alternative compound, the 3,5-diacetyl analogue **181** had a calculated  $IC_{50}$  greater than 50  $\mu\text{M}$ , which is outside the parameters of the experimental design. Of all the stilbene compounds tested, the best  $IC_{50}$  value recorded was seen for the ditrifluoroacetyl compound **182**. It was found to have a 50% inhibitory concentration ( $IC_{50}$ ) of  $28 \pm 4 \mu\text{M}$  against the DLKP cell line. Although the diacetyl derivative had  $IC_{50}$ 's greater than 50  $\mu\text{M}$  for both cell lines, it was estimated from the assay data that at a concentration of 50  $\mu\text{M}$ , there was a 32 and 44 percentage reduction in cell proliferation in DLKP and DLKP-A cell lines. As can be seen in *Table 8.1*, for the 4'-acetyl **161** and the di(trifluoroacetyl) **182** compounds an  $IC_{50}$  value was not possible to determine due to the effects of DMSO on the DLKP-A assays.

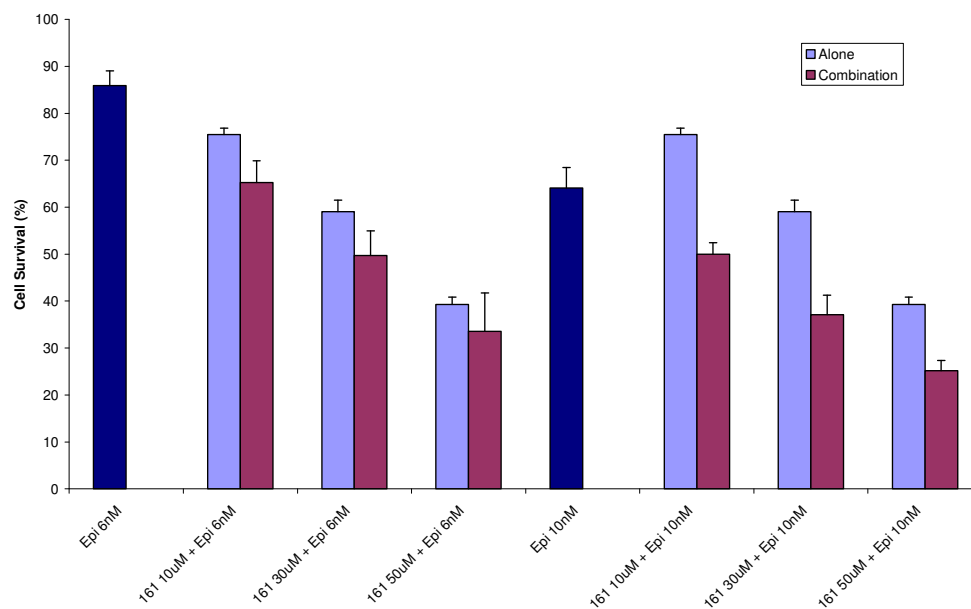


**Figure 8.4:** Combination assay of **161** with epirubicin on the DLKP cell line.

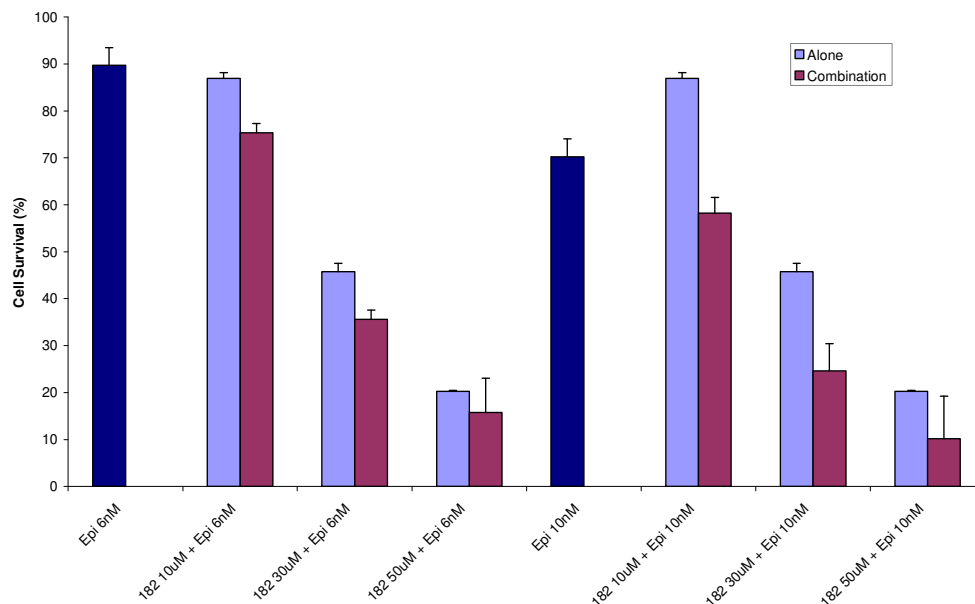


**Figure 8.5:** Combination assay of **182** with epirubicin on the DLKP cell line.

*Figures 8.4* and *8.5* show bar charts demonstrating the increases in activity on the DLKP cell line when stilbenes **161** and **182** are in combination with epirubicin. At a concentration of  $39 \pm 2 \mu\text{M}$ , **161** inhibits growth by 50%, which when compared to that of resveratrol is less toxic. When in combination with epirubicin, an increase in activity is observed. This also suggests that the alterations made to the structure decrease its toxicity while maintaining its ability to interact with pathways relevant to chemotherapy response in the cell. For the ditrifluoroacetyl stilbene **182**, the  $\text{IC}_{50}$  concentration was determined to be of  $28 \pm 4 \mu\text{M}$ . This is again less toxic than resveratrol. As with the other compounds tested and reported so far, when in combination with epirubicin synergy is seen in the DLKP-A cell line.

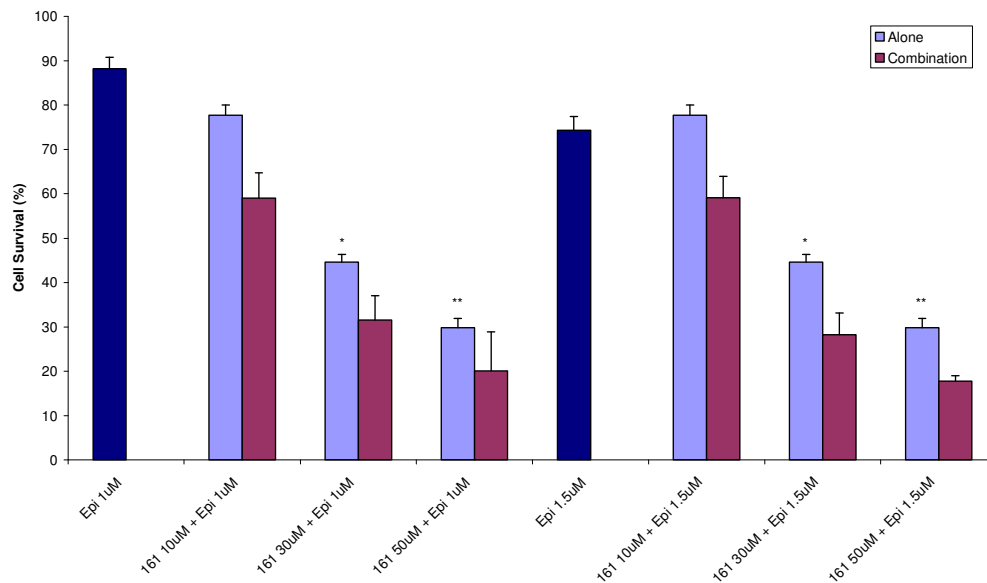


**Figure 8.6:** Combination assay of **161** with epirubicin on the DLKP-A cell line.

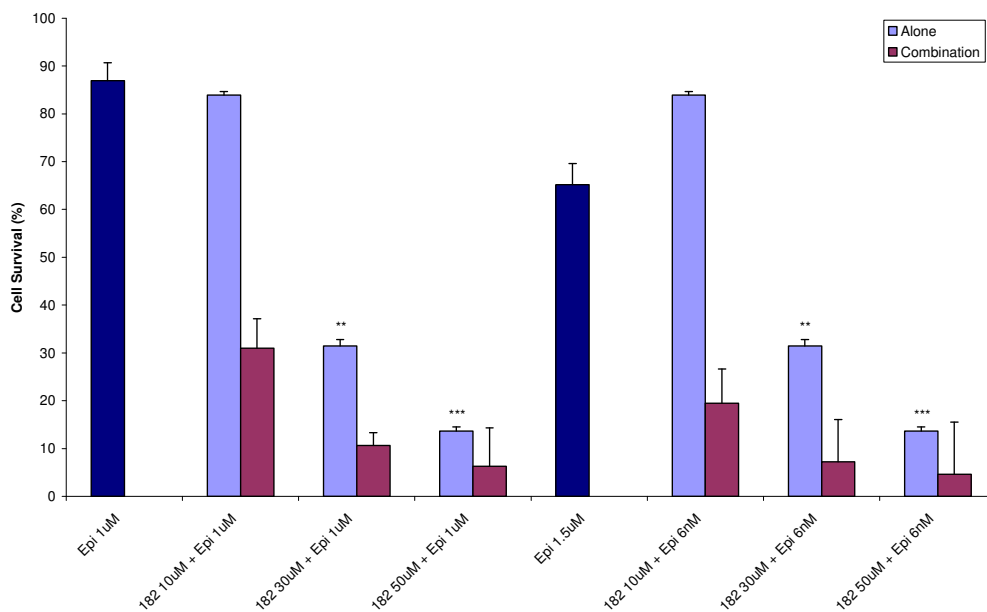


**Figure 8.7:** Combination assay of **182** with epirubicin on the DLKP-A cell line.

**Figure 8.6** illustrates the effect that the analogue **161** can have on the DLKP-A cell line alone and in combination with the known chemotherapeutic drug epirubicin **190**. The IC<sub>50</sub> of **161** is not achievable using this method of analysis due to the adverse effects of DMSO on the cells at the higher concentrations (indicated by stars). However, the combination of 1  $\mu$ M or 1.5  $\mu$ M epirubicin with 10  $\mu$ M stilbene **161**

yields an additive interaction in this cell line. Significant increases in the activity when combined are evident, compared to the values seen individually. As with **161**, the IC<sub>50</sub> of **182** is not achievable due to DMSO concentration (indicated by stars). But again when the combination of 10 µM **182** with 1 µM or 1.5 µM epirubicin is studied, synergy is evident in the DLKP-A cell line.

**Note:**

*Analogue **161** at 10 µM requires a 1% DMSO solution while **182** requires a 1.5% DMSO solution but this has a negligible effect on cell survival.*

\* ***161** 30 µM requires a 3% DMSO solution and causes 10% growth inhibition.*

\*\* ***161** 50 µM and **182** 30 µM, require a 5% DMSO solution and causes 44% growth inhibition.*

\*\*\* ***182** 50 µM requires an 8.6% DMSO solution and causes 70% growth inhibition.*

The final two compounds in this project that were tested were the amino acid salts. Only the deprotected compounds were assayed due to solubility, being caused by the large aliphatic *t*-butyl moiety of the protection group. Once deprotected there was no issue with solubility or with DMSO effects as the deprotected amino acids were isolated as trifluoroacetate salts. This salt formation made the stilbene analogues highly hydrophilic and therefore no DMSO was required to solubilise the products. Both glycine salt analogues (**169** & **188**) were assayed against both the DLKP and DLKP-A cell lines and in combination with the drug epirubicin **190**. The 4'-glycine analogue **169** inhibited cell growth by 20% at 10 µM but when the concentration was increased to 30 µM, the growth inhibition increased to 100%. From this we can conclude that the IC<sub>50</sub> of compound **169** is in the region between 10-30 µM, for the DLKP cell line. The IC<sub>50</sub> of the 3,5-di(glycine) salt **182** was found to be greater than 50 µM and therefore not viable for further individual assay investigations.



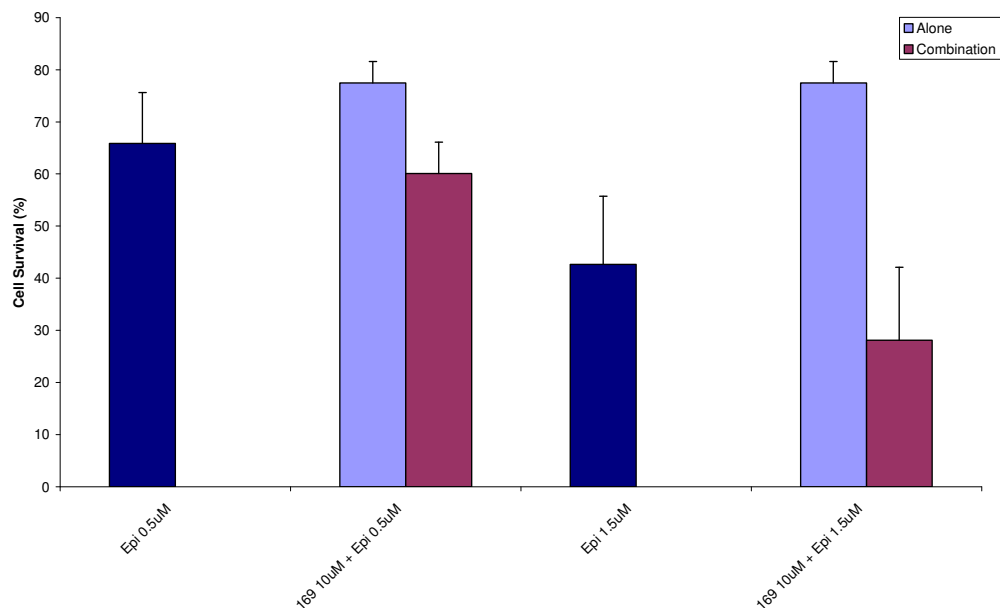


**Figure 8.8:** Combination assay of **169** with epirubicin on the DLKP-A cell line.

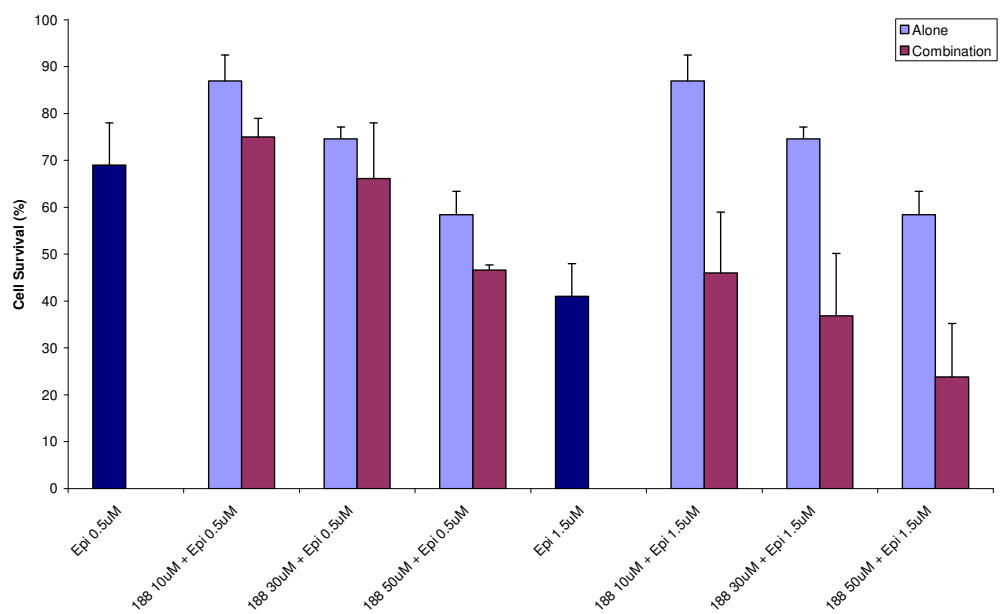


**Figure 8.9:** Combination assay of **188** with epirubicin on the DLKP-A cell line.

From the chart displayed in **Figure 8.8**, we can see the epirubicin has inhibits cell growth by 35% at a concentration of 0.5 µM in DLKP-A, and 58 % when the concentration is increased to 1.5 µM. The 4'-glycine analogue **169** when tested with DLKP-A at 10 µM inhibited growth by 22%. However, when this was combined with

epirubicin (0.5  $\mu\text{M}$ ) the growth inhibition increased to 40% and when the higher concentration of epirubicin was used (1.5  $\mu\text{M}$ ) it increased to almost 74%. Therefore at the higher concentration, the increase was greatest, increasing by almost 28% compared to epirubicin alone.

*Figure 8.9* shows the results from the DLKP-A assays of the di(glycine) salt **188** and epirubicin. As seen in all of the combination assays epirubicin alone inhibits growth by approximately  $30 \pm 7\%$  at a concentration of 0.5  $\mu\text{M}$  and  $60 \pm 8\%$  at 1.5  $\mu\text{M}$ . This bar chart shows combination assays for both P-gp substrate concentrations and at three different stilbene concentrations. It is clear that, as with all the other stilbene compounds that were tested, a noticeable increase in activity is found when both compounds are combined. This amino acid derivative however only really starts to show a significant effect when the concentrations are increased to 50  $\mu\text{M}$ .

A side investigation into the importance of the basic 3,4',5-substitution pattern and the central vinylic bond was assessed by bioassay. Compounds **170-173** were analysed for solubility in the media. From this preliminary screen only the amino version of the diphenylethene analogue **171** was sufficiently soluble to carry out the bioassay against the cell lines, DLKP and DLKP-A. The ethylene derivative **171** was found to remain in solution up to a concentration of 5 mg/ml. However, when assayed with DLKP-A, no effect was seen. When combined with the known chemotherapeutic epirubicin **190**, neither an increase nor decrease in the effect of the drug was seen. This investigation emphasises the importance of the maintaining the basic structure of the resveratrol compound. Whether it is for active site binding factors or for basic solubility reasons, substitutions of both phenyl rings and more importantly maintaining the central vinylic bond are essential.

## 8.4 References

1. Athar, M., Back, J.H., Tang, X., Kim, K.H., Kopelovich, L., Bickers, D.R., Kim, A.L.; *Tox. App. Pharmac.* **2007**, 224, 274.
2. Pettit, G.R., Grealish, M.P., Jung, M.K., Hamel, E., Pettit, R.K., Chapuis, J.C., Schmidt, J.M.; *J. Med. Chem.* **2002**, 45, 2534.
3. <http://www.cancer.gov/cancertopics/what-is-cancer>
4. Aziz, M.H., Kumar, R., Ahmad, N.; *Int. J. Oncol.* **2003**, 23, 17.
5. Ingle, J.N.; *Cancer* **2008**, 112, 695.
6. Fulda, S., Debatin, K.-M.; *Cancer Res.* **2004**, 64, 337.
7. Gao, X., Xu, Y.X., Divine, G., Janakiraman, N., Chapman, R.A., Gautam, S.C.; *J. Nutr.* **2002**, 132, 2076.
8. Dong, Z.; *Mutat. Res.* **2003**, 523-524, 145.
9. She, Q.B., Bode, A.M., Ma, W.Y., Chen, N.Y., Dong, Z.; *Cancer Res.* **2001**, 61, 1604.
10. Andrus, M.B., Liu, J.; *Tet. Lett.* **2006**, 47, 5811.
11. Eddarir, S., Abdelhadi, Z., Rolando, C.; *Tet. Lett.* **2001**, 42, 9127.
12. Anderson, F.P.; “*The synthesis, structural characterisation and biological evaluation of potential chemotherapeutic agents*”, Dublin City University, *PhD Thesis*, **2005**.
13. Thomas, H., Coley, H.M.; *Cancer Control* **2003**, 10, 2, 159.
14. Ferry, D.R., Traunecker, H., Kerr, D.J.; *Eur. J. Cancer* **1996**, 6, 32A, 1070.

## 9.0 Conclusion

In summary, the synthesis and structural characterisation of novel analogues of the stilbene resveratrol was performed. By maintaining the basic resveratrol substitution pattern, derivatives were synthesised with a variety of different atoms and functional groups as substituents. This was achieved with the aim of emulating or surpassing the biological potency of the parent compound resveratrol. Previous work in our laboratory has shown that replacement of the hydroxyl groups by fluorine atoms has minor effects on the biological activity of the stilbene analogues. Bearing this in mind, two contrasting series of fluorinated analogues were synthesised, one with 3,5-fluorine substitution on the 'A' ring and the other with the 4'-hydroxyl replaced with a fluorine. In remaining resveratrol substitution sites, 4'- and 3,5-, respectively, the known hydroxyl chemical isostere, the amino group, was utilised. These fluoro-amino resveratrol derivatives were synthesised from reduction of the corresponding nitro groups. Amino-substituted analogues were also prepared for comparison to hydroxylated derivatives previously reported.

The importance of key components of the resveratrol structure was also investigated and evaluated on their bioactivity. From results gathered it is shown that the central saturated unit of the stilbene structure is critical for maintaining the potency, as is the substitution pattern of the phenyl rings.

Although computer modelling studies of the interaction and binding site of resveratrol have yet to be carried out, it is clear from assays performed, that a few areas of the resveratrol structure are critical for maintaining bioactivity. Firstly, as only the *trans*-isomer of resveratrol shows activity, it can be stated that the planar orientation must be maintained. This was demonstrated in the synthesis of a variety of *cis*-analogues which all showed no effect when tested with cancer cells. Steric repulsion of the phenyl rings and substituents renders the *cis*-isomer non-planar. Another factor is that as resveratrol is such a small simple molecule, this may be the reason for the vast array of biological properties reported. Therefore, preserving the simplicity of the molecule must be an integral part of the design suitable derivatives. For this reason it was attempted to keep the substituents as small and as simple as possible.

Solubility was a major factor in the search for increased activity with the nitro compounds and this led to the synthesis of amino acid derivatives. Although once deprotected, solubility problems did not occur, although the bulk and flexibility of a side chain was a concern. The assays performed on these showed a similar pattern to the amino analogues.

Biological evaluation of these fluoro-amino derivatives was assessed by the interaction with non-small lung cell carcinomas. Solubility was a constant factor in the assays and was the cause of many problems due to required levels of dimethylsulphoxide. From the preliminary results of the assays performed it can be assumed that replacement of the hydroxyl moiety by a nitro or an amino group does not increase the activity, however certain analogues developed have shown encouraging results when in combination with a known chemotherapeutic drug.

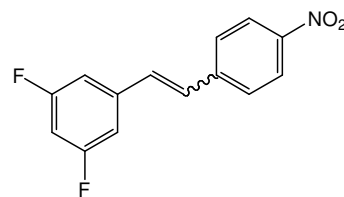
These results indicate that fluorinated amino analogues of resveratrol have the potential to be active inhibitors of carcinogenesis but require further modification. It is hoped that derivatisation of the amino analogues will improve the potency of these derivatives

## 10.0 Experimental

All chemicals were purchased from Sigma-Aldrich, Lennox Chemicals or Fluorochem Limited; and used as received. Commercial grade reagents were used without further purification. When necessary all solvents were purified and dried; and stored under argon. Triethylamine distilled and stored over potassium hydroxide pellets. Riedel-Haën silica gel was used for thin layer and column chromatography. Melting point determinations were carried out using a Stuart melting point (SMP3) apparatus and are uncorrected. Elemental Analysis was carried out by the Microanalytical Laboratory at University College Dublin. Electrospray ionisation mass spectra were obtained on a Bruker Esquire 3000 series ion trap mass spectrometer. IR spectra were obtained on a Perkin-Elmer Spectrum GX FT-IR system. UV spectra were obtained on a UV-Vis-NIR Perkin-Elmer Lambda 900 spectrometer. NMR spectra were obtained on a Bruker AC 400 NMR spectrometer operating at 400 MHz for  $^1\text{H}$  NMR, 376 MHz for  $^{19}\text{F}$  NMR and 100 MHz for  $^{13}\text{C}$  NMR. The  $^1\text{H}$  and  $^{13}\text{C}$  NMR chemical shifts ( $\delta$ ) are relative to trimethylsilane and the  $^{19}\text{F}$  NMR chemical shifts ( $\delta$ ) are relative to trifluoroacetic acid. All coupling constants ( $J$ ) are in Hertz (Hz).

### ***(E/Z)*-3,5-difluoro-4'-nitrostilbene 156/157**

3,5-Difluorobenzyl triphenyl phosphonium bromide (11.7 g, 25 mmol) and 4-nitrobenzaldehyde (4.7 g, 31.25 mmol) were dissolved in dichloromethane (150 ml) and stirred at room temperature. A 50% w/v sodium hydroxide solution was added dropwise to the stirred solution [0.4ml NaOH solution per 1 mmol of aldehyde]. The solution was stirred at room temperature for 1 hour then washed with brine and water. The solvent was removed *in vacuo* to yield both isomers as a yellow solid. Recrystallisation from ethanol gave the *trans* isomer as a bright yellow powder **156** (3.2 g, 49%). Crystals of **156** suitable for X-ray analysis were grown from toluene. The resulting mother liquor was evaporated to dryness to yield the *cis* product as a pale yellow powder **157** (3.0 g, 46%).



### ***Trans* isomer (156)**

m.p. 199-201 °C

Anal. calcd. for  $\text{C}_{14}\text{H}_9\text{NO}_2\text{F}_2$ : C, 64.37; H, 3.47; N, 5.36.

Found C, 64.12; H, 3.47; N, 5.21

IR (KBr):  $\nu$  3085, 2929, 2831, 2442, 2209, 1927, 1793, 1726, 1618, 1589, 1509, 1439, 1336, 1116, 974, 865, 748, 707, 691, 665  $\text{cm}^{-1}$ .

UV ( $\lambda_{\text{max}}$ ) (ACN): 337 nm.

$^1\text{H}$  NMR (400 MHz,  $\text{DMSO-}d_6$ ):  $\delta$  8.27 (2H, d,  $J = 8.8$  Hz, -ArH 3' & 5'), 7.86 (2H, d,  $J = 9.2$  Hz, -ArH 2' & 6'), 7.59 (1H, d,  $J = 16.4$  Hz, -CH), 7.51 (1H, d,  $J = 16.4$  Hz, -CH-), 7.43 (2H, m, -ArH 2 & 6), 7.21 (1H, tt,  $J = 2.4$  & 9.2 Hz, -ArH 4).

$^{13}\text{C}$ -NMR (100 MHz,  $\text{DMSO-}d_6$ ):  $\delta$  162.8 (d,  $J = 244.2$  Hz, -CF), 162.6 (d,  $J = 244.0$  Hz, -CF), 146.6 (-ArC 4'), 143.1 (-ArC 1'), 140.2 (t,  $J = 9.9$  Hz, -ArC 1), 130.8 (-CH), 129.3 (-CH), 127.6 (-ArC 2' & 6'), 124.1 (-ArC 3' & 5'), 109.9 (d,  $J = 25.6$  Hz, -ArC 2 & 6), 103.6 (t,  $J = 25.9$  Hz, -ArC 4).

$^{19}\text{F}$ -NMR (376 MHz,  $\text{DMSO-}d_6$ ):  $\delta$  -109.82 (2F, t,  $J = 9.4$  Hz.).

#### **Cis isomer (157)**

m.p. 73-75  $^{\circ}\text{C}$

Anal. calcd. for  $\text{C}_{14}\text{H}_9\text{NO}_2\text{F}_2$ : C, 64.37; H, 3.47; N, 5.36.

Found C, 64.35; H, 3.67; N, 5.16

IR (KBr):  $\nu$  3106, 3081, 2836, 2442, 1928, 1640, 1587, 1503, 1447, 1432, 1340, 1321, 1179, 1127, 1104, 996, 970, 882, 860, 842, 767, 750, 732, 695, 666  $\text{cm}^{-1}$ .

UV (ACN):  $\lambda_{\text{max}}$  314 nm.

$^1\text{H}$  NMR (400 MHz,  $\text{DMSO-}d_6$ ):  $\delta$  8.17 (2H, d,  $J = 9.2$  Hz, -ArH 3' & 5'), 7.48 (2H, d,  $J = 8.4$  Hz, -ArH 2' & 6'), 7.17 (1H, tt,  $J = 2.4$  & 9.4 Hz, -ArH 4) 6.84-6.92, (4H, m, -ArH 2 & 6, -CH, -CH).

$^{13}\text{C}$ -NMR (100 MHz,  $\text{DMSO-}d_6$ ):  $\delta$  162.4 (d,  $J = 245.0$  Hz, -CF), 162.3 (d,  $J = 244.7$  Hz, -CF), 146.4 (-ArC 4'), 143.0 (-ArC 1'), 139.6 (t,  $J = 9.9$  Hz, -ArC 1), 130.9 (-CH), 130.4 (-CH), 129.8 (-ArC 2' & 6'), 123.7 (-ArC 3' & 5'), 111.6 (d,  $J = 25.5$  Hz, -ArC 2 & 6), 103.3 (t,  $J = 25.8$  Hz, -ArC 4).

$^{19}\text{F}$ -NMR (376 MHz,  $\text{DMSO-}d_6$ ):  $\delta$  -109.57 (2F, t,  $J = 8.0$  Hz.).

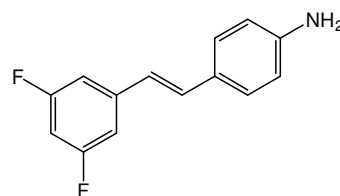
#### **(E)-3,5-difluoro-4'-aminostilbene 158**

(E)-3,5-difluoro-4'-nitrostilbene (1.42 g, 5.4 mmol)

was dissolved in a 10:1 mixture of ethanol and acetic acid (22 ml) and heated to reflux temperature. Iron

(III) chloride hexahydrate (0.25 g, 0.93 mmol),

followed by iron pindust (2.22 g, 39.7 mmol) was added with vigorous stirring and



the solution refluxed for 3 hours. The solution was filtered and diluted with water. The product was extracted with diethyl ether and dried over sodium sulphate. Purification by column chromatography with hexane/ethyl acetate as eluant yielded compound **158** as a brown powder (1.1 g, 88%).

m.p. 110-112 °C

Anal. calcd. for C<sub>14</sub>H<sub>11</sub>NF<sub>2</sub>: C, 72.72; H, 4.79; N, 6.06.

Found C, 72.48; H, 4.90; N, 5.97

Mass Spectrum: [M+H]<sup>+</sup> found 232.4

C<sub>14</sub>H<sub>12</sub>NF<sub>2</sub> requires, 232.24

IR (KBr):  $\nu$  3483, 3466, 3396, 3380, 3206, 3091, 3025, 1894, 1617, 1586, 1447, 1429, 1312, 1268, 1183, 1138, 1116, 997, 979, 965, 881, 839, 818, 670 cm<sup>-1</sup>.

UV (ACN):  $\lambda_{\max}$  315 nm; 242 (sh), 339 (sh) nm.

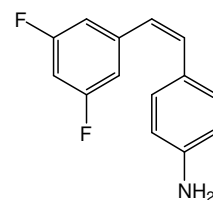
<sup>1</sup>H NMR (400 MHz, DMSO-*d*<sub>6</sub>):  $\delta$  7.20-7.30 (5H, m, -ArH 2', 6', -CH, -ArH 2 & 6), 7.00 (1H, tt, *J* = 2.2 & 9.4 Hz, -ArH 4), 6.89 (1H, d, *J* = 16.4 Hz, -CH), 6.57 (2H, d, *J* = 8.4 Hz, -ArH 3' & 5'), 5.45 (2H, s, -NH<sub>2</sub>).

<sup>13</sup>C-NMR (100 MHz, DMSO-*d*<sub>6</sub>):  $\delta$  162.7 (d, *J* = 242.9 Hz, -CF), 162.6 (d, *J* = 243.0 Hz, -CF), 149.4 (-ArC 4'), 142.1 (t, *J* = 9.8 Hz, -ArC 1), 132.1 (-CH), 128.1 (-ArC 2' & 6'), 123.7 (-ArC 1'), 120.3 (-CH), 113.7 (-ArC 3' & 5'), 108.2 (d, *J* = 25.1 Hz, -ArC 2 & 6), 101.2 (t, *J* = 26.1 Hz, -ArC 4).

<sup>19</sup>F-NMR (376 MHz, DMSO-*d*<sub>6</sub>):  $\delta$  -110.55 (2F, t, *J* = 7.5 Hz).

### **(Z)-3,5-difluoro-4'-aminostilbene 159**

(Z)-3,5-difluoro-4'-nitrostilbene (1.0 g, 3.8 mmol) was dissolved in a 10:1 mixture of ethanol and acetic acid (22 ml) and heated to reflux temperature. Iron (III) chloride hexahydrate (0.18 g, 0.65 mmol), followed by iron pindust (1.56 g, 28.0 mmol) was added with vigorous stirring and the solution refluxed for 3 hours. The



solution was filtered and diluted with water. The product was extracted with diethyl ether and dried over sodium sulphate. Purification by column chromatography with hexane/ethyl acetate as eluant furnished **159** as a brown oil (1.0 g, 80%).

b.p. 180-185 °C

Anal. calcd. for C<sub>14</sub>H<sub>11</sub>NF<sub>2</sub>: C, 72.72; H, 4.79; N, 6.06.

Found C, 72.52; H, 4.93; N, 5.88



IR (ATR):  $\nu$  3461, 3372, 3214, 3010, 1616, 1603, 1583, 1514, 1445, 1429, 1307, 1176, 1113, 988, 966, 871, 830, 794, 666  $\text{cm}^{-1}$ .

UV (ACN):  $\lambda_{\text{max}}$  238 nm; 314, 336(sh) nm.

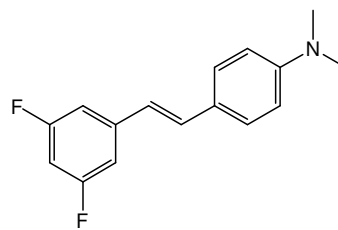
$^1\text{H}$  NMR (400 MHz,  $\text{DMSO-}d_6$ ):  $\delta$  7.05 (1H, tt,  $J = 2.2$  & 9.2 Hz, -ArH 4) 6.93 (4H, d,  $J = 8.4$  Hz, -ArH 2, 6, 2' & 6'), 6.55 (1H, d,  $J = 12.4$  Hz, -CH), 6.46 (2H, d,  $J = 8.4$  Hz, -ArH 3' & 5'), 6.29 (1H, d,  $J = 12.4$  Hz, -CH), 5.34 (2H, s, - $\text{NH}_2$ ).

$^{13}\text{C}$ -NMR (100 MHz,  $\text{DMSO-}d_6$ ):  $\delta$  162.3 (d,  $J = 243.8$  Hz, -CF), 162.2 (d,  $J = 243.7$  Hz, -CF), 148.7 (-ArC 4'), 141.6 (t,  $J = 9.9$  Hz, -ArC 1), 133.0 (-CH), 129.7 (-ArC 2' & 6'), 123.3 (-CH), 122.8 (-ArC 1'), 113.4 (-ArC 3' & 5'), 111.2 (d,  $J = 25.1$  Hz, -ArC 2 & 6), 102.0 (t,  $J = 25.8$  Hz, -ArC 4).

$^{19}\text{F}$ -NMR (376 MHz,  $\text{DMSO-}d_6$ ):  $\delta$  -110.47 (2F, t,  $J = 8.8$  Hz).

### **(E)-3,5-difluoro-4'-dimethylaminostilbene 160**

3,5-Difluorobenzyl triphenyl phosphonium bromide (2.5 g, 5.33 mmol) and 4-dimethylaminobenzaldehyde (0.99 g, 6.66 mmol) were dissolved in dichloromethane (40 ml) and stirred at room temperature. A 50% w/v sodium hydroxide solution (2.6 ml) was added



dropwise to the vigorously stirred solution [0.4ml NaOH solution per 1 mmol of aldehyde] stirring continued at room temperature for a further 3 hours before washing with brine and water. The solvent was removed *in vacuo* to yield a mixture of isomers. Recrystallisation from ethanol gave the *trans* product **160** as yellow crystals (0.45 g, 32%).

m.p. 139-141  $^{\circ}\text{C}$

Anal. calcd. for  $\text{C}_{16}\text{H}_{15}\text{NF}_2$ : C, 74.11; H, 5.83; N, 5.40.

Found C, 74.19; H, 5.96; N, 5.38

IR (KBr):  $\nu$  3094, 3020, 2898, 2862, 2810, 2359, 1883, 1599, 1522, 1445, 1355, 1316, 1220, 1194, 1116, 977, 964, 876, 841, 805, 674  $\text{cm}^{-1}$ .

UV (ACN):  $\lambda_{\text{max}}$  364 nm.

$^1\text{H}$  NMR (400 MHz,  $\text{DMSO-}d_6$ ):  $\delta$  7.43 (2H, d,  $J = 8.8$  Hz, -ArH 3' & 5'), 7.24-7.31 (3H, m, -ArH 2, 6 & -CH), 6.93-7.03 (2H, m, -ArH 4 & -CH), 6.72 (2H, d,  $J = 8.8$  Hz, -ArH 2' & 6'), 2.94 (6H, s, - $\text{CH}_3$ ).

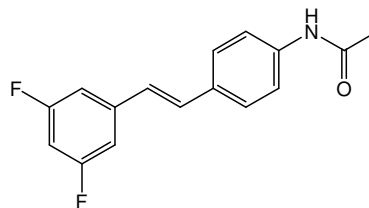
$^{13}\text{C}$ -NMR (100 MHz,  $\text{DMSO-}d_6$ ):  $\delta$  161.2 (d,  $J = 243.0$  Hz, -CF), 162.7 (d,  $J = 243.0$  Hz, -CF), 150.3 (-ArC 1'), 142.1 (t,  $J = 9.5$  Hz, -ArC 1), 132.0 (-CH), 128.0 (-ArC 3'

& 5'), 123.9 (-ArC 4'), 121.1 (-CH), 112.0 (-ArC 2' & 6'), 108.4 (d,  $J = 19$  Hz, -ArC 2 & 6), 101.4 (t,  $J = 26.5$  Hz, -ArC 4), 39.8 (-CH<sub>3</sub>).

<sup>19</sup>F-NMR (376 MHz, DMSO-*d*<sub>6</sub>):  $\delta$  -110.52 (2F, t,  $J = 7.5$  Hz).

### ***(E)*-3,5-difluoro-4'-acetylaminostilbene 161**

*(E)*-3,5-difluoro-4'-aminostilbene (0.96 g, 4.16 mmol) was dissolved in ethyl acetate (5ml) and three drops of pyridine. Acetic anhydride (1.18 ml, 12.47 mmol) was added dropwise to this solution and the reaction was stirred at room temperature for



40 min before washing with water and brine. Recrystallisation from hexane/ethyl acetate yielded the title compound **161** as a white powder (0.79 g, 70%).

m.p. 217-220 °C

IR (KBr):  $\nu$  3290, 3098, 3047, 3021, 1663, 1619, 1584, 1522, 1408, 1369, 1314, 1118, 980, 961, 847, 810, 673 cm<sup>-1</sup>.

UV (ACN):  $\lambda_{\max}$  327 nm.

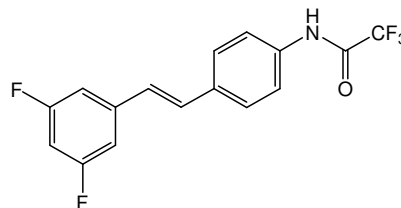
<sup>1</sup>H NMR (400 MHz, DMSO-*d*<sub>6</sub>):  $\delta$  10.07 (1H, s, -NH-), 7.62 (2H, d,  $J = 8.8$  Hz, -ArH 3' & 5'), 7.53 (2H, d,  $J = 8.4$  Hz, -ArH 2' & 6'), 7.30-7.38 (3H, m, -ArH 2, 6 & -CH), 7.06-7.16 (2H, m, -ArH 4 & -CH), 2.06 (3H, s, -CH<sub>3</sub>).

<sup>13</sup>C-NMR (100 MHz, DMSO-*d*<sub>6</sub>):  $\delta$  168.3 (-C=O), 162.7 (d,  $J = 243.0$  Hz, -CF), 162.6 (d,  $J = 243.1$  Hz, -CF), 141.4 (t,  $J = 9.7$  Hz, -ArC 1), 139.5 (-ArC 1'), 131.1 (-CH), 131.0 (-ArC 4'), 127.3 (-ArC 2' & 6'), 124.6 (-CH), 119.0 (-ArC 3' & 5'), 108.9 (d,  $J = 12.0$  Hz, -ArC 2 & 6), 102.2 (t,  $J = 26.0$  Hz, -ArC 4), 24.0 (-CH<sub>3</sub>).

<sup>19</sup>F-NMR (376 MHz, DMSO-*d*<sub>6</sub>):  $\delta$  -110.26 (2F, t,  $J = 7.5$  Hz).

### ***(E)*-3,5-difluoro-4'-(trifluoroacetyl)aminostilbene 162**

*(E)*-3,5-difluoro-4'-aminostilbene (1.45 g, 6.28 mmol) was dissolved in ethyl acetate (10ml) and three drops of pyridine. Trifluoroacetic anhydride (2.62 ml, 18.83 mmol) was added dropwise to this solution and the reaction was stirred at room



temperature for 40 min before washing with water and brine. Recrystallisation from hexane/ethyl acetate yielded compound **162** as a beige powder (1.27 g, 62%).

m.p. 188-191 °C

Anal. calcd. for C<sub>16</sub>H<sub>10</sub>NF<sub>5</sub>O: C, 58.72; H, 3.08; N, 4.28.

Found C, 58.58; H, 3.09; N, 4.19

IR (KBr):  $\nu$  3296, 3095, 1705, 1619, 1589, 1541, 1450, 1291, 1248, 1186, 1155, 1118, 984, 958, 913, 841, 808, 734, 669 cm<sup>-1</sup>.

UV (ACN):  $\lambda_{\max}$  321 nm.

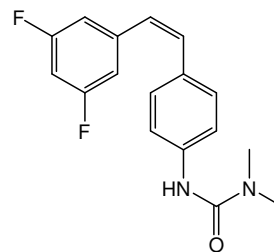
<sup>1</sup>H NMR (400 MHz, DMSO-*d*<sub>6</sub>):  $\delta$  11.38 (1H, s, -NH-), 7.73 (2H, d, *J* = 8.8 Hz, -ArH 3' & 5'), 7.65 (2H, d, *J* = 8.4 Hz, -ArH 2' & 6'), 7.42 (1H, d, *J* = 16.8 Hz, -CH), 7.36 (2H, m, -ArH 2 & 6), 7.24 (1H, d, *J* = 16.8 Hz, -CH), 7.13 (1H, tt, *J* = 2.2 & 9.2 Hz, -ArH 4).

<sup>13</sup>C-NMR (100 MHz, DMSO-*d*<sub>6</sub>):  $\delta$  162.8 (d, *J* = 243.7 Hz, -CF), 162.6 (d, *J* = 243.6 Hz, -CF), 154.4 (q, *J* = 36.8 Hz, -C=O), 141.0 (t, *J* = 9.8 Hz, -ArC 1), 136.3 (-ArC 1'), 133.6 (-ArC 4'), 130.6 (-CH), 127.4 (-ArC 2' & 6'), 126.1 (-CH), 121.1 (-ArC 3' & 5'), 115.7 (q, *J* = 286.9 Hz, -CF<sub>3</sub>), 109.2 (d, *J* = 25.4 Hz, -ArC 2 & 6), 102.6 (t, *J* = 26.0 Hz, -ArC 4).

<sup>19</sup>F-NMR (376 MHz, DMSO-*d*<sub>6</sub>):  $\delta$  -73.83 (3F, s, -CF<sub>3</sub>), -110.14 (2F, t, *J* = 7.5 Hz).

### ***(Z)*-3,5-difluoro-4'-amino(dimethylcarbamoyl) stilbene 163**

(*Z*)-3,5-difluoro-4'-aminostilbene (0.78 g, 3.39 mmol) was dissolved in dichloromethane (10 ml) and cooled to 0°C. Triethylamine (1.04 ml, 7.46 mmol) was added to stirred solution and dimethylcarbamyl chloride (0.62 g, 6.78 mmol) was then added dropwise. The reaction was stirred at 0 °C for 30 min before warming to room temperature.



Purification by column chromatography with hexane/ethyl acetate as eluant furnished *cis*-compound **163** as a white solid (0.19 g, 20%).

m.p. 127-131 °C

Anal. calcd. for C<sub>17</sub>H<sub>16</sub>N<sub>2</sub>OF<sub>2</sub>: C, 67.54; H, 5.33; N, 9.27.

Found C, 67.18; H, 5.47; N, 9.13

IR (KBr):  $\nu$  3276, 3096, 3017, 2924, 1648, 1585, 1512, 1375, 1310, 1255, 1190, 1118, 991, 969, 875, 841, 756, 669 cm<sup>-1</sup>.

UV (ACN):  $\lambda_{\max}$  320 nm.

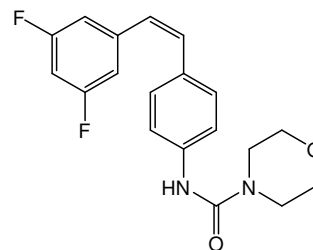
<sup>1</sup>H NMR (400 MHz, DMSO-*d*<sub>6</sub>):  $\delta$  8.36 (1H, s, -NH-), 7.40 (2H, d, *J* = 9.2 Hz, -ArH 3' & 5'), 7.06-7.11 (3H, m, -ArH 4, 2' & 6'), 6.91 (2H, m, -ArH 2 & 6), 6.68 (1H, d, *J* = 12.4 Hz, -CH), 6.48 (1H, d, *J* = 12 Hz, -CH), 2.92 (6H, s, -CH<sub>3</sub>).

$^{13}\text{C}$ -NMR (100 MHz,  $\text{DMSO-}d_6$ ):  $\delta$  162.3 (d,  $J = 245.0$  Hz, -CF), 162.2 (d,  $J = 244.0$  Hz, -CF), 155.5 (-C=O), 140.9 (t,  $J = 9.5$  Hz, -ArC 1), 140.4 (-ArC 4'), 132.3 (-CH), 128.8 (-ArC 1'), 128.6 (-ArC 2' & 6'), 126.1 (-CH), 119.2 (-ArC 3' & 5'), 111.4 (d,  $J = 25.0$  Hz, -ArC 2 & 6), 102.5 (t,  $J = 25.5$  Hz, -ArC 4), 36.2 (-CH<sub>3</sub>).

$^{19}\text{F}$ -NMR (376 MHz,  $\text{DMSO-}d_6$ ):  $\delta$  -110.27 (2F, t,  $J = 8.8$  Hz).

**(Z)-3,5-difluoro-4'-(carbamyl-4-morpholine) stilbene 164**

(Z)-3,5-difluoro-4'-aminostilbene (0.45 g, 1.93 mmol) was dissolved in dichloromethane (10 ml) and cooled to 0 °C. Triethylamine (0.44 ml, 3.85 mmol) was added to the stirring solution and 4-morpholinecarbonyl chloride (0.44 ml, 3.85 mmol) was then added dropwise. The reaction was stirred at 0 °C for 30 min before warming to room temperature. Purification by column chromatography with hexane/ethyl acetate yielded **164** as a white solid (0.19 g, 29%).



m.p. 126-129 °C

Anal. calcd. for  $\text{C}_{19}\text{H}_{18}\text{N}_2\text{O}_2\text{F}_2$ : C, 66.27; H, 5.27; N, 8.14.

Found C, 65.59; H, 5.37; N, 8.03.

IR (KBr):  $\nu$  3224, 3095, 2948, 2854, 1631, 1588, 1522, 1429, 1309, 1253, 1118, 989, 879, 848, 748, 670  $\text{cm}^{-1}$ .

UV (ACN):  $\lambda_{\text{max}}$  301 nm.

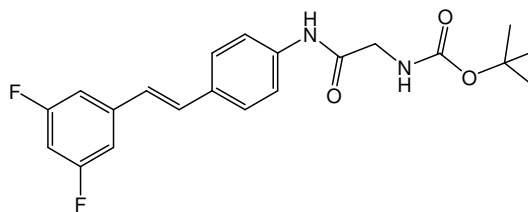
$^1\text{H}$  NMR (400 MHz,  $\text{DMSO-}d_6$ ):  $\delta$  8.64 (1H, s, -NH-), 7.41 (2H, d,  $J = 8.8$  Hz, -ArH 3' & 5'), 7.06-7.12 (3H, m, -ArH 4, 2' & 6'), 6.91 (2H, m, -ArH 2 & 6), 6.69 (1H, d,  $J = 12.4$  Hz, -CH), 6.50 (1H, d,  $J = 12.4$  Hz, -CH), 3.59-3.61 (4H, m, -OCH<sub>2</sub>), 3.41-3.43 (4H, m, -NCH<sub>2</sub>).

$^{13}\text{C}$ -NMR (100 MHz,  $\text{DMSO-}d_6$ ):  $\delta$  162.3 (d,  $J = 243.8$  Hz, -CF), 162.1 (d,  $J = 244.1$  Hz, -CF), 154.8 (-C=O), 140.8 (t,  $J = 9.7$  Hz, -ArC 1), 140.0 (-ArC 4'), 132.2 (-CH), 129.0 (-ArC 1'), 128.7 (-ArC 3' & 5'), 126.2 (-CH), 119.1 (-ArC 2' & 6'), 111.3 (d,  $J = 25.1$  Hz, -ArC 2 & 6), 102.4 (t,  $J = 25.8$  Hz, -ArC 4), 65.9 (-OCH<sub>2</sub>, -VE DEPT), 44.1 (-NCH<sub>2</sub>, -VE DEPT).

$^{19}\text{F}$ -NMR (376 MHz,  $\text{DMSO-}d_6$ ):  $\delta$  -110.21 (2F, t,  $J = 9.4$  Hz).

**(E)-3,5-difluoro-4'-N-(BOC-glycine)aminostilbene 165**

(E)-3,5-difluoro-4'-aminostilbene (0.8 g, 3.85 mmol) was dissolved in dichloromethane (20 ml). *N*-tert-butoxycarbonyl-glycine (0.68 g, 3.85 mmol), 1-hydroxybenzotriazole (0.52 g,



3.85 mmol) and triethylamine (0.54 ml, 3.85 mmol) were added to stirred solution. The reaction mixture was cooled to 0 °C, and *N*-ethyl-*N'*-(3-dimethylaminopropyl) carbodiimide (0.74 g, 3.85 mmol) was added. After 30 min. the solution was raised to room temperature and the reaction was allowed to proceed for 48 hrs. The solution was washed with brine, sat. potassium hydrogen carbonate, 10% citric acid and dried over sodium sulphate. The solvent was evaporated *in vacuo* and purification was achieved by column chromatography with hexane/ethyl acetate. Recrystallisation from ethyl acetate/hexane furnished **165** as a white powder (0.25 g, 17%).

m.p. 189-191 °C

Anal. calcd. for C<sub>21</sub>H<sub>22</sub>N<sub>2</sub>O<sub>3</sub>F<sub>2</sub>: C, 64.94; H, 5.71; N, 7.21.

Found C, 64.81; H, 5.70; N, 7.12.

IR (KBr):  $\nu$  3414, 3277, 3195, 2977, 1679, 1603, 1509, 1447, 1414, 1371, 1313, 1277, 1166, 1117, 1056, 962, 844, 670 cm<sup>-1</sup>.

UV (ACN):  $\lambda_{\max}$  321 nm.

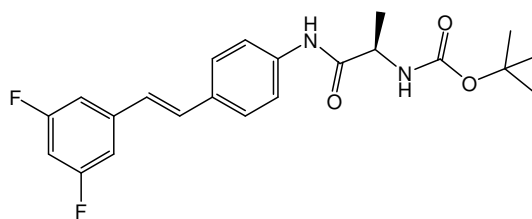
<sup>1</sup>H NMR (400 MHz, DMSO-*d*<sub>6</sub>):  $\delta$  10.05 (1H, s, -NH) 7.63 (2H, d, *J* = 8.4 Hz, -ArH 3' & 5'), 7.55 (2H, d, *J* = 8.8 Hz, -ArH 2' & 6'), 7.31-7.38 (3H, m, -ArH 2, 6 & -CH), 7.15 (1H, d, *J* = 16.4 Hz, -CH), 7.06-7.12 (2H, m, -ArH 4 & -NH), 3.73 (2H, d, *J* = 6.0 Hz, -CH<sub>2</sub>), 1.40 (9H, s, t-CH<sub>3</sub>).

<sup>13</sup>C-NMR (100 MHz, DMSO-*d*<sub>6</sub>):  $\delta$  168.3 (-COCH<sub>2</sub>), 162.8 (d, *J* = 243.3 Hz, -CF), 162.6 (d, *J* = 243.6 Hz, -CF), 155.9 (-COOt-Butyl), 141.4 (t, *J* = 9.9 Hz, -ArC 1), 139.1 (-ArC 4'), 131.2 (-CH), 131.1 (-ArC 1'), 127.4 (-ArC 2' & 6') 124.8 (-CH), 119.1 (-ArC 3' & 5'), 109.0 (d, *J* = 25.4 Hz, -ArC 2 & 6), 102.0 (t, *J* = 26.2 Hz, -ArC 4), 78.0 (-C(CH<sub>3</sub>)<sub>3</sub>), 43.8 (-CH<sub>2</sub>, -VE DEPT), 28.2 (-C(CH<sub>3</sub>)<sub>3</sub>).

<sup>19</sup>F-NMR (376 MHz, DMSO-*d*<sub>6</sub>):  $\delta$  -110.28 (2F, t, *J* = 7.5 Hz).

**(E)-3,5-difluoro-4'-N-(BOC-L-alanine)aminostilbene 166**

(E)-3,5-difluoro-4'-aminostilbene (1.7 g, 7.36 mmol) and *N*-tert-butoxycarbonyl-L-alanine (1.39 g, 7.36 mmol) were used. Purification by column chromatography with



hexane/ethyl acetate as eluant gave the title compound **166** as a white powder (0.54 g, 18%).

m.p. 227-229 °C

Anal. calcd. for C<sub>22</sub>H<sub>24</sub>N<sub>2</sub>F<sub>2</sub>O<sub>3</sub>: C, 65.66; H, 6.01; N, 6.96.

Found C, 65.38; H, 5.96; N, 6.80

IR (KBr):  $\nu$  3335, 2986, 2939, 1674, 1587, 1517, 1444, 1411, 1366, 1316, 1250, 1161, 1112, 1073, 979, 959, 841, 666, 630 cm<sup>-1</sup>.

UV (ACN):  $\lambda_{\max}$  325 nm.

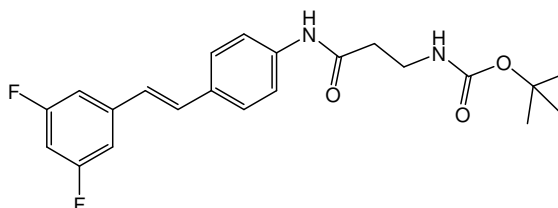
<sup>1</sup>H NMR (400 MHz, DMSO-*d*<sub>6</sub>):  $\delta$  10.08 (1H, s, -NH) 7.66 (2H, d, *J* = 8.8 Hz, -ArH 3' & 5'), 7.56 (2H, d, *J* = 8.8 Hz, -ArH 2' & 6'), 7.32-7.39 (3H, m, -ArH 2, 6 & -CH), 7.06-7.18 (3H, m, -CH, -ArH 4 & -NH), 4.13 (1H, quin, *J* = 7.2,  $\alpha$ -H), 1.39 (9H, s, t-CH<sub>3</sub>), 1.28 (3H, d, *J* = 7.2 Hz, -CH<sub>3</sub>).

<sup>13</sup>C-NMR (100 MHz, DMSO-*d*<sub>6</sub>):  $\delta$  171.9 (-COCH<sub>2</sub>), 162.8 (d, *J* = 243.5 Hz, -CF), 162.6 (d, *J* = 243.5 Hz, -CF), 155.2 (-COOt-Butyl), 141.3 (t, *J* = 10.0 Hz, -ArC 1), 139.2 (-ArC 4'), 131.2 (-CH), 131.0 (-ArC 1'), 127.4 (-ArC 2' & 6') 124.7 (-CH), 119.2 (-ArC 3' & 5'), 109.0 (d, *J* = 25.3 Hz, -ArC 2 & 6), 102.3 (t, *J* = 26.1 Hz, -ArC 4), 78.0 (-C(CH<sub>3</sub>)<sub>3</sub>), 50.4 ( $\alpha$ -C), 28.2 (-C(CH<sub>3</sub>)<sub>3</sub>), 17.9 (-CH<sub>3</sub>).

<sup>19</sup>F-NMR (376 MHz, DMSO-*d*<sub>6</sub>):  $\delta$  -110.24 (2F, t, *J* = 9.4 Hz).

**(E)-3,5-difluoro-4'-N-(BOC- $\beta$ -alanine)amino stilbene 167**

(E)-3,5-difluoro-4'-aminostilbene (0.58 g, 2.51 mmol) and *N*-tert-butoxycarbonyl- $\beta$ -alanine (0.48 g, 2.51 mmol) were used. Purification by column chromatography with



hexane/ethyl acetate as eluant furnished **167** as a white powder (0.12 g, 12%).

m.p. 213-215 °C

Anal. calcd. for C<sub>22</sub>H<sub>24</sub>N<sub>2</sub>F<sub>2</sub>O<sub>3</sub>: C, 65.66; H, 6.01; N, 6.96.

Found C, 65.28; H, 6.07; N, 6.77

IR (KBr):  $\nu$  3353, 2985, 1682, 1619, 1588, 1521, 1446, 1411, 1343, 1281, 1248, 1167, 1113, 980, 958, 841, 667  $\text{cm}^{-1}$ .

UV (ACN):  $\lambda_{\text{max}}$  326 nm.

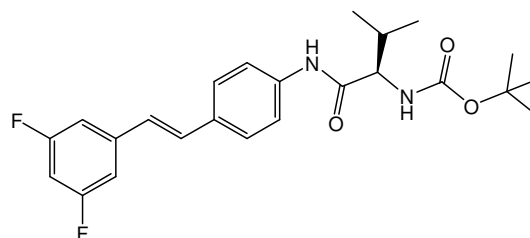
$^1\text{H}$  NMR (400 MHz,  $\text{DMSO-}d_6$ ):  $\delta$  10.07 (1H, s, -NH), 7.64 (2H, d,  $J = 8.4$  Hz, -ArH 3' & 5'), 7.54 (2H, d,  $J = 8.4$  Hz, -ArH 2' & 6'), 7.31-7.38 (3H, m, -ArH 2, 6 & -CH), 7.06-7.17 (2H, m, -CH, -ArH 4), 6.90 (1H, t,  $J = 5.6$  Hz, -NH), 3.23 (2H, q,  $J = 6.4$  Hz,  $\beta$ -H), 2.47-2.52 (m,  $\alpha$ -H), 1.38 (9H, s, t- $\text{CH}_3$ ).

$^{13}\text{C}$ -NMR (100 MHz,  $\text{DMSO-}d_6$ ):  $\delta$  169.5 (-COCH<sub>2</sub>), 162.8 (d,  $J = 243.0$  Hz, -CF), 162.7 (d,  $J = 243.0$  Hz, -CF), 155.5 (-COOt-Butyl), 141.3 (t,  $J = 10.0$  Hz, -ArC 1), 139.3 (-ArC 4'), 131.0 (-CH), 131.0 (-ArC 1'), 127.3 (-ArC 2' & 6') 124.7 (-CH), 119.1 (-ArC 3' & 5'), 109.0 (d,  $J = 25.0$  Hz, -ArC 2 & 6), 102.3 (t,  $J = 26.0$  Hz, -ArC 4), 77.6 (-C( $\text{CH}_3$ )<sub>3</sub>), 36.8 ( $\alpha$ -C, -VE DEPT), 36.4 ( $\beta$ -C, -VE DEPT), 28.2 (-C( $\text{CH}_3$ )<sub>3</sub>).

$^{19}\text{F}$ -NMR (376 MHz,  $\text{DMSO-}d_6$ ):  $\delta$  -110.25 (2F, t,  $J = 7.5$  Hz).

#### (*E*)-3,5-difluoro-4'-*N*-(BOC-*L*-valine)aminostilbene **168**

(*E*)-3,5-difluoro-4'-aminostilbene (0.97 g, 4.20 mmol) and *N*-tert-butoxycarbonyl-*L*-valine (0.91 g, 4.20 mmol) were used. Purification by column chromatography with



hexane/ethyl acetate as eluant yielded **168** as a white powder (0.20 g, 11%).

m.p. 177-180 °C

Anal. calcd. for  $\text{C}_{24}\text{H}_{28}\text{N}_2\text{F}_2\text{O}_3$ : C, 66.96; H, 6.56; N, 6.51.

Found C, 66.71; H, 6.57; N, 6.51

IR (KBr):  $\nu$  3337, 2964, 2871, 1666, 1588, 1516, 1447, 1412, 1367, 1310, 1246, 1168, 1116, 982, 961, 844, 668  $\text{cm}^{-1}$ .

UV (ACN):  $\lambda_{\text{max}}$  307 nm.

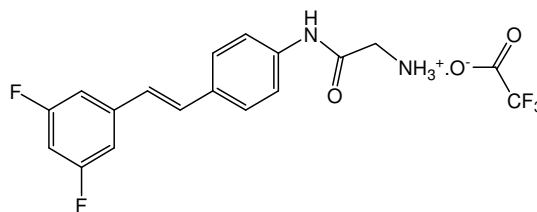
$^1\text{H}$  NMR (400 MHz,  $\text{DMSO-}d_6$ ):  $\delta$  10.06 (1H, s, -NH), 7.65 (2H, d,  $J = 8.4$  Hz, -ArH 3' & 5'), 7.55 (2H, d,  $J = 8.4$  Hz, -ArH 2' & 6'), 7.32-7.39 (3H, m, -ArH 2, 6 & -CH), 7.07-7.18 (2H, m, -CH, -ArH 4), 6.94 (1H, d,  $J = 8.8$  Hz, -NH), 3.92 (1H, t,  $J = 7.8$  Hz,  $\alpha$ -H), 1.96-2.01 (m, -CH( $\text{CH}_3$ )<sub>2</sub>), 1.38 (9H, s, t- $\text{CH}_3$ ), 0.90 (6H, d,  $J = 6.4$  Hz, -CH( $\text{CH}_3$ )<sub>2</sub>).

$^{13}\text{C}$ -NMR (100 MHz, DMSO- $d_6$ ):  $\delta$  170.8 (-COCH<sub>2</sub>), 162.8 (d,  $J$  = 243.5 Hz, -CF), 162.6 (d,  $J$  = 243.5 Hz, -CF), 155.6 (-COOt-Butyl), 141.3 (t,  $J$  = 9.8 Hz, -ArC 1), 139.0 (-ArC 4'), 131.3 (-CH), 131.0 (-ArC 1'), 127.3 (-ArC 2' & 6') 124.8 (-CH), 119.3 (-ArC 3' & 5'), 109.0 (d,  $J$  = 25.3 Hz, -ArC 2 & 6), 102.3 (t,  $J$  = 26.0 Hz, -ArC 4), 78.0 (-C(CH<sub>3</sub>)<sub>3</sub>), 60.6 ( $\alpha$ -C), 30.3 (-C(CH<sub>3</sub>)<sub>2</sub>), 28.1 (-C(CH<sub>3</sub>)<sub>3</sub>), 19.2 (-CH<sub>3</sub>), 18.4 (-CH<sub>3</sub>).

$^{19}\text{F}$ -NMR (376 MHz, DMSO- $d_6$ ):  $\delta$  -110.25 (2F, t,  $J$  = 7.5 Hz).

**(*E*)-3,5-difluoro-4'-(aminoglycine) stilbene trifluoroacetate salt **169****

(*E*)-3,5-difluoro-4'-(amino-BOC-glycine)stilbene (0.22g, 0.57mmol) was dissolved in dichloromethane (5 mls). Trifluoroacetic acid (5 ml) was added and the reaction was stirred at



room temperature for 1 hour. The reaction was monitored by thin layer chromatography. The solvent and excess TFA was evaporated with nitrogen stream. The crude residue was recrystallised from ethyl acetate to yield the title product **169** as a white powder (0.21g, 92%)

m.p. 196-199 °C

IR (KBr):  $\nu$  3260, 3116, 2360, 1677, 1589, 1546, 1509, 1434, 1315, 1263, 1201, 1139, 1121, 958, 842, 800, 724, 670  $\text{cm}^{-1}$ .

UV (ACN):  $\lambda_{\text{max}}$  318 nm.

$^1\text{H}$  NMR (400 MHz, DMSO- $d_6$ ):  $\delta$  10.70 (1H, s, -NH) 8.25 (3H, s, -NH<sub>3</sub><sup>+</sup>), 7.66 (2H, d,  $J$  = 8.8 Hz, -ArH 3' & 5'), 7.61 (2H, d,  $J$  = 8.8 Hz, -ArH 2' & 6'), 7.39 (1H, d,  $J$  = 16.4 Hz, -CH), 7.34 (2H, m, -ArH 2 & 6), 7.19 (1H, d,  $J$  = 16.4 Hz, -CH), 7.11 (1H, tt,  $J$  = 2.2 & 9.4 Hz, -ArH 4), 3.83 (2H, s, -CH<sub>2</sub>).

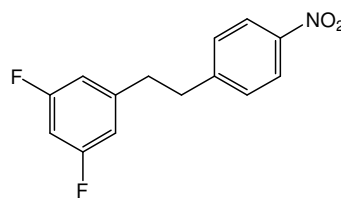
$^{13}\text{C}$ -NMR (100 MHz, DMSO- $d_6$ ):  $\delta$  164.9 (-CO), 162.8 (d,  $J$  = 243.5 Hz, -CF), 162.6 (d,  $J$  = 243.5 Hz, -CF), 158.3 (q,  $J$  = 30.0 Hz, -COCF<sub>3</sub>), 141.2 (t,  $J$  = 9.8 Hz, -ArC 1), 138.3 (-ArC 4'), 131.9 (-ArC 1'), 130.9 (-CH), 127.6 (-ArC 2' & 6'), 125.2 (-CH), 119.2 (-ArC 3' & 5'), 117.2 (d,  $J$  = 298.0 Hz, -CF<sub>3</sub>), 109.1 (d,  $J$  = 25.3 Hz, -ArC 2 & 6), 102.4 (t,  $J$  = 26.4 Hz, -ArC 4), 41.0 (-CH<sub>2</sub>, -VE DEPT).

$^{19}\text{F}$ -NMR (376 MHz, DMSO- $d_6$ ):  $\delta$  -73.61 (3F, s), -110.20 (2F, t,  $J$  = 9.4 Hz).



### ***1-(3,5-difluorophenylethyl)-4'-nitrobenzene 170***

3,5-Difluoro-4'-nitrostilbene (1.26 g, 4.83 mmol) and palladium (II) acetate (0.54 g, 2.41 mmol) were dissolved in anhydrous tetrahydrofuran (40 ml) under an atmosphere of nitrogen. Aqueous potassium fluoride (0.56 g, 9.66 mmol) was added dropwise with



stirring and the solution cooled on an ice bath prior to the very slow addition of PMHS (polymethylhydrosiloxane) (1.16 ml, 19.31 mmol). The reaction was stirred for a further two hours. After all the stilbene starting material had been consumed, the dark black reaction mixture was diluted with diethyl ether and washed repeatedly with water. The organic layers were combined and stirred in celite. This mixture was passed through an alumina/celite plug to yield a brown solution. Purification by column chromatography with hexane/ethyl acetate as eluant yielded the title compound **170** as a beige powder (0.29 g, 23%).

m.p. 102-104 °C

IR (KBr):  $\nu$  3089, 2960, 2851, 1932, 1624, 1593, 1517, 1458, 1341, 1260, 1106, 1013, 867, 851, 798, 749, 705, 668, 662  $\text{cm}^{-1}$ .

UV (ACN):  $\lambda_{\text{max}}$  276 nm.

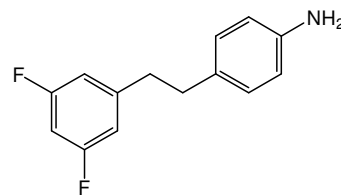
$^1\text{H}$  NMR (400 MHz,  $\text{DMSO}-d_6$ ):  $\delta$  8.02 (2H, d,  $J = 8.8$  Hz, -ArH 3' & 5'), 7.39 (2H, d,  $J = 8.8$  Hz, -ArH 2' & 6'), 6.85-6.92 (3H, m, -ArH 2, 4 & 6) 2.89-2.94 (2H, m, - $\text{CH}_2$ ), 2.81-2.85 (2H, m, - $\text{CH}_2$ ).

$^{13}\text{C}$ -NMR (100 MHz,  $\text{DMSO}-d_6$ ):  $\delta$  162.3 (d,  $J = 243.9$  Hz, -CF), 162.2 (d,  $J = 244.1$  Hz, -CF), 149.3 (-ArC 4'), 145.9 (-ArC 1'), 145.5 (t,  $J = 9.2$  Hz, -ArC 1), 129.7 (-ArC 2' & 6'), 123.4 (-ArC 3' & 5'), 111.5 (d,  $J = 24.2$  Hz, -ArC 2 & 6), 101.4 (t,  $J = 25.6$  Hz, -ArC 4), 35.8 (- $\text{CH}_2$ , -VE DEPT), 35.6 (- $\text{CH}_2$ , -VE DEPT).

$^{19}\text{F}$ -NMR (376 MHz,  $\text{DMSO}-d_6$ ):  $\delta$  -110.53 (2F, t,  $J = 9.4$  Hz).

### ***1-(3,5-difluorophenylethyl)-4'-aminobenzene 171***

3,5-Difluoro-4'-nitrostilbene (1.26 g, 4.83 mmol) and palladium (II) acetate (0.54 g, 2.41 mmol) were dissolved in anhydrous tetrahydrofuran (40 ml) under an atmosphere of nitrogen. Aqueous potassium fluoride (0.56 g, 9.66 mmol) was added dropwise with



stirring and the solution cooled on an ice bath prior to the very slow addition of

PMHS (polymethylhydrosiloxane) (1.16 ml, 19.31 mmol). The reaction was stirred for a further two hours. After all the stilbene starting material had been consumed, the dark black reaction mixture was diluted with diethyl ether and washed repeatedly with water. The organic layers were combined and stirred in celite. This mixture was passed through an alumina/celite plug to yield a brown solution. Purification by column chromatography with hexane/ethyl acetate as eluant furnished the reduced compound **171** as a dark brown oil (0.83 g, 74%).

b.p. 193-196 °C

Anal. calcd. for C<sub>14</sub>H<sub>13</sub>NF<sub>2</sub>: C, 72.09; H, 5.62; N, 6.00.

Found C, 71.74; H, 5.64; N, 5.95

IR (ATR):  $\nu$  1622, 1592, 1516, 1458, 1315, 1274, 1113, 966, 845, 821, 681 cm<sup>-1</sup>.

UV (ACN):  $\lambda_{\max}$  244; 296 nm.

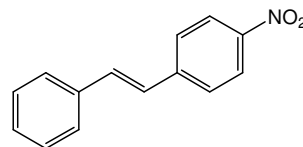
<sup>1</sup>H NMR (400 MHz, DMSO-*d*<sub>6</sub>):  $\delta$  6.99 (1H, tt, *J* = 2.4 & 9.6 Hz, -ArH 4), 6.93 (2H, m, -ArH 2 & 6), 6.86 (2H, d, *J* = 8.0 Hz, -ArH 2' & 6'), 6.49 (2H, d, *J* = 8.0, Hz -ArH 3' & 5'), 4.87 (2H, s, -NH<sub>2</sub>), 2.80-2.84 (2H, m, -CH<sub>2</sub>), 2.68-2.72 (2H, m, -CH<sub>2</sub>).

<sup>13</sup>C-NMR (100 MHz, DMSO-*d*<sub>6</sub>):  $\delta$  162.3 (d, *J* = 244.0 Hz, -CF), 162.4 (d, *J* = 244.0 Hz, -CF), 146.6 (m, -ArC 1 & 4'), 128.7 (-ArC 2' & 6'), 127.8 (-ArC 1'), 113.9 (-ArC 3' & 5'), 111.4 (d, *J* = 24.0 Hz, -ArC 2 & 6), 101.0 (t, *J* = 25.5 Hz, -ArC 4), 37.0 (-CH<sub>2</sub>, -VE DEPT), 35.6 (-CH<sub>2</sub>, -VE DEPT).

<sup>19</sup>F-NMR (376 MHz, DMSO-*d*<sub>6</sub>):  $\delta$  -110.81 (2F, t, *J* = 10.0 Hz).

### ***(E)*-4-nitrostilbene 172**

A suspension of 4-nitrobenzyl triphenyl phosphonium bromide (2.98 g, 6.25 mmol) and benzaldehyde (0.66 g, 6.25 mmol) in dichloromethane (40 ml) was stirred under an atmosphere of nitrogen. To this suspension, potassium



carbonate (0.99 g, 7.19 mmol) and a few crystals of dibenzo-18-crown-6 were added and stirring continued for a further 48 hrs. The solvent was removed *in vacuo* to yield a crude yellow/brown solid. Recrystallisation from ethanol gave the title product **172** as yellow crystalline needles (0.83 g, 59%).

m.p. 157-160 °C

Anal. calcd. for C<sub>14</sub>H<sub>11</sub>NO<sub>2</sub>: C, 74.65; H, 4.92; N, 6.22.

Found C, 73.71; H, 5.08; N, 6.05

IR (KBr):  $\nu$  3102, 3075, 3023, 2918, 2826, 2438, 1632, 1594, 1510, 1449, 1338, 1190, 1109, 1075, 971, 878, 849, 834, 769, 696  $\text{cm}^{-1}$ .

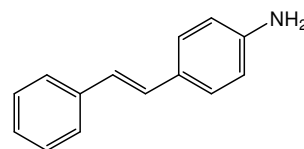
UV (ACN):  $\lambda_{\text{max}}$  350 nm.

$^1\text{H}$  NMR (400 MHz,  $\text{DMSO-}d_6$ ):  $\delta$  8.24 (2H, d,  $J = 8.8$  Hz, -ArH 3 & 5), 7.87 (2H, d,  $J = 8.8$  Hz, -ArH 2 & 6), 7.69 (2H, d, -ArH 2' & 6'), 7.54 (1H, d,  $J = 16.4$  Hz, -CH), 7.34-7.45 (4H, m, -ArH 3', 4', 5' & -CH).

$^{13}\text{C}$ -NMR (100 MHz,  $\text{DMSO-}d_6$ ):  $\delta$  146.1 (-ArC 4), 143.9 (-ArC 1), 136.2 (-ArC 1'), 133.2 (-CH), 128.8 (-ArC 3' & 5'), 128.6 (-ArC 4'), 127.2 (-ArC 2 & 6), 127.1 (-ArC 2' & 6'), 126.3 (-CH), 123.9 (-ArC 3 & 5).

### ***(E)*-4-aminostilbene 173**

4-Nitrostilbene (0.28 g, 1.24 mmol) was dissolved in an ethanol:acetic acid solution [10:1]. Iron (III) chloride hexahydrate (0.06 g, 0.21 mmol) and iron pindust (0.51 g, 9.08 mmol) were added. The impurities were removed by



filtration and recrystallisation from ethyl acetate yielded compound **173** as a beige powder (0.2 g, 94%).

m.p. 140-144 °C

IR (KBr):  $\nu$  3446, 3361, 3027, 1616, 1590, 1515, 1283, 1262, 1179, 967, 819, 754, 694  $\text{cm}^{-1}$ .

UV (ACN):  $\lambda_{\text{max}}$  333 nm.

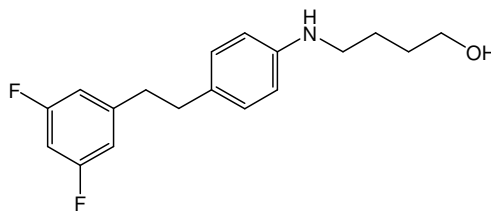
$^1\text{H}$  NMR (400 MHz,  $\text{DMSO-}d_6$ ):  $\delta$  7.50 (2H, d,  $J = 7.2$  Hz, -ArH 2' & 6'), 7.27-7.34 (4H, m, -ArH 2, 6, 3' & 5'), 7.18 (1H, t,  $J = 7.4$  Hz, -ArH 4'), 7.07 (1H, d,  $J = 16.4$  Hz, -CH), 6.90 (1H, d,  $J = 16.4$  Hz, -CH), 6.57 (2H, d,  $J = 8.4$  Hz, -ArH 3 & 5), 5.32 (2H, s, -NH<sub>2</sub>).

$^{13}\text{C}$ -NMR (100 MHz,  $\text{DMSO-}d_6$ ):  $\delta$  148.8 (-ArC 4), 137.9 (-ArC 1'), 129.1 (-CH), 128.6 (-ArC 2' & 6'), 127.6 (-ArC 3' & 5'), 126.4 (-ArC 4'), 125.7 (-ArC 2 & 6), 124.6 (-ArC 1), 122.7 (-CH), 113.9 (-ArC 3 & 5).

### ***4-(4-(3,5-difluorophenylethyl)phenylamino)butan-1-ol 174***

3,5-Difluoro-4'-nitrostilbene (0.5 g, 1.92 mmol) and palladium (II) acetate (0.33 g, 1.44 mmol) were dissolved in anhydrous tetrahydrofuran (20 ml) under an atmosphere of nitrogen. Aqueous potassium fluoride (0.33 g, 5.76 mmol) was added dropwise and solution cooled on an ice bath prior to very slow addition of PMHS

(polymethylhydrosiloxane) (0.69 ml, 11.52 mmol). The reaction was stirred for a further four hours. After all stilbene starting material had been consumed, the dark black reaction mixture was diluted



with diethyl ether and washed repeatedly with water. The organic layers were combined and stirred in celite. This mixture was passed through an alumina/celite plug to yield an orange solution. 3,5-Difluoro-4'-nitrostilbene (1.26 g, 4.83 mmol) and palladium (II) acetate (0.54 g, 2.41 mmol) were dissolved in anhydrous tetrahydrofuran (40 ml) under an atmosphere of nitrogen. Aqueous potassium fluoride (0.56 g, 9.66 mmol) was added dropwise with stirring and the solution cooled on an ice bath prior to the very slow addition of PMHS (polymethylhydrosiloxane) (1.16 ml, 19.31 mmol). The reaction was stirred for a further two hours. After all the stilbene starting material had been consumed, the dark black reaction mixture was diluted with diethyl ether and washed repeatedly with water. The organic layers were combined and stirred in celite. This mixture was passed through an alumina/celite plug to yield a brown solution. Purification by column chromatography with hexane/ethyl acetate as eluant yielded the title compound **174** as a beige powder (0.15 g, 25%).

m.p. 68-70 °C

IR (KBr):  $\nu$  3272, 2920, 2850, 1783, 1616, 1595, 1516, 1495, 1310, 1252, 1116, 1075, 968, 853, 825, 803, 747, 680  $\text{cm}^{-1}$ .

UV (ACN):  $\lambda_{\text{max}}$  254; 303 nm.

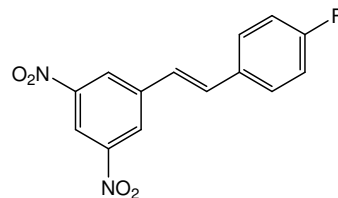
$^1\text{H}$  NMR (400 MHz,  $\text{DMSO-}d_6$ ):  $\delta$  6.90-6.99 (5H, m, -ArH 2'', 4'', 6'', 2' & 6'), 6.46 (2H, d,  $J = 8.4$ , Hz -ArH 3' & 5'), 5.33 (1H, t,  $J = 5.4$  Hz, -NH-), 4.40 (1H, t,  $J = 5.2$  Hz, -OH), 3.42 (2H, q,  $J = 6.2$ , -CH<sub>2</sub> 1), 2.95 (2H, q,  $J = 6.6$ , -CH<sub>2</sub> 4), 2.80-2.84 (2H, m, -CH<sub>2</sub>), 2.69-2.72 (2H, m, -CH<sub>2</sub>), 1.45-1.58 (4H, m, -CH<sub>2</sub> 2 & 3).

$^{13}\text{C}$ -NMR (100 MHz,  $\text{DMSO-}d_6$ ):  $\delta$  162.3 (d,  $J = 244.0$  Hz, -ArCF), 162.1 (d,  $J = 243.0$  Hz, -ArCF), 147.3 (-ArC 4'), 146.2 (t,  $J = 9.4$  Hz, -ArC 1), 128.7 (-ArC 2' & 6'), 127.4 (-ArC 1'), 111.8 (-ArC 3' & 5'), 111.5 (d,  $J = 24.0$  Hz, -ArC 2' & 6'), 101.1 (t,  $J = 25.8$  Hz, -ArC 4), 60.5 (-CH<sub>2</sub> 1, -VE DEPT), 42.9 (-CH<sub>2</sub> 4, -VE DEPT), 37.0 (-CH<sub>2</sub>, -VE DEPT), 35.5 (-CH<sub>2</sub>, -VE DEPT), 30.2 & 25.4 (-CH<sub>2</sub> 2 & 3, -VE DEPT).

$^{19}\text{F}$ -NMR (376 MHz,  $\text{DMSO-}d_6$ ):  $\delta$  -110.84 (2F, t,  $J = 8.0$  Hz).

### **(E)-3,5-dinitro-4'-fluorostilbene 175**

3,5-Dinitrobenzoyl chloride (1 g, 4.35 mmol) and 4-fluorostyrene (0.53 g, 4.35 mmol) were added to a solution of palladium (II) acetate (0.05 g, 0.22 mmol) and *N*-ethylmorpholine (0.5 g, 4.35 mmol) in *p*-xylene



(30 mls). The solution was heated at 120 °C for 18 hrs and then filtered. The solvent was removed *in vacuo* to yield a crude brown solid. Recrystallisation from hexane/ethyl acetate 50:1 gave the title product **175** as a mustard yellow powder (0.91 g, 65%).

m.p. 228-230 °C

Anal. calcd. for C<sub>14</sub>H<sub>9</sub>N<sub>2</sub>FO<sub>4</sub>: C, 58.34; H, 3.15; N, 9.72.

Found C, 58.35; H, 3.12; N, 9.83

IR (KBr):  $\nu$  3012, 2870, 1789, 1592, 1533, 1506, 1411, 1343, 1233, 1214, 1161, 1075, 962, 860, 815, 783, 731, 704, 652 cm<sup>-1</sup>.

UV (ACN):  $\lambda_{\max}$  280 nm.

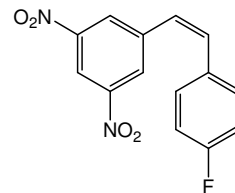
<sup>1</sup>H NMR (400 MHz, DMSO-*d*<sub>6</sub>):  $\delta$  8.84 (2H, d, *J* = 2.0 Hz, -ArH 2 & 6), 8.68 (1H, t, *J* = 1.8 Hz, -ArH 4), 7.73-7.78 (3H, m, -ArH 2', 6' & -CH), 7.54 (1H, d, *J* = 16.4 Hz, -CH), 7.29 (2H, t, *J* = 8.8 Hz, -ArH 3' & 5').

<sup>13</sup>C-NMR (100 MHz, DMSO-*d*<sub>6</sub>):  $\delta$  162.31 (d, *J* = 245.0 Hz, -CF), 148.5 (-ArC 3 & 5), 140.9 (-ArC 1), 132.6 (-CH), 132.6 (d, *J* = 3.3 Hz, -ArC 1'), 129.1 (d, *J* = 8.2 Hz, -ArC 2' & 6'), 125.9 (-ArC 2 & 6), 124.4 (d, *J* = 2.3 Hz, -CH), 116.4 (-ArC 4), 115.8 (d, *J* = 21.5 Hz, -ArC 3' & 5').

<sup>19</sup>F-NMR (376 MHz, DMSO-*d*<sub>6</sub>):  $\delta$  -112.30 (1F, m).

### **(Z)-3,5-dinitro-4'-fluorostilbene 176**

3,5-Dinitrobenzyl triphenyl phosphonium bromide (2.22 g, 4.64 mmol) and 4-fluorobenzaldehyde (0.59 g, 5.57 mmol) were dissolved in dichloromethane (30 ml) and stirred at room temperature. A 50% *w/v* sodium hydroxide solution was added dropwise [0.4ml NaOH solution per 1 mmol of aldehyde].



Stirring continued for a further hour before washing with brine and water. The solvent was removed *in vacuo* to yield both isomers as a yellow solid. Recrystallisation from ethanol gave the *trans* isomer **175** as a mustard yellow powder (0.47 g, 35%). The

resulting mother liquor was evaporated to dryness to yield the *cis* isomer **176** as a pale yellow powder (0.62 g, 46%).

m.p. 93-96 °C

IR (KBr):  $\nu$  3102, 2954, 2922, 2869, 2359, 2341, 1903, 1600, 1535, 1506, 1342, 1314, 1218, 1158, 1076, 955, 916, 860, 841, 826, 816, 752, 730, 644  $\text{cm}^{-1}$ .

UV (ACN):  $\lambda_{\text{max}}$  262 nm.

$^1\text{H}$  NMR (400 MHz,  $\text{DMSO}-d_6$ ):  $\delta$  8.67 (1H, t,  $J = 2.2$  Hz, -ArH 4), 8.40, (2H, d,  $J = 2.0$  Hz, -ArH 2 & 6), 7.31-7.34 (2H, m, -ArH 2' & 6'), 7.17 (2H, t,  $J = 8.8$  Hz, -ArH 3' & 5'), 6.99 (1H, d,  $J = 12.0$  Hz, -CH), 6.87 (1H, d,  $J = 12.4$  Hz, -CH).

$^{13}\text{C}$ -NMR (100 MHz,  $\text{DMSO}-d_6$ ):  $\delta$  161.6 (d,  $J = 244.4$  Hz, -CF), 147.9 (-ArC 3 & 5), 139.7 (-ArC 1), 133.3 (-CH), 131.5 (d,  $J = 3.5$  Hz, -ArC 1'), 130.5 (d,  $J = 8.1$  Hz, -ArC 2' & 6'), 128.6 (-ArC 2 & 6), 126.1 (-CH), 116.7 (-ArC 4), 115.7 (d,  $J = 21.3$  Hz, -ArC 3' & 5').

$^{19}\text{F}$ -NMR (376 MHz,  $\text{DMSO}-d_6$ ):  $\delta$  -113.02 (1F, m).

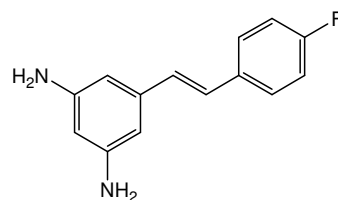
#### **(E)-3,5-diamino-4'-fluorostilbene 177**

(E)-3,5-dinitro-4'-fluorostilbene (1.4 g, 4.86 mmol)

was dissolved in a 10:1 mixture of ethanol and acetic acid (33 ml) and heated to reflux temperature. Iron

(III) chloride hexahydrate (1.31 g, 4.86 mmol),

followed by iron pindust (8.15 g, 0.15 mol) was added with vigorous stirring. The solution was refluxed for 3 hours before filtering and dilution with water. The product was extracted with diethyl ether and dried over sodium sulphate. The title product **177** was purified by column chromatography with hexane/ethyl acetate as eluant, furnishing in a brown powder (0.85 g, 77%).



m.p. 157-160 °C

Anal. calcd. for  $\text{C}_{14}\text{H}_{13}\text{N}_2\text{F}$ : C, 73.66; H, 5.74; N, 12.27.

Found C, 72.93; H, 5.87; N, 11.94.

IR (KBr):  $\nu$  3436, 3397, 3360, 3316, 3198, 3062, 3047, 3021, 1896, 1593, 1507, 1464, 1362, 1333, 1225, 1192, 1159, 1097, 963, 834, 788, 682  $\text{cm}^{-1}$ .

UV (ACN):  $\lambda_{\text{max}}$  312 nm; 260 nm.

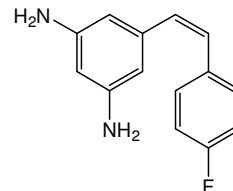
$^1\text{H}$  NMR (400 MHz,  $\text{DMSO}-d_6$ ):  $\delta$  7.59 (2H, m, -ArH 2' & 6'), 7.17 (2H, t,  $J = 8.8$  Hz, -ArH 3' & 5'), 6.90 (2H, d,  $J = 2.0$  Hz, HC=CH), 6.04 (2H, d,  $J = 2.0$  Hz, -ArH 2 & 6), 5.80 (1H, t,  $J = 1.8$  Hz, -ArH 4), 4.76 (4H, s, - $\text{NH}_2$ ).

$^{13}\text{C}$ -NMR (100 MHz,  $\text{DMSO-}d_6$ ):  $\delta$  161.3 (d,  $J = 242.9$  Hz, -CF), 149.3 (-ArC 3 & 5), 137.5 (-ArC 1), 133.9 (d,  $J = 3.0$  Hz, -ArC 1'), 130.0 (d,  $J = 2.1$  Hz, -CH), 128.0 (d,  $J = 7.8$  Hz, -ArC 2' & 6'), 125.1 (-CH), 115.5 (d,  $J = 21.2$  Hz, -ArC 3' & 5'), 101.7 (-ArC 2 & 6), 100.1 (-ArC 4).

$^{19}\text{F}$ -NMR (376 MHz,  $\text{DMSO-}d_6$ ):  $\delta$  -114.97 (1F, m).

**(Z)-3,5-diamino-4'-fluorostilbene 178**

(Z)-3,5-dinitro-4'-fluorostilbene (1.39 g, 4.83 mmol) was dissolved in a 10:1 mixture of ethanol and acetic acid (33 ml) and heated to reflux temperature. Iron (III) chloride hexahydrate (1.3 g, 4.83 mmol), followed by iron pindust (8.09 g, 0.15 mol) was added with vigorous stirring. The solution was refluxed for 3 hours before filtering and dilution with water. The product was extracted with diethyl ether and dried over sodium sulphate. Purification by column chromatography with hexane/ethyl acetate as eluant yielded **178** as a brown oil (0.72 g, 65%).



b.p. 190-195 °C

Anal. calcd. for  $\text{C}_{14}\text{H}_{13}\text{N}_2\text{F}$ : C, 73.66; H, 5.74; N, 12.27

Found C, 73.12; H, 5.76; N, 12.05.

IR (KBr):  $\nu$  3424, 3339, 3208, 3010, 1614, 1585, 1505, 1460, 1420, 1349, 1218, 1190, 1157, 1095, 863, 834, 787, 674  $\text{cm}^{-1}$ .

UV (ACN):  $\lambda_{\text{max}}$  252 nm; 222, 286 nm.

$^1\text{H}$  NMR (400 MHz,  $\text{DMSO-}d_6$ ):  $\delta$  7.32 (2H, m, -ArH 2' & 6'), 7.05 (2H, t,  $J = 9.0$  Hz, -ArH 3' & 5'), 6.39 (2H, d,  $J = 3.2$  Hz, HC=CH), 5.72 (3H, m, -ArH 2, 4 & 6), 4.68 (4H, s, -NH<sub>2</sub>).

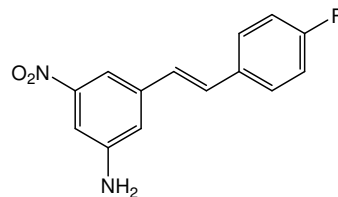
$^{13}\text{C}$ -NMR (100 MHz,  $\text{DMSO-}d_6$ ):  $\delta$  160.9 (d,  $J = 242.6$  Hz, -CF), 149.3 (-ArC 3 & 5), 137.7 (-ArC 1), 133.5 (d,  $J = 3.1$  Hz, -ArC 1'), 131.8 (d,  $J = 1.0$  Hz, -CH), 130.6 (d,  $J = 7.9$  Hz, -ArC 2' & 6'), 127.1 (-CH), 114.8 (d,  $J = 21.1$  Hz, -ArC 3' & 5'), 102.9 (-ArC 2 & 6), 99.3 (-ArC 4).

$^{19}\text{F}$ -NMR (376 MHz,  $\text{DMSO-}d_6$ ):  $\delta$  -114.94 (1F, m).

**(E)-3-nitro-5-amino-4'-fluorostilbene 179**

(E)-3,5-dinitro-4'-fluorostilbene (0.54 g, 1.88 mmol) was dissolved in a 10:1 mixture of ethanol and acetic acid (11 ml) and warmed to reflux temperature. Iron (III) chloride hexahydrate (0.17 g, 0.64 mmol), followed by iron pindust (1.53 g, 27.38

mmol) was added with vigorous stirring. The solution was refluxed for 3 hours before filtering and dilution with water. The product was extracted with diethyl ether and dried over sodium sulphate. The title product



**179** was purified by column chromatography with hexane/ethyl acetate as eluant, furnishing an orange powder (0.08 g, 17%).

m.p. 138-141 °C

Anal. calcd. for C<sub>14</sub>H<sub>11</sub>N<sub>2</sub>FO<sub>2</sub>: C, 65.11; H, 4.29; N, 10.85.

Found C, 64.99; H, 4.32; N, 10.86.

IR (KBr):  $\nu$  3472, 3372, 3224, 3082, 1895, 1620, 1600, 1578, 1531, 1509, 1447, 1413, 1352, 1333, 1241, 1159, 1091, 964, 856, 841, 778, 742, 666 cm<sup>-1</sup>.

UV (ACN):  $\lambda_{\max}$  290 nm.

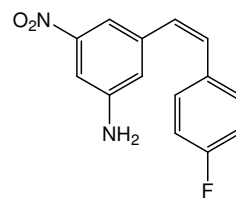
<sup>1</sup>H NMR (400 MHz, DMSO-*d*<sub>6</sub>):  $\delta$  7.70 (2H, m, -ArH 2' & 6'), 7.58 (1H, s, -ArH 2), 7.17-7.31 (5H, m, -ArH 4, 3', 5' & HC=CH), 7.14 (1H, s, -ArH 6), 5.86 (2H, s, -NH<sub>2</sub>).

<sup>13</sup>C-NMR (100 MHz, DMSO-*d*<sub>6</sub>):  $\delta$  161.7 (d, *J* = 242.9 Hz, -CF), 150.1 (-ArC 3), 149.2 (-ArC 5), 138.9 (-ArC 1), 133.09 (d, *J* = 3.0 Hz, -ArC 1'), 130.04 (d, *J* = 2.1 Hz, -CH), 128.0 (d, *J* = 7.8 Hz, -ArC 2' & 6'), 127.0 (-CH), 117.2 (-ArC 6), 115.6 (-ArC 3' & 5'), 107.8 (-ArC 2), 106.3 (-ArC 4).

<sup>19</sup>F-NMR (376 MHz, DMSO-*d*<sub>6</sub>):  $\delta$  -113.58 (1F, m).

#### **(Z)-3-nitro-5-amino-4'-fluorostilbene 180**

(Z)-3,5-dinitro-4'-fluorostilbene (1.39 g, 4.83 mmol) was dissolved in a 10:1 mixture of ethanol and acetic acid (33 ml) and warmed to reflux temperature. Iron (III) chloride hexahydrate (1.3 g, 4.83 mmol), followed by iron pindust (8.09



g, 0.15 mol) was added with vigorous stirring. The solution was refluxed for 3 hours before filtering and dilution with water. The product was extracted with diethyl ether and dried over sodium sulphate. Purification by column chromatography with hexane/ethyl acetate as eluant furnished compound **180** as an orange powder (0.11 g, 23%).

m.p. 116-118 °C

IR (KBr):  $\nu$  3438, 3356, 3232, 3085, 3017, 1635, 1600, 1526, 1508, 1343, 1238, 1221, 1159, 998, 877, 840, 807, 767, 745, 663 cm<sup>-1</sup>.



UV (ACN):  $\lambda_{\max}$  270 nm.

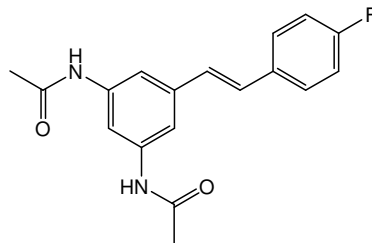
$^1\text{H}$  NMR (400 MHz,  $\text{DMSO-}d_6$ ):  $\delta$  7.26 (3H, m, -ArH 4, 2' & 6'), 7.12 (3H, m, -ArH 2, 3' & 5'), 6.80 (1H, s, -ArH 6), 6.69 (1H, d,  $J = 12.4$  Hz, -CH), 6.59 (1H, d,  $J = 12.0$  Hz, -CH), 5.80 (2H, s, -NH<sub>2</sub>).

$^{13}\text{C}$ -NMR (100 MHz,  $\text{DMSO-}d_6$ ):  $\delta$  168.4 (d,  $J = 214.9$  Hz, -CF), 150.1 (-ArC 1), 148.8 (-ArC 3), 147.4 (-ArC 5), 138.5 (-ArC 1'), 130.6 (d,  $J = 8.0$  Hz, -ArC 2' & 6'), 130.3 (-CH), 128.7 (-CH), 119.4 (-ArC 6), 115.3 (d,  $J = 21.2$  Hz, -ArC 3' & 5'), 109.7 (-ArC 2), 106.0 (-ArC 4).

$^{19}\text{F}$ -NMR (376 MHz,  $\text{DMSO-}d_6$ ):  $\delta$  -113.98 (1F, m).

### ***(E)*-3,5-diacetylamino-4'-fluorostilbene **181****

(*E*)-3,5-difluoro-4'-aminostilbene (0.5 g, 2.19 mmol) was dissolved in ethyl acetate (5 ml) and pyridine (5 ml) and cooled to 0 °C. Acetic anhydride (1.24 ml, 13.16 mmol) was added dropwise to this solution and the reaction was stirred at room



temperature for 40 min before washing with water and brine. Recrystallisation from hexane/ethyl acetate yielded the product **181** as a white powder (0.53 g, 78%).

m.p. 213-215 °C

Anal. calcd. for C<sub>18</sub>H<sub>17</sub>N<sub>2</sub>FO<sub>2</sub>: C, 69.22; H, 5.49; N, 8.97.

Found C, 68.85; H, 5.63; N, 8.83

IR (KBr):  $\nu$  3268, 3099, 1667, 1615, 1599, 1556, 1509, 1456, 1420, 1371, 1276, 1227, 1159, 1038, 998, 964, 848, 609 cm<sup>-1</sup>.

UV (ACN):  $\lambda_{\max}$  258 nm, 298, 307(sh) nm.

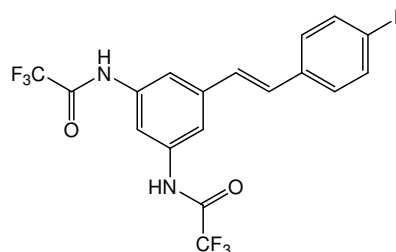
$^1\text{H}$  NMR (400 MHz,  $\text{DMSO-}d_6$ ):  $\delta$  9.99 (2H, s, -NH), 7.76 (1H, s, -ArH 4), 7.69 (2H, m, -ArH 2' & 6'), 7.52 (2H, d,  $J = 1.2$  Hz, -ArH 2 & 6), 7.21 (2H, t,  $J = 9.0$  Hz, -ArH 3' & 5'), 7.14 (1H, d,  $J = 16.4$  Hz, -CH), 7.03 (1H, d,  $J = 16.4$  Hz, -CH), 2.05 (6H, s, -CH<sub>3</sub>).

$^{13}\text{C}$ -NMR (100 MHz,  $\text{DMSO-}d_6$ ):  $\delta$  168.4 (-C=O), 161.7 (d,  $J = 244.0$  Hz, -CF), 139.8 (-ArC 3 & 5), 137.4 (-ArC 1), 133.3 (d,  $J = 2.0$  Hz, -ArC 1'), 128.5 (-ArC 2' & 6'), 128.4 (-CH), 127.2 (-CH), 115.5 (d,  $J = 21.0$  Hz, -ArC 3' & 5'), 112.0 (-ArC 2 & 6), 109.5 (-ArC 4), 24.0 (-CH<sub>3</sub>).

$^{19}\text{F}$ -NMR (376 MHz,  $\text{DMSO-}d_6$ ):  $\delta$  -114.09 (1F, m).

**(E)-3,5-di(trifluoroacetylamino)-4'-fluorostilbene 182**

(E)-3,5-difluoro-4'-aminostilbene (0.56 g, 2.46 mmol) was dissolved in ethyl acetate (5 ml) and pyridine (5 ml). Trifluoroacetic anhydride (2.1 ml, 14.74 mmol) was added dropwise to this solution and the reaction was stirred at room temperature for 40 min before washing with water and brine.



Recrystallisation from hexane/ethyl acetate yielded the title product **182** as a white powder (0.58 g, 56%).

m.p. 247-250 °C

Anal. calcd. for C<sub>18</sub>H<sub>11</sub>N<sub>2</sub>FO<sub>2</sub>: C, 51.44; H, 2.64; N, 6.67.

Found C, 51.85; H, 2.86; N, 6.47.

IR (KBr):  $\nu$  3410, 3325, 3107, 1888, 1732, 1711, 1598, 1562, 1568, 1458, 1322, 1216, 1149, 1006, 959, 938, 914, 890, 849, 815, 791, 738, 674, 623 cm<sup>-1</sup>.

UV (ACN):  $\lambda_{\text{max}}$  260 nm; 296, 307(sh) nm.

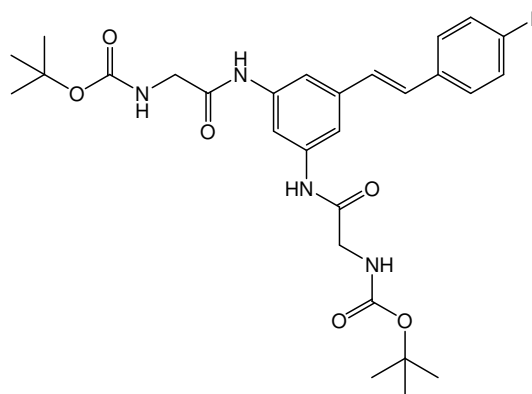
<sup>1</sup>H NMR (400 MHz, DMSO-*d*<sub>6</sub>):  $\delta$  11.47 (2H, s, -NH), 8.02 (1H, t, *J* = 1.6 Hz, -ArH 4), 7.70-7.74 (4H, m, -ArH 2, 6, 2' & 6'), 7.16-7.28 (4H, m, -ArH 3', 5' and HC=CH).

<sup>13</sup>C-NMR (100 MHz, DMSO-*d*<sub>6</sub>):  $\delta$  161.9 (d, *J* = 243.8 Hz, -CF), 154.7 (q, *J* = 36.9 Hz, -C=O), 138.3 (-ArC 1), 137.1 (-ArC 3 & 5), 133.0 (d, *J* = 3.0 Hz, -ArC 1'), 128.7 (d, *J* = 7.9 Hz, -ArC 2' & 6'), 128.7 (-CH), 127.3 (-CH), 115.7 (q, *J* = 287.1 Hz, -CF<sub>3</sub>), 116.2 (-ArC 2 & 6), 115.6 (d, *J* = 21.4 Hz, -ArC 3' & 5'), 113.1 (-ArC 4).

<sup>19</sup>F-NMR (376 MHz, DMSO-*d*<sub>6</sub>):  $\delta$  -73.87 (6H, s), -113.53 (1F, m).

**(E)-3,5-di(N-BOC-glycine)amino-4'-fluoro stilbene 183**

(E)-3,5-diamino-4'-fluorostilbene (0.29 g, 1.27 mmol) was dissolved in dichloromethane (15 ml) with *N*-tert-butoxycarbonyl-glycine (0.67 g, 3.81 mmol), 1-hydroxybenzotriazole (0.52 g, 3.81 mmol) and triethylamine (1.06 ml, 7.62 mmol). The mixture was cooled to 0 °C, and *N*-ethyl-*N'*-(3-dimethylaminopropyl) carbodiimide (0.73 g, 3.81 mmol) was added. After 30 min.



the solution was raised to room temperature and the reaction was allowed to proceed for 48 hrs. The solution was washed with brine, sat. potassium hydrogen carbonate, 10% citric acid and dried over sodium sulphate. The solvent was evaporated *in vacuo* and purification by column chromatography using hexane/ethyl acetate as eluant gave a solid. Recrystallisation from ethyl acetate/hexane furnished **183** as a white powder (0.26 g, 56%).

m.p. 138-140 °C

Anal. calcd. for C<sub>28</sub>H<sub>35</sub>N<sub>4</sub>FO<sub>6</sub>: C, 61.98; H, 6.50; N, 10.33.

Found C, 61.58; H, 6.66; N, 9.82

IR (KBr):  $\nu$  3300, 3103, 2976, 2929, 1675, 1599, 1507, 1452, 1366, 1225, 1160, 1052, 959, 847, 791, 681 cm<sup>-1</sup>.

UV (ACN):  $\lambda_{\max}$  257 nm; 298, 309(sh) nm.

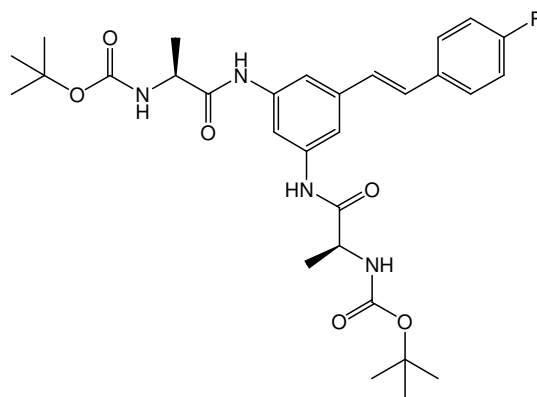
<sup>1</sup>H NMR (400 MHz, DMSO-*d*<sub>6</sub>):  $\delta$  9.99 (2H, s, -NH) 7.80 (1H, s, -ArH 4), 7.70 (2H, m, -ArH 2' & 6'), 7.55 (2H, s, -ArH 2 & 6), 7.15-7.24 (3H, m, -ArH 3', 5' & -CH), 7.04-7.08 (3H, m, -CH & -NH-), 3.75 (4H, d, *J* = 6.4 Hz, -CH<sub>2</sub>), 1.41 (18H, s, t-CH<sub>3</sub>).

<sup>13</sup>C-NMR (100 MHz, DMSO-*d*<sub>6</sub>):  $\delta$  168.3 (-COCH<sub>2</sub>), 161.7 (d, *J* = 243.6 Hz, -CF), 155.9 (-COOt-Butyl), 139.5 (-ArC 3 & 5), 137.6 (-ArC 1), 133.3 (d, *J* = 3.1 Hz, -ArC 1'), 128.5 (-CH), 128.5 (-ArC 2' & 6'), 127.4 (-CH), 115.6 (d, *J* = 21.4 Hz, -ArC 3' & 5'), 112.1 (-ArC 2 & 6), 109.6 (-ArC 4), 78.0 (-C(CH<sub>3</sub>)<sub>3</sub>), 43.7 (-CH<sub>2</sub>, -VE DEPT), 28.2 (-C(CH<sub>3</sub>)<sub>3</sub>).

<sup>19</sup>F-NMR (376 MHz, DMSO-*d*<sub>6</sub>):  $\delta$  -114.02 (1F, m).

#### (*E*)-3,5-di(*N*-BOC-*L*-alanine)amino-4'-fluoro stilbene **184**

(*E*)-3,5-diamino-4'-fluorostilbene (1.21 g, 5.31 mmol) and *N*-tert-butoxycarbonyl-*L*-alanine (3.01 g, 15.92 mmol) were used. Purification by column chromatography with hexane/ethyl acetate as eluant furnished the product **184** as a white powder (1.15 g, 38%).



m.p. 139-141 °C

Anal. calcd. for C<sub>30</sub>H<sub>39</sub>N<sub>4</sub>FO<sub>6</sub>: C, 63.14; H, 6.89; N, 9.82.

Found C, 63.42; H, 6.72; N, 9.66.

IR (KBr):  $\nu$  3292, 2977, 2931, 1672, 1600, 1508, 1452, 1366, 1288, 1164, 1070, 1021, 960, 846, 790, 711, 681  $\text{cm}^{-1}$ .

UV (ACN):  $\lambda_{\text{max}}$  258 nm; 298, 307(sh) nm.

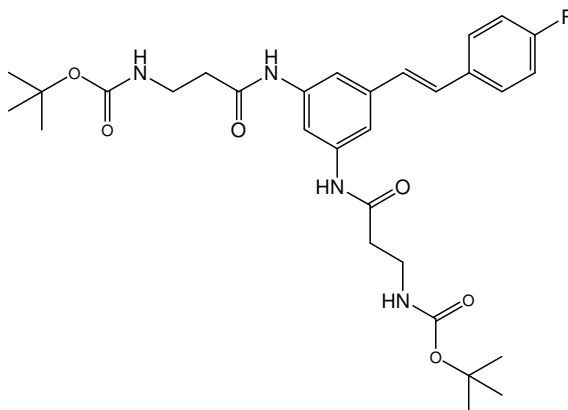
$^1\text{H}$  NMR (400 MHz,  $\text{DMSO-}d_6$ ):  $\delta$  9.98 (2H, s, -NH) 7.84 (1H, s, -ArH 4), 7.69 (2H, m, -ArH 2' & 6'), 7.55 (2H, s, -ArH 2 & 6), 7.14-7.23 (3H, m, -ArH 3', 5' & -CH), 7.04-7.08 (3H, m, -CH & -NH), 4.14 (2H, quin,  $J = 7.2$  Hz,  $\alpha$ -H), 1.39 (18H, s, t- $\text{CH}_3$ ), 1.27 (6H, d,  $J = 7.2$  Hz, - $\text{CH}_3$ ).

$^{13}\text{C}$ -NMR (100 MHz,  $\text{DMSO-}d_6$ ):  $\delta$  172.0 (-COCH<sub>2</sub>), 161.7 (d,  $J = 243.5$  Hz, -CF), 155.1 (-COOt-Butyl), 139.6 (-ArC 3 & 5), 137.5 (-ArC 1), 133.3 (-ArC 1'), 128.54 (-CH), 128.46 (-ArC 2' & 6') 127.4 (-CH), 115.6 (d,  $J = 21.3$  Hz, -ArC 3' & 5'), 112.3 (-ArC 2 & 6), 109.9 (-ArC 4), 78.0 (-C(CH<sub>3</sub>)<sub>3</sub>), 50.4 ( $\alpha$ -C), 28.2 (-C(CH<sub>3</sub>)<sub>3</sub>), 18.0 (-CH<sub>3</sub>).

$^{19}\text{F}$ -NMR (376 MHz,  $\text{DMSO-}d_6$ ):  $\delta$  -114.03 (1F, m).

#### ***(E)*-3,5-di(*N*-BOC- $\beta$ -alanine)amine-4'-fluoro stilbene **185****

(*E*)-3,5-diamino-4'-fluorostilbene (0.52 g, 2.28 mmol) and *N*-tert-butoxycarbonyl- $\beta$ -alanine (1.3 g, 6.84 mmol) were used. Purification by column chromatography with hexane/ethyl acetate as eluant yielded **185** as a white powder (0.52 g, 60%).



m.p. 113-116 °C

Anal. calcd. for  $\text{C}_{30}\text{H}_{39}\text{N}_4\text{FO}_6$ : C, 63.14; H, 6.89; N, 9.82.

Found C, 62.95; H, 7.24; N, 9.64.

IR (KBr):  $\nu$  3303, 3095, 2975, 2928, 1680, 1599, 1508, 1450, 1366, 1247, 1165, 1068, 961, 846, 789  $\text{cm}^{-1}$ .

UV (ACN):  $\lambda_{\text{max}}$  257 nm, 298, 308(sh) nm.

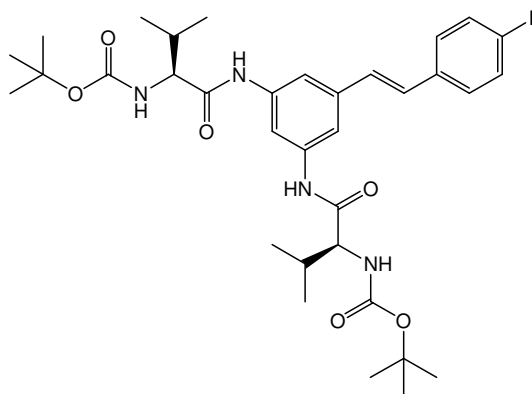
$^1\text{H}$  NMR (400 MHz,  $\text{DMSO-}d_6$ ):  $\delta$  9.99 (2H, s, -NH) 7.79 (1H, s, -ArH 4), 7.68 (2H, m, -ArH 2' & 6'), 7.56 (2H, s, -ArH 2 & 6), 7.21 (2H, t,  $J = 8.8$  Hz, -ArH 3' & 5'), 7.13 (1H, d,  $J = 16.2$  Hz, -CH), 7.03 (1H, d,  $J = 16.2$  Hz, -CH), 6.86 (2H, t,  $J = 5.4$  Hz, -NH), 3.24 (4H, q,  $J = 6.4$  Hz, -CH<sub>2</sub>), 2.47-2.50 (m, -CH<sub>2</sub>), 1.38 (18H, s, t- $\text{CH}_3$ ).

$^{13}\text{C}$ -NMR (100 MHz,  $\text{DMSO-}d_6$ ):  $\delta$  169.5 (-COCH<sub>2</sub>), 161.7 (d,  $J$  = 243.5 Hz, -CF), 155.5 (-COOt-Butyl), 139.7 (-ArC 3 & 5), 137.4 (-ArC 1), 133.3 (d,  $J$  = 3.1 Hz, -ArC 1'), 128.5 (-ArC 2' & 6'), 128.4 (-CH), 127.2 (-CH), 115.6 (d,  $J$  = 21.5 Hz, -ArC 3' & 5'), 112.2 (-ArC 2 & 6), 109.7 (-ArC 4), 77.6 (-C(CH<sub>3</sub>)<sub>3</sub>), 36.7 (-CH<sub>2</sub>, -VE DEPT), 36.5 (-CH<sub>2</sub>, -VE DEPT), 28.2 (-C(CH<sub>3</sub>)<sub>3</sub>).

$^{19}\text{F}$ -NMR (376 MHz,  $\text{DMSO-}d_6$ ):  $\delta$  -114.07 (1F, m).

**(*E*)-3,5-di(*N*-BOC-*L*-valine)amino-4'-fluoro stilbene 186**

(*E*)-3,5-diamino-4'-fluorostilbene (0.62 g, 2.72 mmol) and *N*-tert-butoxycarbonyl-*L*-valine (1.35 g, 6.21 mmol) were used. Purification by column chromatography with hexane/ethyl acetate as eluant gave the title product **186** as a brown wax (0.20 g, 12%).



IR (KBr):  $\nu$  3305, 3091, 2964, 2924, 2873, 2358, 2336, 1670, 1508, 1451, 1366, 1227, 1164, 1024, 847  $\text{cm}^{-1}$ .

UV (ACN):  $\lambda_{\text{max}}$  258 nm; 296, 310 (sh) nm.

$^1\text{H}$  NMR (400 MHz,  $\text{DMSO-}d_6$ ):  $\delta$  10.06 (2H, s, -NH) 7.88 (1H, s, -ArH 4), 7.70 (2H, m, -ArH 2' & 6'), 7.60 (2H, s, -ArH 2 & 6), 7.16-7.23 (3H, m, -ArH 3', 5' & -CH), 7.08 (1H, d,  $J$  = 16.4 Hz, -CH), 6.89 (2H, d,  $J$  = 8.4 Hz, -NH), 3.99 (2H, t,  $J$  = 7.8 Hz,  $\alpha$ -H), 1.94-2.10 (2H, m, -CH), 1.41 (18H, s, t-CH<sub>3</sub>), 0.94 (12H, d,  $J$  = 6.0 Hz, -CH(CH<sub>3</sub>)<sub>2</sub>).

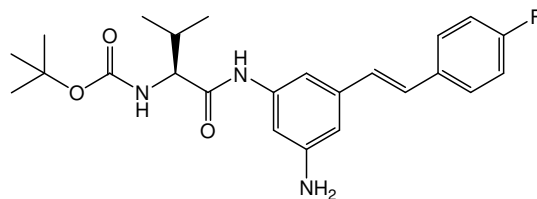
$^{13}\text{C}$ -NMR (100 MHz,  $\text{DMSO-}d_6$ ):  $\delta$  170.8 (-COCH<sub>2</sub>), 161.7 (d,  $J$  = 243.0 Hz, -CF), 155.5 (-COOt-Butyl), 139.4 (-ArC 3 & 5), 137.6 (-ArC 1), 133.3 (d,  $J$  = 3.0 Hz, -ArC 1'), 128.5 (-CH), 128.4 (-ArC 2' & 6') 127.4 (-CH), 115.5 (d,  $J$  = 22.0 Hz, -ArC 3' & 5'), 112.5 (-ArC 3 & 5), 110.0 (-ArC 4), 78.0 (-C(CH<sub>3</sub>)<sub>3</sub>), 60.6 ( $\alpha$ -C), 30.3 (-CH-), 28.1 (-C(CH<sub>3</sub>)<sub>3</sub>), 18.4 & 19.2 (-CH(CH<sub>3</sub>)<sub>2</sub>).

$^{19}\text{F}$ -NMR (376 MHz,  $\text{DMSO-}d_6$ ):  $\delta$  -114.01 (1F, m).

**(*E*)-3-*N*-(BOC-*L*-valine)amino-5-amino-4'-fluoro stilbene 187**

(*E*)-3,5-diamino-4'-fluorostilbene (0.62 g, 2.72 mmol) and *N*-tert-butoxycarbonyl-*L*-valine (1.35 g, 6.21 mmol) were used. Purification by column chromatography with

hexane/ethyl acetate as eluant furnished the title product **184** as a brown powder (0.80 g, 81%).



m.p. 105-109 °C

IR (KBr):  $\nu$  3300, 2964, 1664, 1613, 1507, 1366, 1225, 1160, 1094, 1013, 961, 839, 679  $\text{cm}^{-1}$ .

UV (ACN):  $\lambda_{\text{max}}$  257 nm; 298, 306(sh) nm.

$^1\text{H}$  NMR (400 MHz,  $\text{DMSO-}d_6$ ):  $\delta$  9.69 (1H, s, -NH), 7.64 (2H, m, -ArH 2' & 6'), 7.20 (2H, t,  $J = 8.8$  Hz, -ArH 3' & 5'), 6.92-7.04 (3H, m, -ArH 6 & CH=CH), 6.85 (1H, s, -ArH 2), 6.81 (1H, d,  $J = 8.4$  Hz, -NH), 6.50 (1H, s, -ArH 4), 5.17 (2H, s, -NH<sub>2</sub>), 3.92 (1H, t,  $J = 8.2$  Hz,  $\alpha$ -H), 1.92-2.05 (1H, m, -CH), 1.40 (9H, s, t-CH<sub>3</sub>), 0.92 (6H, d,  $J = 2.0$  Hz, -CH(CH<sub>3</sub>)<sub>2</sub>).

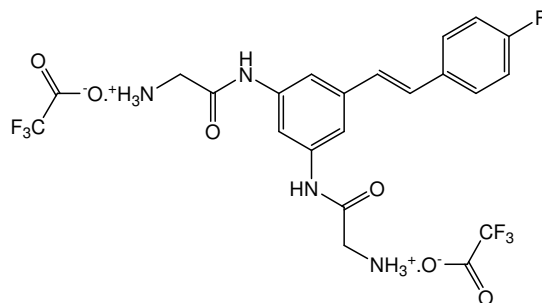
$^{13}\text{C}$ -NMR (100 MHz,  $\text{DMSO-}d_6$ ):  $\delta$  170.5 (-COCH), 161.5 (d,  $J = 243.0$  Hz, -CF), 155.5 (-COOt-Butyl), 149.2 (-ArC 5), 139.7, (-ArC 3), 137.5 (-ArC 1), 133.6 (d,  $J = 3.0$  Hz, -ArC 1'), 129.2 (-CH), 128.2 (d,  $J = 8.0$  Hz, -ArC 2' & 6') 126.2 (-CH), 115.5 (d,  $J = 22.0$  Hz, -ArC 3' & 5'), 107.5 (-ArC 4), 106.0 (-ArC 6), 105.0 (-ArC 2), 78.0 (-C(CH<sub>3</sub>)<sub>3</sub>), 60.5 ( $\alpha$ -C), 30.4 (-CH(CH<sub>3</sub>)<sub>2</sub>), 28.2 (-C(CH<sub>3</sub>)<sub>3</sub>), 19.2 (-CH<sub>3</sub>), 18.4 (-CH<sub>3</sub>).

$^{19}\text{F}$ -NMR (376 MHz,  $\text{DMSO-}d_6$ ):  $\delta$  -114.01 (1F, m).

### **(E)-3,5-di(aminoglycine)-4'-fluorostilbene trifluoroacetate salt 188**

3,5-di(amino-BOC-glycine)-4'-

fluorostilbene (0.22 g, 0.41 mmol) was dissolved in dichloromethane (5 mls). Trifluoroacetic acid (5 ml) was added to this solution and the reaction was stirred at room temperature for an



hour, until all starting material was consumed (monitoring by TLC). The solvent and excess TFA were evaporated with nitrogen stream. The crude residue was recrystallised from ethyl acetate to yield the title product **188** as a white powder (0.22g, 95%)

m.p. 204-206 °C

IR (KBr):  $\nu$  3095, 3002, 1670, 1626, 1560, 1509, 1458, 1199, 1136, 847, 798, 722  $\text{cm}^{-1}$ .

UV (ACN):  $\lambda_{\text{max}}$  254 nm; 298 nm.

$^1\text{H}$  NMR (400 MHz,  $\text{DMSO-}d_6$ ):  $\delta$  10.65 (2H, s, -NH) 8.24 (6H, s,  $-\text{NH}_3^+$ ), 7.88 (1H, s, -ArH 4), 7.71 (2H, m, -ArH 2' & 6'), 7.57 (2H, d,  $J = 1.2$  Hz, -ArH 2 & 6), 7.23 (3H, m, -ArH 3', 5' & -CH), 7.07 (1H, d,  $J = 16.0$  Hz, -CH), 3.28 (4H, s,  $-\text{CH}_2$ ).

$^{13}\text{C}$ -NMR (100 MHz,  $\text{DMSO-}d_6$ ):  $\delta$  164.9 (-CO), 161.5 (d,  $J = 243.8$  Hz, -CF), 158.4 (q,  $J = 32.0$  Hz, -CO), 139.0 (-ArC 3 & 5), 138.0 (-ArC 1), 133.1 (d,  $J = 3.2$  Hz, -ArC 1'), 128.6 (d,  $J = 7.9$  Hz, -ArC 2' & 6'), 128.1 (-CH), 127.9 (-CH), 116.9 (d,  $J = 297.0$  Hz, - $\text{CF}_3$ ), 115.6 (d,  $J = 21.5$  Hz, -ArC 3' & 5'), 112.6 (-ArC 2 & 6), 109.6 (-ArC 4), 41.0 (- $\text{CH}_2$ , -VE DEPT).

$^{19}\text{F}$ -NMR (376 MHz,  $\text{DMSO-}d_6$ ):  $\delta$  -73.84 (6F, s,  $-\text{CF}_3$ ), -113.76 (1F, m, 4'-F).

# *Appendix I*

## **List of abbreviations**

( <i>E</i> )	trans
( <i>Z</i> )	cis
2D COSY	2 dimension correlation spectroscopy
4CL	4-coumarate:CoA ligase
5-FU	5-fluorouracil
Å	angstrom
AA	amino acid
ABTS	2,2'-azinobis(3-ethylbenzthiazoline-6-sulfonic acid)
ACE	angiotensin converting enzyme
ACF	aberrant crypt foci
ACN	acetonitrile
AD	Alzheimers disease
AhR	aryl hydrocarbon receptor
AIDS	acquired immunodeficiency syndrome
AMD	age-related macular degeneration
AML	acute myeloid leukaemia
Anal	analysis
anhyd	anhydrous
AOM	azoxymethane
aq	aqueous
ARA70	androgen receptor-specific coactivator
ARDS	adult respiratory distress syndrome
Arg	arginine
Asn	asparagine
Asp	aspartic acid
ATM	ataxia telangiectasia-mutated
ATP	adenosine triphosphate
ATR	ataxia telangiectasia and rad3-related



ATR	attenuated total reflection
av	average
BABIN	bis(5-amidino-2-benzimidazolyl)methane
BACE	$\beta$ -secretase
BaP	benzo[ <i>a</i> ]pyrene
BMS	Bristol Myers Squibb
Bn	benzyl
BOC	tert-butoxycarbonyl
Bu or n-Bu	n-butyl
Bz	benzoyl
C4H	cinnamic acid 4-hydroxylase
calcd	calculated
Cat	cathepsin
CHCl <sub>3</sub>	chloroform
CHF	chronic heart failure
CHS	chalcone synthase
CL1	cathepsin L
cm <sup>-1</sup>	wavenumber(s)/ per centimetre
CNS	central nervous system
CoA	coenzyme A
conc	concentration
COPD	chronic obstructive pulmonary disease
COX	cyclo-oxygenase
Cyp	cytochrome P450
Cys	cysteine
d	density
<i>d</i> -	deuterated
d	doublet (spectral)
Da	dalton
DBU	1,8-diazabicyclo[5.4.0]undec-7-ene
DCC	1,3-dicyclohexylcarbodiimide
DCM	dichloromethane
dd	double doublets (spectral)
DES	diethylstilbestrol

DFP	diisopropylfluorophosphate
DMBA	7,12-dimethylbenz( <i>a</i> )anthracene
DMPO	5,5-dimethyl-1-pyrroline-N-oxide
DMSO	dimethyl sulfoxide
DNA	deoxyribonucleic acid
dNTPs	deoxyribonucleoside triphosphates
DPPH	1,1-diphenyl-2-picrylhydrazyl
DTP	development therapeutic program
DTT	dithiotheritol
E-64	<i>L-trans</i> -epoxysuccinyl-leucylamide-(4-guanido)-butane
ED <sub>50</sub>	50% effective dose
EDC	N-ethyl-Nϕ-(3-dimethylaminopropyl)carbodiimide
EDTA	ethylenediaminetetraacetic acid
EGTA	ethylene glycol tetraacetic acid
Enz	enzyme (s)
EPR	electron paramagnetic resonance
eq	equation
equiv	equivalent(s)
ER	oestrogen receptor
ESI-MS	electrospray ionisation mass spectrometry
Et	ethyl
EtOAc	ethyl acetate
EtOH	ethanol
FDA	food and drug administration
FMOC	9-fluorenylmethoxycarbonyl
Fxa	serine protease factor Xa
g	gram(s)
GC	gas chromatography
<i>gem</i> -	geminal
Gly	glycine
GSTP1	glutathione S-transferase P1
H <sub>2</sub> O	water
HAP	histo-aspartic proteinase
HAV	hepatitis A virus

HCl	hydrochloric acid
Hex	hexane
Hg	mercury
His	histidine
HIV	human immunodeficiency virus
HLE	human leukocyte elastase
HOBt	1-hydroxybenzotriazole
hr	hour(s)
HRV	human rhinovirus
HSPG	heparan sulphate proteoglycans
HUVEC	human umbilical vein endothelial cells
Hz	hertz
i-Bu	isobutyl
IC <sub>50</sub>	concentration required for 50% growth inhibition
ICE	interlukin-1 converting enzyme
ID <sub>50</sub>	infectious dose to 50% of exposed individuals
IHD	ischaemic heart disease
Ile	isoleucine
i-Pr	isopropyl
IR	infrared
Iva	isovaline
J	coupling constant
$k_{ass}$	rate of irreversible inhibition
kDa	kilodaltons
KF	potassium fluoride
$K_i$	rate of inhibition
$K_m$	Michaelis Menten constant
L	litre(s)
L-Ala	L-alanine
LDL	low density lipoprotein
lit.	literature
LLCs	Lewis lung carcinomas
L-Leu	L-leucine
LPS	lipopolysaccharide

L-Val	L-valine
<i>m</i> -	meta
M	molar (moles per liter)
m	multiplet (spectral)
m/z	mass-to-charge ratio
M <sup>+</sup>	molecular ion
(M+H) <sup>+</sup>	protonated molecular ion
MAPK	mitogen-activated protein kinase
max	maximum
MDR	multidrug resistance
Me	methyl
mEH	microsomal epoxide hydrolase
MeOH	methanol
MgSO <sub>4</sub>	magnesium sulfate
MHz	megahertz
MI	post-myocardial infarction
min	minute(s); minimum
ml	millilitre
mM	millimolar (millimoles per liter)
mmol	millimole(s)
MMP	matrix metalloproteases
mol wt	molecular weight
mol	mole(s)
MOM	methoxymethyl ether
mp	melting point
mpk	milligrams per kilogram
MS	mass spectrometry
N	normal (equivalents per liter)
Na <sub>2</sub> SO <sub>4</sub>	sodium sulfate
NADPH	nicotinamide adenine dinucleotide phosphate
NaOH	sodium hydroxide
NCI	national cancer institute
NEM	<i>N</i> -ethylmorpholine
NF-κB	nuclear factor-kappa B

-NHMeC	7-amino-4-methylcoumarin
-NHNap	4-naphthylamine
nM	nanomolar
NMBA	<i>N</i> -nitrosomethylbenzylamine
nmol/L	nanomoles per litre
NMP	<i>N</i> -methyl-2-pyrrolidone
NMR	nuclear magnetic resonance
NNRTI	non-nucleotide reverse transcriptase inhibitors
NO	nitric oxide
NOESY	nuclear overhauser effect spectroscopy
NRTI	nucleoside reverse transcriptase inhibitors
NtRTI	nucleotide reverse transcriptase inhibitors
Nu	nucleophile
<i>o</i> -	ortho
°C	celsius
ODC	ornithine decarboxylase
<i>p</i> -	para
Pa	pascal
PAH	polycyclic aromatic hydrocarbons
PAL	phenylalanine ammonium lyase
PBM	peripheral blood mononuclear
PE	petroleum ether
PET	positron emission tomography
PGE(2)	prostaglandin E synthase
P-gp	p-glycoprotein
Ph	phenyl
Phe	phenylalanine
PI	protease inhibitor
PI	protease inhibitor (s)
PI3K	phosphoinositide 3-kinase
pK <sub>a</sub>	acid dissociation constant
PMHS	polymethylhydrosiloxane
PMs	plasmepsins
PMSF	phenylmethylsulphonylfluoride

PPE	porcine pancreatic elastase
ppm	part(s) per million
Pr	propyl
Pro	proline
PSA	prostate-specific antigen
q	quartet (spectral)
quin	quintet (spectral)
r.t.	room temperature
RAS	renin-angiotensin system
Ref.	reference (in tables)
RNA	ribonucleic acid
ROS	reactive oxygen species
RPE	retinal pigment epithelium
RR	ribonucleoside reductase
s	singlet (spectral); second(s)
SAR	structural activity relationship
SARS	severe acute respiratory syndrome
SARS-CoV M <sup>PRO</sup>	severe acute respiratory syndrome coronavirus main proteinase
sat.	saturated
s-Bu	sec-butyl
Ser	serine
sex	sextet (spectral)
soln	solution
Sta	statine
STS	stilbene synthase
t	triplet (spectral)
t-Bu	tert-butyl
TEA	triethylamine
Temp	temperature (in tables)
TFA	trifluoroacetic acid
TGF- $\alpha$	transforming growth factor- $\alpha$
THF	tetrahydrofuran
TIMP	tissue inhibition of metalloproteases
TLC	thin-layer chromatography

TLCK	tosyl-lysine chloromethyl ketone
TMS	tetramethylsilane
TMS	trimethylsilyl
TNF- $\alpha$	tumour necrosis factor- $\alpha$
TPA	12- <i>O</i> -tetradecanoylphorbol-13-acetate
TPCK	tosylamido-2-phenylethylchloromethyl ketone
Trp	tryptophan
tt	triplet of triplets
UV	ultraviolet
UVA	ultraviolet A (long range)
UVB	ultraviolet B (medium range)
v/v	volume per unit volume (volume-to-volume ratio)
vol	volume
w/w	weight per unit weight (weight-to-weight ratio)
wt	weight
Z-/CBz	benzoxycarbonyl
ZBG	zinc-binding group
Zn <sup>2+</sup>	zinc
Z-VAD.FMK	carbobenzyloxy-valyl-alanyl-aspartyl-[ <i>o</i> -methyl]-fluoromethyl ketone
$\beta$ -Ala	$\beta$ -alanine
$\gamma$ -ABA	$\gamma$ -aminobutyric acid
$\delta$	chemical shift (ppm)
$\mu$ M	micromolar